UNIVERSITY OF OKLAHOMA
GRADUATE COLLEGE

FUNCTION AND DEGRADATION OF TWO CELL-CYCLE INHIBITORS FOR INITIATION OF SEED FORMATION IN *ORYZA SATIVA L.*

A DISSERTATION
SUBMITTED TO THE GRADUATE FACULTY
in partial fulfillment of the requirement for the
Degree of
Doctor of Philosophy

By
HENGPING XU
Noman, Oklahoma
2021

FUNCTION AND DEGRADATION OF TWO CELL-CYCLE INHIBITORS FOR INITIATION OF SEED FORMATION IN *ORYZA SATIVA L.*

A DISSERTATION APROVED FOR THE

DEPARTMENT OF MICROBIOLOGY AND PLANT BIOLOGY

BY THE COMMITTEE CONISTING OF

Dr. Scott Russell, Chair

Dr. Anne Dunn

Dr. Christina Bourne

Dr. Laura Bartley

Dr. Marc Libault

Contents

Abstract

The cell cycle controls cell division and proliferation of all eukaryote cells and is important to development of all multi-cellular organisms. The cell cycle of sexually reproducing organisms is founded by the zygote and needs to be re-established in the founding generations of new organism. Without control and synchronization of the cell-cycle, gametes cannot be assured that the DNA complement of both gametes is activated and numerically correctly represented; thus, neither double fertilization nor embryo formation would be possible. According to studies in all eukaryotes, including yeast, animals and the model plant Arabidopsis, the cell cycle consists of four different phases (M, G1, S and G2), each of which is tightly regulated at checkpoints by the cooperation of several critical regulatory factors.

However, due to the difficulty in accessing to gametic and zygotic cells in flowering plants, which are controlled in single cells deeply embedded in multiple tissues, little is known about how molecular mechanisms underlying the initiation of plant embryogenesis may reflect or contrast from such systems in other eukaryotes. Fortunately, Dr. Russell lab has developed an approach of cell isolation that opened a pathway to examine the developmental status of rice gametes and zygotes, which make it possible to manipulate cell cycle control factors involved ultimately in the initiation of the seed formation.

In this project, we employed various approaches to identify the components involved in rice zygotic cell cycle and characterize their functions and regulation. The methods and results are reported in four chapters. The main points of each chapter will be stated as the following.

Firstly, we optimized the previous procedure to isolate more, pure and viable rice egg cells and zygotes from different developmental stages, and also developed a new efficient approach, Blender method, to purify rice sperm cells. Both isolated rice egg cells and sperm cells were

identified with marker genes and used in the published study of siRNAs in rice gametes and zygotes. Our practice shows that the isolated rice gametes and zygotes are featured with viability, transparency, purity and intactness, and thus serve as an ideal system for research in cellular and molecular biology and biochemistry.

Secondly, based on our study, we established a model of arrested core complex involved in rice zygotic cell cycle control. It consists of four major regulatory components including CDKB1, CYCD5, KRP5 and KRP4. CDKB1 is the first major player in cell cycle progression; KRP4 and KRP5 function as CDKB1 inhibitors, as proved in the CDK activity analysis; more importantly, KRP5 and KRP4 act in a coordinate, or heterodimer-like, manner, as indicated in the results of Y2H, yeast growth in serial dilutions, BiFC and Kinase activity assay. Besides, this coordinate inhibition might exist in the cell cycle control of other living organisms.

Thirdly, as a novel rice F-box protein, Fb3 is preferentially expressed in rice egg cells and zygotes. It interacts with both KRP5 and KRP4 and mediates the degradation of these two KRP inhibitors through 26S proteasome pathway. This is evidenced in the protein degradation assay and supported by its reversal effect on KRP inhibition on the Kinase activity of CDKB. Our results identify Fb3 as a regulator of the two KRP inhibitors of rice zygotic cell cycle.

In addition, our phenotypic observation, genetic analysis, seed setting test and complementation trial in the rice mutant plants demonstrate that all KRP5, KR4 and Fb3 are rice specific proteins involved in initiation of rice seed formation. We also found that these mutations result in abnormal morphology in rice female germ units and compromised function in rice sperm cells.

Since rice genetics is well documented as the second sequenced flowering plant and the most abundant of human’s crops around the world, the knowledge from this effort may enrich

our understanding of the molecular mechanism underlying cell cycle control in embryogenesis initiation; in agriculture, it may facilitate crop breeding for better rice production to meet the high food demand from increasing global population.

Key Words

Rice zygote, cell cycle control, core complex, KRP inhibitors, coordinate inhibition, F-box protein, FBP mediated degradation, Blender method, microdissection

Introduction

I. Why rice was chosen as the material for this project

It is obvious that we are faced with unprecedented challenges in grain production due to the increasing need for food. Based on statistical data of the United Nations, the world population would be about 7 billion by 2011 and 8 billion by 2024. Meanwhile, arable land is decreasing due to urbanization in developing countries, increasing the urgency for agriculture improvement.

Rice was domesticated 10,000 ~ 15, 000 years ago in China and is the most abundant human's crop. About 50% of the human population consumes rice every day. Moreover, rice is the model monocot plant having the best documented record in agronomy and genetics during the past decades and particularly its genomic sequence is available for molecular manipulation as well as phylogenetic analysis. Therefore, rice is one of the best models in monocot plants for studying the mechanisms underlying the seed formation to achieve higher grain yield for the increasing global population.

II. Double fertilization is the key event for formation of grain seeds in flowering plants (angiosperms)

Seeds of flowering plants vary in shape, size and color depending the type of plant, but in major structure, consist of just embryo and endosperm. The embryo is a typically diploid structure consisting of half sperm and half egg cell genetic that forms a precocious baby plant, the endosperm is a triploid fusion product of the sperm and a maternal tissue of the central cell, forming the bulk of food of the embryo during seed germination. Both parts are derived from a unique process called double fertilization.

Double fertilization is a complicated process involved in multiple tissues and organs in flowering plants. Male gametes begin to migrate when a pollen grain lands on the surface of the stigma of the carpel, the female organ of a flower. After the pollen becomes sufficiently hydrated, the pollen grain germinates into a pollen tube which elongates through the style to the embryo sac to deliver two sperm cells (male gametes) within the ovary where the egg cell and central cell (two female gametes) are located. As a result, one sperm cell adheres and fuses with the egg cell to form a diploid zygote, and the other sperm cell combines with the larger central cell (containing 2 polar nuclei) to form a large triploid cell (Russell 1992, Dresselhaus 2016 and Sprunk 2020).

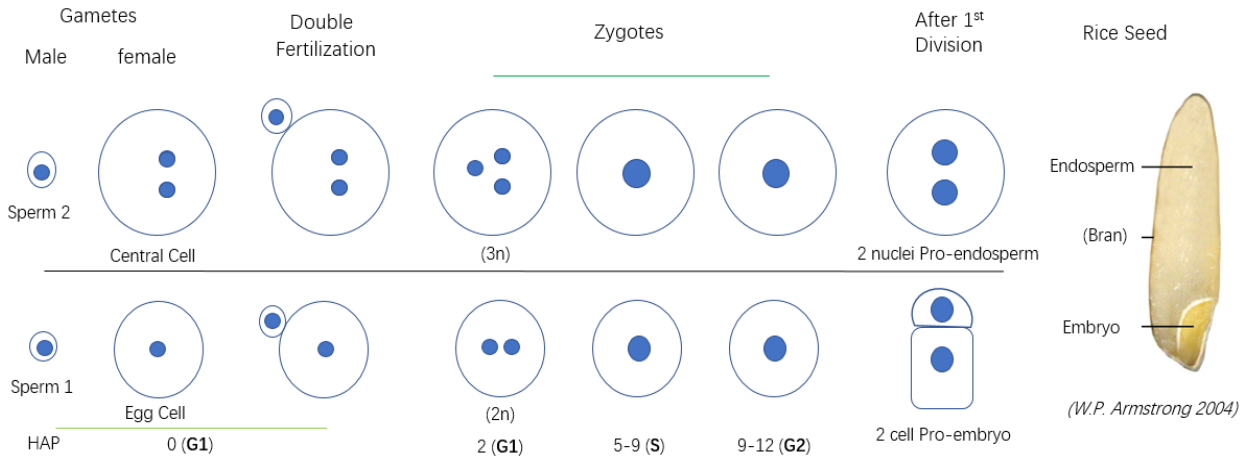

Fig. 1 The early embryogenesis in rice from the double fertilization to the first zygotic division. HAP: hour after pollination; G1, S and G2: the cell cycle phase for growth, DNA synthesis, and growth and preparation for mitosis.

The zygote is the earliest developmental stage of embryo. After its first mitosis division, the zygote is divided into two asymmetrical parts: a smaller apical cell on the top with rich cytoplasmic content, and a larger basal cell on the bottom containing large vacuoles. Unlike dicot

plants, the monocots, like rice, wheat and maize, divide their apical and basal cells in multiple planes, thus develop into pro-embryo and ultimately the embryo. In parallel, maturation in the central cell will initiate a triploid cell that will grow into the endosperm, a nutrient-rich tissue that provides nutrition for the embryo to grow into a new plant (Kranz et al 1992, Khanday and Sundaresan 2021). All the above pathways can be simply generalized as Figure 1.

III. The relationship of cell cycle to double fertilization and seed formation

The double fertilization acts as the central stage for seed formation, however, both its prior event (gametogenesis) and its post one (embryogenesis) are cell cycle related. Without the cell cycle, however, neither sperm cells nor egg/central cells would be synchronically formed for the right fertilization embryogenesis.

Numerous studies show that the cell cycle controls cell proliferation of all eukaryotic cells and regulates development within the cells of all multi-cellular organisms. The cell cycle of sexually reproduced organisms needs to be re-established in each generation in the new organism and is founded by the zygote, establishing the cell cycle as a fundamental tissue of the plant body. The cell cycle is tightly controlled to ensure it is properly regulated and synchronized via myriad regulatory factors. In sexual reproduction of higher plants, for instance, without synchronization of the cell-cycle, the DNA complement of both gametes cannot be assured to be activated and numerically correctly represented; then neither double fertilization nor embryo-formation would be possible, thus no seed production (Friedman, 1999 and Tian, et al., 2005).

IV. Cell cycle and control elements

The cell cycle, also called “cell-division cycle”, is a series of coordinated events that result in cell division of daughter cells. It consists of four different phases (G1, S, G2 and M), each of

which is tightly controlled or regulated at several checkpoints with multiple coordinated players.

It is well known that the Gap 1 phase (G1) is for active cellular growth by making proteins and organelles, the S phase (S) is for DNA synthesis, the Gap 2 phase (G2) is for more cellular growth, and Mitosis phase (M) is for cell division with proper chromosome arrangement. As indicated in Fig. 2 (blue arrows) there are two checkpoints which are crucial in decision if a cell continues to divide or not. One is from G1 to S, the other is from G2 to M.

Each of these checkpoints is tightly regulated by several critical factors. If the cell cycle machinery is not properly regulated at the checkpoints, cell proliferation will become inappropriately controlled as happens in various cancers, which permit the existence of too many cells. (Collins et al 1997, Foster 2008, Williams and Stoeber 2012, Otto and Sicinski 2017).

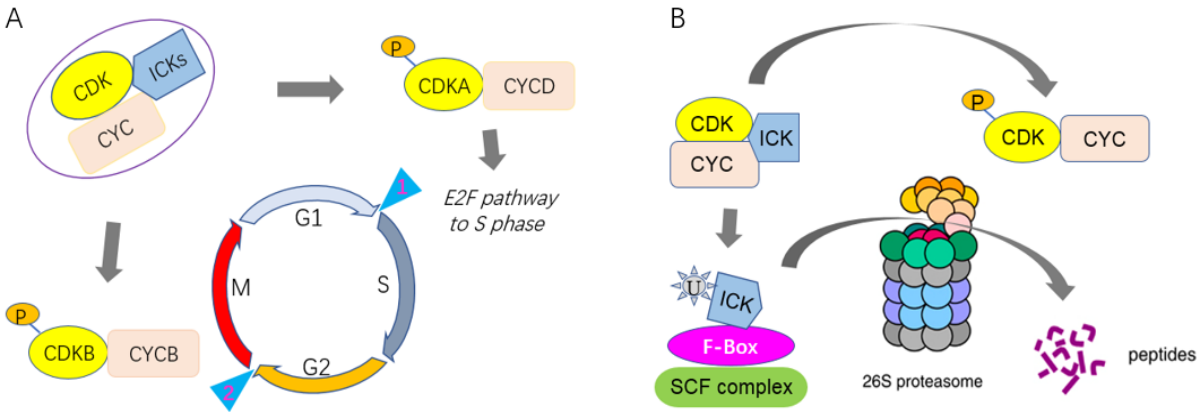

Fig. 2 Models of cell cycle control and regulation. A. Core complex factors in the control of cell cycle in Arabidopsis. CDK: Cyclin dependent kinase; ICKs: Inhibitors of CDK; CYC: Cyclin (protein). B. Degradation of the inhibitory proteins (ICKs) by the F-box protein associated SCF complex in yeast. SCF: Skp1-Cullin1-F-box; U: ubiquitin (8.5 kD). The blue arrowhead #1 and #2 indicate the two checkpoints in cell cycle: #1 is for S phase entry; #2 for mitosis, cell dividing.

As shown in Figure 2A, the first two main players are Cyclins (CYC, tissue specific) and Cyclin-Dependent Kinases (CDKs, for protein phosphorylation). Three scientists (Lee Hartwell, Paul Nurse and Tim Hunt) won the 2001 Nobel Prize in Medicine for their contributions in discovering CDKs and Cyclins in yeast. Once a specific CDK associated with Cyclin is activated, the transcription factor named E2F will be released from its inhibitor (retinoblastoma protein) to activate a group of genes required for DNA replication to enter the S phase from G1.

Both CDK and Cyclin conjugate with their third partner, Inhibitor of Cyclin Dependent Kinase (ICK). ICK is called Sim related proteins (SMR, in Arabidopsis), or Kip Related Protein (KRP, in all plants). It is 200~300 amino acid residue long, having 2 motifs at the C' terminal for interactions with CDK and Cyclin (Wang 1997, Stals and Inze 2001, De Veylder et al 2001, Barroco et al 2006, Mizutani et al 2010, Yang et al 2011, Cheng et al 2013, Dante et al 2014, Pedroza-Garcia, et al 2016 and Ramos Coelho et al 2017). Without removing the inhibition from the inhibitors, CDKA can't be activated for the S-phase entry (see the check point 1 in Fig. 1 A), and CDKB, the marker for mitosis, won't be activated either for cell dividing (see the check point 2, Fig. 1 A). The same will take place for other CDKs to pass other check points of the cell cycle. Therefore, another family of proteins encoded by F-box genes are crucial to the cell cycle progression.

The F-box motif has ~ 50 amino acid residues and is usually located at the N'-terminal. Studies in yeast and humans show that the F-box protein associates to form a protein complex, Skp1-Cullin1-F-box (SCF), which binds the inhibitor ICK and marks it for ubiquitination (by adding a small 8.5 KD ubiquitin protein) and is thus subsequently degraded via 26S proteasomes (see Fig. 2B) (Bai et al 1996, Schulman et al 2000, Kipreos and Pagano 2000, Ho et al 2006 and Marrocco et al 2010). Studies in Arabidopsis also demonstrate that plant sperm cell formation is under the

control of two cell cycle inhibitors, AtKRP6 and AtKRP5, which are degraded in the proteasome pathway via a specific F-box protein (FBL17) associated SCF complex (Kim et al 2008).

V. Cell isolation as a technique allowing cell cycle to be examined in plant gametes and zygotes

As aforementioned, the living plant gametes and zygotes are deeply embedded in multiple layers of tissues, thus it is difficult to access these cells to observe their developmental status at the molecular level. That is why little is known about the cell cycle in female gametogenesis and embryogenesis in plants, particularly, the molecular control of the first cell division from the diploid zygote into the small cytoplasm-rich apical cell and large vacuolated basal cell.

However, significant progress has been made since about 20 years ago. To our knowledge, the first protocol for mass isolation of rice sperm cells was reported in 1999 (Gou et al 1999 and Russell et al 2017). Sperm cells were released from collected fresh pollen and enriched in pure cell collections using a discontinuous Percoll gradient centrifugation protocol. In the same year, a simple mechanical method was developed to isolate rice egg cells and zygotes and the isolated zygote were used for *in vitro* culture to generate fertile rice plants. (Zhang et al 1999 and Zhao et al 2000). In addition, similar dissection but with more careful manual manipulation was applied in isolating the larger central cells (Zhao et al 2000 and Uchiumi et al 2006). The isolated rice egg cells and sperm cells were also used for *in vitro* fusion for artificial zygote (Khalequzzaman and Haq 2005).

All these isolation procedures were also systematically optimized in Dr. Russell lab, which made the rice gametes and zygotes relatively accessible for molecular profiling and manipulation

Russell et al 2011, Jones 2014 and Anderson et al 2013) and opened a window to examine the developmental status of plant gametes and zygotes.

Isolated rice sperm cells and egg cells were used for RNA sequencing (RNAseq). It was found that the transcriptomes of two opposite gametes are highly divergent and their distinctive expression profiles are involved in chromatin conformation (Anderson et al, 2013).

Isolated zygotes were also used for RNAseq later. It showed that zygotic genome activation (ZGA) takes place soon after fertilization with unequal parental contribution where most genes are expressed primarily from the maternal genome and during ZGA a number of maternal genes (2898) are downregulated indicating the removal of maternal transcript (Anderson et al 2017).

Most recently, the isolated rice gametes and zygotes were also used in the studies on small RNA transcriptomes. It is observed that the distribution of 24 nt small interfering RNA (siRNA) loci is reset in rice sperm cells and egg cells (Li et al 2020) and this pattern is returned to the canonical one in the zygotes (Li et al 2021). These observations demonstrate that chromatin modifications such as methylation and acetylation are likely taken placed in plant gametes and contributed to the next generation via the zygotes; and it is important to study the epigenetic mechanisms underlying the specific gene expression for zygotic development (Khanday and Sundaresan 2021).

VI. Objectives and significance of this research project

Even though the recent progress was made from the isolated rice gametes and zygotes, little is known about the cell cycle in gametogenesis and embryogenesis of crop plants, particularly, the molecular control of the first cell division from the diploid zygote into the small cytoplasm-rich apical cell and large vacuolated basal cell.

Based on the relevant studies in yeast, human and Arabidopsis, and the fact that there are more cell cycle control factors in rice plants, we assume that more motor-like CYC-CDKs, more brake-like KRPs and other cell cycle regulators would be involved in the event of rice zygotic division. Specifically, three questions as the following should be answered in this study:

1. What are the major players for the cell cycle control in rice egg cells and zygotes, that is, which CDK kinases, which cyclins and which KRPs will interact to form the core complex for important cell cycle checkpoints such as the S-phase entry and mitosis? Does any rice KRP protein work as the inhibitor of the kinase activity of CDKs and how does it perform this function?
2. Is there any F-box protein associated complex responsible for degrading the inhibitory KRPs?
3. How would these KRP and F-box proteins affect the phenotype, especially the seed formation in the mutant plants?

Therefore, the major objectives and corresponding approaches employed in this project will include:

1. Optimize the previous methods and develop new procedures for isolation and culture of rice leaf protoplast cells, rice sperm cells, rice egg cells and zygotes for cellular localization by transient transfection with artificial constructs.
2. Collect and screen for the candidate factors of cell cycle core complexes, particularly for those preferentially expressed in rice egg cells and zygotes, then detect interactions among those components and identify the function of KRPs in inhibiting the kinase activity of CDKs using Yeast Two Hybridization (Y2H) (Ferro and Trabalzini, 2013; Fields and Song, 1989), Co-immunoprecipitation (Co-IP) (Liu et al 2017 and Louche et al 2017), measurement of

phosphorylation level of relevant CDKs (Manning et al 2002, Grant 2009, Lewis 2013, Atkins and Cross 2018) and Bimolecular Fluorescent Complementation (BiFC) (Kudla and Bock, 2016; Horstman, 2014; Lee and Gelvin 2014, Morell et al, 2008; Walter et al., 2004).

3. Detect the interactions of KRPs and F-box proteins and analyze how the inhibitory function of KRP proteins is regulated by the partner F-box protein. Then methods include measuring the kinase activity and examining the protein degradation (Kim et al 2008, Chen et al 2012 and Teixeira et al 2013) as well as BIFC. The relevant assays will be conducted not only in yeast system, rice leaf protoplasts (Bart et al 2006 and Xu et al 2012), and rice gametes and zygotes (Li et al 2019) at different developmental stages.
4. Observe the phenotypical changes especially the seed-setting rate in rice mutant plants (An et al 2003 and Jeong et al 2006), conduct cross pollination between two mutant lines for double mutant and complementation and reciprocal pollination between the wildtype and its mutant line, and test the complementation (Liu et al 1999 and Hudson et al 2016) in the mutant plants transformed with fluorescent labelled KRP and F-box proteins expressed under the native promoters.

Since the rice genetics is well documented as the second sequenced flowering plant and the most abundant of human's crops around the world, the knowledge from the above effort may enrich our understanding of the molecular mechanism underlying cell cycle control in embryogenesis initiation; in agriculture, it may facilitate crop breeding for better rice production to meet the high food demand from increasing global population.

References

An, S., Park, S., Jeong, D. H., Lee, D. Y., Kang, H. G., Yu, G. H., Hur, J., Kim, S. R., Kim, Y.H., Lee, M., Han, S., Kim, S. J., Yang, J., Kim, E., Wi, S. J., Chung, S. H., Hong, J. P., Choe,

V., Lee, H. K., Hee, J. H., Nam, C. J., Kim, S. R., Park, P. B., Park, K. Y., Kim, W. T., Choe, S., Lee, C. B. and An G. (2003). Generation and Analysis of End Sequence Database for T-DNA Tagging Lines in Rice. Plant Physiology, 133, 2040–2047

Anderson, S.N., Johnson, C.S., Chesnut, J., Jones, D. S., Khanday, I., Woodhouse, M., Li, C., Conrad, L. J., Russell, S.D. and Sundaresan V.(2017) The zygotic transition is initiated in unicellular plant zygotes with asymmetric activation of parental genomes. Dev Cell, 43, 349-358

Anderson, S.N., Johnson, C.S., Jones, D.S., Conrad, L.J., Gou, X., Russell, S.D. and Sundaresan, V. (2013) Transcriptomes of isolated *Oryza sativa* gametes characterized by deep sequencing: evidence for distinct sex-dependent chromatin and epigenetic states before fertilization. Plant J, 76, 729-741

Atkins KC and Cross FR (2018) Interregulation of CDKA/CDK1 and the Plant-Specific Cyclin-Dependent Kinase CDKB in Control of the Chlamydomonas Cell Cycle. The Plant Cell. 30, 429–446

Bai, C., Sen, P., Hofmann, K., Ma, M., Goebl, M., Harper, J.W., and Elle S. J. (1996). SKP1 Connects Cell Cycle Regulators to the Ubiquitin Proteolysis Machinery through a Novel Motif, the F-Box. Cell *86*, 263–274

Barrôco, R. M., Peres, A., Droual, A. M., De Veylder, L., Nguyen le, S. L., De Wolf, J., Mironov, V., Peerbolte, R., Beemster, G.T., Inzé, D., Broekaert, W.F., Frankard, V. (2006). The cyclin-dependent kinase inhibitor Oryza; KRP1 plays an important role in seed development of rice. Plant Physiol. 142, 1053-1064

Bart, R., Chern, M., Park, C.J., Bartley, L., and Ronald, P.C. (2006). A novel system for gene silencing using siRNAs in rice leaf and stem-derived protoplasts. Plant Methods *2*, 1746-1748

Chen, B. B., Glasser, J. R., Coon, T. A., Zou, C., Miller, H. L., Fenton, M., McDyer, J. F.,

Boyiadzis, M. and Mallampalli, R. K. (2012). F-box protein FBXL2 targets cyclin D2 for ubiquitination and degradation to inhibit leukemic cell proliferation. BLOOD, 119 (13), 3132-3141

Cheng, Y., Cao, L., Wang, S., Li, Y., Shi, X., Liu, H., Li, L., Zhang, Z., Fowke, L.C., Wang, H., Zhou, Y. (2013). Downregulation of multiple CDK inhibitor ICK/KRP genes upregulates the E2F pathway and increases cell proliferation, and organ and seed sizes in Arabidopsis. Plant J. 75, 642-655

Collins, K., Jacks, T. and Pavletich, N. (1997). The cell cycle and cancer. PNAS, 94, 2776-2778

Dante RA, Larkins BA and Sabelli PA (2014) Cell cycle control and seed development. Frontiers in Plant Science. 493, 1-14

De Veylder, L., Beeckman, T., Beemster, G.T., Krols, L., Terras, F., Landrieu, I., van der Schueren, E., Maes, S., Naudts, M., and Inzé, D. (2001). Functional analysis of cyclin-dependent kinase inhibitors of Arabidopsis. Plant Cell *13*, 1653-1668

Dresselhaus, T., Sprunck, S., and Wessel, G. M. (2016) Fertilization Mechanisms in Flowering Plants. Current Biology. 26, R125-R139

Ferro, E., and Trabalzini, L. (2013). The yeast two-hybrid and related methods as powerful tools to study plant cell signaling. Plant Mol. Biol. *83*, 287-301

Fields, S. and Song, O. (1989). A novel genetic system to detect protein–protein interactions. Nature 340, 245-246

Foster, I. (2008). Cancer: A cell cycle defect. Radiography, 14, 144-149

Friedman, W. E., (1999). Expression of the cell cycle in sperm of Arabidopsis: implication for understanding patterns of gametogenesis and fertilization in plants and other eukaryotes. Development *126*, 1065–1075

Grant SK. (2009). Therapeutic protein kinase inhibitors. Cell Mol Life Sci., 66(7), 1163-1177

Ho, M. S., Tsai, P. I., and Chien, C. T. (2006). F-box proteins: the key to protein degradation. J. Biomed. Sci. 13, 181-191

Horstman, A., Tonaco, I. A. N., Boutilier, K., Immink, R. G. H. (2014). A Cautionary Note on the Use of Split-YFP/BiFC in Plant Protein-Protein Interaction Studies. International Journal of Molecular Sciences 15, 9628-9643

Hudson, A. O., Harkness, T. C. M., Savka, M. A. (2016). Functional Complementation Analysis (FCA): A Laboratory Exercise Designed and Implemented to Supplement the Teaching of Biochemical Pathways. Journal of Visualized Experiments, 112, 1-11

Jeong, D. H., An, S., Park, S., Kang, H. G., Park, G. G., Kim, S. R., Sim, J., Kim, Y.O., Kim, Kim S-R., Kim, J., Shin, M., Jung M. and An, G. (2006). Generation of a flanking sequence-tag database for activation-tagging lines in japonica rice The Plant Journal, 45, 123–13

Jones, D. (2014). Reproductive development in two plant models: in situ visualization of the female gametophyte and transcriptomic analysis of cell cycle regulation in Oryza sativa post-fertilization. Master's degree Thesis, University of Oklahoma

Kenneth C. Atkins and Frederick R. Cross (2018). Interregulation of CDKA/CDK1 and the Plant-Specific Cyclin-Dependent Kinase CDKB in Control of the Chlamydomonas Cell Cycle. The Plant Cell, 30, 429–446

Khalequzzaman M and Haq N (2005) Isolation and in vitro fusion of egg and sperm cells in *Oryza sativa*. Plant Physiol Biochem. 43, 69–75

Khanday, I. and Sundaresan, V. (2021) Plant zygote development: recent insights and applications to clonal seeds. Current Opinion in Plant Biology. 13: 1-10

Kim, H.J., Oh, S.A., Brownfield, L., Hong, S.H., Ryu, H., Hwang, I., Twell, D., and Nam, H.G.

(2008). Control of plant germline proliferation by SCFFBL 17 degradation of cell cycle inhibitors. Nature *455*, 1134-1137

Kipreos, E. T. and Pagano, M. (2000). The F-box protein family. Genome Biol. 1, 1-7

Ko, S. S., Li, M. J., Sun-Ben Ku, M., Ho, Y. C., Lin, Y. J., Chuang, M. H., Hsing, H. X., Lien, Y. C.,

Kudla, J., and Bock, R. (2016). Lighting the Way to Protein-Protein Interactions: Recommendations on Best Practices for Bimolecular Fluorescence Complementation Analyses. Plant Cell 28, 1002-1008

Kranz, E, Lorz H., Digonnet, C. and Faure J.E. (1992). In vitro fusion of gametes and production of zygotes. In Russell, S. D. and Dumas, C. (eds.), Sexually Reproduction in Flowering Plants. Acdemic Press, Inc, pp357-390

Lee, L.Y. and Gelvin, S. B. (2014). Bimolecular Fluorescence Complementation for imaging protein interactions in plant hosts of microbial pathogens. In Annette C. Vergunst and David O'Callaghan (eds.), Host-Bacteria Interactions: Methods and Protocols, Methods in Mol. Biol., Springer Science+ Business Media New York *1197*, pp185-208

Lewis, C. W., Taylor, R. G., Kubara, P. M., Marshall, K., Meijer, L., Go, R. M. (2013). A western blot assay to measure cyclin dependent kinase activity in cellsor in vitro without the use of radioisotopes. FEBS Letters, 587, 3089-3095

Li, C., Gent, J.I., Xu, H., Fu, H., Russell, S. D. and Sundaresan, V. (2021) Resetting of 24-nt siRNA landscape is initiated in the unicellular zygote in rice 2021 (to be submitted)

Li, C., Xu, H., Fu, F.F., Russell, S. D., Sundaresan, V. and Gent, J.I. (2020) Genome-wide redistribution of 24-nt siRNAs in rice gametes. Genome Res, 30, 173-184

Li, C., Xu, H., Russell, S.D., Sundaresan, V. (2019). Step-by-step protocols for rice gamete

isolation. Plant Reprod. 32:5–13

Liu, X., Liu, R., Li, Y., Shen, X., Zhong, S., and Shi, H. (2017). EIN3 and PIF3 Form an Interdependent Module That Represses Chloroplast Development in Buried Seedlings. The Plant Cell, 29, 3051–3067

Liu, Y. G., Shirano, Y., Fukaki, H., Yanai, Y., Tasaka, M., Tabata, S. and Shibata, D. (1999). Complementation of plant mutants with large genomic DNA fragments by a transformation-competent artificial chromosome vector accelerates positional cloning. PNAS, 96, 6535– 6540

Louche, A., Salcedo, S. P. and Bigot, S. (2017) Chapter 20. Protein–Protein Interactions: Pull-Down Assays. Laure Journal and Eric Cascales (eds) Bacterial Protein Secretion Systems: Methods and Protocols, Methods in Molecular Biology, Springer Science+Business Media LLC, vol. 1615, pp247-255

Manning, G., Whyte, D. B., Martinez, R.,Hunter, T., Sudarsanam S. (2002). The protein kinase complement of the human genome. Science, 298, 1912-1934.

Marrocco, K., Bergdoll, M., Achard, P., Criqui, M. C., and Genschik, P. (2010). Selective proteolysis sets the tempo of the cell cycle. Cur. Opin. Plant Biol. *13*, 631–639

Mizutani, M., Naganuma, T., Tsutsumi, K. N., and Saitoh, Y. (2010). The syncytium-specific expression of the Orysa; KRP3 CDK inhibitor: implication of its involvement in the cell cycle control in the rice (*Oryza sativa L*.) syncytial endosperm. J Exp Bot. *61*, 791-798

Morell, M., Espargaro, A., Aviles, F.X., and Ventura, S. (2008). Study and selection of in vivo protein interactions by coupling bimolecular fluorescence complementation and flow cytometry. Nat. Protoc. *3*, 22-33

Otto, T. and Sicinski, P. (2017). Cell cycle proteins as promising targets in cancer therapy. Nat Rev Cancer; 17(2): 93–115

Pedroza-Garcia, J. A., Domenichini, S., and Raynaud, C. (2016). Plant cell cycle transitions. In: Molecular cell biology of the growth and differentiation of plant cells, edited by Rose, R. J. CRC Press, pp3-21

Ramos Coelho, R., Vieira, P., Antonino de Souza Junior, J. D., Martin-Jimenez, C., De Veylder, L., Cazareth, J., Engler, G., Grossi-de-Sa, M. F., and de Almeida Engler, J. (2017). Exploiting cell cycle inhibitor genes of the KRP family to control root-knot nematode induced feeding sites in plants. Plant Cell Environ, 40(7):1174-1188

Russell, S. D. (1992). Double fertilization. In Russell, S. D. and Dumas, C. (eds.), Sexually Reproduction in Flowering Plants. Acdemic Press, Inc, pp357-390

Russell, S.D., X. Gou,C.E. Wong,X. Wang,T. Yuan,X. Wei,P.L. Bhalla,M. B. Singh (2012) Genomic profiling of rice sperm cell transcripts reveals conserved and distinct elements in the flowering plant male germ lineage. New Phytologist, 195(3), 560-573

Schulman, B.A., Carrano, A.C., Jeffrey, P.D., Bowen, Z., Kinnucan, E.R., Finnin, M.S., Elledge, S.J., Harper, J.W., Pagano, M., and Pavletich, N.P. (2000). Insights into SCF ubiquitin ligases from the structure of the Skp1–Skp2 complex. Nature 408, 381-386

Sprunck, S. (2020). Twice the fun, double the trouble: gamete interactions in flowering plants. Opinion in Plant Biology 2020, 53, 106-116

Stals, H. and Inze, D. (2001). When plant cells decide to divide. Trends in Plant Science *6*, 359-364

Tavva, V. S., Dinkins, R. D., Palli, S. R., and Collins, G. B. (2006). Development of a methoxyfenozide-responsive gene switch for applications in plants. Plant J. *45*, 457-469

Teixeira,F. R., Manfiolli, A. O., Soares,C. S., Baqui,M. M. A., Koide, T., Gomes, M. D. (2013) The F-box protein FBXO25 promotes the proteasome-dependent degradation of

ELK-1 protein. J Biol Chem, 288(39), 28152-62

Tian, H. Q., Yuan, T., and Russell, S. (2005). Relationship between double fertilization and the cell cycle in male and female gametes of tobacco. Sex. Plant Reproduction *17*, 243-252

Uchiumi, T., Komatsu, S., Koshiba, T., Okamoto, T. (2006). Isolation of gametes and central cells from *Oryza sativa* L. Sex Plant Reprod 19, 37-45

Walter, M., Chaban, C., Schütze, K., Batistic, O., Weckermann, K., Näke, C., Blazevic, D., Grefen, C., Schumacher, K., Oecking, C., Harter, K., and Kudla, J. (2004). Visualization of protein interactions in living plant cells using bimolecular fluorescence complementation. Plant J. *40*, 428-38

Wang, H and Fowke LC (1997): A plant cyclin-dependent kinase inhibitor gene. Nature *386*, 451-452

Williams, G. H. and Stoeber, K. (2012). The cell cycle and cancer. J Pathol, 226, 352–364

Xu, C., Wang, Y., Yu, Y., Duan, J., Liao, Z., Xiong, G., Meng, X., Liu, G., Qian Q., and Li, J. (2012). Degradation of MONOCULM 1 by APC/C^{TAD1} regulates rice tillering. Nature Communications 3, 1-9

Yang, R., Tang, Q., Wang, H., Zhang, X., Pan, G., Wang, H., Tu, J. (2011). Analyses of two rice (Oryza sativa) cyclin-dependent kinase inhibitors and effects of transgenic expression of OsiICK6 on plant growth and development. Ann. Bot. 107, 1087-1101

Zhang J, Dong WH, Galli A and Potrykus I (1999) Regeneration of fertile plants from isolated zygotes of rice (*Oryza sativa*). Plant Cell Rep 19:128–132

Zhao J, Zhou C and Yang HY (2000) Isolation and in vitro culture of zygotes and central cells of *Oryza sativa L*. Plant Cell Rep. 19, 321–326

Chapter 1. Isolation and Transfection of Rice Gametes and Zygotes

Abstract

Plant gametes and zygotes are founding cells for seed formation, but little is known about how molecular mechanisms underlying the initiation of plant embryogenesis since these single cells are deeply embedded in multiple tissues. During the past decade, Dr. Russell Lab had made rice gametes and zygotes relatively accessible. Here we optimized the previous protocol to get more, pure and living rice egg cells and zygotes from different developmental stages. We also developed a new efficient approach, Blender method, to purify rice sperm cells. Both isolated rice gametes were identified with specific marker genes and successfully used in the study of siRNAs of rice gametes. Our practice shows that isolated rice gametes and zygotes are featured with purity, viability, transparency and intactness, thus can serve as an ideal system for research in cellular and molecular biology and biochemistry.

Background

The plant sexual reproduction is one of fundamental issues for human. It includes the double fertilization as the central stage in the life cycle of higher plants, referring one sperm cell to bind and fuse with the egg cell then develop into the embryo and the other with the central cell into the endosperm for the nutrition of the embryo. Both embryo and endosperm are the two major components of seeds to feed human and animals. This unique process was firstly described in 1898 by Sergius Nawaschin and 1899 by Leon Guignard in *Lilium martagon* (Russell 1992 and Hu 1998). Since then, intensive research has been devoted to the observation and characterization of the diverse reproduction process and the method invention particularly in electron microscopy to rich the knowledge of gametogenesis and embryogenesis in angiosperms.

However, the molecular mechanisms underlying the double fertilization, the gamete formation and zygote development are very limited until today due to inaccessibility to these cells deeply embedded in multiple plant tissues as well the lower expression level of those major biochemical components in the process for seed formation.

On the other hand, the significant progress has been made in the manual isolation of plant gametes, mainly sperm cells and egg cells, in numerous studies during the past decades (Russell et al 1990, Roeckel et al 1990, Theunis 1991, Zhang et al 2010 and Lin et al 2021). But only some of these studies would be briefly reviewed in the following as the background for this PhD program.

I. Isolation of non-rice plant gametes

1. Male gametes (sperm cells)

One of the earliest efforts in isolation of plant sperm cells can be tracked back to 1973 (Cass) from barley, *Hordeum vulgare*. The spherical shape was observed after released from pollen grain and used for observing the ultrastructure. However, the sperm cell isolation in mass has not been achieved until 1986 from *Plumbago zeylanica* (Russell 1986). Since then, the sperm isolation has been undertaken using at least 29 different plant species, including those with economic importance such as maize (*Zey mays*), rice (*Oryza sativa*), wheat (*Triticum aestivum*), rape (*Brassica spp*), spinach (*Spinacia oleracea*), lily (*Lilium longiflorum*) and leek (*Allium tuberosum Roxb*)..

The procedure for isolation of plant sperm cells can be generalized into 4 major steps.

(1). Break pollen or pollen tubes by grinding or osmotic shocking

For tricellular pollen grain in which the generative cell has divided into 2 sperm cells, it can be broken by grinding or osmotic shocking. The grinding method was used in the sperm cell

isolation in lily, but the yield was lower (Tanaka 1988); the popular way is using the solution with appropriately lower osmotic pressure to burst the pollen grain and keep the released sperm cell intact and viable (Russell 1985, 1986, 1990, Zhang et al 1992, Xu and Tsao 1997a).

For the bicellular pollen grain (e.g. from tobacco), the sperm cells are formed in pollen tube. Therefore, the pollen must be germinated and cultured in media, then the pollen tubes are treated with the low osmotic solution to release the sperm cells (Xu et al 2002).

To facilitate bursting the pollen grain or pollen tube, the osmotic shock can be added with cell wall digestion enzymes, a mixture of cellulase, pectinase and pectolyase (Zou et al 1990 and Shivanna et al 1988).

(2). Separate sperm cells from broken pollen grains

A filter with a proper opening size (30~40 μm), depending the size of pollen grain or pollen tube, is used for this purpose (Zou et al 1988 and Hough et al 1986).

(3). Enrich sperm cells

The filtrate from the step (2) will be centrifuged on a density gradient solution of sucrose (Russell 1986 and Cass and Fabi 1988) or percoll (a medium with low viscosity) (Dupius et all 1987, Nielsen and Olesen 1988). The sperm cells will be enriched on the special gradient interface and collected for further purification by repeating the same step.

(4). Examine the yield and viability of isolated sperm cells in microscopy

The sperm cell yield can be calculated with the number of recovered cells divided by the total cell number from the starting material. The rate was 20 ~ 30% from maize (Dupuis et al 1987 and Roeckel et al 1988), and up to 75% from *Plumbargo zeylanica* (Russell 1986). To test the viability, the most popular way is staining the isolated cell with Fluorescein Diacetate (FDA), a cell-permeant substrate for cellular esterase. The fluorescence observed under the microscope

indicates the viability and membrane integrity of the stained sperm cells.

2. Female gametes (the egg and central cells)

Plant female gametes are located within the embryo, specifically, in a structure called embryo sac. The isolation of viable embryo sacs was succeeded in in *Nicotiana tabacum* in 1970s (Solntseva and Levkovskii 1978). During 1980s, the viable embryo sacs and egg cells were isolated in China from several plant species including *Antirrhinu majus* (Zhou 1985, Zhou and Yang 1984, Hu et al 1885, Hu 2002). Then, a large quantity of female gametes was isolated in Europe and America (Mol 1986, Huang and Russell 1989, Huang et al 1990, Van and Kwee 1990, Wagner et al 1988, Kranz et al 1991, Cao and Russell 1997). The number of plant species used for this purpose are over 48, including 12 crop plants.

The major isolation technique was manual micro-dissection with or without the aid of cell wall enzymatic digestion. The micro-dissection needs micro-knives, thin needles, micro-capillaries and inverted microscope. Without enzymatic digestion in this method, it is easier to control the quality and purity of isolated products, but the disadvantage is that it requires great skill and patience. With aid of enzymatic digestion in a mixture of cellulase and pectinase to soften the surrounding tissues, a large quantities of female gametes can be isolated, but the potential issue is hard to avoid residual degrading on the viable cells (Hu et al 1985, Zhou and Yang 1985 , Russell et al 1989 and Kranz 1991).

3. Application of isolated <u>non-rice</u> plant gametes in studies of current biology

There are at least three major application of the isolated plant gametes in biological studies.

(1) *In vitro* fertilization

Through intensive efforts, the isolated and viable gametes from many plant species become accessible. However, it is questionable if these isolated gametes can function same as those *in*

vivo in fertilization and embryogenesis. During the past decades maize has been used as one of model systems (Dumas and Mogensen 1993) to address this issue. Based on the two studies of *in vitro* fertilization, isolated maize sperm cell and egg cell work in fusion into a zygote, and the zygote is successfully developed into an embryo (Kranz and Lort 1994 and Faure et al 1994). This *in vitro* fertilization system can be very useful in future for testing the molecular function of some specific gamete surface proteins, which may be involved in the mechanisms underlying the double fertilization and embryogenesis.

(2) Cell surface recognition molecules

According to the observation of Dr. Russell (1985 and 1992), the preferential fertilization may exist at least in some plant species like Plumbago and maize. In Plumbago, the cytoplasmic organelles are unevenly distributed between two sperm cells. One sperm cell (Sua, not associated with the vegetative nucleus) contains many more plastids but many fewer mitochondria than the other (Svn). In 94% of examined cases, the Sua sperm cell fuses with the egg cell. This is very interesting since it indicates the possible existence of specific gametic surface proteins as the determinants for the recognition, adherence and fusion during the double fertilization. Therefore, several studies were carried out to detect and identify the plasma membrane proteins from isolated plant sperm cells.

First, six different fluorescein isocyanate (FITC) labeled lectins (ConA, RCA I, WGA, SBA, PHA-L and UEA I) were used to label the plasma membrane of isolated viable maize sperm cells. It is found that the sperm cell surface is positively reacted with FITC-Con A, indicating that the sperm cell has the surface glycoproteins containing mannosyl and glucosyl residues (Xu and Tsao 1997b). Then the maize sperm cells were accumulatively isolated from totally up to two kilograms of fresh pollen for purification of plasma membrane and the surface glycoproteins (Xu

and Tsao 1997c). As a result, multiple glycol-polypetides with size form 68 kD to 32 kD were purified and immunolocalized on the isolated maize sperm cells (Xu and Tsao 1997d).

By comparing the difference in surface proteins between leaf and sperm cells in lily using the probe N-hydroxysuccinimido- (NHS) or sulfo-NHS-biotin, two sperm cell specific proteins, 63 and 67 kD, were identified (Blomstedt et al 1992). In addition, it is observed that two monoclonal antibodies to arabinogalactan proteins, JIM8 and JIM13, bound to the sperm cells of Brassica and Lilium, either in pollen tubes or isolated, suggesting that these sperm cells contain arabinogalactan proteins (Southworth and Kwiatkowski, 1996).

All these sperm cell specific surface proteins or glycoproteins are likely playing a role in the recognition, adhesion and fusion at the double fertilization. Although three sperm surface proteins (DMP8/9, GEX2 and HAP2) and egg cell excretive protein EC1 are recently found involved in the *in vitro* fertilization in Arabidopsis (Mori et al 2014, Dresselhaus et al 2016 and Sprunck 2020), it is unknown if they are glycoproteins or not and if they are universal players in the double fertilization of angiosperms including the crop plants like rice of our interest. It is important to learn this information, since the sugar chains of the glycoproteins play the role in the cell-to-cell recognition and fusion based on the relevant studies in animal and human (Xu and Tsao 1997).

(3) Specifically expressed genes

One more fascinating issue is about the genes specifically expressed in plant gametes and involved in the process of the unique fertilization and the zygotic development into two major components of seed: embryo and endosperm. For this purpose, mRNAs are extracted from the isolated gametes and used to construct a cDNA library, which will be screened against various vegetative tissues (stem, leaf, root, pollen, ovary, etc.). LGC1 is one of examples, a specific cell

gene identified from lily sperm cells. Its gene product is located at the sperm plasma membrane (Xu et al 1999). Similarly, two sperm-cell specific transcripts, NtS1 and NtS2, were identified from the initial screening of 396 clones from the tobacco sperm cell cDNA library (Xu et al 2002).

The above strategy is more suitable for analyzing the gene expression in cytologically dimorphic sperm cells of Plumbago. As aforementioned about the preferential fertilization, in each mature pollen, one smaller sperm cell, Sua, is rich in plastids and targets egg cell to form zygote and develop into embryo, the other in larger size, Svn, contains more mitochondria and usually fuses the central cell for forming endosperm. Therefore, two different cDNA libraries were constructed from 12,000 Sua and 12,000 Svn separately, followed with microarray hybridization, sequence analysis, qPCR and *in situ* hybridization. As a result, a number of genes were found differentially expressed in the two dimorphic sperm cells: in Sua, the genes for transcription and translation are up-regulated, whereas in Svn, those for hormone biosynthesis are increased. This unique expression pattern may matter in the early development of embryo and endosperm (Gou et al 2009, and Russell et al 2010).

II. Isolation of **rice** gametes and zygotes and the application of isolated cells in epigenetic studies

As one of staple crop plants, the rice has great potential in helping us meet the challenge of increasing global population. Meanwhile, as the best model of monocot plants, rice has a relatively smaller genome (~440 Mb) and excellently documented record in agronomy, genetics and cell biology. Particularly, its genomic sequence is available for years to carry out molecular manipulation and phylogenetic analysis. That is why the special procedures to isolate rice gametes and zygotes were inevitably developed and optimized during the past decades to

facilitate studying mechanisms underlying rice seed formation for better rice production.

To our knowledge, the first protocol for mass isolation of rice sperm cells is reported in 1999 (Gou et al 1999 and Russell et al 2017). Briefly, the sperm cells were released from manually collected fresh pollen and enriched using discontinuous Percoll gradient centrifugation. In the same year a simple mechanical method was developed to isolate rice egg cells and zygotes, and the isolated zygote were used for *in vitro* culture to generate fertile rice plants. (Zhang et al 1999 and Zhao et al 2000). In addition, the similar dissection but with more careful manual manipulation was applied in isolating the larger central cells (Zhao et al 2000 and Uchiumi et al 2006). The isolated rice egg cells and sperm cells were also used for *in vitro* fusion for artificial zygote (Khalequzzaman and Haq 2005).

Soon after, all procedures for the isolation of rice gametes and zygotes were systematically optimized in Dr. Russel Lab and the isolated products have higher purity and sufficient quantity for a number of relevant studies, including *cis*-regulatory elements and transcriptomes of rice sperm cells and egg cells (Sharma et al 2011, Russell et al 2012 and Anderson et al 2013), large-scale transcriptomic changes in rice zygotes (Anderson et al 2017) and the landscape of small interference RNA (siRNA) in rice gametes and zygotes (Li et al 2020 and 2021).

It is found that the transcriptomes of two opposite gametes are highly divergent and their distinctive expression profiles are involved in chromatin conformation (Anderson et al, 2013). The RNAseq of isolated zygotes shows that the zygotic genome activation (ZGA) takes place soon after fertilization with unequal parental contribution where most genes are expressed primarily from the maternal genome and during ZGA a number of maternal genes (2898) are downregulated indicating the removal of maternal transcript (Anderson et al 2017).

Most recently, the isolated rice gametes and zygotes were also used in the studies on small RNA transcriptomes. It is observed that the distribution of 24nt small interfering RNA (siRNA) loci is reset in rice sperm cells and egg cells (Li et al 2020) and this pattern is returned to the canonical one in the zygotes (Li et al 2021). These observations demonstrate that chromatin modifications such as methylation and acetylation are likely taken placed in plant gametes and contributed to the next generation via the zygotes; and it is important to study the epigenetic mechanisms underlying the specific gene expression for zygotic development (Khanday and Sundaresan 2021).

In this chapter I will present our optimized protocols for isolation of rice gametes and zygotes, the representative isolated rice cells and their transient transformation with artificial constructs. At the end, some existing issues in the isolation procedure and potential applications of isolated rice gametes and zygotes in the future will be discussed.

Material and Methods

Plant material

The seeds of rice (the variety *Kitaake and IR50*) are treated with 20% bleach for 10 min and followed by 3 washes with autoclaved water, 10-15 minutes each, then germinated with sterile water in petri dishes in dark at room temperature for 5 days. The seedlings are transplanted to soil in pot (4-6 inch) and maintained in greenhouse until blooming for sample collection. The temperature of greenhouse is kept around 27°C during daytime (12 hours) and 25°C for nighttime (12 hours). The daytime light is controlled to the level of 500 μmol $m^{-2}s^{-1}$. Rice plants are irrigated with deionized water every day and fertilized twice each week by filling the headspace in pots with 300-350 ppm Nitrogen (Jack's 20-10-20).

Procedures for isolation of rice gametes and zygotes and transient transformation for cellular localization

The two major parts of rice floret are anther and ovary. The anther engulfs pollen grains each of which contains 2 sperm cells; the ovary is where the egg cell or fertilized egg cell (zygote), embedded (Fig. 1 upper panel). The procedures from the isolation to transient transformation include multiple steps as shown in the flowchart (Fig. 1, lower panel).

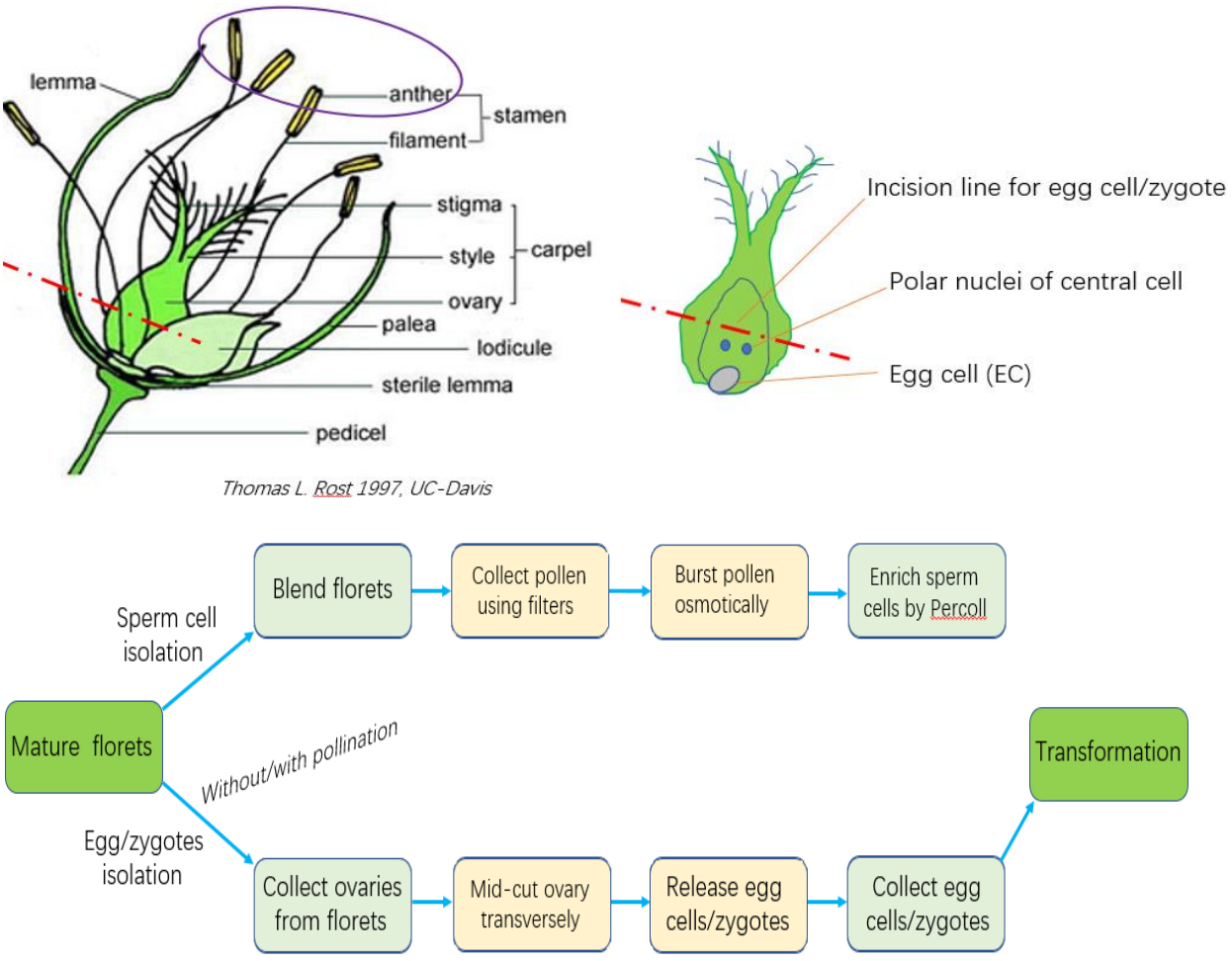

Fig. 1 Scheme of rice floret structure (upper panel) and flowchart for isolation of rice gametes and gametes (lower panel). The scheme (the upper left) is to show the anther filled with pollen grains containing sperm cells and the incision line at the mid region of ovary for transversely

cutting to release the egg cell or zygote from the lower part.

I. Isolation of sperm cells using Blender method

The sperm cell isolation is based on the previous protocol (Gou et al 1999 and Russell et al 2017), but with optimization, particularly in the preparation for pollen grains, as stated as the following.

1. Select ~ 50 rice branches with mature florets around 10 am (for variety *Kitaake*) before anthesis, cut stems at the lower part and place them into the bucket with ~ 200 ml water to keep fresh.
2. Collect all mature florets into the blender (Hamilton Beach) containing ~ 150 ml of 45% sucrose.
3. Blend tissues for 3 times to release pollen grains from anthers into the sucrose solution: 30 seconds each time with a pause of ~ 30 seconds.
4. Separate pollen containing solution into a flask from the blended mixture using 100 μm nylon mesh on a funnel.
5. To get rid of chloroplasts and other impurities, pass the filtrate through 30 μm nylon mesh to trap the pollen on the mesh.
6. Carefully transfer the mesh with pollen onto a beaker, rinse pollen in 45% sucrose from the mesh into the container using a transfer pipet, then add ~ 50 ml more same solution and swirl the beaker for ~ 1 minute.
7. Repeat Step 5 and 6 two more times until the filtered sucrose solution is clear to get intact and pure pollen grains.
8. To burst pollen for sperm isolation, quickly rinse the pollen (1 ~2 ml) to a 50 ml tube in ~ 20 ml 15% sucrose, seal the cap and rotate slowly at room temperature for ~ 25 min.
9. Filter the mixture through 30 μm mesh to separate sperm cells from sperm-depleted

pollen.

10. Layer each 9~10 ml filtrate slowly using the syringe with the tip-bent needle onto each top of 15 % Percoll solution in two isolation tubes.
11. Centrifuge at 4^{o}C, 4000 x g for 45 min with slower acceleration and deceleration (Thermo Scientific Heraeus Multifuge X3R Centrifuge, with acceleration set at 8 and deceleration at 9, to prevent the interface of Percoll gradient from being disturbed); the sperm rich portion at the interface of 40/15% Percoll will be visible after centrifuging.
12. Pipet out the supernatant until 0.5~1 cm above the interface, and collect sperm rich layer using the syringe with the tip-bent needle up to ~ 0.5 ml from each tube; dilute in 4 volumes of 15% sucrose in a new tube, and filter in 10 μm mesh to prevent the potential agglutination of sperm cells (aggregated sperms may form a new layer on the surface of 15% Percoll mixed with impurity, and thus reduce the yield of sperm cells).
13. Add the filtrate to the top of 15% Percoll in a new isolation tube, and centrifuge at 4^{o}C, 3000 x g for 25 min.
14. For higher purity (but lower sperm cell yield), repeat Step 12 and 13 once more.
15. Collect 0.2~0.5 ml from the interface, add 3 ml of 15% sucrose, and centrifuge at 4^{o}C, 1000 x g for 10 min.
16. Pipet out the most supernatant but leave the bottom 0.1~ 0.2 ml, add ~1 ml of 15% sucrose, and centrifuge again (4^{o}C, 1000 x g, 10 min).
17. Remove the supernatant with caution and leave the bottom 30~50 μl in the tube.
18. Use 1 μl for microscopy; save the rest in a new Eppendorf tube at -80^{o}C; for RNA isolation, use DEPC treated Eppendorf tube and freeze it in liquid Nitrogen, then store at -80^{o}C until use.

II. Isolation and collection of rice egg cells and zygotes

The isolation and collection for rice egg cells and zygotes follows the previous description (Anderson et al 2013 and 2017, and Li et al 2019) but with minor modifications.

1. The mature and still closed florets (in which anther occupies most of the floret prior to anthesis) for egg cell isolation or pollinated open florets for zygote isolation are collected into 0.4 M mannitol in a 10 mL petri dish in the morning (8-10 am for variety IR-50; 9-11 am for *Kitaake* under our growth conditions).
2. The 6-10 florets are gently carefully dissected on a microscope slide (treated with 70 Ethanol) one by one, using one pair of fine tweezers in right hand and the fingernails of thumb and index in left hand, to separate the intact carpel from other non-carpel structures including the palea, lemma, stamen, lodicule and pedicel (Fig. 1).
3. Collect the ovaries with the needle (B-D Sub-Q, 26G 5/8, #305115) and rinse them twice on the slide with the same sugar solution 0.4 M mannitol to clean pollen grains off.
4. Transversely cut the ovaries along the incision line (Fig. 1) under a dissecting stereomicroscope using a thin and sharp razor blade (Merkur double edge razor blades), remove the upper portion with style and stigma.
5. Quickly rinse the basal portion of ovaries twice on the slide with a drop of same sugar solution to ensure no pollen grain to be associated and transfer them into a fresh mannitol droplet (10-15µl) on the slide.
6. Mount the slide under an inverted phase contrast microscope (10× objective lens), use an acupuncture needle or insect pin to press the basal gently to help release the egg cell from the ovary.
7. Collect the cells using a special micropipette. The micropipette is made by pulling a

microcapillary (World Precision Instruments, Inc., Sarasota, Florida USA TW120F-4) with the instrument PUL-1 (WPI, Inc.)

8. The captured cells can be immediately used for fluorescent microscopy or transformation for cellular localization; if for RNA extraction later, they will be frozen in liquid nitrogen then stored at -80°C freezer.

III. PCR for identification of isolated gametes

The procedure is as previously described (Li et al 2019). Briefly, total RNA is efficiently extracted from isolated rice gametes (low input material) using the Ambion RNaqueous Micro Total RNA kit, in which, the small RNAs (shorter than 200 nt) can be recovered and used for miRNA and siRNA profiling.

For cDNA synthesis from the RNA with low concentration, NuGEN Ovation RNA-seq System V2, or iSript Select cDNA Synthesis Kit (BIO-RAD 1708896), is adapted to produce ~1 µg cDNA from RNA as low as 1 ng. Then we use Qiagen MinElute Reaction Cleanup Kit to purify cDNA products and the Nanodrop spectrophotometer or Qubit fluorometric instrument (Thermo Fisher Scientific) for quantification.

To identify the isolated rice cells, the specific gamete marker genes (MGH for sperm cell and ECA-like 1 or 2) and other vegetative cell markers are used to design primers, as listed in supplementary Table 1, for PCR.

IV. PCR cloning for cellular localization in rice cells

The mRNA from young rice flowers (*Kitaake*) are purified using Oligotex mRNA Mini Kit (Qiagen 70022) and cDNAs are synthesized with RevertAid First Strand cDNA Synthesis Kit (Thermo Scientific Inc, K1621).

For the products of coding sequence (CDS) from the PCR reactions of rice KRP5 (LOC_Os03g04490.1), KRP4 (LOC_Os10g33310.1) and the F-box gene, Fb3 (LOC_Os08g09750), we used 3 pairs of specific primers, HX65/66, HX63/64 and HX 59/60, respectively (supplementary Table 1) with Q5 High Fidelity DNA Polymerase (NEB, M0491) or Phusion High Fidelity DNA Polymerase (Thermo Scientific Inc F530S).

Then, Fb3 CDS product is ligated to the vector pE3150 (supplementary Fig.2) (Lee et al 2008, Lee and Gelvin 2014) at XhoI and HindIII to fuse with Enhanced Yellow Fluorescent Protein (EYFP) at C' terminus; the similar ligation for the product of KRP5 is at EcoRI and SalI, and that of KRP4 at EcoRI and SalI.

In addition, mCherry with nuclear localization signal peptides in the vector pE3275 (generally offered by Dr. Marc Libault) is used as the positive control for the nuclear localization (Supplementary Fig. 3).

V. Isolation of rice leaf protoplasts

Since the isolation of rice gametes and zygotes demands greater effort and consume more time than that for rice leaf protoplasts, the latter is prepared and transfected according to the procedure described by Wang et al (2013). This pre-trial is to test if the construct of the rice gene fused with EYFP work or not prior to the formal transfection of isolated rice gametes and zygotes.

VI. Transfection of isolated rice cells with EYFP fused rice KRP and F-box genes for cellular localization

The specific protocol and recipe for transfection of isolated rice egg cell and zygotes are developed and optimized according to the previous reports (Koiso et al 2017 and Toda et al 2019). The general procedure is summarized as the following, which requires both patience and

caution.

1. Isolate and store 3-6 cells in ~8 µl MMG (4 mM Mes-KOH, pH5.7, 15mM MgCl2 in 0.4M mannitol) on a microslide within a moisture chamber.
2. Add 2 µl plasmid DNA: pE3275 and EYFP fused KRP or Fb3 construct.
3. Add 10 µl of 30% PEG with 100 mM CaCl2 in 0.4M mannitol.
4. Immediately and gently mix twice with a micro pipet.
5. Incubate at room temperature for ~10 min.
6. Carefully wash cells for 3 times by very slow capillary sucking ~ 10 µl of the droplet solution, then add same volume fresh MMG solution back.
7. Carefully wash cells 3 times in fresh modified W5 solution (W5: 154 mM NaCl, 125 mM $CaCl_2$, 5 mM KCl, 2 mM MES; plus 500 mM Glucose), as step 6.
8. Culture the cells with ~10 µl W5 solution plus Ampicillin (100µg/ml) at 25^{o}C in dark for overnight in the moisture chamber.
9. Surround the droplet on the slide with cream (Petrolatum, Fisher Scientific, P66-1) to make a square chamber covered with a coverslip for fluorescent microscopy.

VI. Fluorescent microscopy and image processing

Aniline blue fluorescence is used to monitor the pollen germination on stigma and growth along the style. For this purpose, the stigma and style assocaitd with the upper portion of ovary are stained in Aniline blue solution (0.005% in 0.15M K_2HPO_4 at pH8.2) for 10 min at room temperature, then viewed under the fluorescent microscope Axiovert 10 (Zeiss).

To examine the viability and observe the nuclear, isolated gametes and zygotes or pollen grains are stained with Fluorescine Diacetate (FDA, excited at 48-510 nm and emited at 535-585 nm) and 4′,6-Diamidino-2-phenylindole (DAPI, excited at 358 nm and emited at 461 nm),

separately, as follows:

1. Make a square chamber on a clean slide with the Petrolatum cream and transfer isolated cells in 5-10 µl 0.3 M mannitol into it.

2. Add the same volume of 2x FDA or DAPI staining solution which is diluted in 1:1000 from the stock (1µg/µl) in 0.3M mannitol.

3. Keep the slide in a moist chamber (a petri-dish with a wet paper tower) in dark for 3-5 minutes for FDA, or ~ 30 minutes for DAPI.

4. Put a coverslip over the cream chamber for microscopy (Axiovert 10).

To observe transfected rice cells, Nikon Eclipse Ni matched with the light source of X-Cite 120LED is used with appropriate filters for EYFP (excitation at 514 nm and emission at 527 nm) and for mCherry (excitation at 587 nm, emission at 610 nm).

Results

I. Isolated rice sperm cells and identification with the marker gene

To isolate sperm cells from rice, the first step is pollen collection. As described previously (Gou et al 1999 and Russell et al 2017), this is done from manually picked mature anthers. It has

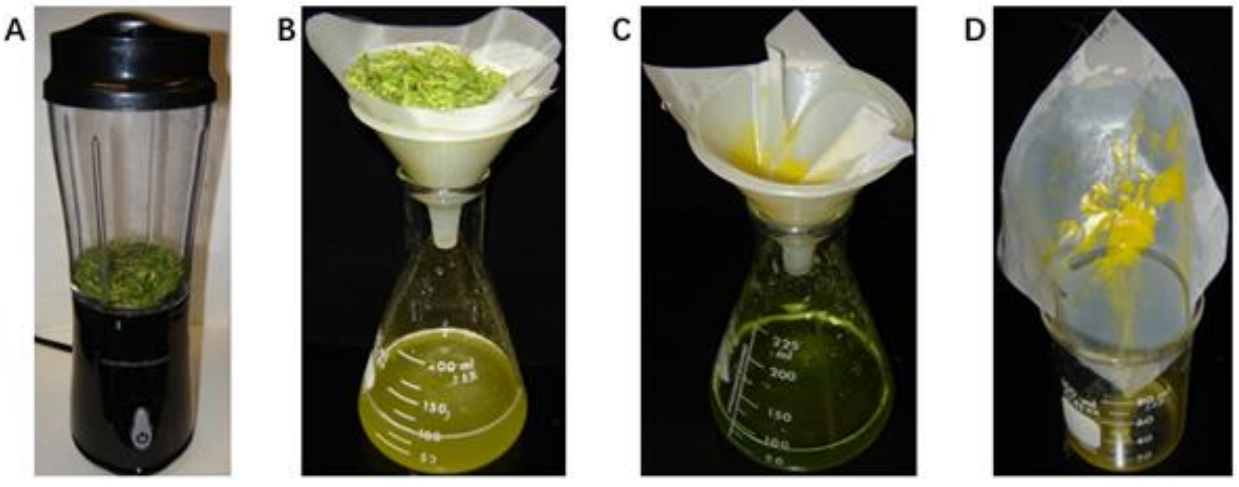

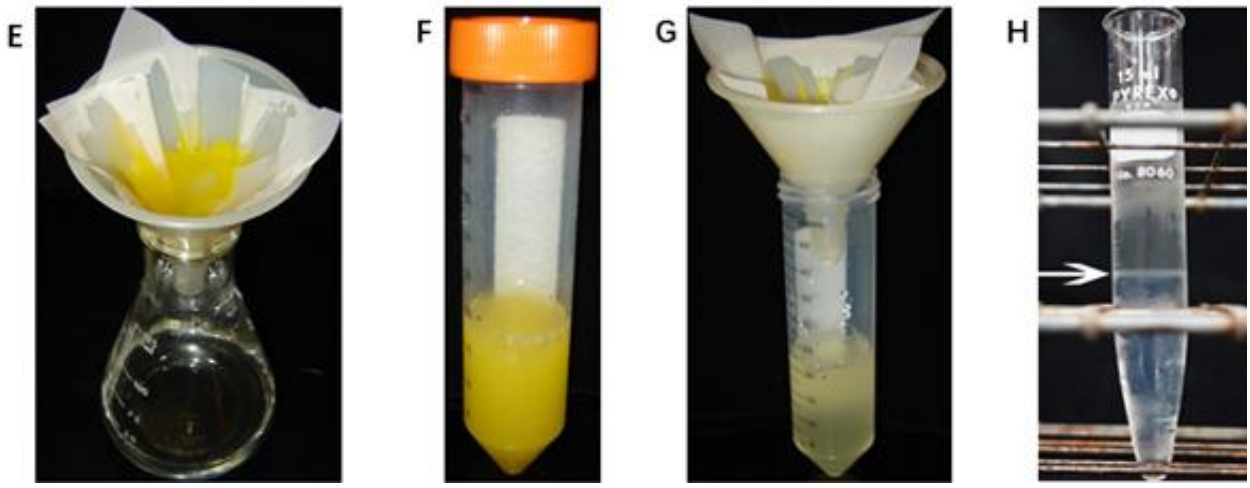

Fig. 2: Key steps for rice sperm cell isolation using blender method. A. rice florets collected into the blender containing 45% sucrose solution; B. pollen containing solution in flask separated from the blended mixture through 100 μm mesh; C. pass the filtrate of step B through 30 μm mesh; D. pollen with the mesh from step C transferred to a clean beaker for washing in 45% sucrose; E. pollen washed twice; F. the pure pollen incubated with 15% sucrose to release sperm cells; G sperm containing filtrate in 50 ml tube; H. sperm-cell enriched layer indicated by arrow at the interface of 40/15% Percoll (Russell et al 2017 and Li et al 2019).

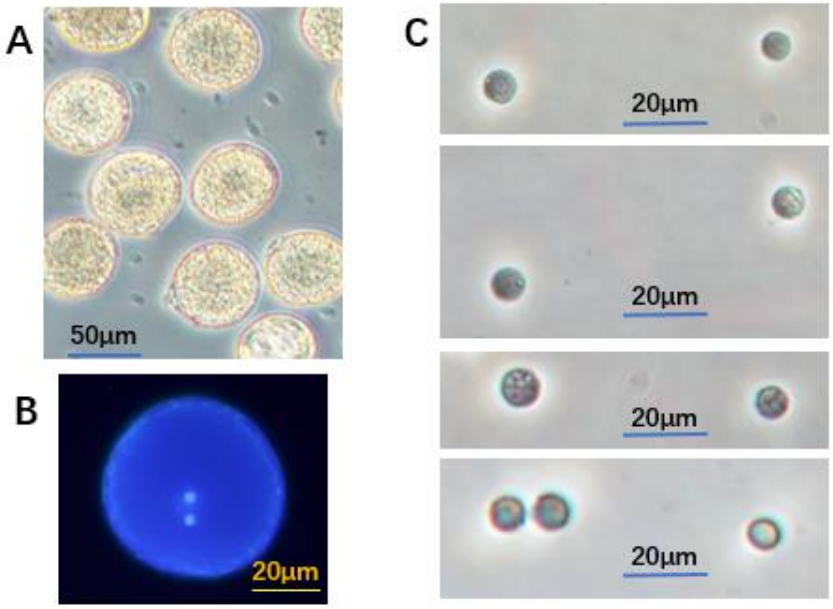

Fig. 3 Collected rice pollen grains and isolated sperm cells. A. the pollen grains after rinsing with 45% sucrose; B. the pollen grain stained with DAPI showing the two sperm nuclei; C. sperm cells observed under microscope from different isolations.

worked well for small amount preparation and the isolation product was used for the studies of cis-regulatory elements and transcriptomics of rice gametes (Sharma et al 2011, Russell et al 2012 and Anderson et al 2013 and 2017). But this procedure demands more in both time and labor. Therefore, we employed the blender method to replace it. In this part, the mature florets were disrupted in minutes and pollen grains were collected and purified through repeated fiteration in 1-2 hours (Fig. 2).

One of most concerned issues here is the potential contamination in pollen by the broken sporophytic tissue debris, especially the chloroplasts. However, it is significantly reduced after two to three times of filteration, as demonstrated in Fig. 2 E. Then, sperm cells are enriched by 2 or 3 times of discontinuous Percoll density gradient centrifuge. From the mature florets of 50 flowering panicles, about 1 ml of pure fresh pollen can be harvested, from which about 2000 sperm cells will be collected. As shown in Fig. 3 C, this isolation rate has an ideal repeatability; the isolated rice sperm cells is 5 ~ 7 μm in diameter; its nuclear is heterochrmatic surounded by a small volume of cytoplasm.

More importantly, the sperm cells enriched from the new procedure also have much better purity. This is confirmed by the semi-quantitative RT-PCR using specific primers for the marker genes (Fig. 4 and supplementary Table 1). For addressing this issue, we used OsMGH3 (Anderson et al 2013 and Okada et al 2005) as the sperm marker gene, OsLAT52 as the pollen vegetative cell marker gene, OsMADS3, marker gene for stamen and bracts (lemma and palea); OsMADS7 as the marker gene for stamen, OsRBCS as the marker gene for chloroplasts in the green tissues

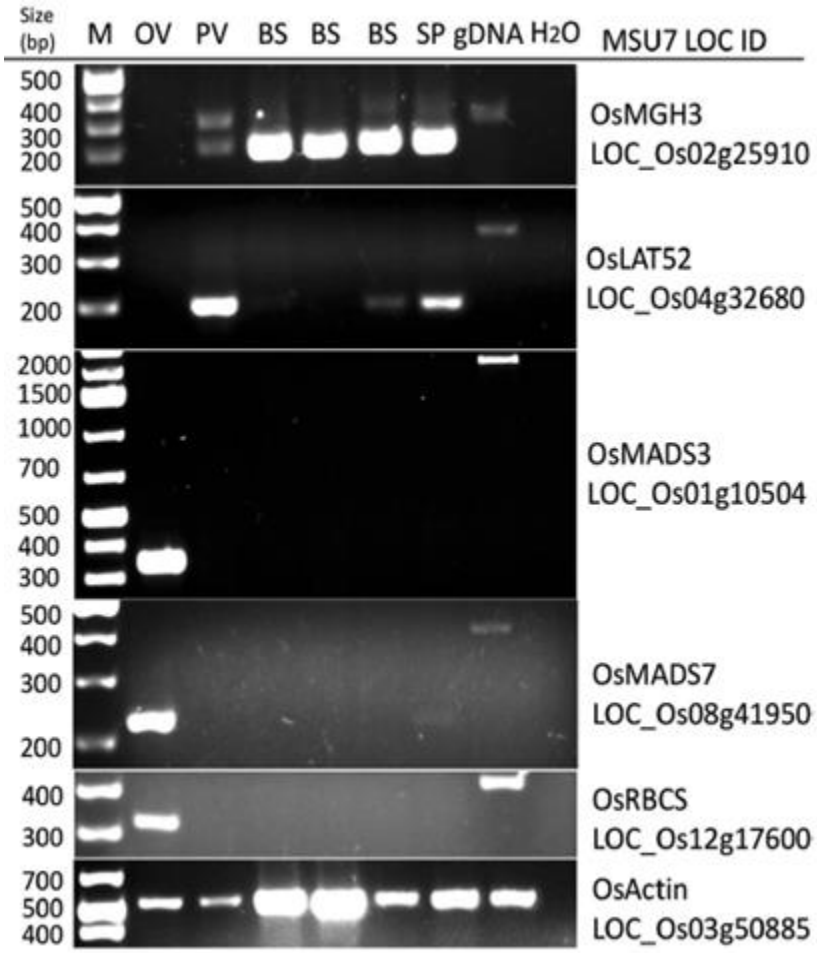

Fig. 4 RT-PCR for sperm cell identification (Li et al 2019). M, DNA ladder; OV, ovary; PV, pollen vegetative cells; BS, sperm cells collected by blender method; SP, sperm cells collected using non-blend method (Russell et al. 2017); gDNA, Genomic DNA; OsMGH3, sperm cell marker gene; OsLAT52, pollen vegetative cell marker gene; OsMADS3, marker gene for stamen and bracts (lemma and palea); OsMADS7, marker gene for stamen and tapetum; OsRBCS, marker gene for chloroplasts in green tissue (Rubisco small unit); OsActin, housekeeping gene in all type of cells.

(Rubisco small unit) and OsActin as the housekeeping gene in all type of cells (Li et al2019). As demonstrated by the DNA gel image, all three samples of sperm cells isolated using the blender method (BS) give the strong signal of sperm cell marker gene, OsMGH3, but very weak to the

pollen vegetative cell marker gene, OsLAT52, and undetectable for other tissue marker genes, suggesting that sperm samples collected by the new method is almost free of the contamination from the floral organ and sporophytic tissue (Li et al 2019).

II. Isolated rice egg cells and the identification with the marker gene

The procedure for isolating rice egg cells looks relatively simple (Anderson et al 2013 and 2017, and Li et al 2019), yet to be productive, it requires highly motivated patience and skill.

The images of two representative isolated rice egg cells are shown as in Fig. 5 A. They appear transparent with numerous inner vacuoles. This morphological feature is remarkably different from that of their partner cells, synergids (supplementary Fig.1), which have slightly smaller size, opaque appearance and occasional presence while the egg cells are collected, but it is easy to distinguish it from the egg cells. In addition, in contrast to the tiny sperm cell, the egg cell has a significantly larger size, around 50 μm in diameter, comparable to its pollen grain; and also, unlike the sperm cell, the egg cell nuclear is not condensed, as demonstrated in DAPI staining. Besides, from FDA staining (in green under the fluorescent microscope), we learned that the isolated egg cell keeps viable for hours after isolation, and this viability may last for overnight

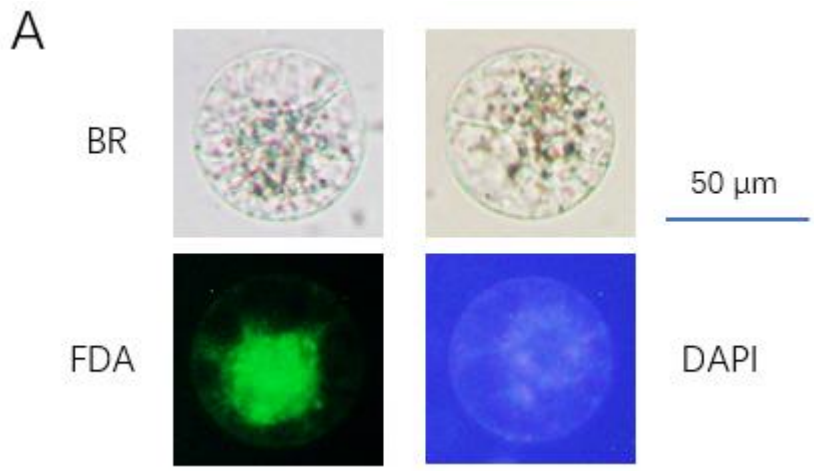

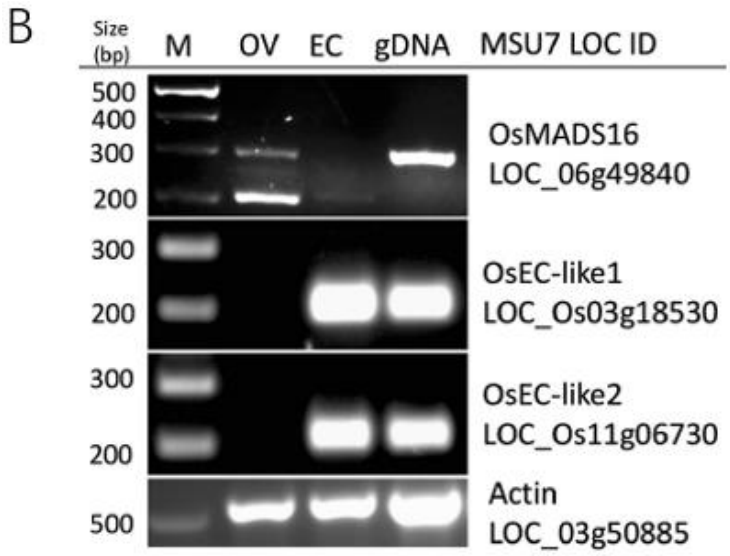

Fig. 5 Isolated rice egg cells and the identification. A. Isolated rice egg cells labelled with FDA (green) and DAPI (bright blue). B. RT-PCR to identify isolated egg cells (Li et al 2019). M, DNA ladder; OV, ovary; gDNA, genomic DNA; OsMADS16, ovary marker gene; OsEC-like1/2, marker gene for the rice egg cell; Actin, housekeeping gene in all type of cells.

(See the other part of this chapter, transient transfection of rice egg cells and zygotes).

To identify the isolated egg cells and particularly ensure they are not or less contaminated from other vegetative tissues, we carried out the parallel RT-PCR using OsEC-like1 and OsEC-like 2 as the marker genes (Ohnishi et al 2011) for the rice egg cell, OsMADS16 as the ovary marker gene, and Actin as the housekeeping gene for all types of cells (Li et al 2019). As shown in the DNA gel image (Fig. 4B), the egg cell (EC) sample gives very strong signal to the probes of EC marker genes, OsEC-like 1 and 2, but very weak one for that of ovary marker gene, OsMADS16, demonstrating that contamination in the isolated egg cell sample from the sporophytic ovary is minimum. This is also confirmed by the study of siRNA in rice gametes (Li et al 2020).

Regarding isolation rate for rice egg cells, it is influenced by multiple factors including seasonal change, daily weather status and some unknown elements. Nevertheless, no single factor is

dominant. It seems that the combination of those factors determines the physical status of rice plants, particularly, the turgor pressure within the ovary. It is likely that this sort of internal force helps the egg cell or zygote flow out from the lower portion of ovary, which may explain why some egg cells or zygotes automatically present at the interface in a couple of minutes after cutting along the incision line even without pressing the ovary using the fine needle.

The best season for the isolation is spring, and the better day seems one with higher humidity (>50%) and something else. Under these conditions, for two skillful manipulators, the average isolation rate can reach daily 10 cells. With the necessary funding, about 3000 of isolated cells can be accumulated annually. Although still limited, it is promising to use this amount of material for some preliminary but valuable data in studies of epigenetics and proteomics including finding the double-fertilization-recognition related surface glycoproteins from crop plants such as rice and maize.

III. Isolated rice zygotes and identification

To isolate rice zygotes, we adopted the same protocol for isolating rice egg cells, but did polination prior to the floret collection at the desired time for either self-polinated zygotes or the cross hybrid ones.

For self polination, the selected mature florets are carefully slightly open with the aid of tweezers. In a couple of minutes, we start timing and slightly flicking those open florets with finger to help pollen grains fall onto the stigma. For cross pollination, we follow the procedure described by Dr. Susan McCouch, Department of Plant Breeding and Genetics, of Cornell University (*http://ricelab.plbr.cornell.edu/cross_pollinating_rice*), including anther removal from the recipient florets (emasculation) and 3-5 times of quick addition of the pollen freshly collected from the donor plants.

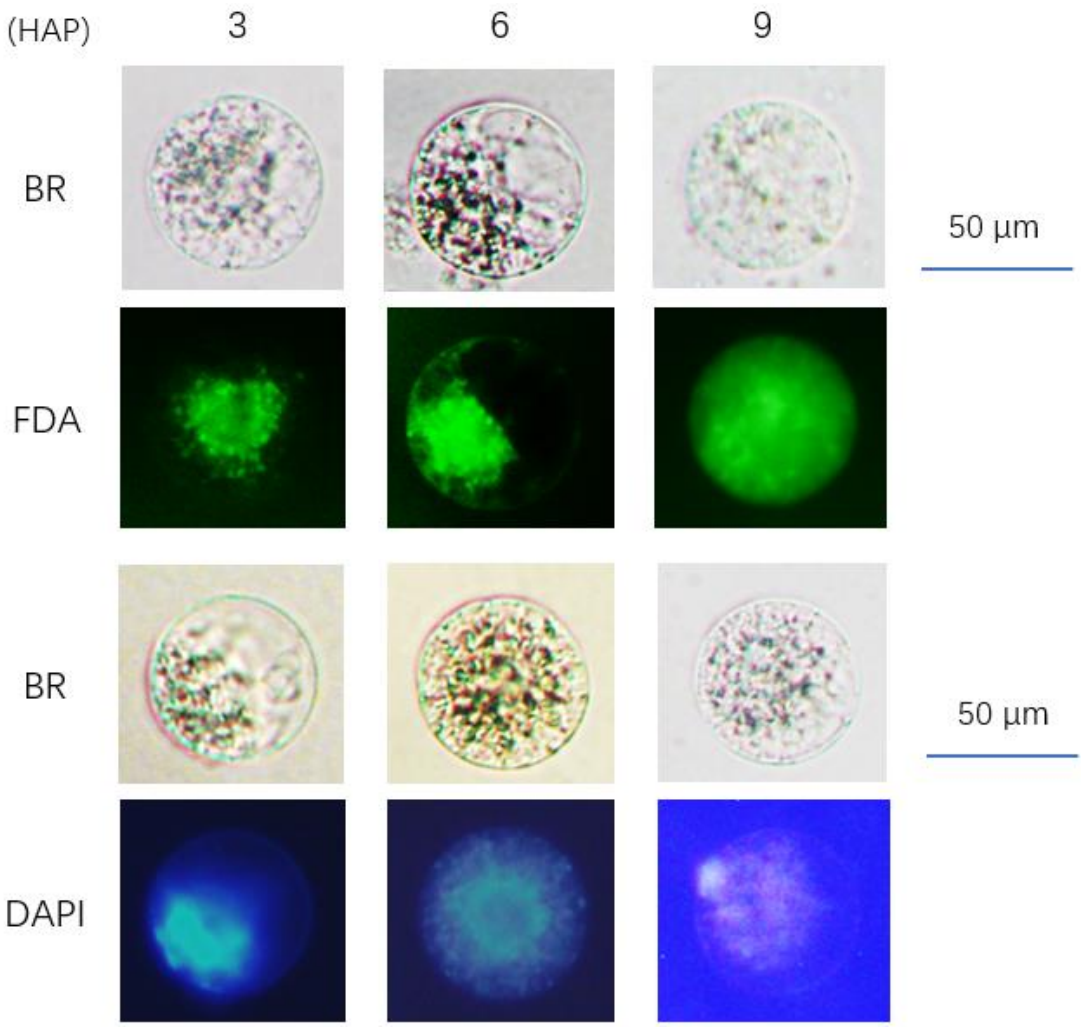

Fig. 6 Isolated rice zygotes stained with FDA and DAPI. HRP, hours after pollination showing zygotes isolated at different developmental stages; BR, differential interference contrast images of isolated zygotes; FDA, the fluorescent signal (green) indicating the viability of isolated zygotes stained with FDA; DAPI, the fluorescent signal (bright blue) from nuclei of isolated zygotes stained with DAPI.

The representative images of isolated rice zygotes from 3 different stages (3, 6 and 9 HAP) are shown as in Fig. 6. They have the similar morphology to the isolated egg cells except slightly smaller size. As demonstrated in FDA staining, they are viable for hours after isolation if

cultured in the appropriate solution or culture medium. Like the isolated egg cell the isolated zygote has a much larger nuclear with active euchromatin.

One of common concerns of the isolated zygotes is, if any, how many unfertilized egg cells could be mixed with the fertilized zygotes in the isolation. Since the marker gene method does not help address this issue, we adopted two other different measures. One is the microscopy with Aniline Blue fluorescence to isolate the self zygotes at 2 HAP (Fig. 7). Once finding the pollen tube(s) growing along the stigma which indicates the higher chance of fertilization, the corresponding lower portion ovary will be taken for zygote isolation. The other is seed setting assay (Table 1). Under the condition we set in greehouse for rice growth, the seed-set rate is ca. 97% for WT, which told us that, if any, the rate of unfertilized egg cells is lower than 3% in our isolated zygote sample; in contrast, the seed set rate is only 1% in the minus control of emasqulated florets without pollination. In conclusion, the quality of our isolated self zygotes is reliable for further studies like siRNA analysis, the transfection for cellular localization and Bimolecular Fluorescent Complementation (BiFC).

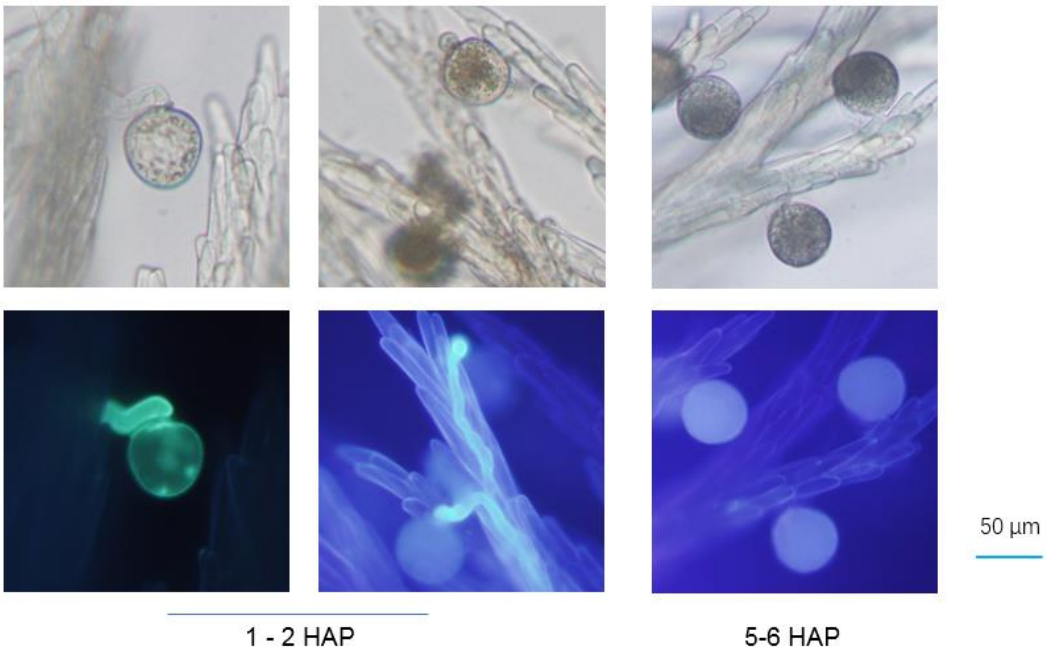

Fig. 7 Rice pollen grain and pollen tube located on stigma and grown along the style. The upper portion of carpel is stained with Aniline Blue and observed under fluorescent microscope. HAP: hour after pollination

Table 1. Rice (*Kitaake*) Seed Setting Assay

	Emasqulated without pollination				*Self-Pollinated*		
Panicle #	Emas. floret #	Seed #	Seedset (%)		Pol-floret #	Seed #	Seedset (%)
1	11	1			9	8	
2	20				7	7	
3	21	1			9	9	
4	24				8	8	
5	22				10	9	
6	13				12	12	
7	14				11	10	
8	12				8	8	
9					9	9	
10					10	10	
11					8	8	
Sub total	137	2	*1*		101	98	*97*

IV. Transient transfection of rice leaf protoplasts with EYFP-fused three putative rice cell cycle genes

According to the rice genomic database data, three rice genes, KRP5, KRP4 and Fb3 are putative cell cycle genes. Therefore, we are interested in testing their subcellular localization in isolated rice gametes and zygotes. To ensure that the fluorescent-molecule fused constructs and the transfection procedure work prior to using the valuable isolated rice cells, we took rice leaf protoplasts as the pretrial material since they are widely used before in analysis of protein-protein interactions (PPI) and cellular localization (Wang et al 2013, Lv Q et al 2014 and Shi et al 2019).

As shown in Fig. 8 A, B, the typical isolated rice leaf protoplast presents as transparent sphere in size of 30 ~ 50 μm. Due to the pressure of big central vacuoles, their nuclei are pushed to plasma

membrane region (the edge of 2D image) and accurately localized by transfection with $mCherry_{NSL}$ (red signal). In the minus control (Fig. 8 A, the top image #3 from left), EYFP is expressed in both nuclear and protoplasm, but both EYFP-KRP5 and EYFP-KRP4 are only expressed in nuclei (Fig. 8 A) and this rate is up to over 90% (Fig. 8 C), indicating KRP5 and KRP4 are nuclear protein, which is consistent with their putative molecular function in cell cycle control. We also observed that EYFP-Fb3 is expressed in either nuclei or cytoplasm with about 50% of chance for each (Fig. 8 B, C), and each truncated Fb3 fused with EYFP has higher chance of expression in cytoplasm, indicating both F-box domain and LRR region contribute to the determination of Fb3 localization in rice protoplasts.

In a word, the constructs of EYFP-KRP5, EYFP-KRP4 and EYFP-Fb3 as well as the procedure for transient trasfection work well for the cellular localization in rice protoplasts, and hopefuuly they will work too in isolated rice egg cells and and zygotes.

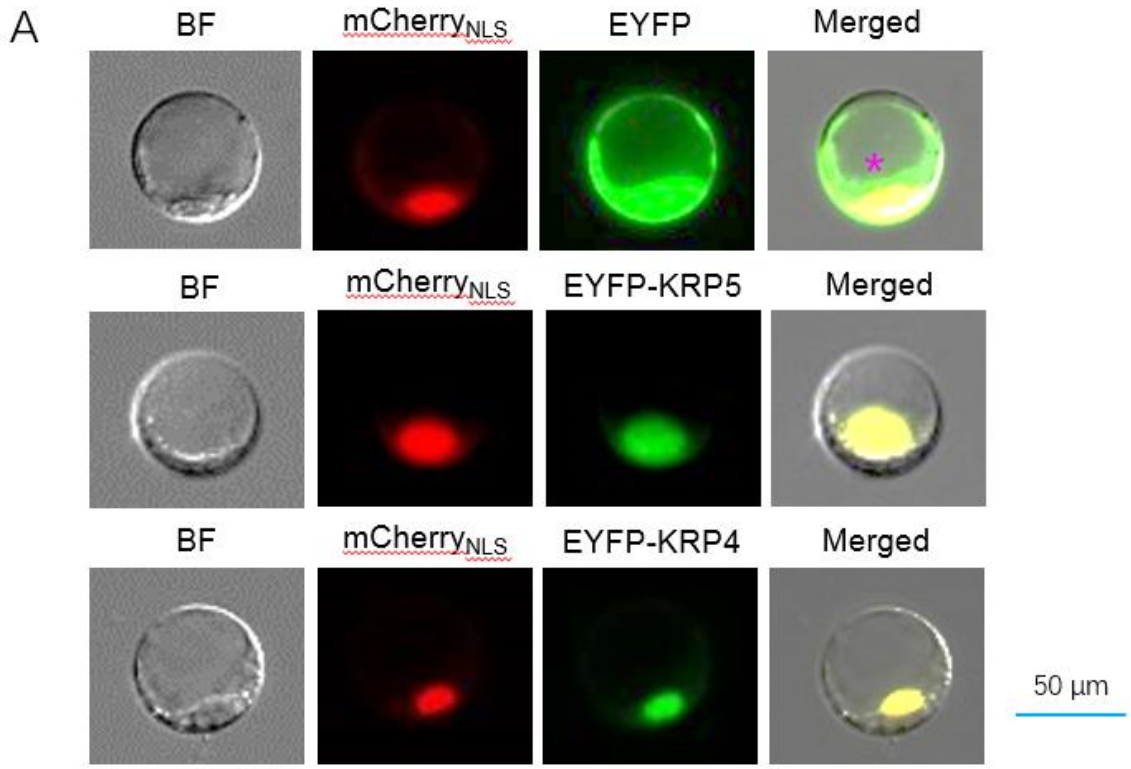

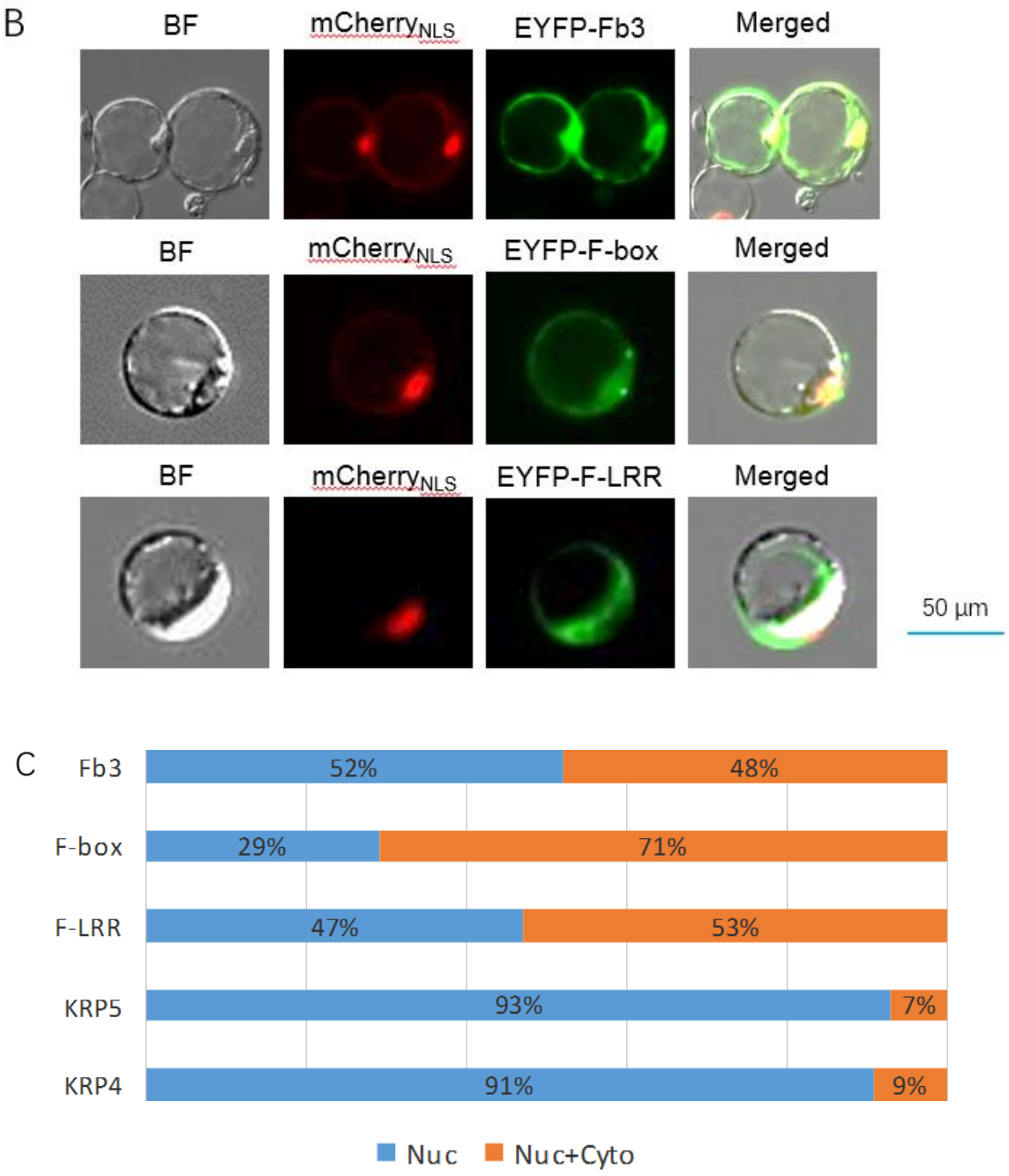

Fig. 8 Transfection of rice leaf protoplasts with EYFP-fused 3 putative rice cell cycle genes for cellular localization driven by cauliflower mosaic virus promoter (CaMV 35S). A. Transient transfection of the protoplasts with KRP5 and KRP4 gene fused with EYFP at N-terminus (EYFP-KRP5 and EYFP-KRP4); EYFP as control. The mCherry$_{NLS}$ represents mCherry linked

*with Nuclear Localization Sequence (NLS, 12 amino acid residues) and is used as the nuclear marker. BR represents the images of bright field. Merged refers the overlaid image from the other three in each transfection. * indicates the central vacuole in in the protoplasts. B. Transient transfection of the protoplasts with EYFP fused Fb3, F-box (300bp from 3' terminus of Fb3 gene with the F-box domain) and F-LRR (1.4 kb of Fb3 from 5' terminus with Leucine Rich Region) at N-terminus. C. Localization frequency of EYFP fused rice genes (KRP5, KRP4 and Fb3) and Fb3 fragments (F-box and F-LRR). Blue bars represent the percentage of protoplasts with Nuclear (Nuc) localization. Red bars indicate the percentage of protoplasts with nucleus-cytoplasm (Nuc+Cyto) localization.*

V. Transient transfection of isolated rice egg cells and zygotes with EYFP-fused three putative rice cell cycle genes (KRP5, KRP4 and Fb3)

Although the above constructs and procedure work well in transfecting rice protoplasts, it is difficult to apply them to isolated rice egg cells and zygotes. They are not only limited in number,

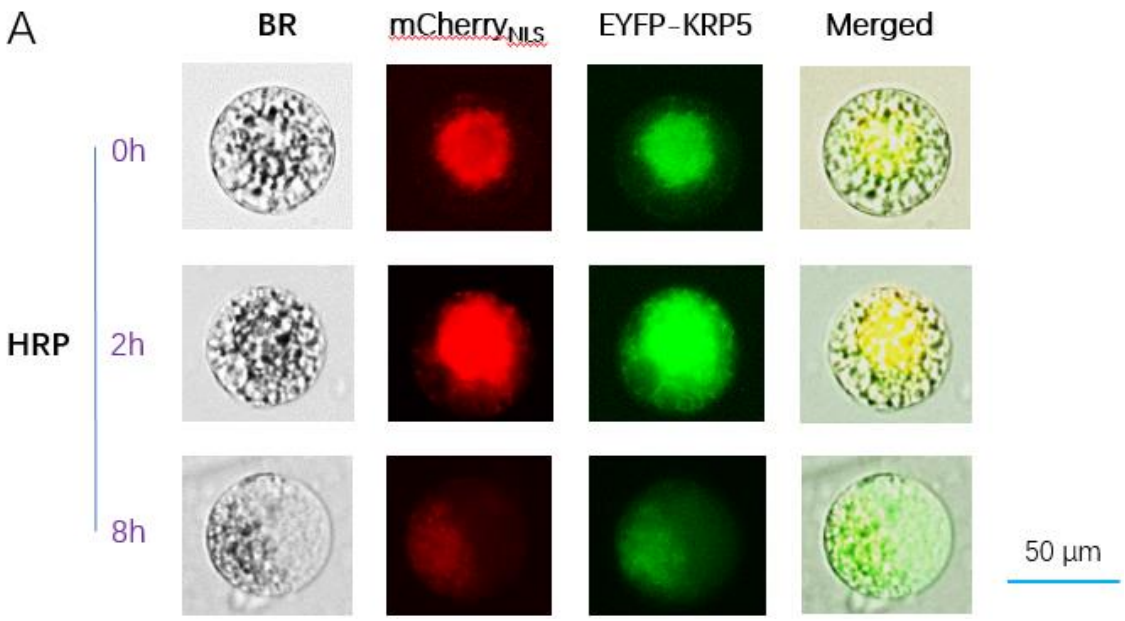

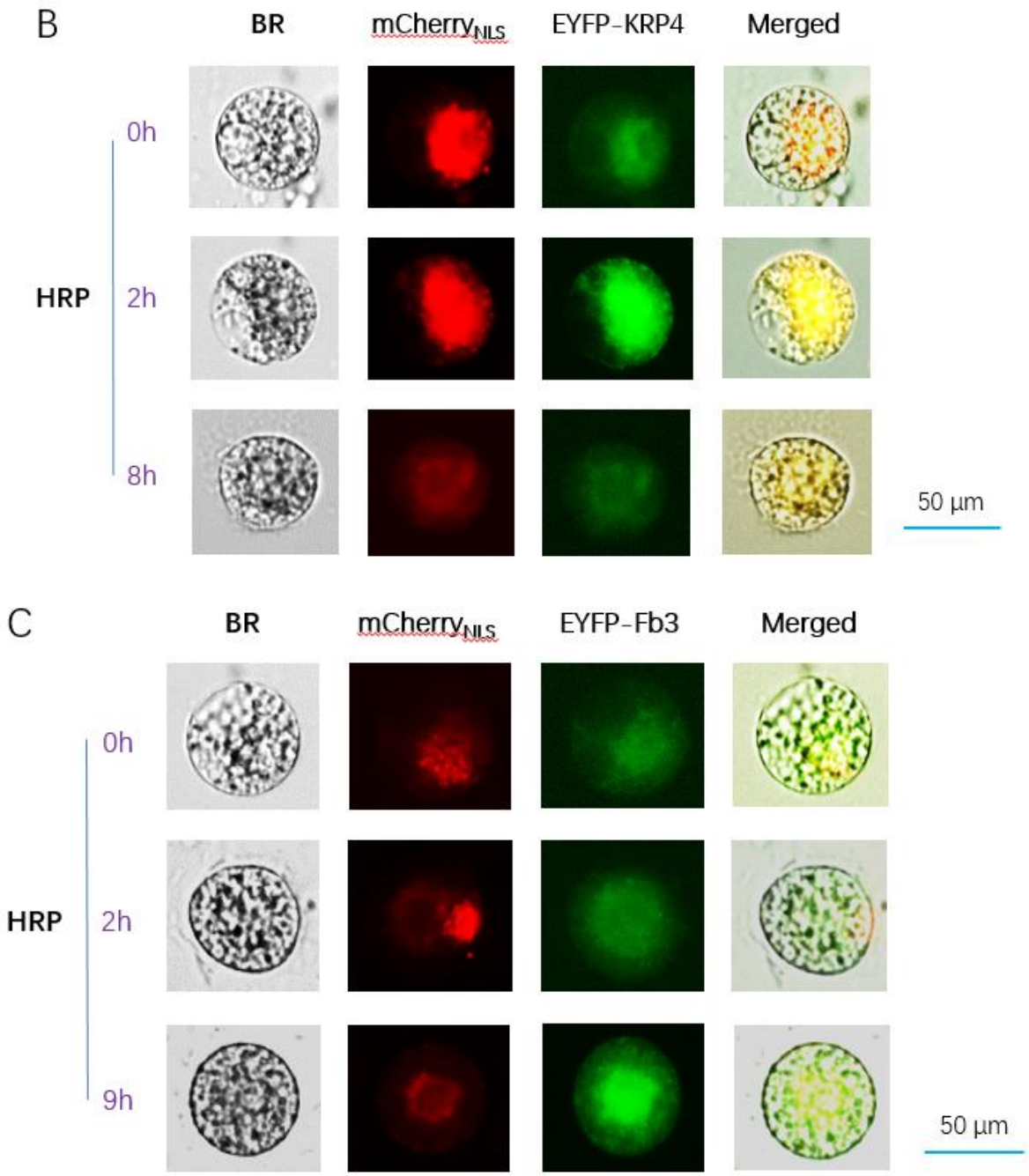

Fig. 9 Transfection of isolated rice egg cells and zygotes for cellular localization with EYFP-fused 3 putative rice cell cycle genes. A. Transient transfection of rice egg cells and zygotes with EYFP-KRP5. B. The transfection of rice egg cells and zygotes with EYFP-KRP4. C. The transfection of rice egg cell and zygote with EYFP-Fb3. HRP, hour after pollination. BR, bright field for the gray images. mCherry$_{NLS}$, mCherry linked with Nuclear Localization Sequence

(NLS)), served as the nuclear marker.

and also very vulnerable to multiple transferring and washing during the process of transfection. Therefore, the special caution was taken to carry out the procedure as stated in the part of Methods.

As a result, the transfection worked through with isolated rice egg cells and zygotes. As shown in Fig. 9 A and B, $mCherry_{NLS}$ expressed in all nuclei (red signal) of the egg cells (0 HAP) and zygotes at 2 HAP and 9 HAP; the co-transformed EYFP-KRP5 and EYFP-KRP4 also expressed in the similar pattern (green signal). The merged images demonstrate the nuclear localization of KRP5 and KRP4 in rice egg cells and zygotes, consistent with our observation in the transfected rice protoplasts. However, as shown in Fig. 9 C, the expression patterns of $mCherry_{NLS}$ (red signal) and EYFP-Fb3 (green signal) in the transfected cells are not overlapped well, indicating the localization of EYFP-Fb3 mainly in nuclei and partially in cytoplasm.

It is also interesting to compare the fluorescent intensity of the transfected cells at different developmental stages. In Fig. 9 A and B, both EYFP-KRP5 and EYFP-KRP4 give stronger signal in the egg cells and zygotes at 2 HAP (both in G1 phase of cell cycle) but weaker signal in zygotes of 8 HAP (S-G2 phase of cell cycle). In contrast to Fig. 9 C, the expression level of EYFP-Fb3 in the egg cell and zygote of 2 HAP (the G1 phase) is obviously lower than that of zygote at 9 HAP (the G2 phase). This feature needs more observation to confirm. If the case is true, it indicates the putative function of these proteins in cell cycle and demonstrates this transient transfection system could be useful in testing the expression level of other specific genes in plant gametes and zygotes.

The same procedure for cellular localization also has been applied in Bimolecular Fluorescent Complementation (BiFC) in isolated rice egg cells and gametes at different developmental stages

and it is successful (see Chapter 2 and 3). Put these two parts together, we totally used 546 isolated egg cells and zygotes, among which the first 128 was consumed in the pre-test and the rest 418 for the formal transfection. From the latter, 148 transfected cells survived through the overnight incubation for protein expression and 86 of these cells were observed with expected fluorescent signal. Thus, the surviving rate after transfection is 35.4% and successful co-transfection rate is 20.5%, an efficiency not lower than what we expected. To our knowledge, this is the first trial using hundreds of isolated rice egg cells and zygotes for the purpose of cellular localization as well as BiFC for protein to protein interaction (next 2 chapters).

Discussion

Based on the above results, we will briefly discuss four features of those isolated rice gametes and zygotes and the prospects of their application in the study of plant molecular biology.

1. Stage-Specific

As we know, the sperm cell and the egg cell are specific cell types of different sex prepared for fertilization, and the zygote is the immediate product of the fertilization. Both sperm and egg cells are haploid (with 50% of genomic DNA content), but different in their chromosome status and cytoplasm volume. The former has the condensed nuclei simply wrapped with much reduced cytoplasm (3 ~ 7 μm) and the latter's nuclei is de-condensed and surrounded with a large amount of cytoplasm (~ 50 μm). Comparing the egg cell with the zygote, they share almost same size and the loose chromatin status, but the former is haploid and the latter diploid (with 100% of gDNA content). However, all these 3 types of cells are naked and transparent without plant unique cell wall and green chloroplast, i.e. so-called protoplasts. To make the leaf protoplasts, specific enzymes must be used to remove and cell wall; in contrast, the enzymes are unnecessary for isolated rice gametes and zygotes. *In vivo*, they are naturally protoplasts; even after isolation

or in the *in vitro* transfection, they are still semi-natural protoplasts.

Just due to this Stage-Specific feature, they are suitable for fluorescent microscopy to detect the labeled gene expression within these cells without interfering of autofluorescence from cell wall and chloroplasts. Based on this feature and our practice, the isolated rice egg cell and gamete can be used in the routine lab work for cellular localization and BiFC to monitor individual gene expressions and protein-protein interactions with development.

2. Pure

Our samples of isolated rice gametes and zygotes have higher purity. This is confirmed by using the marker genes in RT-PCR (Fig. 3, Fig. 5 and Li et al 2019) and the study of siRNAs in rice gametes and zygotes (Li et al 2020 and 2021).

Based on the study of siRNA in rice gametes and zygotes, it is important to study the epigenetic modifications in rice gametes and zygotes, like the genomic wide removal of the Polycomb complex-directed H3K27me3 repressive epigenetic mark in Arabidopsis sperm cells (Imtiyaz and Sundaresan 2021), to reveal the mechanism underlying the zygotic development and cell cycle in rice. Due to the purity in our isolation, if properly funded, we can isolate and collect annually up to ~ 3000 even more rice egg cells and zygotes for studying the large-scale chromatin modifications during rice zygotic development.

3. Viable

As shown in the cell images of FDA staining, almost all isolated egg cell and zygote are viable; and according to the statistic of our transfected rice cells, after overnight incubation, the surviving rate is still 35.4%.

Because of this viability, the isolated rice egg cells and zygotes have been used for PEG-Ca^{++} mediated transfection and tissue culture for permanently transformed rice plants, as reported by

Koiso et al (2017) and Toda et al (2019). If this technique is routinized in more labs for rice research, the present restriction or difficulty in obtaining the permanent rice transformants will be much bettered; and hopefully we may get the embryo-sac specific cell marker lines particularly for rice gametes and zygotes like those in Arabidopsis (Chamberlin and Lawi 2017), which will greatly facilitate the studies of molecular mechanism underlying the initiation of rice seed formation.

4. Intact

As describe in the part of Methods, the sperm cells are released from pollen grains by osmotic shock before collection; the egg cells and zygotes automatically flow out from ovary to the excision interface, which is likely driven by the internal turgor pressure within ovary or the slight exterior force by the thin needle. Since no cell-wall digestion enzymes are used in the whole microdissection, the isolated rice gametes and zygotes are intact without losing any elements from the cell surface.

This advantage makes the isolated rice gametes, especially the egg cells, suitable for the study of the surface glycoproteins which may be involved in the double-fertilization-recognition as well as the zygotic development in crop plants.

Referencing to the relevant studies in animal and human, the sugar chains of the glycoproteins play the role in the cell-to-cell recognition and fusion (Xu and Tsao 1997). Although as aforementioned four gamete proteins are recently found involved in the *in vitro* fertilization in Arabidopsis (Mori et al 2014, Dresselhaus et al 2016 and Sprunck 2020), it is unknown if they are glycoproteins or not and if they are universal players in the double fertilization of angiosperms like crop plants. Therefore, it is important to learn the information of glycoproteins using isolated rice egg cells.

For this purpose, ~ 3000 isolated egg cells may be required. If the necessary funding is available, this goal is hopefully reachable.

References

Anderson SN, Johnson CS, Chesnut J, Jones DS, Khanday I, Woodhouse M., Li C, Conrad LJ, Russell SD and Sundaresan V (2017). The zygotic transition is initiated in unicellular plant zygotes with asymmetric activation of parental genomes. Dev Cell, 43, 349-358

Anderson SN, Johnson CS, Jones DS, Conrad LJ, Gou X, Russell SD and Sundaresan V (2013) Transcriptomes of isolated *Oryza sativa* gametes characterized by deep sequencing: evidence for distinct sex-dependent chromatin and epigenetic states before fertilization. Plant J, 76, 729-741

Blomstedt CK, Xu H, Singh MB and Knox RB (1992). The isolation and purification of surface specific proteins of somatic and reproductive protoplasts of lily and rapeseed. Physiol Plant, 85, 396-402

Cao Y and Russell SD (1997) Mechanical isolation and ultrastructural characterization of viable egg cells in *Plumbago zeylanica*. Sex Plant Reprod. 10, 368-373

Cass DD and Fabi GC (1988) Structure and properties of sperm cells isolated from the pollen of Zea mays. Can J Bot, 66, 819 825

Chamberlin MA and Lawi SJ (2017) Chapter 5 Development and Observation of Mature Megagametophyte Cell-Specific Fluorescent Markers. In: Anja Schmidt (ed), Plant Germline Development, Methods and Protocols. Humana Press, pp55-65

Dresselhaus T, Sprunck S and Wessel GM (2016) Fertilization Mechanisms in Flowering Plants. Current Biology. 26, R125-R139

Dumas C and Mogensen HL (1993) Gametes and Fertilization: Maize as a Model System for Experimental Embryogenesis in Flowering Plants. The Plant Cell, 5, 1337-1348

Dupuis I, Roeckel P, Matthys-Rochon E, Dumas C (1987) Procedure to isolate viable sperm cells from corn Zea mays L. pollen grains. Plant Physiol, 85, 876-878

Faure JE, Digonnet C and Dumas C (1994) An *in vitro* system for adhesion and fusion of maize gametes. Science, 263, 1598-1600.

Gou X-P, Wang S-H, Chen F (1999) Isolation and cytological observation of viable sperm cells of rice (in Chinese). Acta Bot Sin. 41, 669–671

Gou X, Yuan T, Wei X and Russell SD (2009) Gene expression in the dimorphic sperm cells of *Plumbago zeylanica*: transcript profiling, diversity, and relationship to cell type. Plant J, 60, 33-47

Hu SY (1998) Centenary on SG Nawaschin's discovery of double fertilization: retrospects and prospects. Acta Bot Sin, 40, 1-13

Hu SY (2002) Development of plant embryology in China. Acta Bot Sin, 44(9), 1022-1042

Hu SY and Xu HP: Chapter 8, Gamete fusion and membrane fusion mechanism. In Hu SY and Yang HY (eds) *Biology of Angiosperm Fertilization*, Chinese Scientific Publishing House, Beijing. 2002, pp149-158

Hu S-Y, Li LG, Zhu C (1985) Isolation of viable embryo sacs and their protoplasts of *Nicotiana tabacum.* Acta Bot Sin, 27, 343-347

Huang BQ, Russell SD (1989) Isolation of fixed and viable eggs, central cells and embryo sacs from ovules of *Plumbago zeylaniea*. Plant Physiol, 90:9-12

Huang BQ, Russell SD, Strout GW, Mao LJ (1990) Organization of isolated embryo sacs and eggs of *Plumbago zeylanica (Plumbaginaceae)* before and after fertilization. Am J Bot, 77, 1401-1410

Khalequzzaman M and Haq N (2005) Isolation and in vitro fusion of egg and sperm cells in

Oryza sativa. Plant Physiol Biochem. 43, 69–75

Khanday, I. and Sundaresan, V. (2021) Plant zygote development: recent insights and applications to clonal seeds. Current Opinion in Plant Biology. 13: 1-10

Koiso N, Toda E, Ichikawa M, Kato N, Okamoto T (2017) Development of gene expression system in egg cells and zygotes isolated in rice and maize, Plant Direct, 1-10

Kranz E, Bautor J and Lorz H (1991) *In vitro* fertilization of single, isolated gametes of maize mediated by electrofusion. Sex Plant Reprod, 4, 12-16

Kranz E and Lorz H (1994) *In vitro* fertilization of maize by single egg and sperm cell protoplast fusion mediated by high calcium and high pH. Zygote, 2 (2), 125-128

Lee LY, Fang MJ, Kuang LY and Gelvin SB (2008) Vectors for multi-color bimolecular fluorescence complementation to investigate protein-protein interactions in living plant cells. Plant Methods. 4, 24-34

Lee L. and Gelvin, SB **(**2014) Bimolecular Fluorescence Complementation for imaging protein interactions in plant hosts of microbial pathogens. In Annette C. Vergunst and David O'Callaghan (eds.), Host-Bacteria Interactions: Methods and Protocols, Methods in Mol. Biol., Springer Science+ Business Media New York *1197*, pp185-208

Li C, Gent JI, Xu H, Fu H, Russell SD and Sundaresan V (2021) Resetting of 24-nt siRNA landscape is initiated in the unicellular zygote in rice 2021 (to be submitted)

Li C, Xu H, Fu FF, Russell SD, Sundaresan V and Gent JI (2020) Genome-wide redistribution of 24-nt siRNAs in rice gametes. Genome Res, 30, 173-184

Li C., Xu H., Russell SD and Sundaresan V (2019) Step-by-step protocols for rice gamete isolation. Plant Reprod. 32, 5-13

Lin YH, Lin MZ, Chen YQ and Tian HQ (2021) Isolation of male and female gametes, zygotes and proembryos of leek (Allium tuberosum Roxb). Zygote. 28, 278-285.

Mol R (1986) Isolation of protoplasts from female gametophytes of *Toreniafournieri*. Plant Cell Rep, 3, 202-206

Mori T, Igawa T, Tamiya T, Miyagishima S, Berger F (2014) Gamete Attachment Requires GEX2 for Successful Fertilization in Arabidopsis. Current Biology. 24, 170-175

Lv Q, Zhong Y, Wang Y, Wang Z, Zhang L, Shi J, Wu Z, Liu Y, Mao C, Yi K and Wu P (2014) SPX4 negatively regulates phosphate signaling and homeostasis through its interaction with PHR2 in rice. The Plant Cell. 26, 1586-159

Nielsen JE, Olesen P (1988) Isolation of sperm cells from the trinucleate pollen of sugar beet (Beta vulgaris). In: Wilms H J, Keijzer CJ (eds) Plant sperm cells as tools for biotechnology. Pudoc, Wageningen, pp 111-122

Ohnishi T, Takanashi H, Mogi M, Takahashi H, Kikuchi S, Yano K, Okamoto T, Fujita M and Kurata N and Tsutsumi N (2011) Distinct Gene Expression Profiles in Egg and Synergid Cells of Rice as Revealed by Cell Type-Specific Microarrays. Plant Physiology, 155 (2), 881-891

Okada, T., Endo, M., Singh, M. B., & Bhalla, P. L. (2005). Analysis of the histone H3 gene Family in rabidopsis and identification of the male-gamete-specific variant AtMGH3. Plant Journal, 44 (4), 557-568.

Russell SD (1984) Ultrastructure of the sperm of Plumbago zeylanica II. Quantitative cytology and three-dimensional organization. Planta, 162, 385-391

Russell SD (1985) Preferential fertilization in Plumbago: ultrastructural evidence for gamete-level recognition in an angiosperm. PNAS, 82, 6129-6132

Russell SD (1986) Isolation of sperm cells from the pollen of Plumbago zeylanica. Plant Physiol, 81, 317-319

Russell SD (1990) Isolation and characterization of the angiosperm gamete. In: Dale B(ed) Mechanism of fertilization. plants to humans. Springer, Berlin Heidelberg New York, pp 3- 15

Russell, SD (1992). Double fertilization. In Russell, S. D. and Dumas, C. (eds.), Sexually Reproduction in Flowering Plants. Acdemic Press, Inc, pp357-390

Russell SD, Huang BQ, Strout GW (1989) Preliminary intermediate voltage electron microscopic observations of the isolated embryo sacs and eggs of Plumbago zeylanica L (Plumbaginaceae). In: Pare J, Bugnicourt M (eds) Some aspects and actual orientations in plant embryology. Universit~ de Picardie, Fa- cult6 des Sciences, Picardie, pp 109-119

Russell SC, Cresti M, Dumas C (1990) Recent progress on sperm characterization in flowering plants. Physiol Plant, 80, 669-676

Russell SD, Gou X, Wei X and Yuan T (2010) Male gamete biology in flowering plants. Biochemical Society Transactions, 38, 598-603

Russell SD, Gou X, Wong CE, Wang X, Yuan T, Wei X, Bhalla PL, Singh M (2012) Genomic profiling of rice sperm cell transcripts reveals conserved and distinct elements in the flowering plant male germ lineage. New Phytologist. 195(3), 560-573

Russell SD, Jones DS, Anderson S, Wang X, Sundaresan V and Gou X (2017) Isolation of rice sperm cells for transcriptional profiling. In: Schmidt A (ed) Plant germline development: methods and protocols. Springer, New York, pp 211–219.

Roeckel P, Dupuis I, Detchepare S, Matthys-Rochon E, Dumas C (1988) Isolation and viability of sperm cells from corn (Zea mays) and kale (Brassiea oleracea) pollen grains. In: Wilms H J, Keijzer CJ (eds) Plant sperm cells as tools for biotechno- logy. Pudoc, Wageningen, pp 105-109

Roeckel P, Matthys-Rochon E, Dumas C (1990) Pollen and isolated sperm cell quality in Zea mays. In: Barnabas B, Liszt K (eds) Characterization of male transmission units in higher plant. MTA copy, Budapest, pp 41-48

Sharma N, Russell SD, Bhalla and Singh M (2011) Putative *cis*-regulatory elements in genes highly expressed in rice sperm cells. BMC Research Notes, 4, 319-329

Shi L, Zhang XB, Shi YF, Xu X, He Y, Shao G, Huang QN and Wu JL (2019) OsCDC48/48E complex is required for plant survival in rice (*Oryza sativa L.*). Plant Molecular Biology 100:163–179

Shivanna KR, Xu H, Taylor P, Knox RB (1988) Isolation of sperms from the pollen tubes of flowering plants during fertil- ization. Plant Physiol, 87, 647-650

Southworth D and Kwiatkowski S (1996) Arabinogalactan proteins at the cell surface of *Brassica sperm* and *Lilium* sperm and generative cells. Sex Plant Reprod, 9, 269-272

Sprunck S (2020) Twice the fun, double the trouble: gamete interactions in flowering plants. Current Opinion in Plant Biology, 53, 106–116

Tanaka I (1988) Isolation of generative cells and their protoplasts from pollen of *Lilium longiflorum*. Protoplasma, 142, 68- 73

Theunis CH, Pierson ES and Cresti M (1991). Isolation of male and female gametes in higher plants. Sex Plant Reprod, 4, 145-154

Toda E, Koiso2 N, Takebayashi A, Ichikawa M, Kiba T, Osakabe K, Osakabe Y, Sakakibara H, Kato N and Okamoto T (2019) An efficient DNA- and selectable-marker-free genome-editing system using zygotes in rice. Nature Plants. **5**, 363-368

Uchiumi T, Komatsu S, Koshiba T and Okamoto T (2006) Isolation of gametes and central cells from Oryza sativa L. Sex Plant Reprod. 19, 37-45

Van Went JL, Kwee HS (1990) Enzymatic isolation of living embryo sac of Petunia. Sex Plant Reprod, 3, 257-262

Wagner VT, Song YC, Matthys-Rochon E, Dumas C (1988) The isolated embryo sac of Zea mays: structural and ultrastruc- tural observations. In: Cresti M, Gori P, Pacini E (eds) Sexual reproduction in higher plants. Springer, Heidelberg Berlin New York, pp 125-130

Wang K, Liu Y and Li S (2013) Bimolecular Fluorescence Complementation (BIFC) Protocol for Rice Protoplast Transformation. Bio-protocol. 3(33), 1-5

Xiao H, Wang Y, Liu D, Wang W, Li X, Zhao X, Xu J, Zhai W and Zhu L (2003). Functional analysis of the rice AP3 homologue OsMADS16 by RNA interference. *Plant Molecular Biology*, *52*(5), 957-966.

Xu HL, Swoboda I, Bhalla PL, Singh MB (1999) Male gametic cell-specific gene expression in flowering plants. PNAS, 96, 2554-2558

Xu H and Tsao TH (1997a) An improved procedure for the mass isolation of viable sperm cells from pollen of *Zea mays L*. Acta Phytophysiol Sin, 39, 218-221

Xu H and Tsao TH (1997b) Labeling the plasma membrane of isolated viable sperm cells of *Zea mays* L. by fluorophore-conjugated lectins. Acta Phytophysiol Sin, 23, 399-404

Xu H and Tsao TH (1997c) Purification of plasma membrane of maize sperm cells by aqueous polymer two-phase partitioning, *Acta Bot Sin*, 39, 218-221

Xu H and Tsao T (1997d) Detection and immunolocalization of glycoproteins of the plasma membrane of maize sperm cells. Protoplasma, 198, 125-129

Xu H, Weterings K, Vriesen W, Feron R, Xue, Y, Derksen J and Mariani C (2002) Isolation and characterization of male-germ-cell transcripts in *Nicotiana tabacum*. Sex Plant Reprod, 4, 339-346

Zhang G, Williams CM, Campenot MK, McGann LE, Cass DD (1992) Improvement of longevity and viability of sperm cells isolated from pollen of *Zea mays L*. Plant Physiol, 100, 47-53

Zhang J, Dong WH, Galli A and Potrykus I (1999) Regeneration of fertile plants from isolated zygotes of rice (*Oryza sativa*). Plant Cell Rep 19:128-132

Zhang YN, Wei DM, He EM, Miao S, Tian HQ and Russell SD (2010) Isolation of male and female gametes of rice. Crop Science. 50, 1-7

Zhao J, Zhou C and Yang HY (2000) Isolation and in vitro culture of zygotes and central cells of *Oryza sativa L*. Plant Cell Rep. 19, 321-326

Zhou C, Wu X-J (1990) Mass isolation and purification of generative cells from pollen grains. Acta Bot Sin, 32, 404-406

Zhou C, Orndorff K, Daghlian CP, DeMaggio AE (1988) Isolated generative cells in some angiosperms: a further study. Sex Plant Reprod, 1, 97-102

Supplementary Data

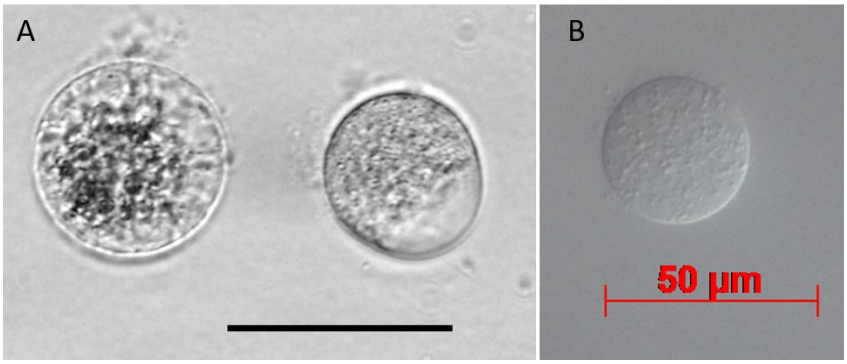

*Supplementary **Fig. 1** Comparison of egg and synergid morphology.*

A: Left: egg cell, right synergid; B: An isolated synergid. Bar = 50 µm.

Supplementary **Table 1-A** Primers for PCR identification

Primers	Sequences 5' - 3'	Product size (bp)
Actin F	GAAGGATATGCTCTCCCCCATG	524
Actin R	GGATCCTCCAATCCAGACACTG	
lat52 F	CAAGGCCGTGTCTACTGTGA	192
lat52 R	GATGTCCTCCTCATGGCTGT	
MADS3F1	GACACCTCCAACTCTGGC	341
MADS3R1	GCTGCCCCCATCATGTTC	
MADS4F	GGAGGACGAGCACAAGATGT	103
MADS4R	CCTGTCGTCGTGGTGGTAG	
MADS7F	CTGGAGGAAAGCAACCATGT	220
MADS7R	ATGGGGGCATGTAGGTGTT	
MADS16F	GAGATCAAGCGGATCGAGAA	198
MADS16R	CTGGTAGCGGTCAAAGATCC	
MGH3F	ACGGAGCTGCTGATAAGGAA	197
MGH3R	CGTCTTTGGACATGATGGTG	
cabF	GCAGCAGTAGCTGAGCTTGA	275
cabR	GTGTCCCACCCGTAGTCG	
RBCSF	GCAGCAGTAGCTGAGCTTGA	318
RBCSR	GTGTCCCACCCGTAGTCG	
EC-like1F	AGCAGTGCTGGGAGGTTCT	200
EC-like1R	GCAGTAGCCCTTGAGCATGT	
EC-like2F	CGCCGTCCTCCTACTACTTG	209
EC-like2R	CCGTTGACGAAGAAGAGCAC	

Supplementary **Table 1-B** Primers for vector construction-cellular localization

Primers	Sequences 5'-3'	Product size (bp)
Fb3-EYFP-F-XhoI (H59)	TGTCTCGAGCTATGCTCGGGAGGAACGCCAT	
Fb3-EYFP-R-HindIII (H60)	TGCAAGCTTCGGAACTCCATATCTGAATCCTC	1684
KRP4-EYFP-F-EcoRI (H63)	GTCGAATTCTATGGGCAAGTACATGCGCAA	
KRP4-EYFP-R-SalI (H64)	TGCGTCGACGTCTAGCTTGACCCATTCAAA	609
KRP5-EYFP-F-EcoRI (H65)	GTCGAATTCTATGGGGAAGTACATGCGGAAG	
KRP5-EYFP-F-SalI (H66)	TGCGTCGACGCAGTCTAGCCTTGTCCATTC	690

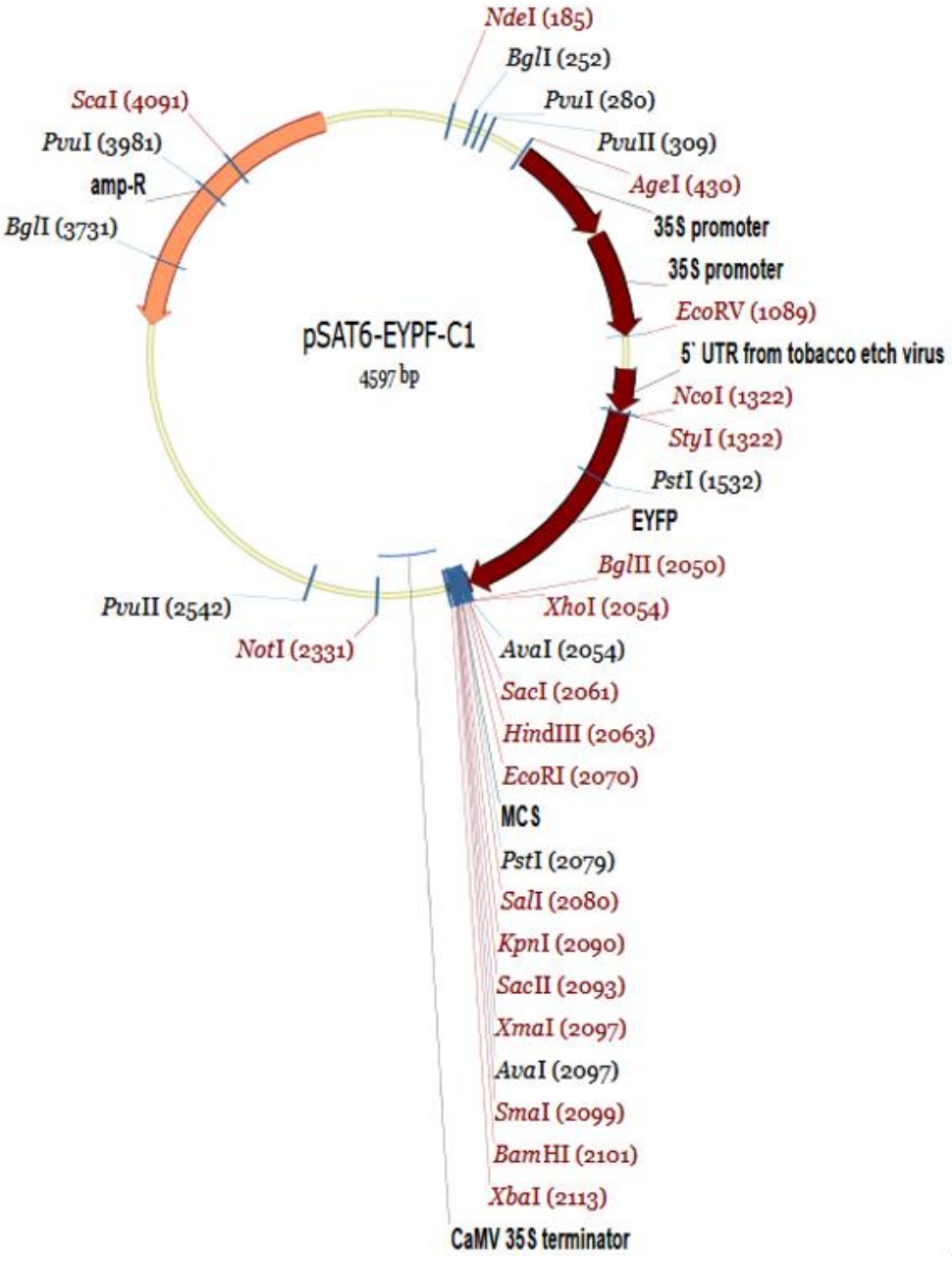

Supplementary Fig. 2 pE3150 for cloning rice genes KRP4, KRP5 and Fb3 (Lee and Gelvin 2014)

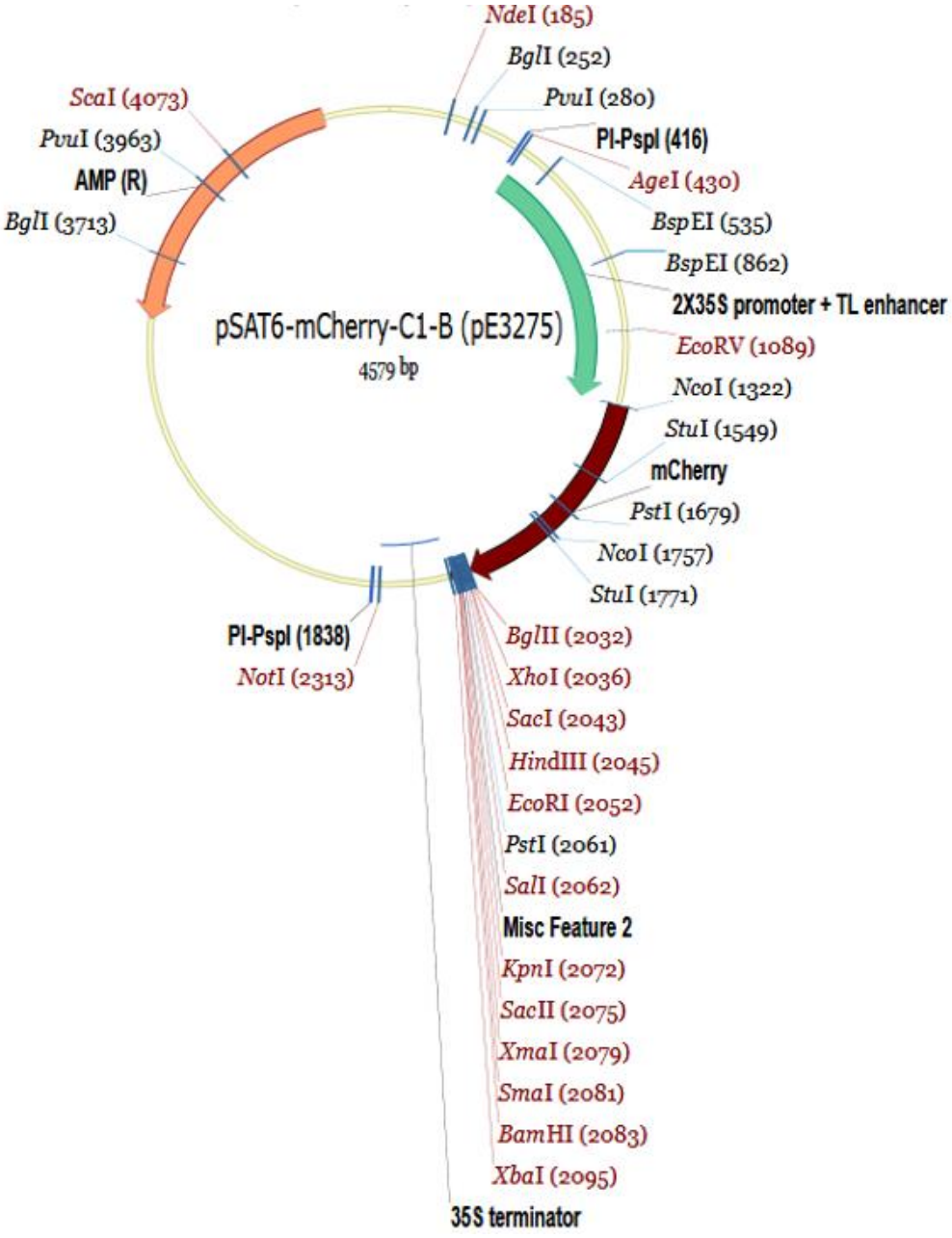

Supplementary Fig.3 pE3275 with mCherry for nuclear localization (from Dr Libault, Lee and Gelvin 2014)

Chapter 2. The Coordinate Function of OsKRP5 and OsKRP4 in Rice Zygotic Cell Cycle Control

Abstract

Zygotic cell cycle control is fundamental in initiation of the seed formation. Due to the long-term inaccessibility to gametes and zygotes in flowering plants, it is still an unexplored issue hitherto. Based on our results from various assays, we established a model called arrested core complex involved in rice zygotic cell control. It consists of four major regulatory components including CDKB1, CYCD5, OsKRP5 and OsKRP4. In this model, CDKB1 is the first major player in cell cycle progression; KRP4 and KRP5 function as CDKB1 inhibitors to arrest the zygotic cell cycle from moving forward. More importantly, OsKRP5 and OsKRP4 act in a coordinate, or heterodimer-like, manner, as indicated in the results of Y2H, yeast growth in serial dilutions, BiFC and Kinase Activity Assay. This coordinate inhibition might exist in the cell cycle control of other living organisms.

Introduction

As aforementioned, rice is one of staple food crops and excellent model monocotyledonous plants. It is a wise choice to use rice to study the mechanisms underlying seed formation for higher production. In flowering plants, the unique double fertilization is the central event for the seed formation. In this event the separate fusions of two sperm cells with the egg cell and central cell result in two inequivalent zygotes. One develops into the embryo of a new seed; the other into nutritious endosperm in seed.

However, the both processions are initiated and carried out by cell cycle for cell proliferation, differentiation and regulated development. That is why the cell cycle is one of fundamental

issues in modern biology. It is due to this importance that the cell cycle is tightly regulated to ensure it properly timed or synchronized with different factors. Without synchronization of the cell-cycle in plant sexual reproduction, the DNA complement of both gametes cannot be assured activated and numerically correctly represented. As a result, neither double fertilization nor embryogenesis would be possible, thus no seed formation (Friedman WE 1999 and Hui Qiao Tian *et al* 2005).

Cell cycle consists of four different phases (M, G1, S and G2), each of which is controlled at several checkpoints by some core complexes consisting with multiple regulatory proteins. Among the members of such core complex, the first group of major players are Cyclins (tissue specific) and the second, Cyclin-Dependent Kinases (CDKs, for protein phosphorylation). Three scientists (Lee Hartwell, Paul Nurse and Tim Hunt) won 2001 Nobel Prize in Medicine for their contributions in discovering CDKs and Cyclins in yeast. Once a specific CDK associated with a Cyclin is activated, the transcription factor E2F will be released from its inhibitor (retinoblastoma protein) to activate a bunch of genes required for DNA replication, entering the S phase from G1.

Due to the requirement for their sessile lifestyle, plants developed a larger set of CDKs and Cyclins for a potentially more combinations as core complexes of cell cycle (Wang et al 1997, Stals and Inze 2001, De Veylder et al 2001 and 2007, Barroco et al 2006, Mizutani et al 2010, Van Leene et al 2011, Yang et al 2011, Cheng et al 2013, Dante et al 2014, Pedroza-Garcia, et al 2016 and Ramos Coelho et al 2017). As listed in Table 1, compared to yeast and human, flowering plants like rice and Arabidopsis have many more different types of CDK proteins (Dudits et al 2007) and Cyclins (Wang et al 2004, La et al 2006, Hu et al 2010, Ma et al 2013, Lin et al 2014 and Pettko - Szandtner et al 2015)

Table 1 Core complex components of cell cycle in model organisms

Models	CDKs	Cyclins	Inhibitors
Budding Yeast	1	9	3 (e.g., Sic1)
Human	4	9	7 (e.g., $p16^{INK4A}$)
Chlamydomonas	3	3	
Arabidopsis	5~11	31	7 (KRPs), 14 (SMRs)
Rice	9	27~48	6 (KRPs)

Nevertheless, both CDK and Cyclin are conjugated with the third partner, inhibitor of Cyclin Dependent Kinase (ICKs) for inhibition of CDK activity. Otherwise, the cell cycle could be out of control without the role of these ICKs (Verkest et al 2005, Pedroza-Garcia et al 2016). In plants, the ICKs are called Kip Related Proteins (KRPs) (except Arabidopsis, whose inhibitors include both KRP and SIAMESES, SIM). These KRPs is a family of nuclear proteins with length of 100 ~ 300 amino acid residues. Different plant species have different number of KRPs. During the past 2 decades, a number of KRP encoding genes have been identified and studied in various plant species, such as Arabidopsis (Wang et al 1997, Liu et al 2000, De Veylder et al 2001, Zhou et al 2002, Kim et al 2008, Cheng et al 2013, Jegu et al 2013 and Cheng et al 2015, Cao et al 2018), tobacco (Jasinski et al 2003), tomato (Bisbis et al 2006), orchid (Lin et al 2014), maize (Coelho et al 2005 and Xiao et al 2017), rice (Barroco et al 2006, Guo et al 2007, Acosta et al 2011, Yang et al 2011, Pettko-Szandtner et al 2015 and Ajadi et al 2020) and Chlamydomonas (Atkins KC and Cross FR 2018).

In rice, there are six different putative KRP proteins based on the genomic data base. As shown in Fig. 1, five conserved motifs are identified in the six rice KRP proteins. The function of motif # 3 ~ 5 is unknown, but the other two, #1 and 2 (in the red circle) at the C' termini of each KRP are known responsible for interactions with CDK and Cyclin. In addition, all these KRPs have

putative nuclear localization signals (NLS) toward N' termini, including both KRP5 and KRP4 (circled in green) which are of our interest in this chapter.

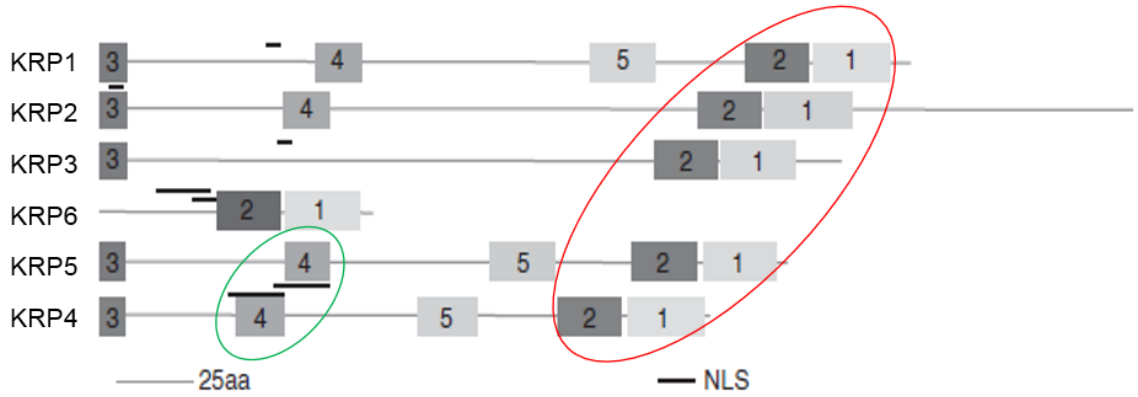

Fig .1 Schematic overview of six rice KRP proteins. Five motifs (box 1-5) identified by MEME. The putative nuclear localization signal (NLS) is marked as dark grey bar (Yang et al 2011).

Regarding the function of plant KRP proteins, extensive studies have been performed with dicot species, particularly Arabidopsis. Only a few will be numerated here. First, The KRP expression is regulated by environmental factors. For example, AtKRP1 and alfalfa KRPMt are induced by abscisic acid (ABA) and salt stress (Wang et al 1998, Pettko-Szandtner et al 2006 and Ruggiero et al 2004), but AtKRP2 is suppressed by auxin (Himanen et al 2002 and Richard et al 2002) Second, over-expression of KRP genes significantly changes plant growth and development with reduced plant size, serrated leaf, reduced cell number but enlarged cell volume (Wang et al 1997, De Veylder et al 2001, Barroco et al 2006, Yang et al 2011). Third, AtKRPs also play a role in the embryo sac formation (Cao et al 2018). In most normal plants, only one embryo sac is produced from the megaspore mother cell (MMC) via cell cycle; but in the septuple mutant (all 7 KRP genes inactivated), supernumerary MMCs and embryo sacs were formed; moreover, this phenotype can be complemented by KRP4 and KRP7, indicating multiple KRPs function

redundantly in restricting the production of extra MMCs and ensuring to develop one embryo sac for one embryo per ovule.

Several studies have also performed on the function of rice KRPs. OsKRP1 is found playing an important role in plant growth and seed formation (Barroco 2006). The rice plant with overexpressed KRP1 reduced cell proliferation in leaf development; KRP1 overexpression also drastically reduced seed filling by the drop in the endoreduplication of endosperm. It is also reported that OsKRP1 and OsKRP2 were significantly induced in developing seeds by applied plant hormone, abscisic acid (ABA) and Brassinosteriod (BR); the smaller seeds with reduced grain weight were produced from the plants with overexpressed OsKRP1 and OsKRP2 suggesting that disturbing the normal state of OsKRP1 and OsKRP2 inhibit cell proliferation and thus blocks the seed development (Ajadi et al 2020). In addition, Over-expression of OsKRP4 caused rice leaves rolled abnormally toward the abaxial side, pollen viability dropped, and seed setting rate lowered (Yang et al 2011).

However, little is known about the components of core complexes of cell cycle control in the development of rice gametes and zygote, particularly about inhibitory function of KRP proteins in the zygotic cell cycle progression, the initiation for embryo formation. This is mainly because the egg cells and zygotes are deeply embedded within multiple layers of plant tissues. Therefore, it is unknown which KRPs play the inhibitory role in zygotic development and which CDKs and cyclins interact with these KRPs to form the core complex to initiate the embryonic cell cycle.

Since the egg cell and zygote have become relatively accessible in Dr. Russell Lab, it is possible for us as the first to carry out a study to address these very fundamental issues in the field of plant reproduction.

Material and Methods

Plant material

The growth of rice plants and the cell isolation for leaf protoplasts, egg cells and zygotes are conducted as previously described in Chapter 1.

Methods

I. RNA isolation, RT-PCR and qRT-PCR

For RNA extraction, samples (~ 100 mg each) were collected from 8 weeks old wildtype (*Kitaake*) plants. The leaf and stem were cut into ~ 0.5 cm^2 pieces and frozen immediately in liquid nitrogen (LN). The root was frozen after a quick washing with distilled water. The individual fresh florets were collected and frozen right way or immerged in 0.3 M mannitol for dissecting anther, lemma/padea and pistil followed by freezing in LN. The total RNA was extracted using Qiagen RNAeasy Plant Mini Kit (Cat# 74904) following the manufacturer's protocol. The reverse transcription was performed with the RevertAid First Strand cDNA Synthesis Kit (Thermo Scientific, Cat# 1621) to synthesize the first-strand cDNA from DNaseI-treated RNA with an oligo (dT)18 primer as the kit instruction.

RT-PCR was conducted on BioRad C1000 Touch Thermal Cycler system with Phusion High Fidelity (Thermo Scientific, Cat#F530S) or Q5 High-Fidelity DNA Polymerase (NEB, Cat# M0491S) for DNA amplification. For qRT-PCR, PowerUp™SYBR™ Green Master Mix Kit (Thermo Scientific Cat# A25741) Kit and BioRad CFX Connect™ Real-Time system were employed and the rice 18S rRNA gene was used as the internal control.

The RT-PCR product was examined in 1% agarose gel containing SYBR safe DNA gel stain (Invitrogen, P/N S33102). The relative transcript abundances from qRT-PCR were calculated using the $2^{-\Delta\Delta Ct}$ method (Schmittgen and Livak 2008). The primers for RT-PCR and qRT-PCR are listed in Supplementary Table 2.

II. Yeast two hybridization (Y2H)

The Y2H assays were conducted using Matchmaker Gold Yeast Two-Hybrid System (Clontech). The full-length complementary DNAs (cDNAs) of rice OsKRP1, OsKRP4, OsKRP5 and 5'-315 bp of OsKRP4 (*KRP4mut*) and 5'- 530 bp of OsKRP5 (*KRP5mut*) were amplified in PCR and then cloned into the vector pGBKT7 at the specific restriction sites as the bait constructs for Y2H; similarly, the cDNAs of 6 OsCDKs and 11 OsCyclins (supplementary Table 1) were PCR-cloned into pGADT7 AD as the prey constructs for Y2H. The primers with the restriction sites are listed in supplementary Table 2.

The component cells of yeast strain Y2H Gold were transformed with the bait constructs and Y187 with the prey constructs as the manufacturer instructed. The transformed or hybrid cells were cultured on the selective medium of Di-Drop-Out (DDO, SD/-Trp-Leu) or Quodra-Drop-Out (QDO, SD/-Trp-Leu-His-Ade), both containing X-α-gal and Aureobasidin A (AbA) at 30°C for ~ 3 days. The protein-protein interactions are indicted by the yeast spots in blue.

III. Isolation of yeast nuclei (for Co-IP)

The isolation of yeast nuclei was based on previous descriptions (Dove et al 1998 and Reese et al 2008) and optimized according to the lab equipment available. Since it is a one-week long procedure and important for the successful Co-IP assay of nuclear proteins, the main steps will be described as the following.

1. Culture yeast cells containing c-Myc or HA tagged constructs (c-Myc-OsKRP5, cMyc-OsKRP4, HA-OsCDKB1 and HA-OsCDKB2), on -Leu-Trp agar medium at 30^{o}C for 3 days.
2. Inoculate 3.5 ml -Leu-Trp liquid medium with the fresh yeast colonies (2 - 3 mm^2) and incubate at 30^{o}C, 220 rpm, for 8-9 hours.
3. Transfer the above culture to 20-25 ml of -Leu-Trp medium and grow (30^{o}C, 220 rpm) for

overnight (o/n).

4. Inoculate ~220 ml -Leu-Trp with the o/n culture, briefly vortex and grow for 6.5 hours (30^{o}C, 220 rpm) until OD600 reach ~1 (~200 mg cells/100ml; longer growth may cause protease activity increasing).
5. Centrifuge in 50 ml tubes (1000g, 5 min, 4^{o}C), and finally pellet into one tube.
6. Resuspend cells in 50 ml dH_2O and centrifuge (1000g, 5 min, 4 ^{o}C).
7. Resuspend each pellet with 3.5 ml Zymolyase Buffer (1M Sorbitol, 50mM Tris-Cl pH7.5, 10mM $MgCl_2$) and add 0.5 µ1 ß-me (final ~2mM).
8. Incubate cells at 30^{o}C for 15 minutes with gentle shaking at 100 rpm.
9. Pellet cells at 4500g for 5 minutes.
10. Resuspend each pellet in 3 ml Zymolyase Buffer and add 2 ml -Leu-Trp/S (-Leu-Trp with 1M Sorbitol).
11. Add 2-3 mg Zymolyase 100T (USB, Cat# Z1004, or Sigma L-4025-50KU: ~6 mg for 200ml culture) and incubate at 30^{o}C for 1.5 -2 hours with gentle shaking (to test spheroplasts at ~ 1 hour, mix 4 µl samples with 4 µl 1% SDS on a slide; the completion will reach > 80%).
12. Add 10 ml -Leu-Trp/S and pellet cells at 4500g for 5 minutes.
13. Resuspend pellet in 25 ml -Leu-Trp/S and pellet cells at 4500g at 4^{o}C for 5 minutes.
14. Repeat Step 7 but in ice cold -Leu-Trp/S.
15. Resuspend pellet in 20 ml 1M Sorbitol (ice cold) and pellet cells at 4500g at 4^{o}C for 5 minutes.
16. Core mix Buffer N (Nuclei buffer: 30 mM Hepes pH7.6, 0.05 mM CaCl2, 5 mM MgSO4.7H2O, 1 mM EDTA, 10% Glycerol, 0.5% NP40, 7.2 mM Spermidine Hexahydrate) with protease inhibitors (PI) and PMSF: to each 8 ml Buffer N, add 20 µl PI (Sigma, P8215),

1.5 µl PMSF (500x, final 1 mM) and 1 µl ß-me.

17. Resuspend each pellet in 6.5 ml the Buffer N into Teflon Dounce homogenizer (on ice) and pass cells through at top speed for 10-12 strokes by an electric drill.

18. Decant the lysate to the same 50 ml tube, rinse the homogenizer once in 1.2 ml Buffer N, and pellet cellular debris at 3000g at 4^{o}C for 5 min.

19. Pipet each supernatant to 4 x 2 ml tubes (w/o pellet junk), to collect the Nuclei at 14000g at 4^{o}C for 10 min, then discard the supernatant, and store pellets at -20^{o}C for later use.

IV. Co-immunoprecipitation (Co-IP) assay

Pierce™ Co-Immunoprecipitation Kit (Thermo Scientific™, Cat # 26149) was used and the manufacturer's protocol was followed. Briefly, the frozen nuclei was suspended in Lysis Buffer containing 25 mM Tris (pH7.5), 150 mM NaCl, 1 mM EDTA, 1% NP40, 5% glycerol 10mM NaF, 1 mM Na3VO4 and freshly added with protease inhibitor cocktail (Sigma, P8215) plus PMSF (final 1 mM), and incubated on ice for 10-15 minutes with periodic flicking. The cell debris was removed by centrifuge (13,500g, 4^{o}C, 8 min), and the resulting supernatant was transferred to a new tube on ice: 1 µl was used to determine protein concentration at A280 with Geno 5 instrument and the rest lysate was precleared with 40 µl control agarose beads.

To make antibody immobilized agarose beads, 25 µg of anti-HA (GenScript, Cat #A01244) or anti-c-Myc mAb (GenScript, Cat #A00702) was used for coupling with 50 µl AminoLink PlusCoupling Resin as the manufacturer's instructions, and incubated with the above precleared nuclear proteins at room temperature for 1.5 - 2 hours or at 4^{o}C for overnight with gentle automatic mixing.

The incubated beads were washed 4 times with Wash Buffer (25 mM Tris, pH 7.5, 150 mM NaCl, 1 mM EDTA, 1% NP40, plus 1 mM PMSF and protease inhibitor cocktail). Then the

immunoprecipitated proteins were eluted with elution buffer (pH 2.8 containing primary amine, the kit provided).

V. Western blot assay

For Western blotting, the eluted proteins (~10 μg) were separated in 12% SDS–PAGE gel and transferred to PVDF membrane (Bio-Rad) using BioRad apparatus. The membrane was incubated with Blocking Solution (20 mM Tris-Cl, pH7.5, 150 mM NaCl, and 0.1%Tween 20, containing 3% BSA or 5% nonfat milk) at room temperature for 1 hour, then with primary antibody (Anti-HA or anti-c-Myc, mouse mAb) in Blocking Buffer at 4°C for overnight.

The membrane was washed with TBST (20 mM Tris-Cl, pH7.5, 150 mM NaCl, and 0.1%Tween 20) for three times (5 min each) and incubated with the horseradish peroxidase (HRP) - conjugated secondary antibodies (goat anti mouse, Invitrogen Cat# 31430, with dilution 1:2000) in Blocking Solution at room temperature for 1 hour.

After washing (5 min x 3), the bound antibodies on the membrane were visualized with One Step Ultra TMB-blotting Solution (Thermo Fisher Cat# 37574) or SuperSignal™ West Pico PLUS Chemiluminescent Substrate (Thermo Scientific, ref 34577) using BioRad ChemDoc XRS system.

VI. CDK activity assay

To avoid using the traditional radioactive material to detect kinase activity, ADPsensor™ Universal Kinase Activity Assay Kit (BioVision, Cat # K212-100) was adopted. Briefly, the purified proteins (HA-tagged OsCDKB1, OsCDKB2 and OsCYCD5 and c-Myc- tagged OsKRP5 and OsKRP4) from Co-IP were used in setting kinase reactions; the reaction product,

ADP, was converted to an intermediate by the ADP Sensor Mix (the kit provided) and then generated a strong and stable fluorescence signal by reacting with a probe.

The fluorescence was scanned at Ex/Em = 535/587 nm in the multiple plate reader (Dr. Bourne Lab, OU) for 60 min (once every 5 min).

VII. Bimolecular Fluorescent Complementation (BiFC)

For BiFC assay, the CDS of OsKRP5 or OsKRP4 were cloned into pE2913 (Supplemental Fig. 3A, Lee et al 2014) for the construct KRP5-nEYFP or KRP4-nEYFP, and the CDS of OsCDKB1 or OsKRP4 into pE2914 (Supplementary Fig. 3B, Lee et al 2014) for CDKB1-cEYFP or KRP4-cEYFP; the native promoters of $OsKRP5_{promoter}$, maize $Ubiquitin(Ubiq)_{promoter}$ and $OsCDKB1_{promoter}$ were added to 5' termini of the construct KRP5-nEYFP, KRP4-nEYFP (also KRP4-cEYFP) and CDKB1-cEYFP, respectively.

To test the interaction of OsCDKB1 and OsKRP5 or OsKRP4, the construct $CDKB1_{promoter}$-CDKB1-cEYFP was linked to $KRP5_{promoter}$-KRP5-nEYFP and $Ubiq_{promoter}$-KRP4-nEYFP, separately, using Gibson Assembly kit (NEB, E5510S).

To test the interaction of OsKRP5 and OsKRP4, the construct $KRP5_{promoter}$-KRP5-nEYFP was linked to $Ubiq_{promoter}$-KRP4-cEYFP by Gibson Assembly. The relevant primers are listed in Supplementary Table 2.

The rice egg cells and zygotes were manually isolated, transfected with above constructs and observed in epi-fluorescent microscopy as previously described (Chapter 1, Wang et al 2013, Koiso et al 2017 and Toda et al 2019).

VIII. Multi-color BiFC (mcBiFC)

For mcBiFC assay, the CDS of OsKRP4 was cloned into pE3233 (Supplemental Fig. 4A, Lee et

al 2014) for the construct KRP4-nVenus, the CDS of OsKRP5 into pE3247 (Supplementary Fig. 4B, Lee et al 2014) for KRP5-nCerulean, and the CDS of OsCDKB1 into pE3449 (Supplemental Fig. 4C, Lee et al 2014) for CDKB1-cCFP; then the native promoters of maize Ubiquitin(Ubiq)$_{promoter,}$ OsKRP5$_{promoter}$, and OsCDKB1$_{promoter}$ were added to 5' termini of the construct KRP4-nVenus, KRP4-nCerulean and CDKB1-cCFP, respectively, as the three semi-constructs (or cassettes).

To detect the interactions of OsCDKB1 to both OsKRP5 and OsKRP4 in transfected rice egg cells or zygotes, the three cassettes were linked into one same plasmid by Gibson Assembly (see the relevant primers listed in Supplementary Table 2).

The detected fluorescent signal of Venus (emitted at ~528 nm) from transfected cells indicates the interaction of OsCDKB1 with OsKRP4 and the signal of Cerulean (at ~ 475 nm) suggests the interaction of OsCDKB1 with OsKRP5.

The same procedure for cell transfection and microscopy in BiFC assay was followed for mcBiFC.

IX. Phylogenetic analysis

The coding sequences (CDS) of 6 rice KRP genes, KRP1 to KRP6, were used for the search in Basic Local Alignment Search Tool (BLAST; NCBI). These sequences are downloaded from rice genomic database (http://rice.plantbiology.msu.edu) using gene locus number (see Supplemental table 1).

To select the homologous sequences to each of 6 KRP query sequences, the cutoff score of identity is above 70% within over 60% of query-cover (except the 2 used as the outgroup), with E value lower than $2e^{-33}$. As a result, 20 members were selected, in which Arabidopsis and Brassica were used as the out group.

The 20 sequences are aligned with MEGA 6 (Tamura et al 2013) for the phylogenetic tree.

Results and Disscussion

I. The expression profile survey and RT-PCR screening for candidate components of cell cycle core complexes in rice pistil

The core complexes of cell cycle control include three different types of components: CDKs, Cyclins and ICKs/KRPs. As shown in the interactome study in *Arabidopsis*, the interactions among those components are complicated (Leene et al 2011). But no similar information in rice, particularly, in gametes and zygotes. To fill up this gap, we carefully investigeted the relevant literature and genomic database and collected 39 candidates according to their expression profile in rice flowers (Supplementary Table 1). Then these candidates were screened in RT-PCR. As a result, 19 genes were cloned for further study in Y2H including 3 KRPs (KRP1, KRP4 and KRP5), 6 CDKs (CDKA1;1, CDKA2;1, CDKB1;1, CDKB2;1, CDKC1;2 and CDKE1) and 10 Cyclins as listed in Table 1.

As shown in Fig. 1A, the transcription levels of KRP4 and KRP5 are much higher than other KRPs in rice flowers; and qRT-PCR in different tissues (Fig. 1B and C) indicates that the expressions of KRP4 and KRP5 are preferentil in rice pistil. Since the pistil consists of stigma, style and ovary, and the ovary contains the egg cell and central cell (before the double fertilization) or zygotes (after the fertilization), it is likely that both KRP5 and KRP4 are preferentially expressed in rice egg cells and zygotes. This point is confirmed by RNAseq conducted by the Russell Lab and the Sundar Lab (Supplementary Fig.1).

Table 1 Screened candidate genes (19/39) **for cell cycle control proteins in rice zygotes**

KRPs (3/6)	CDKs (6/9)	CYCs(10/24)
KRP1	CDKA1;1	CYCA2;1
KRP4	CDKA2;1	CYCA3;1
KRP5	CDKB1;1	CYCA3;2
	CDKB2;1	CYCB1;1
	CDKC1;2	CYCB2;1
	CDKE1	CYCB2;2
		CYCD2;1
		CYCD5;1
		CYCD6;1
		CYCT1;4

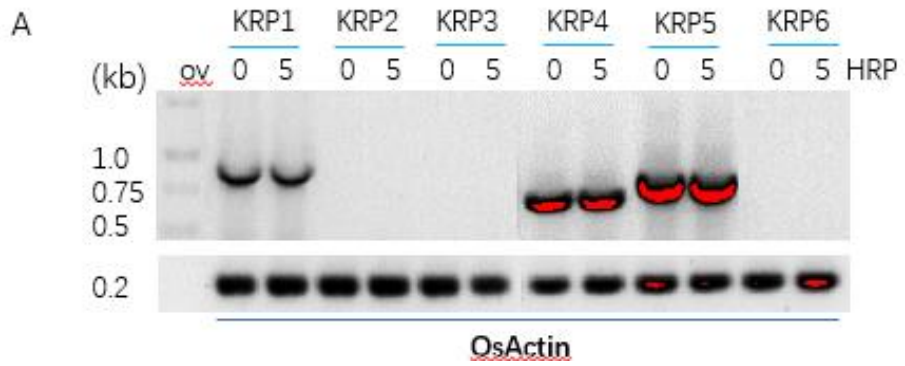

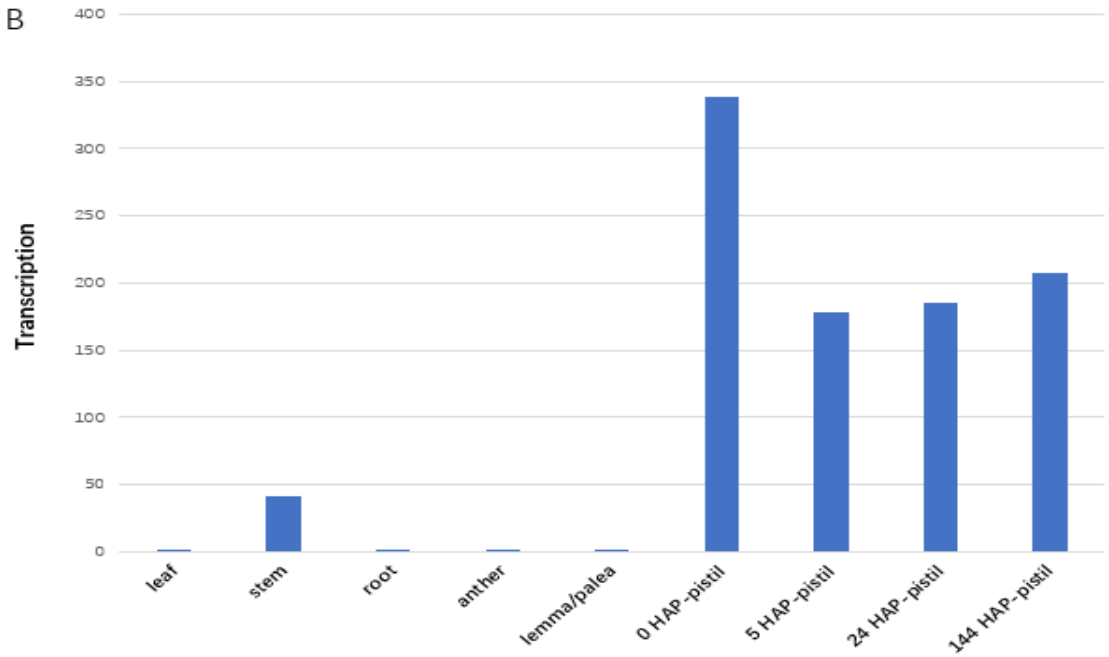

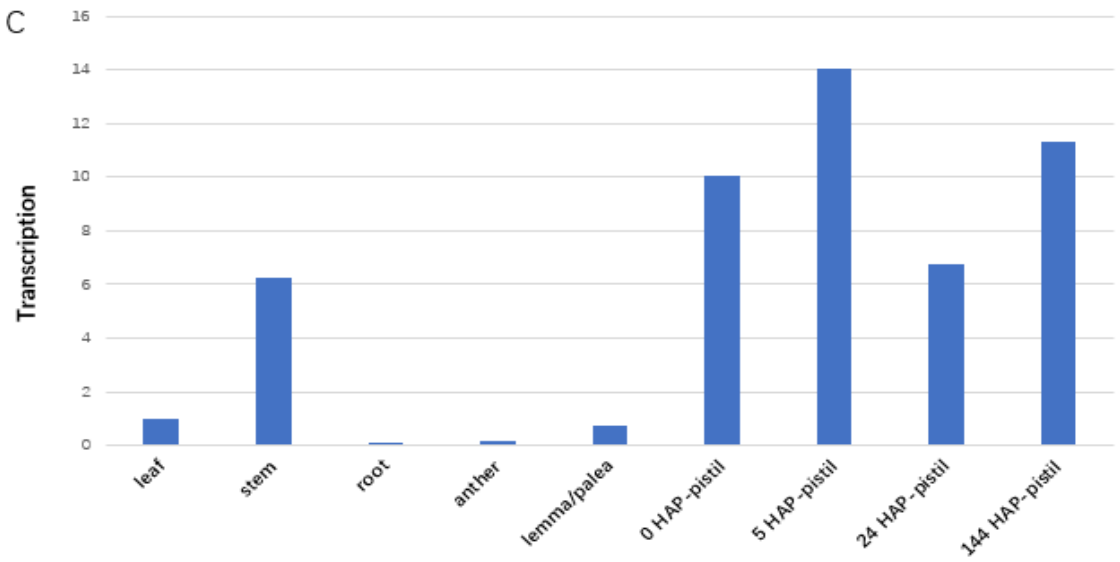

Fig. 1 Expression profile of OsKRP genes in rice plant. A. RT-PCR from rice florets at 0 and 5 HAP (hours after pollination). M, DNA ladder; OsActin, housekeeping gene as the control for equal loading. B and C, qRT-PCR for the transcription level of OsKRP5 (B) and OsKRP4 (C) in different tissues. The transcription in leaf is used to calculate the fold change of transcription in other tissues.

II. Y2H assay-based interaction networks (interactome) of cell cycle core complex proteins in rice egg cells and zygotes

Yeast 2 hybrid (Y2H) is an economic and practical *in vivo* assay for the detection of PPIs (Fields and Song 1989, Leene et al 2011 and Ferro and Trabalzini 2013). It has been widely adopted for a high-throughput screen.

To gain information for the interactome of cell cycle core complex proteins in rice egg cell and zygote, we firstly used KRP1, KRP4 and KRP5 as the baits (recombined to the vector pGBKT7) and other cell cycle components (CDKs and Cyclins) as preys (recombined to pGADT7) for Y2H assay. Once the bait interacts with the prey, the downstream reporter genes (AUR1-C, ADE2, HIS3, and MEL1) will be activated and detected as blue spots on the selective media (DDO,

SD/–Leu/–Trp, or SD/–Ade/–His/–Leu/–Trp, supplemented with the substrate X-α-gal A and antibiotic Aureobasidin A).

Interactions of OsKRPs with OsCDKs in Yeast							
(**Bait**/Prey)	Vector	1. CDKA1;1	2. CDKA2;1	3. CDKB1;1	4. CDKB2;1	5. CDKC1;1	6. CDKE1
KRP1				+			
KRP4		+	+	+	+	++	
KRP5		++	++	++	++	++	+
KRP4mut							
KRP5mut							

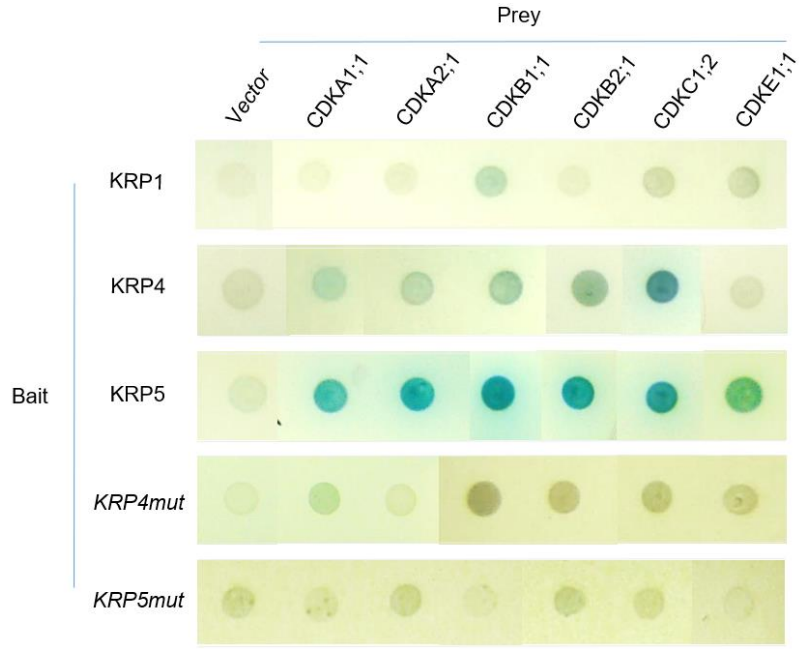

Fig. 2 A. Y2H assay to detect the interactions of OsKRPs with different OsCDKs. "+" in the table (upper panel) shows the intensity of blue signal detected in yeast spots (lower panel). The blue spots on the selective medium (SD/-Leu/-Trp/-His/-Ade with X-α-gal and antibiotic AureobasidinA, AbA) indicate the interactions of OsKRP with OsCDKs. The vector for prey (pGADT7), KRP4 mut (5'-315 bp) in pGBKT7 and KRP5 mut (5'-530 bp) in pGBKT7 are used for the negative control. (n=3).

As shown in Fig.2 A, KRP5 interreacted with all 6 CDKs (CDKA1;1, CDKA2;1, CDKB1;1, CDKB2;1, CDKC1;1 and CDKE1). Beside the interreaction of KRP5 with CDKE1, the other 5 are stronger as scored in the upper panel. Similarly, KRP4 interreacted with all 5 CDKs except CDKE1, including the stronger interaction with CDKC1;1. In contrast, KRP1 interacted only with CDKB1;1.

Since both KRP5 and KRP4 interacted with most selected CDKs (Fig. 2 A), does KRP5 reacts with KRP4 or *vice versa*? Therefore, we used KRP5 and KRP4 as either baits or preys for the 2nd Y2H assay. As a result (Fig. 2 B), the two strongly interacted each other. To our knowledge, this is the first interaction detected between the two putative inhibitory KRP proteins.

Interactions of OsKRP4 with OsKRP5 in Yeast

(**Bait**/Prey)	KRP1	KRP4	KRP5
KRP1	NA	-	-
KRP4	NA	NA	++
KRP5	NA	+	NA

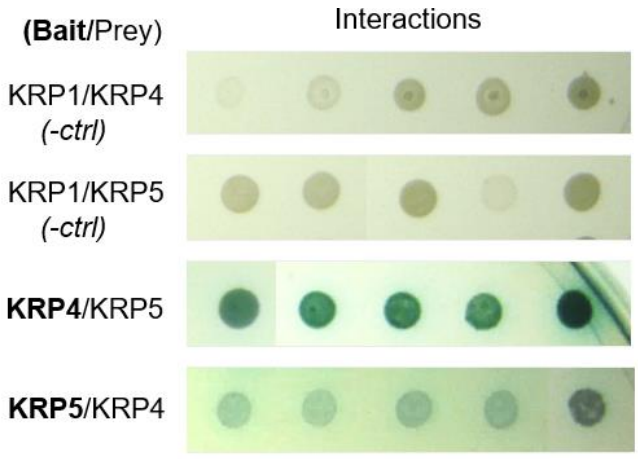

Fig. 2 B. Y2H assay to detect the interaction between OsKRP5 and OsKRP4. "+" in the

table (upper) shows the intensity of blue signal detected in yeast spots (lower panel); NA, not applicable. The blue spots on the selective medium (SD/-Leu/-Trp/-His/-Ade with X-α-gal and antibiotic AureobasidinA, AbA) indicate the interaction of OsKRP5 with OsKRP4. The interaction of OsKRP1 with OsKRP4 or OsKRP5 was used as the negative control. (n > 10)

Interactions of OsCDKs with OsCYCs in Yeast											
(**Bait**/Prey)	Vector	7.CYCA2;1	8. CYCA3;1	9. CYCA3;2	10. CYCB1;1	11. CYCB2;1	12. CYCB2;2	13. CYCD2;1	14. CYCD5;1	15. CYCD6;1	16. CYCT1;4
1. **CDKA1;1**											
2. **CDKA2;1**							++	++	+	++	++
3. **CDKB1;1**									++		
4. **CDKB2;1**		++	+		+		++	+	++	+	
5. **CDKC1;1**											
6. **CDKE1**											

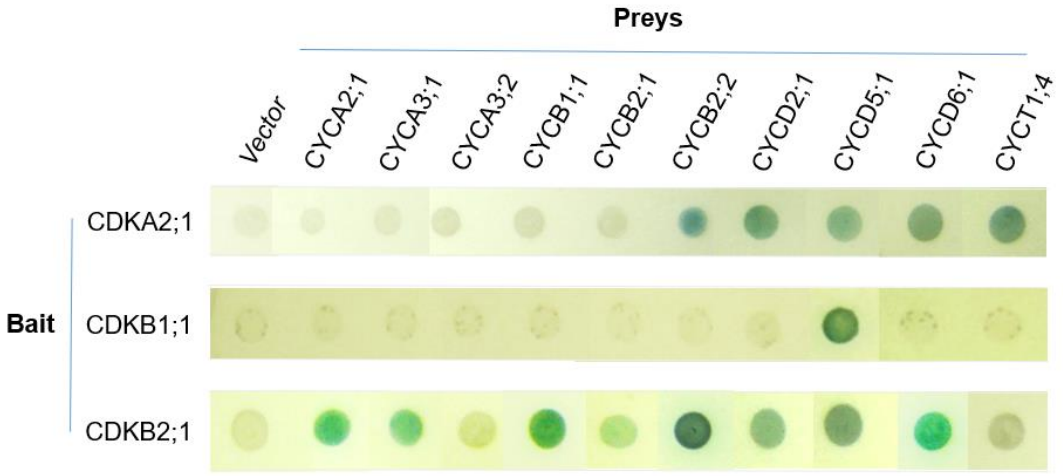

Fig. 2 C. Y2H assay to detect the interactions of OsCDKs with different rice Cyclins, OsCYCs. "+" in the table (upper panel) shows the intensity of blue signal detected in yeast spots (lower panel). The blue spots on the selective medium (SD/-Leu/-Trp/-His/-Ade with X-α-gal and antibiotic AureobasidinA, AbA) indicate the interactions of OsCDKA2;1, OsCDKB1;1 and

OsCDKB2;1 with different OsCYCs. The vector for prey (pGADT7) is used as the negative control. OsCDKB1 interacts with CYCD5 only. (n=3)

All 6 rice CDKs were also used as baits to detect their interactions with 11 different rice Cyclins. The results with positive PPIs are shown as Fig. 2 C. CDKA2;1 interacted with 5 CYCs (CYCB2;2, CYCD2;1, CYCD5;1, CYCD6;1 and CYCT1;4), CDKB1;1 interacted only with 5 CYCD5;1; whereas CDKB2;1 reacted with 7 Cyclins (CYCA2;1, CYCA3;1, CYCB1;1, CYCB2;2, CYCD2;1, CYCD5;1 and CYCD6;1).

In addition, KRP1, KRP4 and KRP5 were used as baits for interactions with different Cyclins (Fig. 2 D), Only KRP5 was found reacted with CYCD5;1 (stronger) and CYCT1;4 (weaker).

Interactions of OsKRPs with OsCYCs in Yeast

(Bait/Prey)	Vector	7. CYCA2;1	10. CYCB1;1	12. CYCB2;2	14. CYCD5;1	15. CYCD6;1	16. CYCT1;4
KRP1							
KRP4							
KRP5					+++		+

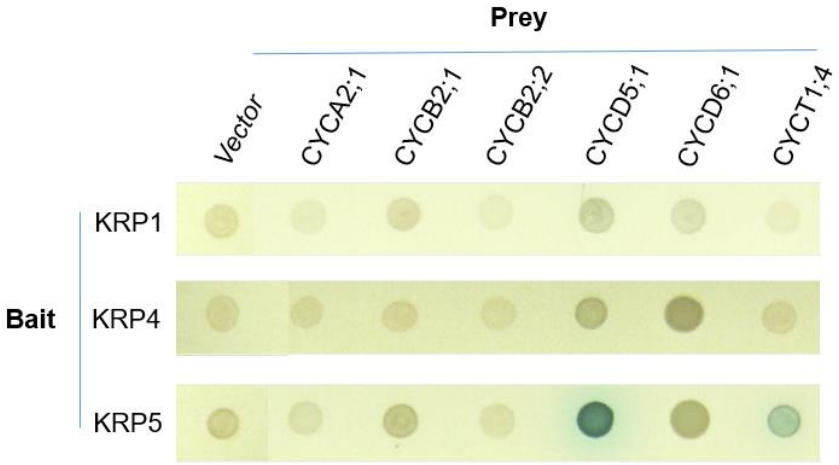

Fig. 2 D. Y2H assay to detect the interactions of OsKRPs with different rice Cyclins, OsCYCs. "+" in the table (upper panel) shows the intensity of blue signal detected in yeast spots (lower

panel). The blue spots on the selective medium (SD/-Leu/-Trp/-His/-Ade with X-α-gal and antibiotic AureobasidinA, AbA) indicate the interactions of OsKRPs with OsCYCs. The vector for prey (pGADT7) is used as the negative control. The lower panel shows that OsKRP5 interacts with CYCD5 and CYCT1:4. (n=3)

From the above Y2H assay, totally 26 positive interactions were detected. They are represented in the scheme of Fig. 2 E. This small network is not so comprehensive to work as the interactome of all rice cell cycles in different tissues, but it is a reliable and specific PPI network for rice pistil, which will be useful in determining the core complex components of cell cycle control in rice egg cells and zygotes.

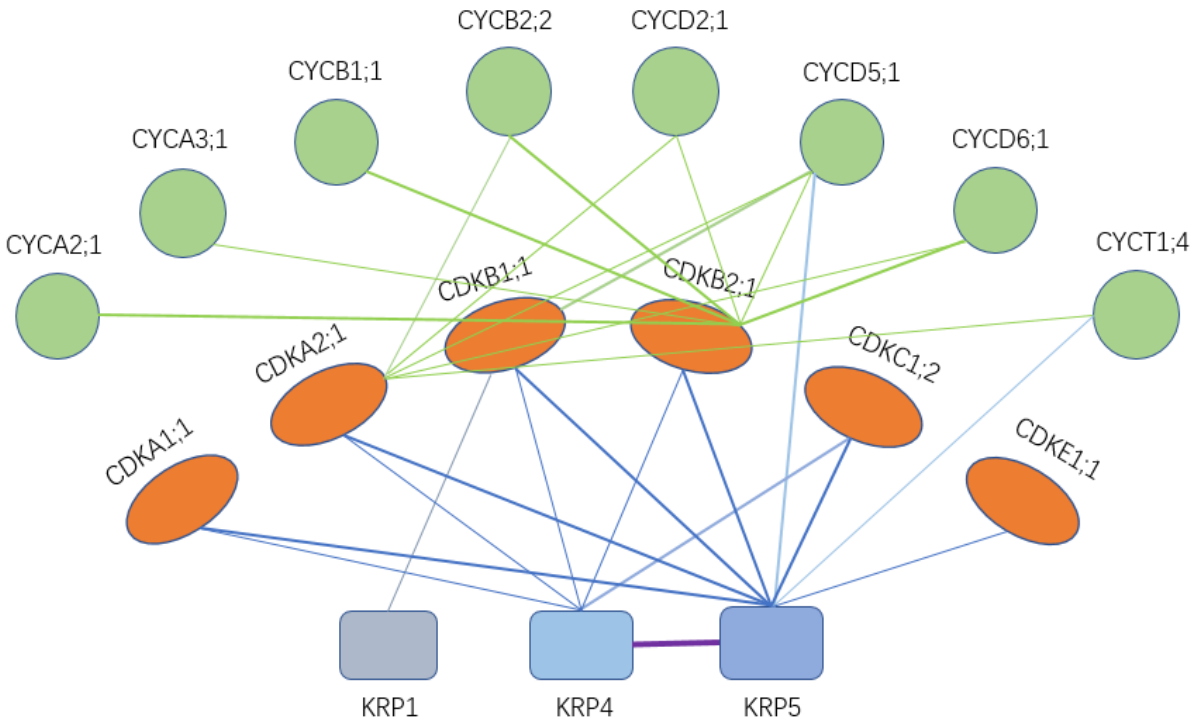

Fig. 2 E. The scheme representing Y2H based interactome of cell cycle core complexes in rice egg cells and zygotes.

III. Verification of the protein interactions in co-immunoprecipitation (Co-IP)

In the above PPI networks, there are four types of rice CDKs (A, B, C and E) interacting with both KRP5 and KRP4. According to previous studies in plants, these CDKs play important roles in plant cell cycle and plant development. CDKA is a key regulator at the checkpoints of G1-S and G2-M, essential for the male gametogenesis (Nowack et al 2006, Dissmeyer et al 2007 and Harashima et al 2007); CDKC works with CYCT for the elongation and splicing in transcription (Kitsios et al 2008); CDKE functions in leaf cell expansion and floral cell-fate specification (Wang and Chen 2004). However, only CDKB proteins are plant specific. There are two major classes of CDKB (B1 and B2) expressed during S-G2 (B1) or G2-M (B2) and active at the G2-M boundary. Therefore, CDKB proteins are essential for cell division (mitosis) which is required for normal cell cycle progression in plants (Boudolf et al 2004, Andersen et al 2008, Leene et al 2011 and Atkins and Cross 2018). Considering our limited research resource, we focus on analyzing the PPIs of the two putative rice CDKB (B1 and B2) with rice KRP5 and KRP4 in Co-IP assay (Liu et al 2017 and Louche et al 2017) and the growth of yeast cells transformed with OsCDKB and OsKRPs on selective media in serial dilutions.

In the Co-IP assay, the budding yeast cell (*Saccharomyces cerevisiae*) were co-transformed with HA (9 amino-acid peptide of human influenza virus hemagglutinin) tagged CDKB1 (CDKB1-HA) and c-Myc (10 aa peptide human c-Myc protein) tagged both KRP5 and KRP4 (KRP5-Myc and KRP4-Myc). Due to the very low expression level of rice nuclear protein in yeast, it is difficult to detect the Co-IP signal from Western blotting. Therefore, we developed a practical procedure to isolate yeast nuclear protein and it is proved solving the problem for the Co-IP assay. As shown in Fig. 3 A (the purple bands), both c-Myc tagged KRP5 and KRP4 and HA-tagged CDKB1 are pulled down by the added mouse Anti-Myc monoclonal antibody from the total yeast nuclear proteins, demonstrating the interactions of both OsKRP5 with OsCDKB1 and

OsKRP4 with OsCDKB1 in yeast nuclei. Similarly, the blue signals detected in Fig. 3 B indicate the interactions of both OsKRP5 with OsCDKB2 and OsKRP4 with OsCDKB2. Following the same principle, the solid interaction between OsKRP5 and OsKRP4 is verified in Fig. 3 C.

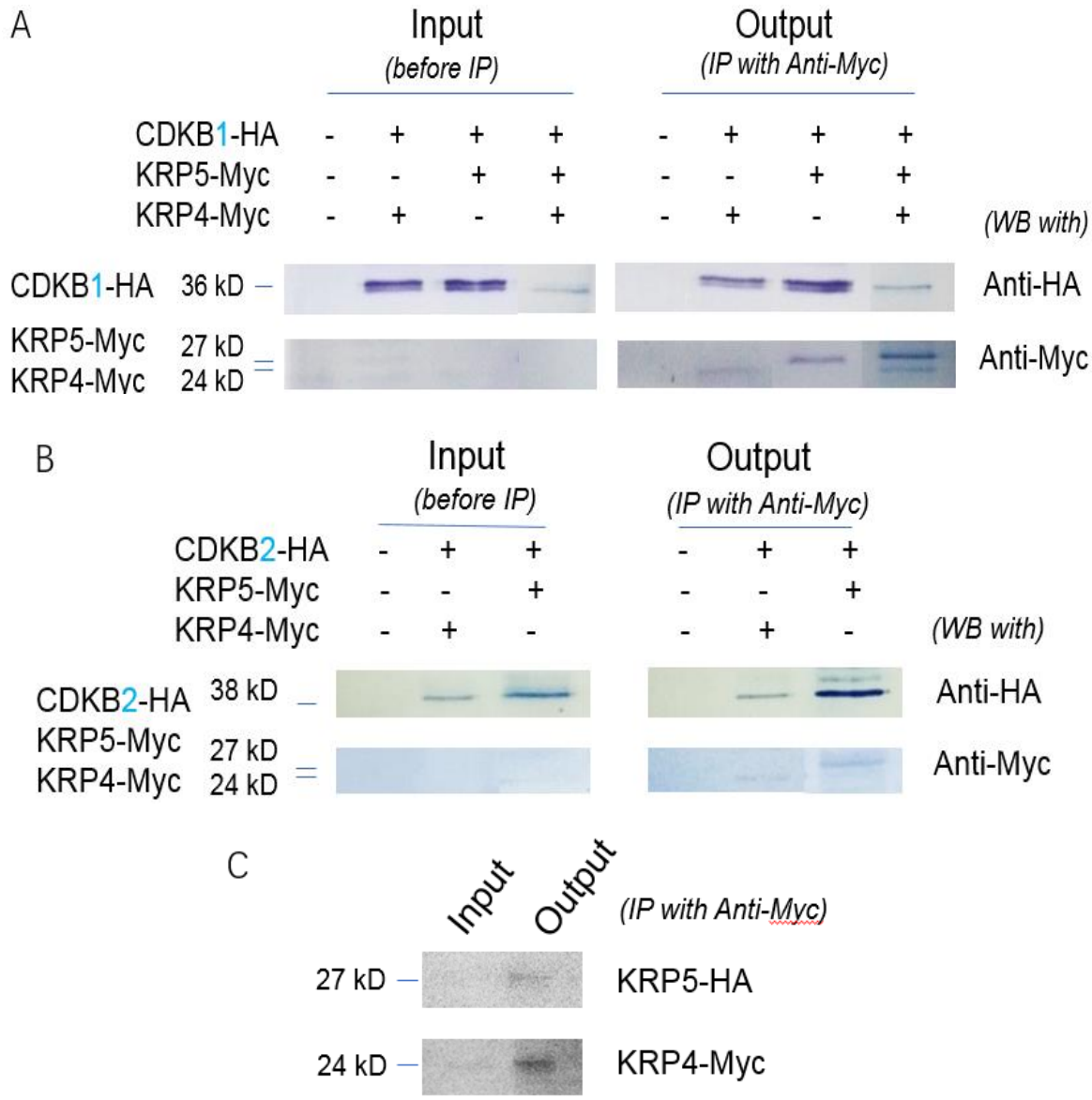

Fig.3 Co-IP assay for interactions of OsKRP5/OsKRP4 with CDKB1/CDKB2 and OsKRP5 with OsKRP4 in yeast. A. Nuclear proteins extracted from yeast cells harboring CDKB1-HA with KRP4-c-Myc or/and KRP5-cMyc; B. Nuclear proteins extracted from the cells harboring CDKB2-HA with KRP4-c-Myc or KRP5-cMyc; C. Nuclear proteins extracted from the cells

harboring both KRP5-HA and KRP4-c-Myc. Anti-HA and anti-c-Myc antibodies were to detect proteins with corresponding tags. The blots of A and B were visualized using 3, 3', 5, 5'-tetramethylbenzidin (*TMB) as the substrate of horseradish peroxidase (HRP); the blot of C was detected in chemiluminescent system.*

IV. The effect of rice cell cycle control proteins on yeast growth

The yeast growth assay (Fig. 4 A) shows us that the transformation with single rice cell cycle

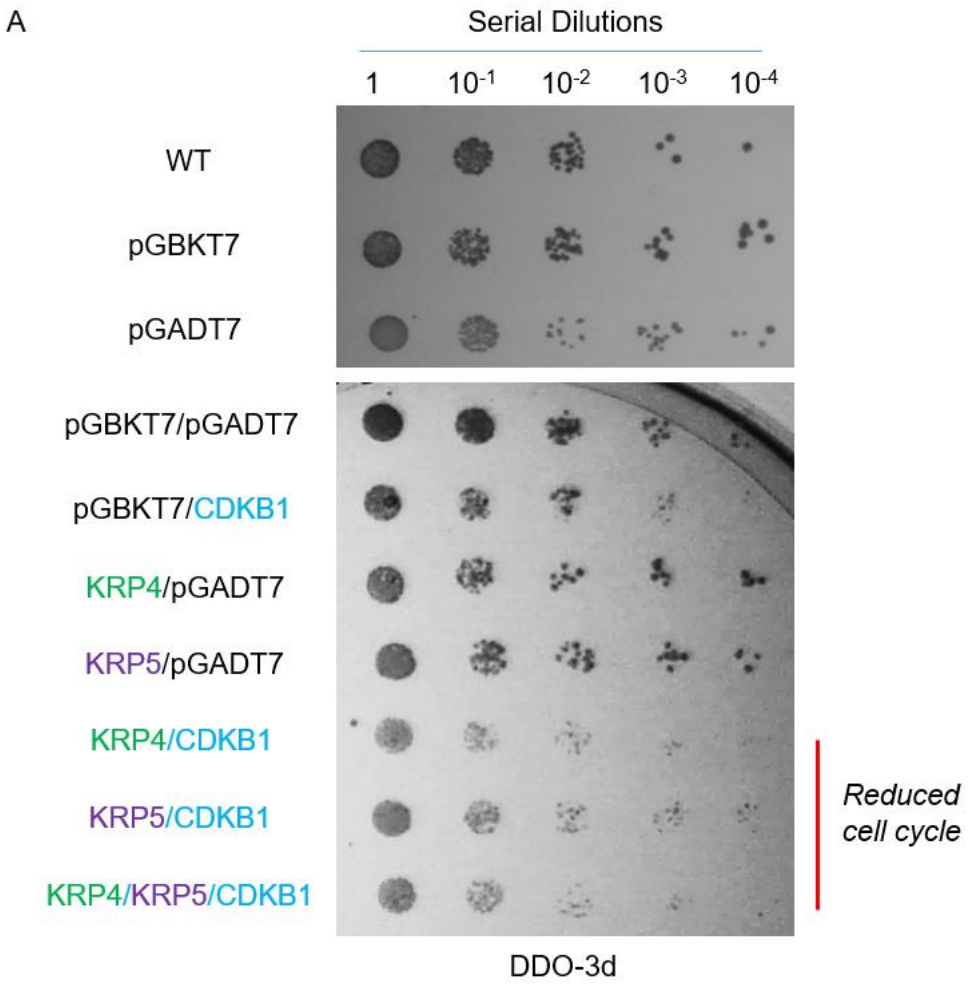

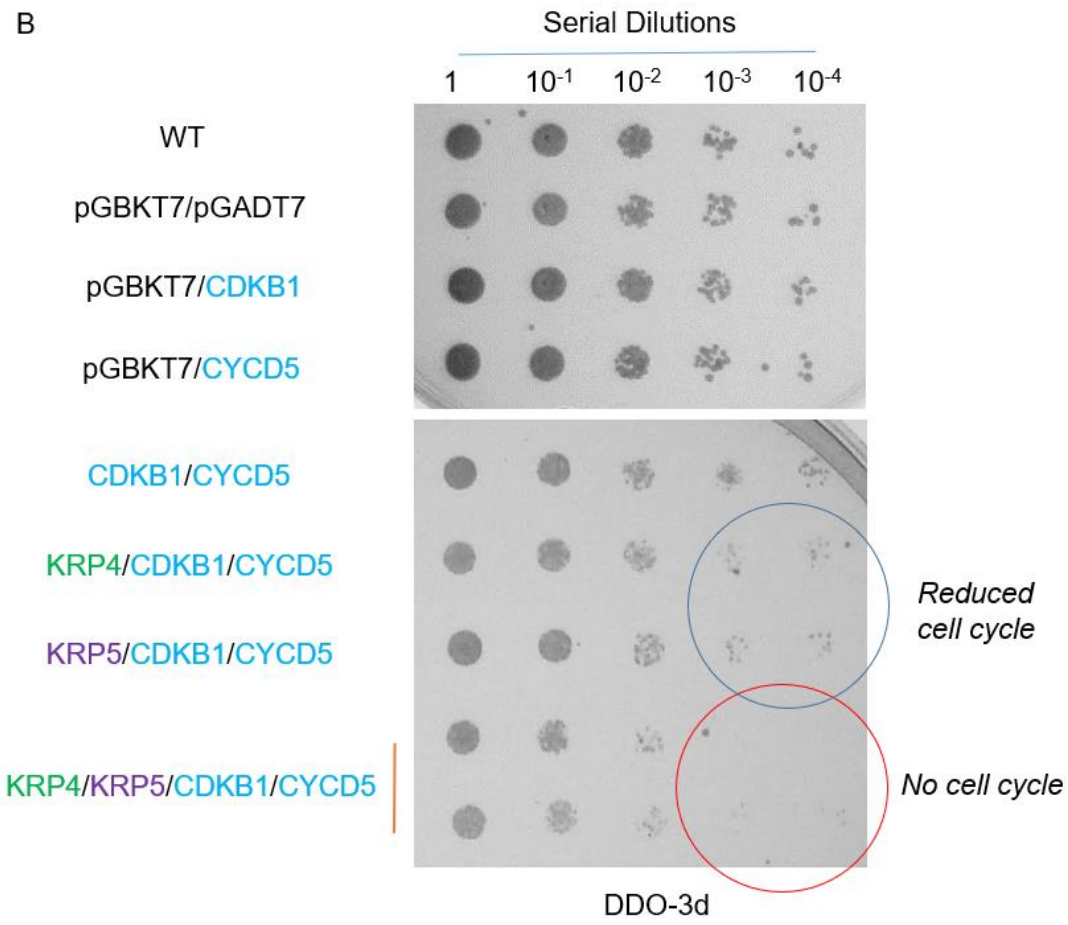

Fig. 4 The growth in serial dilutions of yeast cells transformed with rice cell cycle encoding genes indication the interaction of rice CDKB1 with KRP5 and KRP4. A. Yeast cells harboring OsCDKB1 and OsKRP4 or/and OsKRP5 genes have reduced growth rate; B. Yeast cells harboring OsCDKB1 and OsKRP4 or/and OsKRP5 plus CYCD5 genes have significantly reduced growth rate. DDO-3d, growth on the selective medium SD/-Leu-Trp for 3 days.

control protein, either CDKB1 or KRP5 or KRP4, brought no obvious effect on yeast growth in serial dilutions in the selective DDO medium in contrast to the wildtype and other controls (yeast cells transformed with blank vectors).

But the co-transformation of OsCDKB1 with OsKRP5 or/and OsKRP4 significantly slower the

growth rate on DDO, indicating not only the *in vivo* interaction of OsCDKB1 with OsKRP5 or/and OsKRP4, and also the interfering or disruptive effect of these protein-protein interactions on the yeast growth.

From Fig. 4 B, co-transformation of OsKRP5 or OsKRP4 with both OsCDKB1 and OsCYCD5 did not result in significant change in yeast growth, however, the co-transformation of both OsKRP5 and OsKRP4 together with OsCDKB1 and OsCYCD5 obviously disrupted the normal yeast cell cycle and thus reduced the yeast growth rate on DDO medium, suggesting the potential cooperative relation between OsKRP5 and OsKRP4 in their molecular function to OsCDKB1.

V. Coordinated inhibitory effect of OsKRP5 and OsKRP4 on OsCDKB1;1 kinase activity

Both OsKRP5 and OsKRP4 have been previously regarded as inhibitors of OsCDK based on genomic database, but this is only putative without any biochemical evidence. In this study, we are the first in verifying their inhibitory function by measuring their effect on the kinase activity of OsCDKB1. The kinase activity had been traditionally tested in radioactive method (Manning et al 2002, Grant 2009 and Atkins and Cross 2018); due to unavailability of the required facility and for the safety, we adopted nonradioactive approach (Lewis et al 2013) using ADPsensor^{TM} Universal Kinase Activity Assay Kit (BioVision). In Fig. 5 A, the kinase activity of OsCDKB1 is about 52,000 in relative fluorescent unit (RFU) which is enhanced further to 62,000 RFU by OsCYCD5 (CDKB1+CYCD5); whereas the activity of OsCDKB1 is reduced to about 40,000 RFU with OsKRP4 and below 40,000 RFU with OsKRP5, respectively. Moreover, the CDK activity is dropped further to only 20,000 RFU when OsKRP4 is added with OsKRP5 (CDKB1+KRP4+KRP5). In contrast, this additive inhibition effect on CDKB1 activity is reversed in the reaction of with one mutated OsKRP (CDKB1 +KRP5 + KRP4m or CDKB1

+KRP4 + KRP5m). The similar inhibitory effect of OsKRP4 and OSKRP5 is observed on the activity of OsCDKB2 as shown in Fig. 5 B. The difference is that the additive inhibition of OsKRP4 + OsKRP5 to OsCDKB2 is not as significant as to OsCDKB1.

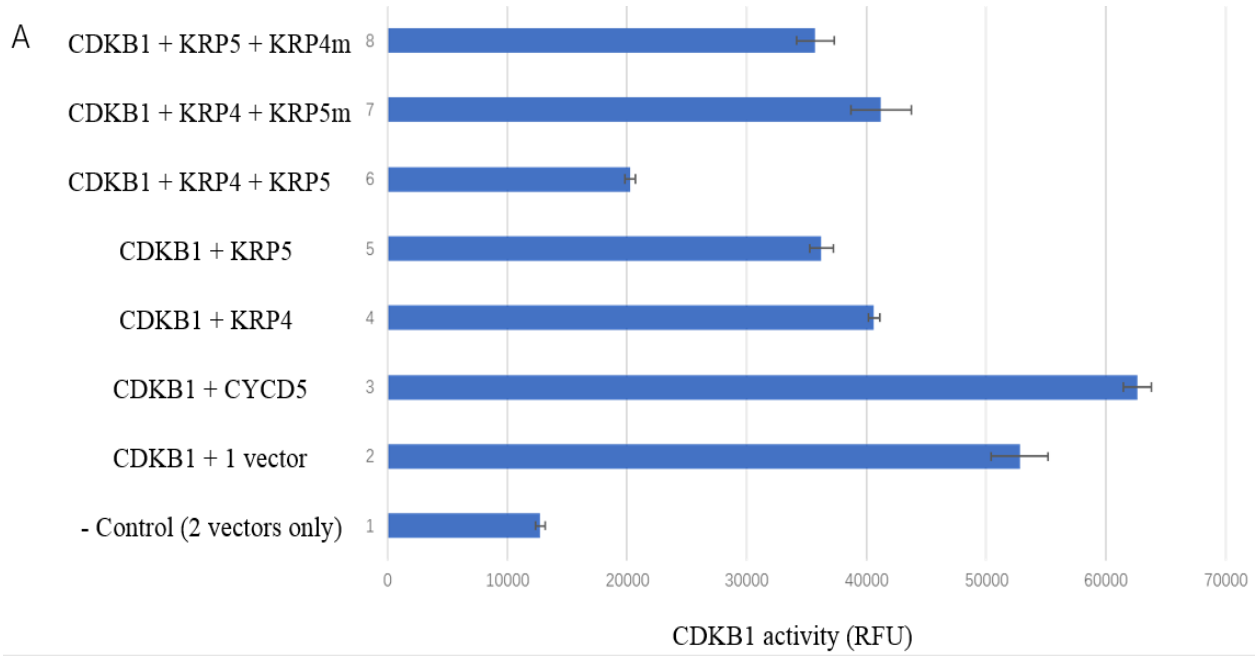

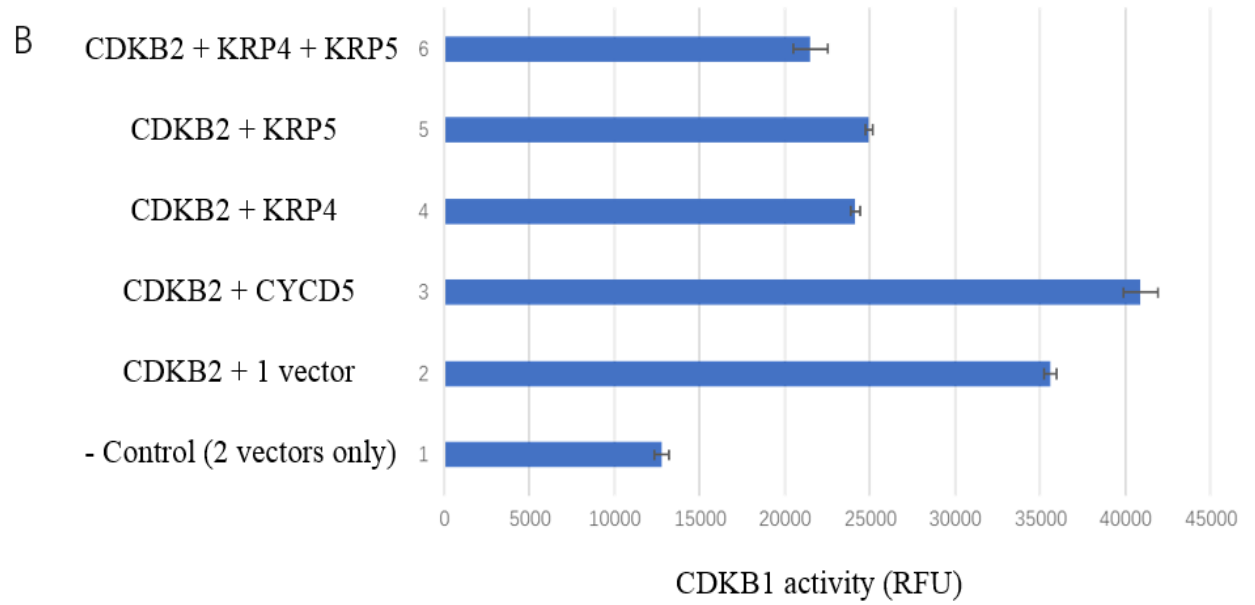

Fig. 5 Inhibitory Effect of OsKRP5 and OsKRP4 on Kinase Activity of OsCDKB1 (A) and

OsCDKB2 (B). The Kinase activity is measured in relative fluorescent unit (RFU) at EX/Em of 535/587 nm. KRP4m, truncated protein encoded by 5'-315 bp of OsKRP4; KRP5m, truncated protein encoded by 5'-530 of OsKRP5; CYCD5, rice Cyclin D5;1. The activities of CDKB1 (A) and CDKB2 (B) are raised by CYCD5 but inhibited by KRP5 and KRP4. The vector pGBKT7 and pGADT7 were used for the negative control. Error bar, Standard Deviation; n=3 (3 biological replicates).

VI. BiFC assay for interactions of cell cycle control proteins in rice egg cells and zygotes

In Bimolecular Fluorescent Complementation (BiFC), the two split fluorescent molecules (N'- and C'- fragments without fluorescence on their own) are fused with two candidate interaction partners, separately. If the two protein interact each other, the two separate fluorescent fragments will be re-associated as the complex emitting the fluorescence to be detected in microscopy. Numerous studies have proved BiFC as an inexpensive but sensitive and *in vivo* assay for detection of protein-protein interactions (PPIs), and thus have been widely used (Walter et al 2004, Morell et al 2008, Leene et al 2011, Wang et al 2013, Horstman 2014, Lee and Gelvin 2014, Kudla and Bock 2016, Koiso et al 2017 and Toda et al 2019). However, because of the restriction in accessibility to the cells deeply embedded within plant ovary and the difficulty in manipulating manually isolated and very vulnerable cells, no BiFC in plant egg cells or zygotes has previously reported. In order to verify the above observed PPIs among components of rice cell cycle complexes, we developed an efficient procedure for BiFC in rice egg cells and zygotes. As shown in Fig. 6 A, the green fluorescent signals under the mark "BiFC" represent the positive interactions between OsKRP4 and OsCDKB1 in rice egg cell (0h) and zygotes (2h after pollination), and these interactions take place in nuclei as indicated by their overlapping with the red signal of $mCherry_{NLS}$ (the positive control for nuclear localization). This is consistent with

the known feature of OsKRP4 as the nuclear protein (Chapter 1). The PPIs of OsKRP5 with OsCDKB1 were also observed in rice egg cell (0h) and zygotes (2h and 8h after pollination) (Fig. 6 B); they are nuclear localized, too, consistent with the nuclear feature of OsKRP5 (Chapter 1).

Just as what is observed in the assays of Y2H, Co-IP, yeast growth and Kinase activity measurement, is OsCDKB1 bound by both OsKRP5 and OsKRP4 in rice egg cells and zygotes? To address this issue, we performed multi-color BiFC (mcBiFC, Lee and Calvin 2008 and 2014). The regular BiFC tests the interaction between one bait protein and one prey preotein, but the mcBiFC detects PPIs of one bait protein with two prey proteins. In our mcBiFC, OsCDKB1-Ccfp was used as the bait and OsKRP4-nVenus and OsKRP5-nCerulean used as the two preys. As a result, both OsKRP5 and OsKRP4 positively react with OsCDKB1 in rice egg cells (0h) transfected with the construct $CDKB1_{promoter}$-CDKB1-cCFP::$Ubiquitin_{promoter}$-KRP4-nVenus:: $KRP5_{promoter}$- KRP5-nCerulean (Fig.7).

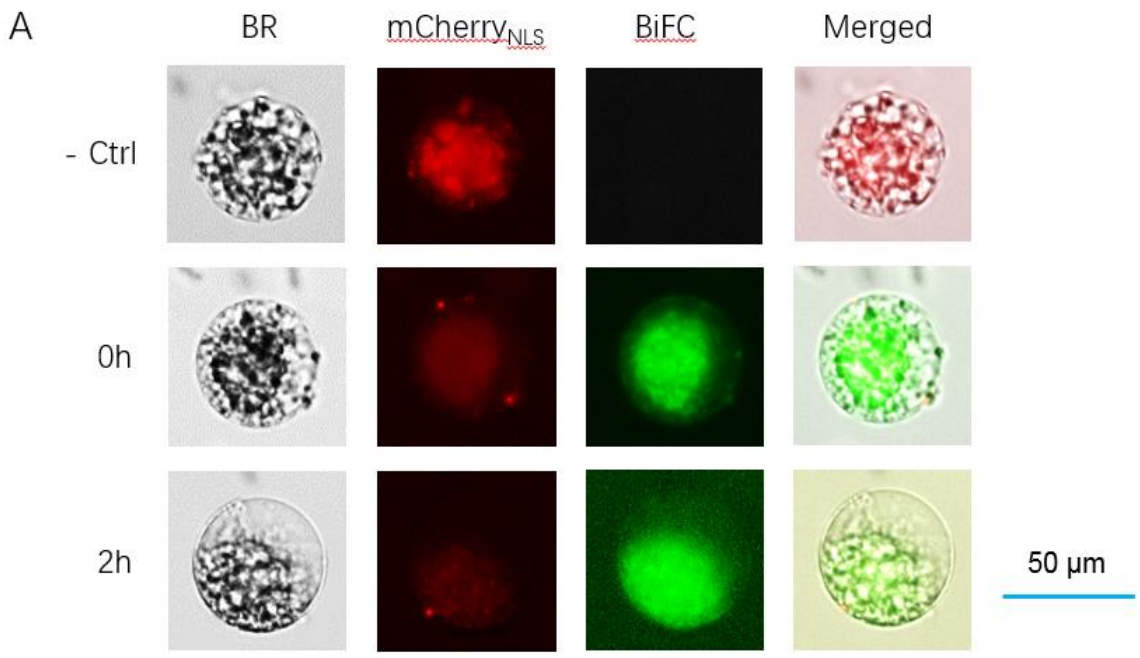

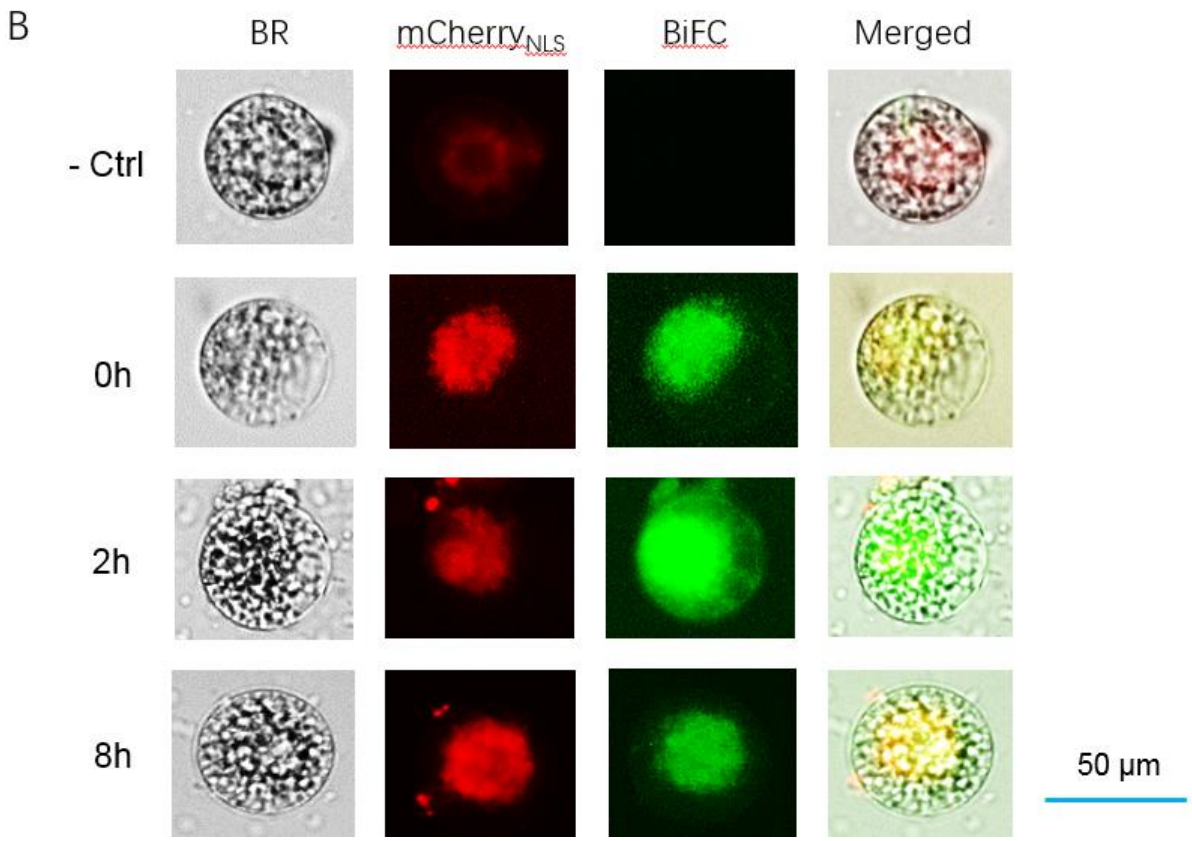

Fig. 6 BiFC assay for interactions of core cell cycle proteins in rice egg cells and zygotes. ***A****. BiFC shows the interaction of OsKRP4 with OsCDKB1 in the egg cell (0h) and zygote (2 HAP) transfected with the construct Ubiq$_{promoter}$-KRP4-nEYFP::CDKB1$_{promoter}$-CDKB1- cEYFP;* ***B****. BiFC shows the interaction of OsKRP5 with OsCDKB1 in the egg cell (0h) and zygotes (2 HAP and 8 HAP) transfected with the construct KRP5$_{promoter}$-KRP5 -nEYFP::CDKB1$_{promoter}$-CDKB1-cEYFP. The construct nEYFC with cEYFC is used as negative control; mCherry$_{NLS}$ is used for nuclear localization; BR is to show the cell images in gray under the bright field; Merged image is derived from overlapping all other images to show that the different fluorescent signals are detected from the same cell.*

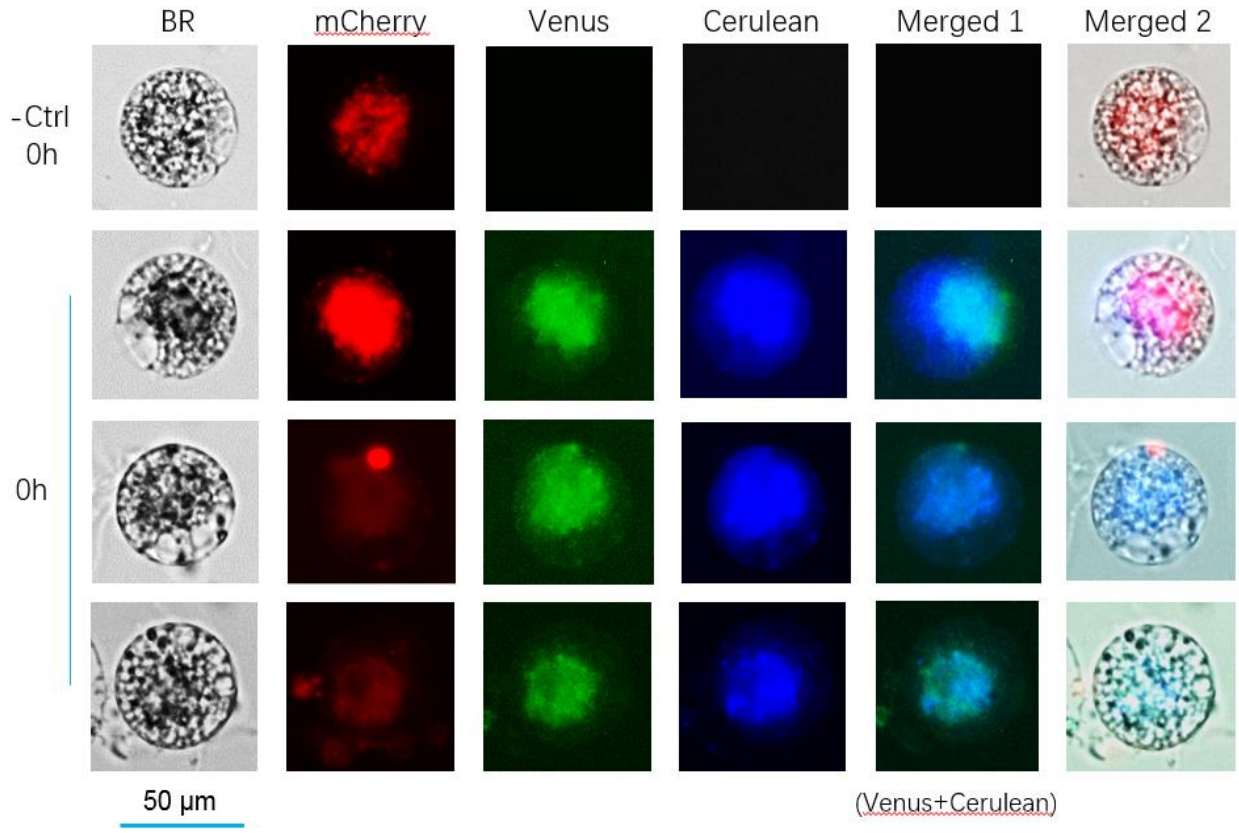

Fig. 7. Multi-color BiFC (mcBiFC) assay for interactions of both OsKRP5 and OsKRP4 with OsCDKB1 in rice egg cells (0h) transfected with the construct CDKB1-cCFP :: KRP4- nVenus + KRP5-nCerulean under native promoters. Venus indicates the interaction of OsKRP4 with OsCDKB1 and Cerulean is for the interaction between OsKRP5 and OsCDKB1. The construct nEYFC and cEYFC are used as negative control; $mCherry_{NLS}$ is used for nuclear localization; BR is to show the cell images in gray under the bright field; Merged image is derived from overlapping other two images (as indicated for Merged 1) or all other images (Merge 2) to show that the different fluorescent signals are detected from the same cell.

KRP proteins in rice zygotes and had at least three observations for each different developmental stages (0 HAP, 2 HAP and 9 HAP). Fig. 8 A shows the representive BiFC images at the three

developmental stages each of which indicates the positive interaction; Fig. 8 B shows the mean intensity of fluorescent signals (RFU) from the transfected cells at each stage. The signal intensity is slightly increased in 2 HAP-zygotes compared to the egg cells (0h), but significantly decreased in 8 HAP-zygotes. Considering that both OsKRP5 and OsKRP4 function as the

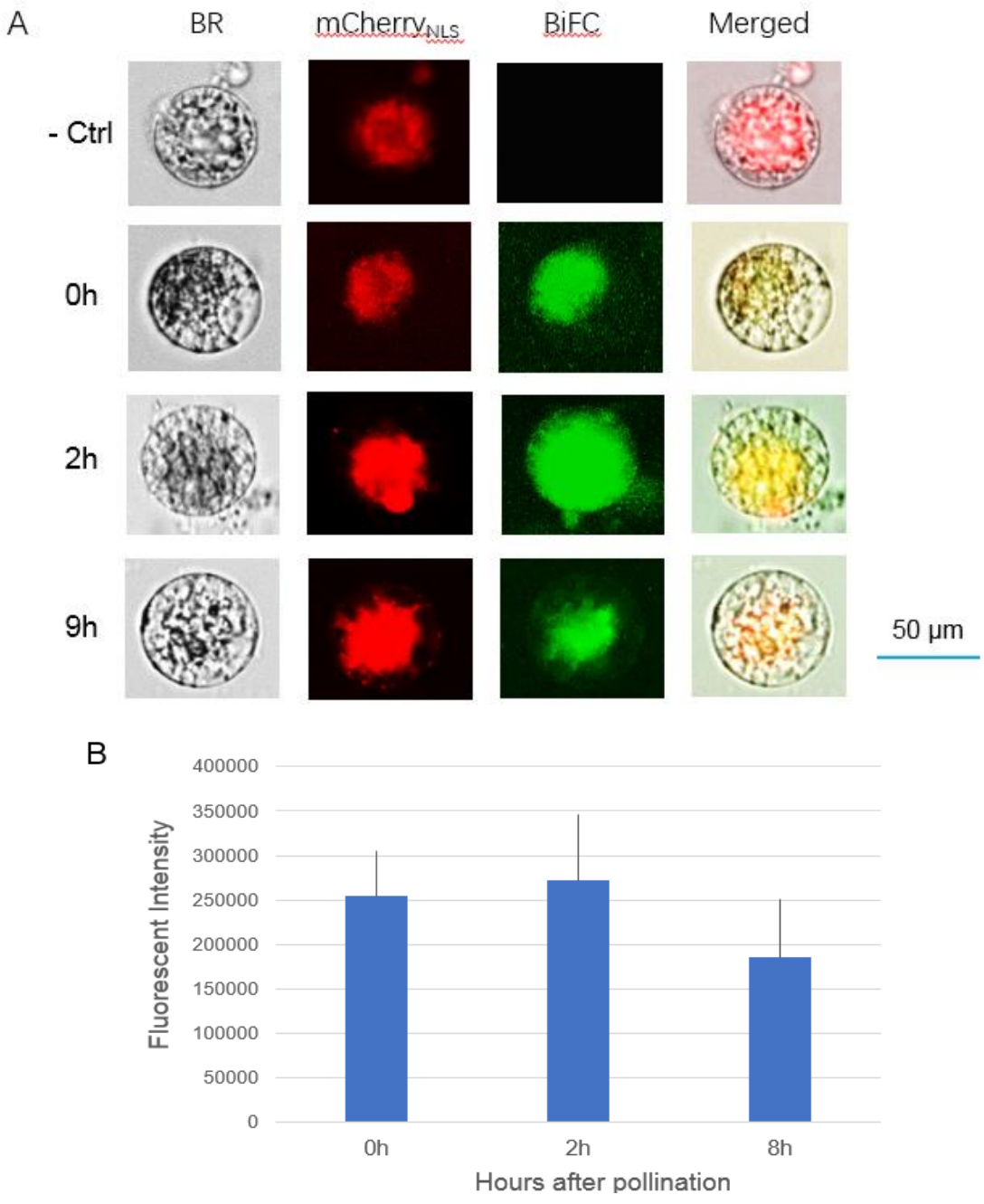

Fig. 8 BiFC assay for the interaction of OsKRP4 and OsKRP5 in rice egg cell and zygotes. ***A***.

BiFC shows the interaction of OsKRP4 with OsKRP5 in the egg cell (0h) and zygotes (2 AHP and 8 HAP) transfected with the construct $Ubiq_{promoter}$*-KRP4-nEYFP::KRP5*$_{promoter}$*-KRP5-cEYFP. The construct nEYFC with cEYFC is used as negative control;* $mCherry_{NLS}$ *is used for nuclear localization; BR is to show the cell images in gray under the bright field; Merged image is derived from overlapping other two images to show that the different fluorescent signals are detected from the same cell.* ***B****. The mean fluorescence intensity from the transfected cells at different developmental stages. Error bar, standard deviation; n = 3 ~ 6.*

inhibitors of OsCDKB1 and OsCDKB2 (Fig.5), the lowered signal intensity at 9 HAP reflects the reasonable regulation when cell cycle procession is approaching to the crucial developmental stage: the first zygotic division (around 12 HAP).

To sum up, we established a model for one of core complexes in rice zygotic cell cycle (Fig. 9). The model is simple but supported by the evidence from multiple assays including Y2H, Co-IP, yeast growth, CDK activity change and BiFC in rice zygotes at different developmental stages. It demonstrates three main points as the following.

1. Kinase activity of OsCDKB1 is CYCD5 dependent but inhibited by OsKRP5 and OsKRP4.
2. OsKRP5 and OsKRP4 physically interact each other and functionally cooperate in inhibiting CDKB1. The two KRP proteins may simply work as a heterodimer. The advantages of such a coordination for cell cycle control may include its stablilty and redundancy which is important to keep the cell cycle progression (at least partially) in case one of the two is disfunctioned.

   The coordinate relation between OsKRP5 and OsKRP4 might be universal in the cell cycle control in plants (even in animal and human?). For instance, both KRP6 and KRP7 present in

the spermatogenesis in Arabidopsis, and both KRP1 and KRP2 are preferntically expressed in rice sperm cells as indicated in supplemental Fig. 1. More examples need to be further investigated.

3. This core complex is essential for the control at the checkpoint of zygotic mitosis, the first step of embryo development for rice seed formation.

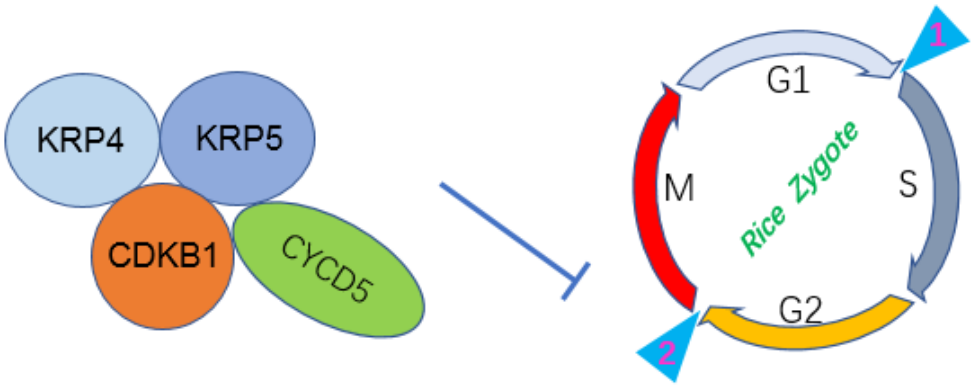

Fig. 9 The model of core complex *for rice zygotic cell cycle control at the checkpoint G2-M. The blue arrowheads indicate two important checkpoints in cell cycle control (#1 is for S-phase entry and # 2 for mitosis). Both KRP5 and KRP4 coordinately inhibit CDKB1 activity against mitosis for the first division of rice zygote.*

- Other clues for supporting the model of core cell cycle complex in rice zygotes

In addition, we did the phylogenetic analysis of OsKRP5 and OsKRP4. As shown in Fig.10, all four KRP5 members of cereal crop plant (in blue circle) and all four KRP4 members of cereal crop plant (in green circle) are clustered, separately, but the two clusters are relatively closer, showing their evolutionary relationship of the two KRP genes, as an indirect support for their cooperation in molecular function. Regarding other KRPs, one KRP6, three KRP3, two KRP2 and four KRP1 species of plant are grouped relatively closer together than those of KRP4 and

KRP5.

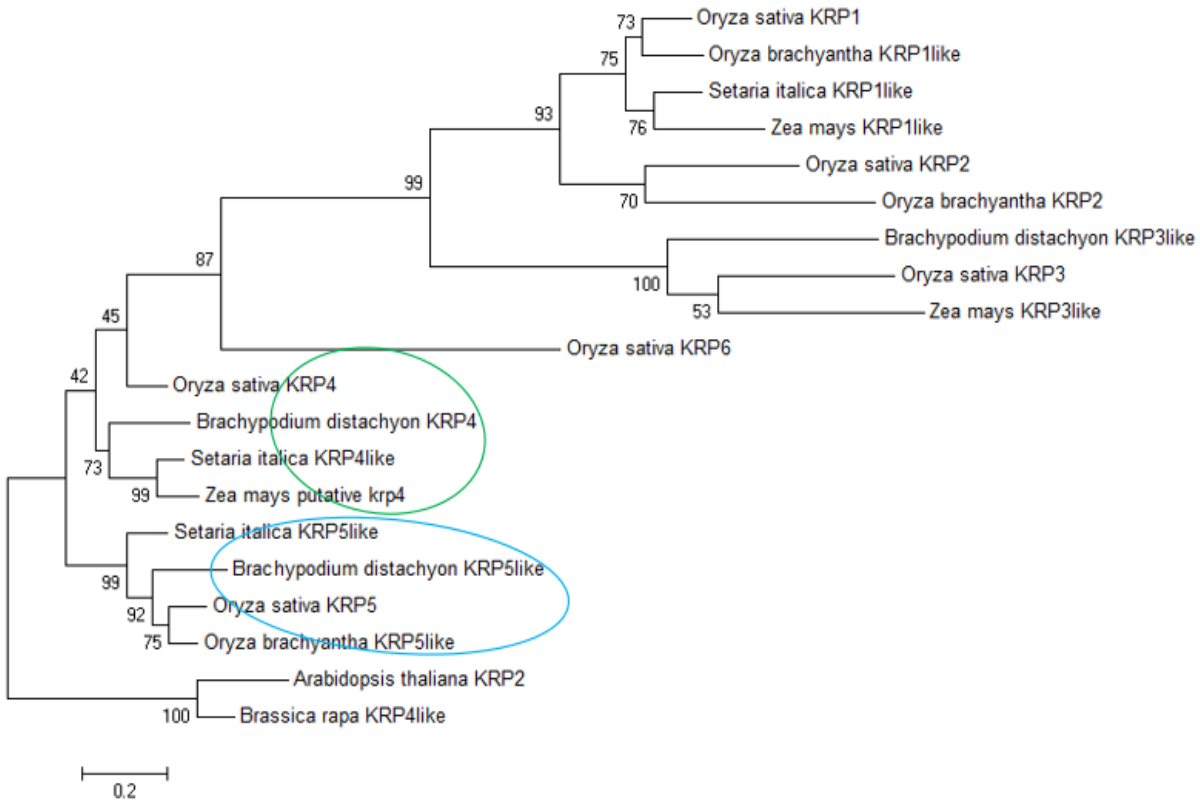

Fig. 10 Phylogenetic analysis of cereal crop plant KRPs. The coding sequences of 20 KRP genes were aligned and the tree was produced using MEGA6, illustrating the closer phylogenetic relationship of KRP5 and KRP4 encoding genes. The number to the scale indicates the percentage of genetic variation (the total phylogenetic distance should <=1).

According the previous studies in rice (Juan Antonio Torres Acosta, et al 2011, Masanori Mizutani 2010 and Ruifang Yang, et al 2011), KRP1~3 and KRP6 are involved in the vegetative growth and development in plants; on the other hand, our study shows that KRP5 and KRP4 are involved in the cell cycle control in rice egg cells and zygotes. Given this context, the clustering patterns of KRP5 and KRP4 seems corresponding to their patterns of interaction or molecular function. In addition, considering the coding sequence (CDS) is the original sequencing data,

instead of translated protein sequence or derived secondary structure, the evolutionary relationship reflected in this tree makes a better sense.

References

Acosta JAT, Fowke LC and Wang H (2011) Analyses of phylogeny, evolution, conserved sequences and genome-wide expression of the ICK/KRP family of plant CDK inhibitors. Ann Bot 107, 1141-1157

Ajadi AA, Tong X, Wang H, Zhao J, Tang L, Li Z, Liu X, Shu Y, Li S, Wang S, Liu W, Tajo SM, Zhang J, and Wang Y (2020) Cyclin-dependent kinase inhibitors KRP1 and KRP2 are involved in grain filling and seed germination in rice (*Oryza sativa L.*). International Journal of Molecular Sciences. 21 (245), 1-16

Andersen SU, Buechel S, Zhao Z, Ljung K, Novák O, Busch W, Schuster C, Lohmann JU (2008) Requirement of B2-typecyclin-dependent kinases for meristem integrity in Arabidopsis thaliana. Plant Cell 20, 88-100

Atkins KC and Cross FR (2018) Interregulation of CDKA/CDK1 and the Plant-Specific Cyclin-Dependent Kinase CDKB in Control of the Chlamydomonas Cell Cycle. The Plant Cell. 30, 429–446

Barrôco RM, Peres A, Droual AM, De Veylder L, Nguyen le SL, De Wolf J, Mironov V, Peerbolte R, Beemster GT, Inzé D, Broekaert WF, Frankard V (2006) The cyclin-dependent kinase inhibitor Oryza; KRP1 plays an important role in seed development of rice. Plant Physiol. 142, 1053-1064

Bisbis B, Delmas F, Joubes J, Sicard A, Hernould M, Inzé D, Mouras A, Chevalier C (2006) Cyclin-dependent kinase (CDK) inhibitors regulate the CDK-cyclin complex activities in

endoreduplicating cells of developing tomato fruit. Journal of Biological Chemistry. 281, 7374-7383

Boudolf V, Vlieghe K, Beemster GTS, Magyar Z, Acosta JAT, Maes S, Schueren EVD, Inzé D, De Veylder L (2004) The plant-specific cyclin-dependent kinaseCDKB1;1 and transcription factor E2Fa-DPa control the balance of mitotically dividing and endoreduplicating cells in Arabidopsis. Plant Cell. 16, 2683-2692

Cao L, Wang S, Venglat P, Zhao L, Cheng Y, Ye S, Qin Y, Datla R, Zhou Y and Wang H (2018) Arabidopsis ICK/KRP cyclin-dependent kinase inhibitors function to ensure the formation of one megaspore mother cell and one functional megaspore per ovule. PLOS Genetics, 1-30

Cheng, Y., Cao, L., Wang, S., Li, Y., Shi, X., Liu, H., Li, L., Zhang, Z., Fowke, L.C., Wang, H., Zhou, Y. (2013). Downregulation of multiple CDK inhibitor ICK/KRP genes upregulates the E2F pathway and increases cell proliferation, and organ and seed sizes in Arabidopsis. Plant J. 75, 642-655

Cheng Y, Liu H, Cao L, Wang S, Li Y, Zhang Y, Jiang W, Zhou Y, Wang H (2015) Down-regulation of multiple CDK inhibitor ICK/KRP genes promotes cell proliferation, callus induction and plant regeneration in Arabidopsis. Front Plant Sci. 13(6), 825

Coelho CM, Dante RA, Sabelli PA, Sun YJ, Dilkes BP, Gordon-Kamm WJ, Larkins BA et al. (2005) Cyclin-dependent kinase inhibitors in maize endosperm and their potential role in endoreduplication. Plant Physiology. 138, 323-2336

Dante RA, Larkins BA and Sabelli PA (2014) Cell cycle control and seed development. Frontiers in Plant Science. 493, 1-14

De Veylder L, Beeckman T, Beemster GT, Krols L, Terras F, Landrieu I, van der Schueren E,

Maes S, Naudts M, and Inzé D (2001) Functional analysis of cyclin-dependent kinase inhibitors of Arabidopsis. Plant Cell *13*, 1653-1668

De Veylder L, Beeckman T and Dirk Inzé (2007) The ins and outs of the plant cell cycle. Nature Reviews Molecular Cell Biology. 8, 655-665

Dissmeyer N, Nowack MK, Pusch S, Stals H, Inzé D, Grini PE, Schnittger A (2007) T-loop phosphorylation of Arabidopsis CDKA;1 is required for its function and can be partially substituted by an aspartate residue. Plant Cell1. 9, 972-8561

Dove E, Brockenbrough JS and Aris JP (1998) Isolation of Nuclei and Nucleoli from the Yeast *Saccharomyces cerevisiae*. J Methods Cell Biol. 53, 33-46

Dudits D, Cserháti M, Miskolczi P, and Horváth G V (2007) "The growing family of plant Cyclin-Dependent Kinases with multiple functions in cellular and developmental regulation," in *Annual Plant Reviews*, Vol. 32, *Cell Cycle Control and Plant Development*, ed. D. Inzé (Oxford: Blackwell Publishing Ltd), pp1–30

Ferro E and Trabalzini L (2013) The yeast two-hybrid and related methods as powerful tools to study plant cell signaling. Plant Mol. Biol. *83*, 287-301

Fields S and Song O (1989) A novel genetic system to detect protein–protein interactions. Nature 340, 245-246\

Friedman WE (1999) Expression of the cell cycle in sperm of Arabidopsis: implication for understanding patterns of gametogenesis and fertilization in plants and other eukaryotes. Development, 126, 1065-1075

Grant SK (2009) Therapeutic protein kinase inhibitors. Cell Mol Life Sci., 66(7), 1163-1177

Guo J, Song J, Wang F, Zhang XS (2007) Genome-wide identification and expression analysis of rice cell cycle genes. Plant Mol Biol. 64(4), 349-60

Harashima H, Shinmyo A, Sekine M (2007) Phosphorylation of threonine 161 in plant cyclin-dependent kinase A is required for cell division by activation of its associated kinase. Plant J. 52, 435-44862

Himanen K, Boucheron E, Vanneste S, de Almeida Engler J, Inze D, Beeckman T (2002) Auxin-mediated cell cycle activation during early lateral root initiation. *Plant Cell.* 14, 2339-2351

Horstman A, Tonaco IAN, Boutilier K, Immink RGH (2014) A Cautionary Note on the Use of Split-YFP/BiFC in Plant Protein-Protein Interaction Studies. International Journal of Molecular Sciences 15, 9628-9643

Hu X, Cheng X, Jiang H, Zhu S, Cheng B and Xiang Y (2010) Genome-wide analysis of cyclins in maize (Zea mays). Genet. Mol. Res. 9, 1490-1503

Jasinski S, Leite CS, Domenichini S, Stevens R, Raynaud C, Perennes C, Bergounioux C and Glab N (2003) NtKIS2, a novel tobacco cyclin-dependent kinase inhibitor is differentially expressed during the cell cycle and plant development. *Plant Physiology and Biochemistry.* 41:667-676

Jégu T, Latrasse D, Delarue M, Mazubert C, Bourge M, Hudik E, Blanchet S, Soler MN, Charon C, De Veylder L, Raynaud C, Bergounioux C, Benhamed M (2013) Multiple functions of Kip-related protein5 connect endoreduplication and cell elongation. Plant Physiol. 161(4), 1694-1705

Jing Guo J, Song J, Wang F and Zhang XS (2007) Genome-wide identification and expression analysis of rice cell cycle genes. Plant Mol Biol, 64, 349-360

Jones, D (2014). Reproductive development in two plant models: in situ visualization of the female gametophyte and transcriptomic analysis of cell cycle regulation in Oryza sativa post-fertilization. Master's degree Thesis, University of Oklahoma

Kelley LA, Mezulis S, Yates CM, Wass MN and Sternberg MJE (2015) The Phyre2 web portal

for protein modeling, prediction and analysis. Nature Protocols, 10, 845-858

Kim, H.J., Oh, S.A., Brownfield, L., Hong, S.H., Ryu, H., Hwang, I., Twell, D., and Nam, H.G. (2008) Control of plant germline proliferation by SCFFBL 17 degradation of cell cycle inhibitors. Nature *455*, 1134-1137

Kitsios G, Alexiou KG, Bush M, Shaw P, Doonan JH (2008) A cyclin-dependent protein kinase, CDKC2, colocalizes with and modulates the distribution of spliceosomal components in Arabidopsis. Plant J.54, 220-235

Koiso N, Toda E, Ichikawa M, Kato N, Okamoto T (2017) Development of gene expression system in egg cells and zygotes isolated in rice and maize, Plant Direct, 1-10

Kudla J and Bock R (2016) Lighting the Way to Protein-Protein Interactions: Recommendations on Best Practices for Bimolecular Fluorescence Complementation Analyses. Plant Cell 28, 1002-1008

La H, Li J, Ji Z, Cheng Y, Li X, Jiang S, Venkatesh PN and Ramachandran S (2006) Genome-wide analysis of cyclin family in rice (*Oryza Sativa L.*). Mol. Genet. Genomics 275, 374-386

Lee LY, Fang MJ, Kuang LY and Gelvin SB (2008) Vectors for multi-color bimolecular fluorescence complementation to investigate protein-protein interactions in living plant cells. Plant Methods. 4, 24-34

Lee L. and Gelvin, SB **(**2014) Bimolecular Fluorescence Complementation for imaging protein interactions in plant hosts of microbial pathogens. In Annette C. Vergunst and David O'Callaghan (eds.), Host-Bacteria Interactions: Methods and Protocols, Methods in Mol. Biol., Springer Science+ Business Media New York *1197*, pp185-208

Leene JV, Boruc J, De Jaeger G, Russinova E and De Veylder L (2011) A kaleidoscopic view of the Arabidopsis core cell cycle interactome. Trends in Plant Science, 16 (3), 141-150

Lewis CW, Taylor RG, Kubara PM, Marshall K, Meijer L, Golsteyn RM (2013) A western blot assay to measure cyclin dependent kinase activity in cellsor in vitro without the use of radioisotopes. FEBS Letters. 587, 3089-3095

Lin HY, Chen JC, Wei MJ, Lien YC, Li HH, Ko SS, Liu ZH, Fang SC (2014) Genome-wide annotation, expression profiling, and protein interaction studies of the core cell-cycle genes in Phalaenopsis Aphrodite. Plant Mol Biol. 84, 203-26

Liu X, Liu R, Li Y, Shen X, Zhong S and Shi H (2017) EIN3 and PIF3 Form an Interdependent Module That Represses Chloroplast Development in Buried Seedlings. The Plant Cell, 29, 3051-3067

Louche A, Salcedo S P and Bigot S (2017) Chapter 20. Protein–Protein Interactions: Pull-Down Assays. Laure Journal and Eric Cascales (eds) Bacterial Protein Secretion Systems: Methods and Protocols, Methods in Molecular Biology, Springer Science + Business Media LLC, vol. 1615, pp247-255

Lui H, Wang H, Delong C, Fowke LC, Crosby WL, Fobert PR (2000) The Arabidopsis Cdc2a-interacting protein ICK2 is structurally related to ICK1 and is a potent inhibitor of cyclin-dependent kinase activity *in vitro*. Plant Journal. 21:379-385

Ma Z, Wu Y, Jin J, Yan J, Kuang S, Zhou M, Zhang Y and Guo AY (2013). Phylogenetic analysis reveals the evolution and diversification of cyclins in eukaryotes. Mol. Phylogenet. Evol. 66, 1002-1010

Manning G, Whyte D B, Martinez R, Hunter T, Sudarsanam S (2002) The protein kinase complement of the human genome. Science, 298, 1912-1934.

Mizutani, M., Naganuma, T., Tsutsumi, K. N., and Saitoh, Y. (2010) The syncytium-specific expression of the Orysa; KRP3 CDK inhibitor: implication of its involvement in the cell cycle

control in the rice (*Oryza sativa L.*) syncytial endosperm. J Exp Bot. *61*, 791-798

Morell M, Espargaro A, Aviles FX and Ventura S (2008) Study and selection of in vivo protein interactions by coupling bimolecular fluorescence complementation and flow cytometry. Nat. Protoc. 3, 22-33

Nowack MK, Grini PE, Jakoby MJ, Lafos M, Koncz C and Schnittger A (2006) A positive signal from the fertilization of the egg cell sets off endosperm proliferation in angiosperm embryogenesis. Nat. Genet. 38, 63-67

Pedroza-Garcia JA, Domenichini S and Raynaud C (2016) Plant cell cycle transitions. In: Rose RJ (ed) Molecular Cell Biology of the Growth and Differentiation of Plant Cells, CRC Press, pp 1-21

Schmittgen TD and Livak KJ (2008) Analyzing real-time PCR data by the comparative C-T method. Nat Protoc. 3, 1101-1108

Pettkó-Szandtner A, Cserháti M, Barrôco RM, Hariharan S, Dudits D and G. Beemster GTS (2015) Core cell cycle regulatory genes in rice and their expression profiles across the growth zone of the leaf. Journal of Plant Research. 128, 953-974

Pettko-Szandtner A, Meszaros T, Horvath GV, Bakó L, Csordás-Tóth E, Blastyák A, Zhiponova M, Miskolczi P, Dudits D (2006) Activation of an alfalfa cyclin-dependent kinase inhibitor by calmodulin-like domain protein kinase. Plant Journal. 46, 111-123

Ramos Coelho R, Vieira P, Antonino de Souza Junior JD, Martin-Jimenez C, De Veylder L, Cazareth J, Engler G, Grossi-de-Sa MF and de Almeida Engler J (2017) Exploiting cell cycle inhibitor genes of the KRP family to control root-knot nematode induced feeding sites in plants. Plant Cell Environ. 40(7), 1174-1188

Reese JC, Zhang H and Zhang Z (2008) Isolation of Highly Purified Yeast Nuclei for Nuclease

Mapping of Chromatin Structure. In Methods in Molecular Biology (MIMB) 463, pp43-53

Richard C, Lescot M, Inze D, De Veylder L (2002) Effect of auxin, cytokinin, and sucrose on cell cycle gene expression in *Arabidopsis thaliana* cell suspension cultures. Plant Cell, Tissue and Organ Culture. 69, 167-176

Ruggiero B, Koiwa H, Manabe Y, Quist TM, Inan G, Saccardo F, Joly RJ, Hasegawa PM, Bressan RA, Maggio A (2004) Uncoupling the effects of abscisic acid on plant growth and water relations. Analysis of sto1/nced3, an abscisic acid-deficient but salt stress-tolerant mutant in Arabidopsis. Plant Physiology. 136, 3134-3147

Schmittgen TD, Livak KJ (2008) Analyzing real-time PCR data by the comparative C-T method. Nat Protoc. 3, 1101-1108

Stals H and Inze D (2001) When plant cells decide to divide. Trends in Plant Science, 6 (8), 359-364

Szandtner AP, Cserháti M, Barrôco RM, Hariharan S, Dudits D and.Beemste GTS (2015) Core cell cycle regulatory genes in rice and their expression profiles across the growth zone of the leaf. J Plant Res. 128, 953-974

Tamura K, Stecher G, Peterson D, Filipski A, and Kumar S (2013) MEGA6: Molecular Evolutionary Genetics Analysis Version 6.0. Mol Biol Evol. 30(12), 2725-2729.

Tian, H. Q., Yuan, T., and Russell, S. (2005). Relationship between double fertilization and the cell cycle in male and female gametes of tobacco. Sex. Plant Reproduction 17, 243-252

Toda E, Koiso N, Takebayashi A, Ichikawa M, Kiba T, Osakabe K, Osakabe Y, Sakakibara H, Kato N and Okamoto T (2019) An efficient DNA- and selectable-marker-free genome-editing system using zygotes in rice. Nature Plants. **5**, 363-368

Van Leene J , Boruc J, Jaeger JD, Russinova E and Veylder LD (2011) A kaleidoscopic view of

the Arabidopsis core cell cycle interactome. Trends Plant Sci. 16(3), 141-50

Verkest A, Weinl C, Inzé D, De Veylder L and Schnittger A (2005) Switching the Cell Cycle. Kip-Related Proteins in Plant Cell Cycle Control. Plant Physiol. 139(3), 1099-1106

Walter M, Chaban C, Schütze K, Batistic O, Weckermann K, Näke C, Blazevic D, Grefen C, Schumacher K, Oecking C, Harter K and Kudla J (2004) Visualization of protein interactions in living plant cells using bimolecular fluorescence complementation. Plant J. *40*, 428-38

Wang G, Kong H, Sun Y, Zhang X, Zhang W, Altman N, DePamphilis CW and Ma H (2004) Genome-wide analysis of the cyclin family in Arabidopsis and comparative phylogenetic analysis of plant cyclin-like proteins. Plant Physiol. 135, 1084-1099

Wang H, Fowke LC and Crosby WL (1997): A plant cyclin-dependent kinase inhibitor gene. Nature *386*, 451-452

Wang H, Qi Q, Schorr P, Cutler AJ, Crosby WL, Fowke LC (1998) ICK1, a cyclin-dependent protein kinase inhibitor from *Arabidopsis thaliana* interacts with both Cdc2a and CycD3, and its expression is induced by abscisic acid. *Plant Journal.* 15, 501-510

Wang K, Liu Y and Li S (2013) Bimolecular Fluorescence Complementation (BIFC) Protocol for Rice Protoplast Transformation. Bio-protocol. 3(33), 1-5

Wang W and Chen X (2004) HUA ENHANCER3 reveals a role for a cyclin-dependent protein kinase in the specification of floral organ identity in Arabidopsis. Development. 131, 3147-3156

Xiao Q, Zhang C, Li H, Wei B, Wang Y, Huang H, Li Y, Yu G, Liu H, Zhang J, Liu Y, Hu Y and Huan Y (2017) Identification and functional analysis of the ICK gene family in maize. Scientific Reports. 7, 1-12

Yang R, Tang Q, Wang H, Zhang X, Pan G, Wang H, Tu J (2011) Analyses of two rice (*Oryza sativa*) cyclin-dependent kinase inhibitors and effects of transgenic expression of OsiICK6 on

plant growth and development. Ann. Bot. 107, 1087-1101

Zhou Y, Fowke LC, Wang H (2002). Plant CDK inhibitors studies of interactions with cell cycle regulators in the yeast two-hybrid system and functional comparisons in transgenic Arabidopsis plants. Plant Cell Reports. 20, 967-975

Supplementary Data

Supplementary Table 1 Expression profile survey of core cell-cycle genes (39) in rice flowers

Name	LOC Os# / Size (bp)	RT-PCR[1]	RNAseq[2]	RNAseq[3]	RT-PCR[4]	Cloned
KRP1	02g52480 / 798	-	26 ~ 27	0~5	+++	Y
KRP2	06g11050 / 1233	na	~0	0~3		
KRP3	11g40030 / 678	na	2 ~ 4	0~3		
KRP4	10g33310 / 585	+	~ 65	70~30	++++	Y
KRP5	03g04490 / 666	+	15 ~ 31	200~70	++++	Y
KRP6	01g37740 / 615	na	~0	~0		
CDKA1;1	03g02680 / 999	+++	35 ~ 45	~40	+	Y
CDKA2;1	02g03060 / 1131	+++	14 ~ 37	na	++	Y
CDKB1-1	01g67160.1 / 912	++	25 ~ 47	50~120	++++	Y
CDKB2-1	08g40170.1 / 981	+++	55 ~ 60	50~120	+++	Y
CDKC1;1	05g32360 / 1560	+	17 ~ 18	na		
CDKC1;2	01g72790 / 1542	+++	38 ~ 58	na	+++	Y
CDKC3;1	08g35220 / 975	++	6 ~ 12	na		
CDKD1	05g32600 / 1275	++	13 ~ 17	na		
CDKE1	10g42950 / 1428	+++	15 ~ 35	na	++++	Y
CYCA2;1	12g31810 / 1473	+++	6 ~ 8	10~55	++++	Y
CYCA3;1	03g41100 / 1122	+	5 ~ 13	2~10	++	Y
CYCA3;2	12g39210 / 1158	-	~8	2~25	+	Y
CYCB1;1	01g59120 / 1350	+++	24 ~ 33	20~40	++++	Y
CYCB1;3	05g41390 / 1350	na	12 ~ 20	na		
CYCB2;1	04g47580 / 1263	+++	12 ~ 16	15~35	+++	Y
CYCB2;2	06g51110 / 1260	+++	8 ~ 16	5~30	+++	Y
CYCD1;1	08g32540 / 1065	-	8 ~ 10	na		
CYCD1;2	06g12980 /1092	na	~ 0	na		
CYCD2;1	09g21450 / 690	+++	6 ~ 15	0~2	+	Y
CYCD3;1	09g02360 / 1095	na	10 ~ 23	2~23	++	
CYCD4;1	07g42860 / 1071	+++	8 ~14	na		
CYCD4;2	06g11410 / 1029	++	8 ~ 21	na		
CYCD4;3	08g37390 / 1152	na	8 ~ 18	na		
CYCD4;4	09g29100 / 1071	na	10 ~ 15	na		
CYCD4;5	03g27420 / 1218	na	~ 0	na		
CYCD5;1	03g10650 / 1038	+++	18 ~ 60	na	+++	Y
CYCD5;2	03g42070 / 1104	-	5 ~ 8	na		
CYCD5;3	12g39830 / 1098	na	15 ~ 18	na		
CYCD6;1	07g37010 / 963	++++	43 ~ 48	na	++	Y
CYCD7;1	11g47950 / 963	++	~ 0	na		
CYCH1;1	03g52750 / 993	++	6 ~ 7	na		
CYCT1;1	02g04010 / 1341	+++	25 ~30	na		
CYCT1;4	12g30020 /1632	+++	22 ~ 34	na	++++	Y

1. Guo et al 2007

2. RNAseq in FPKM, MSU (http://rice.plantbiology.msu.edu)

3. Jones D 2014; RNAseq in rice gametes and zygotes in TPM, UC-Davis (http://sundarlab.ucdavis.edu/cgi-bin/rice_zygote/DEgenescollate.alpha.pl)

4. Carried out by Hengping Xu, 2018

+, signal intensity of RT-PCR product in DNA gel; na, not applicable; Y, Yes.

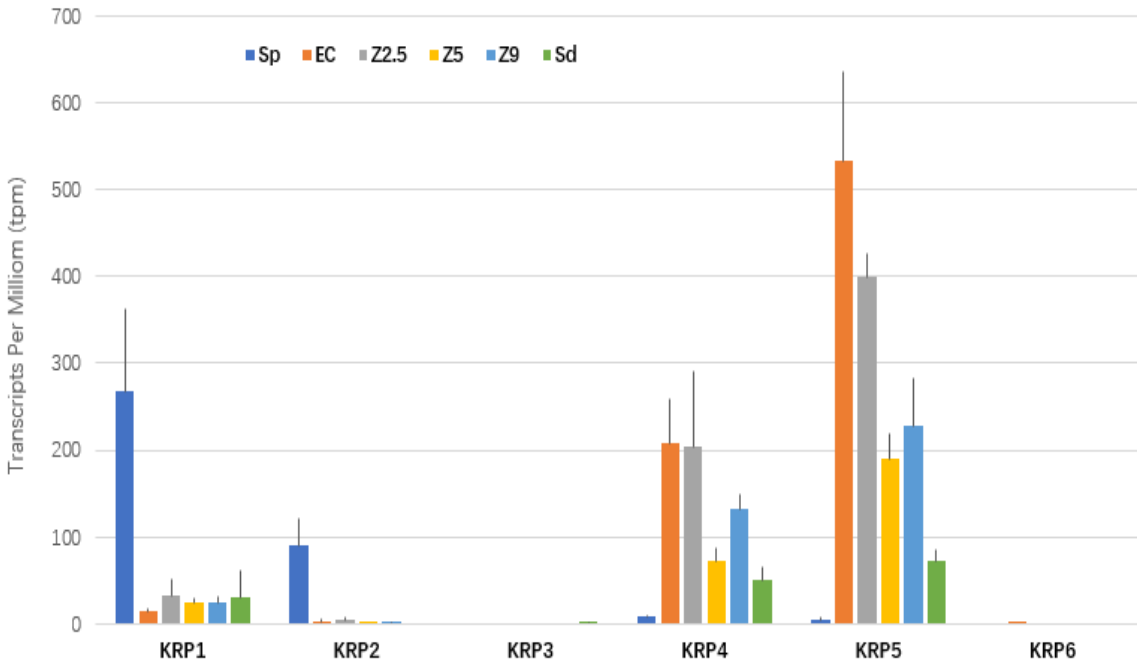

Supplementary Fig. 1 KRP1 and KRP2 are preferentially expressed in rice sperm cells but KRP4 and KRP5 are preferentially expressed in rice egg cells and zygotes based on RNAseq (http://sundarlab.ucdavis.edu/cgi-bin/rice_zygote/DEgenescollate.alpha.pl). Sp, sperm cell; EC, egg cell; Z2.5, zygote at 2.5 hours after pollination (HAP); Z5, zygote of 5 HAP; Z9, zygote of 9 HAP; Sd, seedling.

*Supplementary **Table 2** Primer sequences (chapter 2)*

Primer names	Sequences 5' -3'
RT-PCR	
KRP1-RT-F (H342)	ATGGGCAAGTACATGAGGAAG
KRP1-RT-R (H343)	TCAGCTTCGGCTGCTGAC C
KRP2-RT-F (H347)	GACTGAATTCATGGGGAAGAAGAAGAAGC
KRP2-RT-R (H348)	CTGAGGATCCTCAGTGAACGCGGAGGCG
KRP3-RT-F (H349)	GTCACATATGATGGGCAAGTACCTCAGGAG
KRP3-RT-R (H350)	CAGTCTCGAGTCACATGTCAGTGACATCCTT
KRP4-RT-F (H13)	GAGGCCGAATTCATGGGCAAGTACATGCGCAA
KRP4-RT-R (H14)	GTCGACGGATCCTCAGTCTAGCTTGACCCATTC
KRP5-RT-F (H15)	GAGGCCGAATTCATGGGGAAGTACATGCGGAAG
KRP5-RT-R (H16)	GTCGACGGATCCCTAGCAGTCTAGCCTTGTCCA
KRP6-RT-F (H51)	GTGCCCCGGGATGCTCGGGAGGAACGCCA
KRP6-RT-R (H52)	CGTGCCTCGAGCTCCTCCGGCGGCTCGCT
OsActin-RT-F (H139)	CTTTGCCTTGAGATGGACGC
OsActin-RT-R (H140)	TCACCAGGACACCACCAAAC
qRT-PCR	
KRP4-qRT-F (H168)	CCGATACGATTAGCACCCCT
KRP4-qRT-R (H169)	AGGGCAGTCATTCACAGGAT
KRP5-qRT-F (H185)	ACCAACACCTCGATCAGTTCC
KRP5-qRT-R (H186)	CTAGCAGTCTAGCCTTGTCC
18S- qRT-F (H177)	TTAGGCCACGGAAGTTTGAG
18S-qRT-R (H178)	GCATTCCTCGTTGAAGACCA
Vector construction	
Y2H	
KRP1-Y2Hbait-F-EcoRI (H342c)	GACTGAATTCATGGGCAAGTACATGAGGAAG
KRP1-Y2Hbait-R-BamHI (H343c)	CTGAGGATCCTCAGCTTCGGCTGCTGAC C
KRP4-F-EcoRI (H13)	GAGGCCGAATTCATGGGCAAGTACATGCGCAA
KRP4-R-BamHI (H14)	GTCGACGGATCCTCAGTCTAGCTTGACCCATTC
KRP5-F-EcoRI (H15)	GAGGCCGAATTCATGGGGAAGTACATGCGGAAG
KRP5-R-BamHI (H16)	GTCGACGGATCCCTAGCAGTCTAGCCTTGTCCA
CDKA1;1-Y2Hprey-F-EcoRI (H31)	CTGCGAATTCATGGAGCAGGTGAGCGCCT
CDKA1;1-Y2Hprey-R-BamHI (H32)	GTCTGGATCCTCATTGTACCATCTCAAGGT

CDKA2;1-Y2Hprey-F-EcoRI (H320c)	CTGAGAATTCATGCCACAAGCCCAACCCA
CDKA2;1-Y2Hprey-R-BamHI (H321c)	GACTGGATCCCTACGCCACTTCCAGGTCC
CDKB1;1-Y2Hprey-F-NdeI (H274b1c)	GTCACATATGATGGAGAAGTACGAGAAGCTG
CDKB1;1-Y2Hprey-R-XhoI (H275b1c)	CAGTCTCGAGCTAGAACGTGGACTTGTCGA
CDKB2;1-Y2Hprey-F-EcoRI (H274b2c)	CTGAGAATTCATGGCGGCGCTCCACCAC
CDKB2;1-Y2Hprey-R-BamHI(H275b2c)	GACTGGATCCTCAGTAGAGCTCCTTGTTCAC
CDKC1;2-Y2Hprey-F-NdeI (H322c)	GTCACATATGATGGCGGTGGCGGCGCC
CDKC1;2-Y2Hprey-R-EcoRI (H323c)	CTGAGAATTCCTATTGCCAGTTTCCATACTG
CDKE1-Y2Hprey-F-NdeI (H326c)	GTCA CAT ATG ATG GGG GAC GGC CGC GT
CDKE1-Y2Hprey-R-EcoRI (H327c)	CTGA GAA TTC TCA GAA CCG CCT GTT CTG TT
CYCA2;1-Y2Hprey-F-NdeI (H282)	CGTGCCATATGATGGCTGGAAGGAAGGAAAAT
CYCA2;1-Y2Hprey-R-XhoI (H283)	CGTGCCTCGAGTACGCTGAAGAGTGACTGCC
CYCA3;1-Y2Hprey-F-NdeI (H284)	CGTGCCATATGATGGCCGGCAAGGAGAACG
CYCA3;1-Y2Hprey-R-XhoI (H285)	CGTGCCTCGAGCTACTCGTTTAGGTCTTCGAA
CYCA3;2-Y2Hprey-F-EcoRI (H286)	CTGCGAATTCATGGCTGACAAGGAGAACTC
CYCA3;2-Y2Hprey-R-BamHI (H287)	GTCTGGATCCCTACTCTGTTAAATCTTGGAGG
CYCB1;1-Y2Hprey-F-EcoRI (H292)	CTGCGAATTCATGGCGACACGCAGCCAG
CYCB1;1-Y2Hprey-R-BamHI (H293)	GTCTGGATCCTTATTTGCAGAGTTCCACTGC
CYCB2;1-Y2Hprey-F-NdeI (H294)	CGTGCCATATGATGGATAGGGCGAGCGAGA
CYCB2;1-Y2Hprey-R-XhoI (H295)	CGTGCCTCGAGTCAACAAGGCTGCTTCTGAAG
CYCB2;2-Y2Hprey-F-NdeI (H296)	CGTGCCATATGATGGAGAACATGAGATCTGAG
CYCB2;2-Y2Hprey-R-XhoI (H297)	CGTGCCTCGAGTTACAGTGCCACGCTCTTGA
CYCD2;1-Y2Hprey-F-NdeI (H288)	CGTGCCATATGATGCCGGCCGACGACGAC
CYCD2;1-Y2Hprey-R-XhoI (H289)	CGTGCCTCGAGTCACCCAGCAAAAACATCTGT
CYCD5;1-Y2Hprey-F-EcoRI (H332c)	CTGAGAATTCATGGGGGACGCCTCGGC
CYCD5;1-Y2Hprey-R-BamHI (H333c)	GACTGGATCCCTACTGGCGCTGAGGCGA
CYCD6;1-Y2Hprey-F-EcoRI (H336c)	CTGAGAATTCATGGACATGGCGACGGGG
CYCD6;1-Y2Hprey-R-BamHI (H337c)	GACTGGATCCTCACTCATCAGGGCCGCC
CYCT1;4-Y2Hprey-F-NdeI (H340c)	GTCACATATGATGGCTATGATGCCAAGTGAT
CYCT1;4-Y2Hprey-R-XhoI (H341c)	CAGTCTCGAGCTAACCTTCAGGCCGAGGC
BiFC	
KRP4-F- KpnI (H124)	TGTGGTACCATGGGCAAGTACATGCGCAA
KRP4-R-SmaI (H125)	TGTCCCGGGCCGTCTAGCTTGACCCATTCAAA
UBIQprom-F-AgeI (H118)	TGTACCGGTCTGCAGTGCAGCGTGACCC
UBIQprom-R-HindIII (H119)	TGCAAGCTTCTGCAGAAGTAACACCAAACAA

KRP5-F- EcoRI (H65)	GTCGAATTCTATGGGGAAGTACATGCGGAAG
KRP5-R- SalI (H66)	TGCGTCGACGCAGTCTAGCCTTGTCCATTC
KRP5prom-F-AgeI (H205)	CGTGTACCGGTGGTGACACATCGGTGGAGC
KRP5prom-R-SmaI (H206)	CGTGTCCCGGGGGCCAAGGCGCGCGCGG
CDKB1-F- PstI (H442)	GTCACTGCAGATGGAGAAGTACGAGAAGCTG
CDKB1-R- KpnI (H443)	CAGTGGTACCCTAGAACTGGGACTTGTCGA
CDKB1-cEYFP-F(H403)	CATCGGGGATTCGGGATCGATGGAGAAG TACGAGAAGCTG
CDKB1-cEYFP-R(H406)	CTATTATGGGATTTATGGGTGCTGCGGCCG CGTCACTGGA
CDKB1prom - F (H401)	CTAAAACCAAAATCCAGTGACGCGTGG TTTTGTGAAACTACACTAC
CDKB1prom – R (H402)	CAGCTTCTCGTACTTCTCCATCGATCCCG AATCCCCGATG
UBIQprom-KRP4-cEYFP-F (H419b)	CATAATAGCTGTTTGCCAACTGCAGTGC AGCGTGACC
UBIQprom-KRP4-cEYFP-R (H406) *(Gibson Assembly for p212)*	CTATTATGGGATTTATGGGTGCTGCGGCC GCGTCACTGGA
mcBiFC	
CDKB1;1-F-XhoI (H444)	GTCACTCGAGATGGAGAAGTACGAGAAGCTG
CDKB1;1-R-EcoRI (H445)	CAGTGAATTCGAACTGGGACTTGTCGAGG
KRP4-F-EcoRI (H63)	GTCGAATTCTATGGGCAAGTACATGCGCAA
KRP4-R-SalI (H64)	TGCGTCGACGTCTAGCTTGACCCATTCAAA
UBIQprom-KRP4-nVenus-F (H447)	TAAAACCAAAATCCAGTGACGCCTGCAGTGC AGCGTGACC
UBIQprom-KRP4-nVenus-R (H448)	GCTCCACCGATGTGTCACCGCGTCACTGG ATTTTGGTTTTA
KRP5prom-F-AgeI (H205)	CGTGTACCGGTGGTGACACATCGGTGGAGC
KRP5prom-R-XhoI (H446)	CAGTCTCGAGGGCCAAGGCGCGCGCG
KRP5prom-KRP5-nCerullean-F (H449)	TAAAACCAAAATCCAGTGACGCGGTGACACA TCGGTGGAGC
KRP5prom-KRP5-nCerulean-R-NotI (H450)	TACGGCGCGCCGCGGCCGCGTCACTGGATTTT GGTTTTA

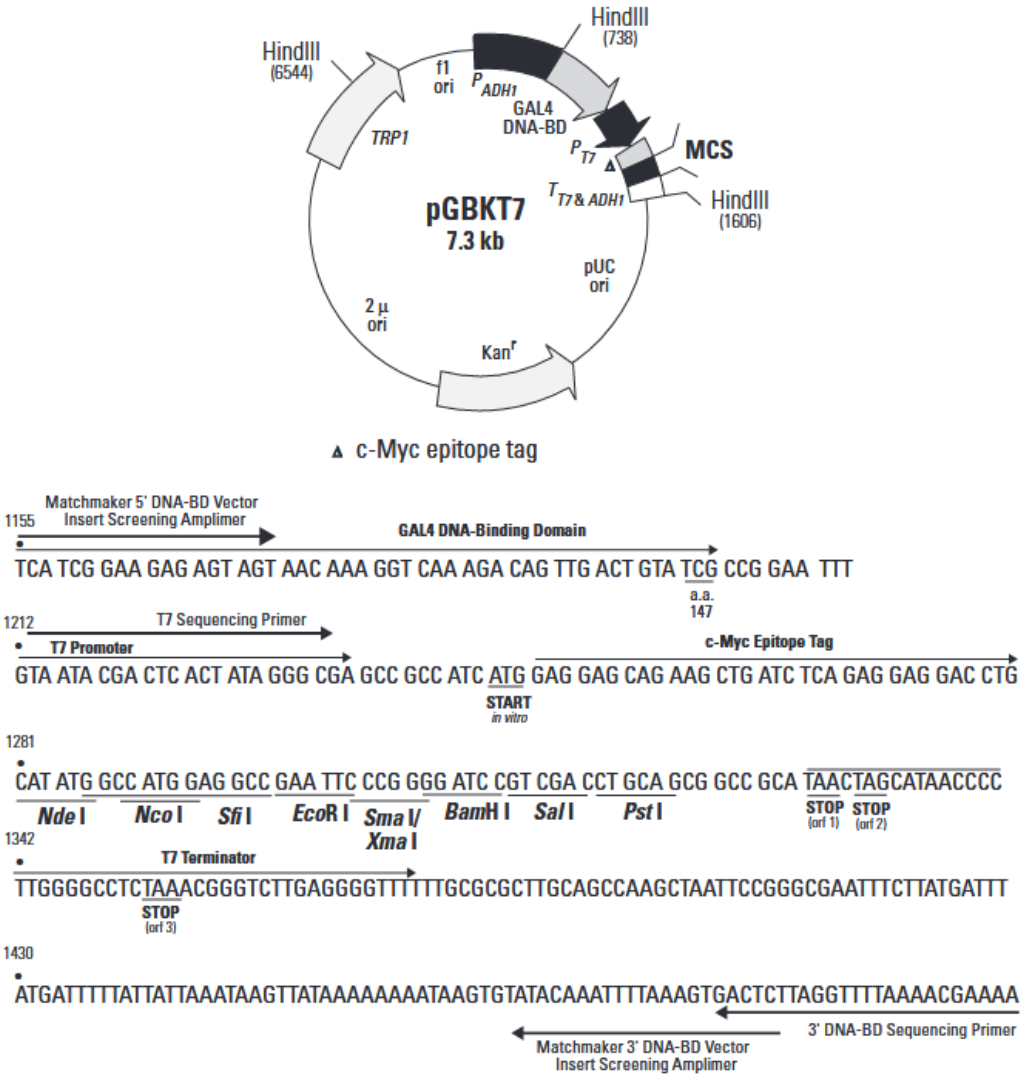

Supplementary Fig. 2 A Map and multiple cloning sites (MCS) of pGBKT7 for Y2H bait construct

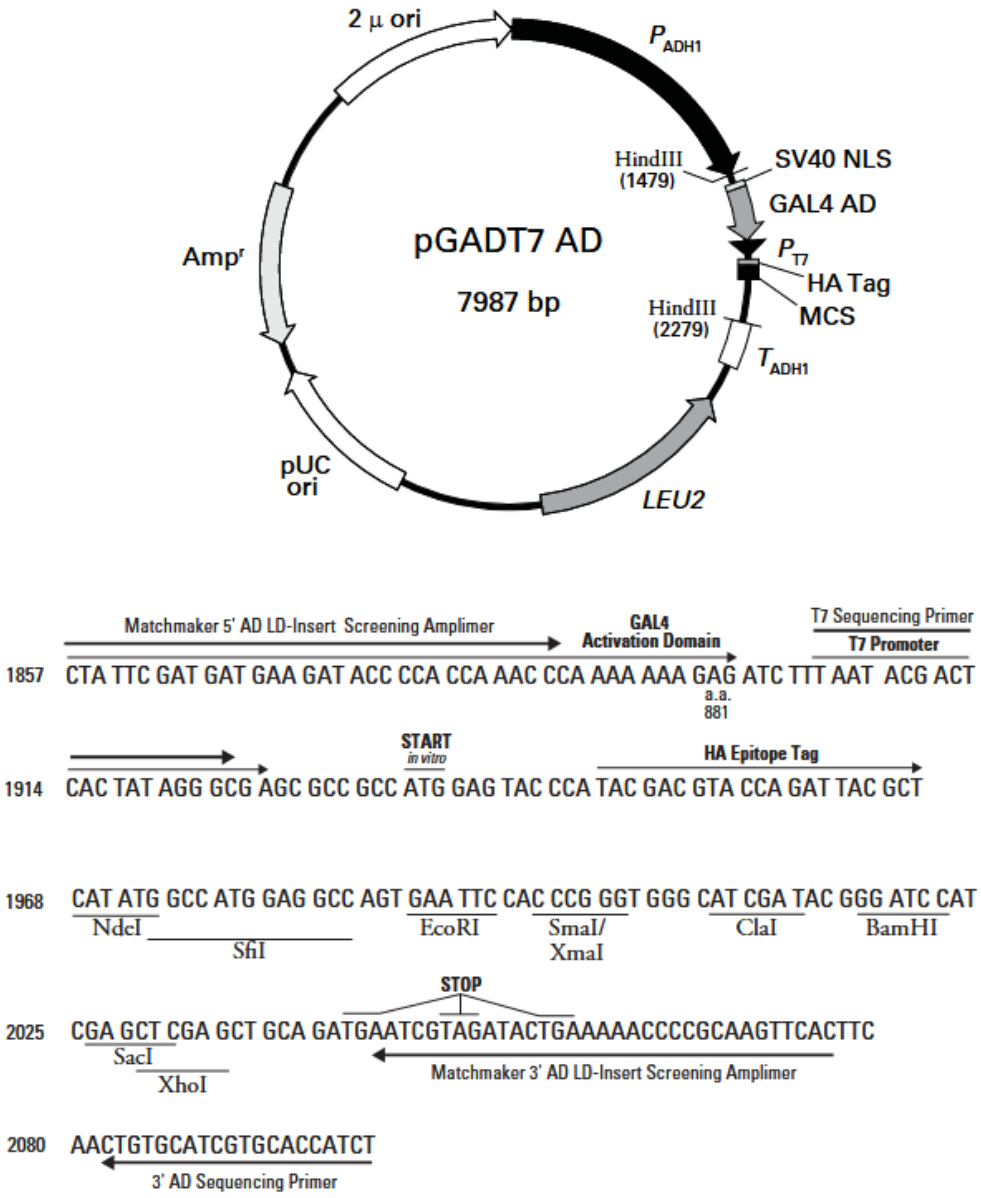

Supplementary Fig. 2 B. Map and multiple cloning sites (MCS) of pGADT7 AD for Y2H prey constructs

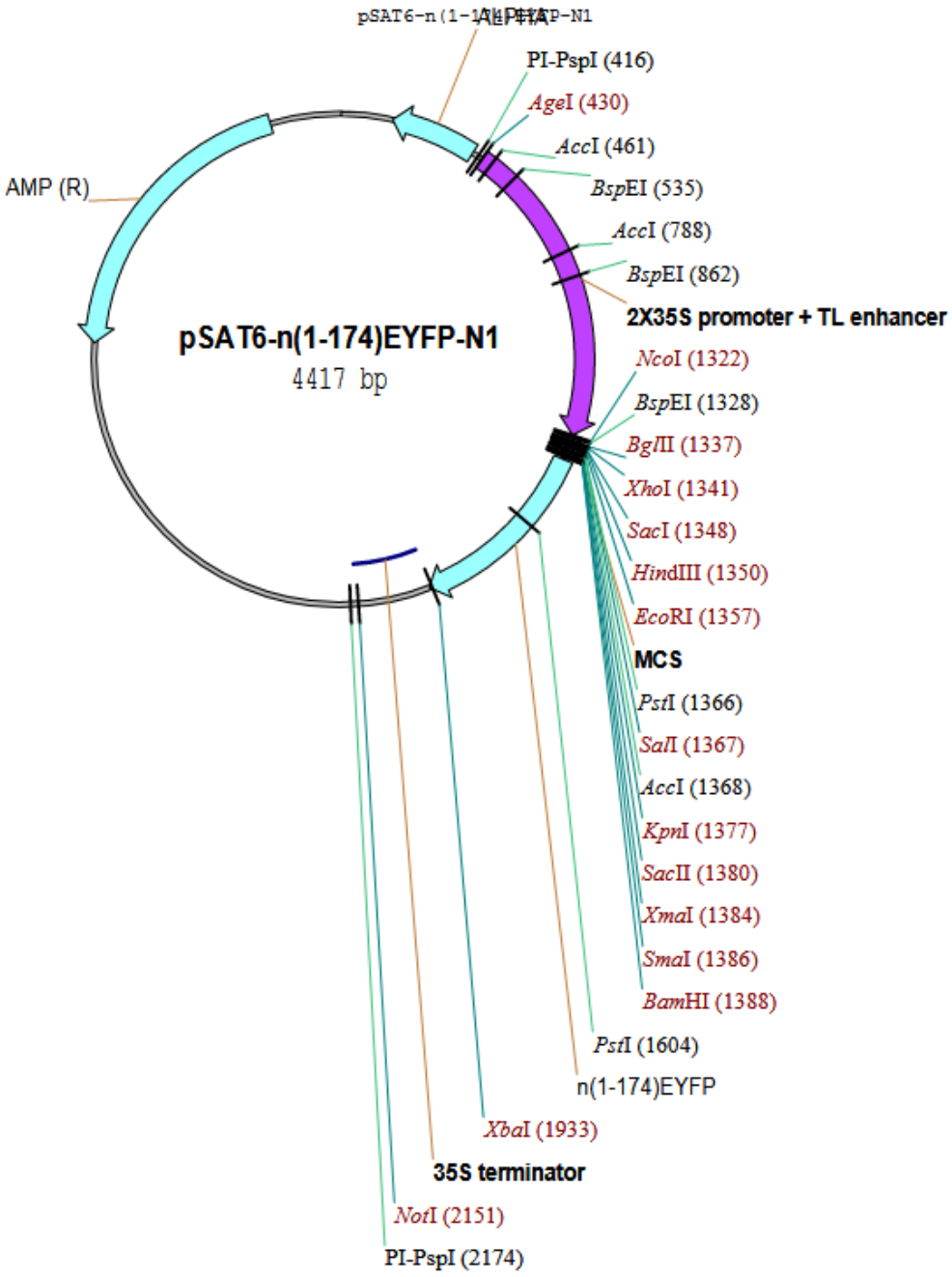

Supplementary Fig. 3 A. Map and multiple cloning sites (MCS) of pE2913 with nEYFP for BiFC (Lee and Gelvin 2014)

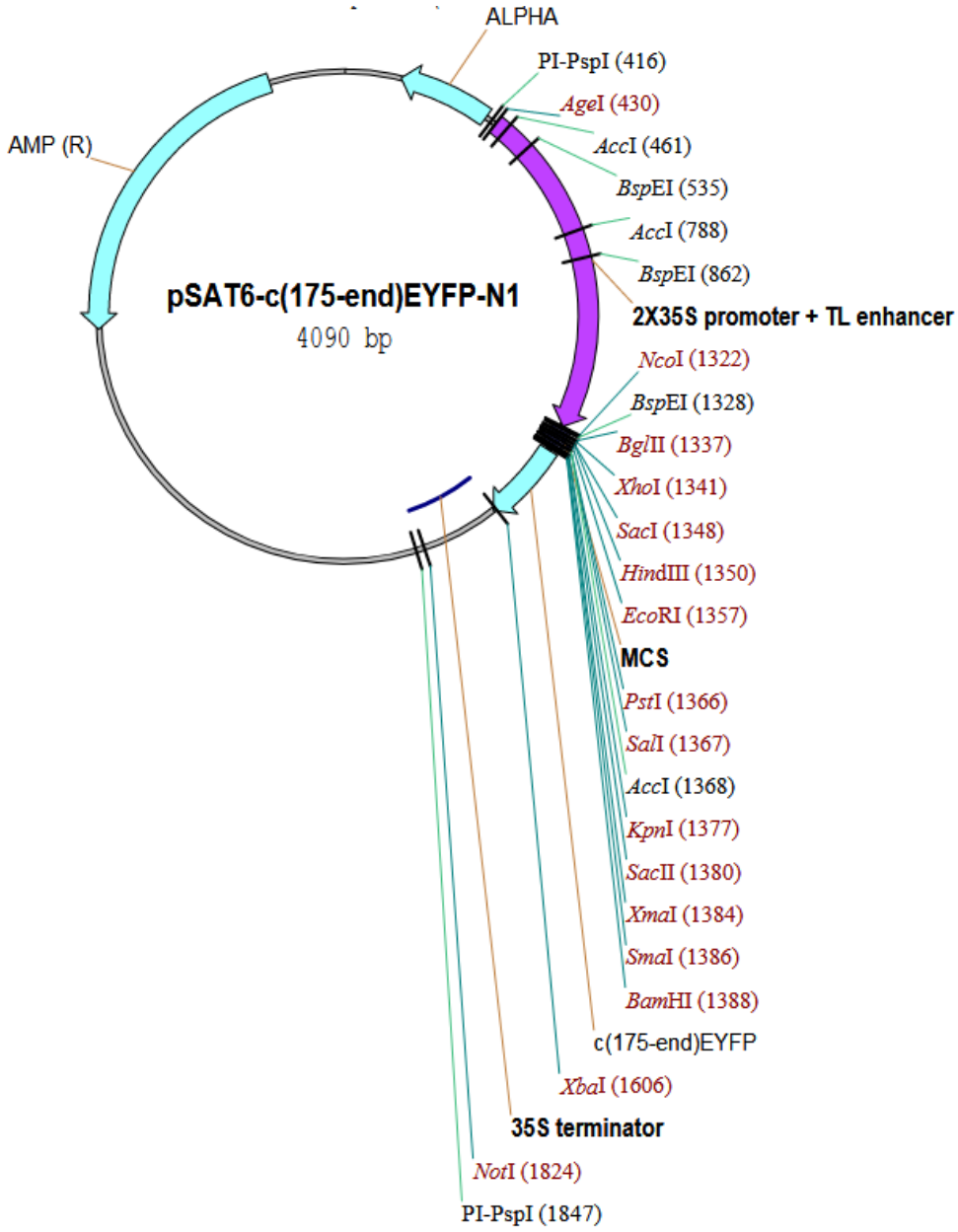

Supplementary Fig. 3 B. Map and multiple cloning sites (MCS) of pE2914 with cEYFP for BiFC (Lee and Gelvin 2014)

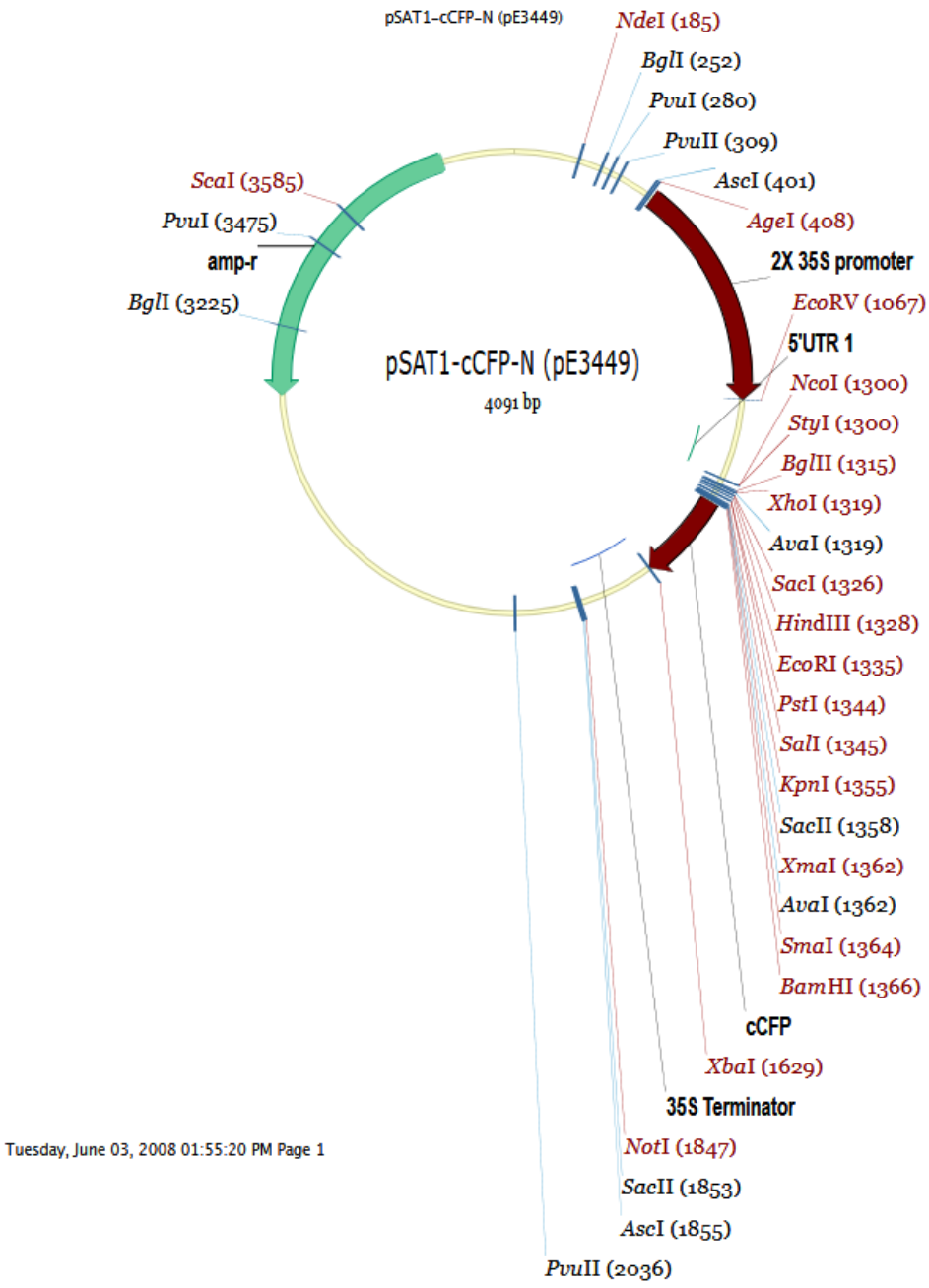

Supplementary Fig. 4 A. Map and multiple cloning sites (MCS) of pE3449 with cCFP for mcBiFC (Lee and Gelvin 2014)

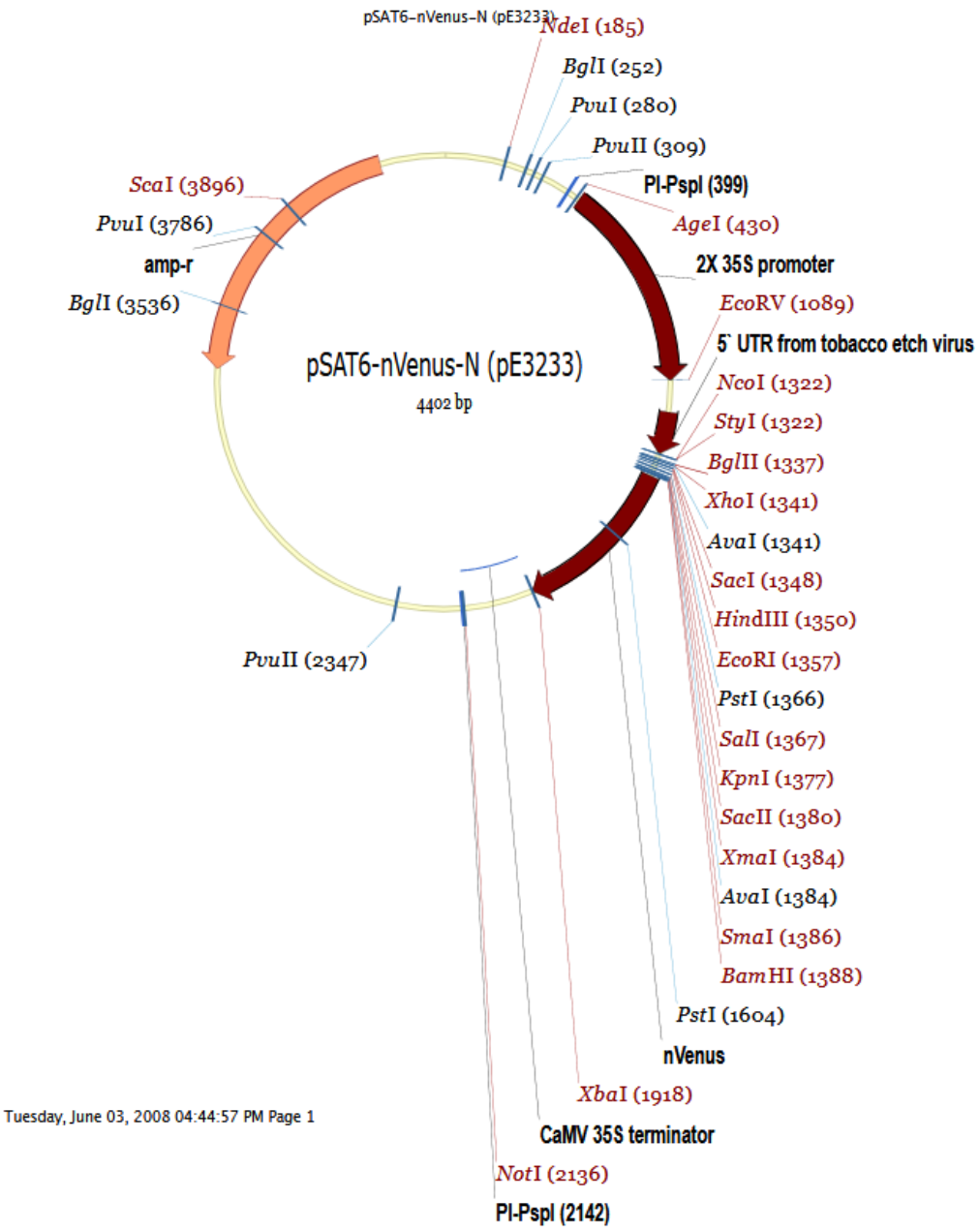

Supplementary Fig. 4 B. Map and multiple cloning sites (MCS) of pE3233 with nVenus for mcBiFC (Lee and Gelvin 2014)

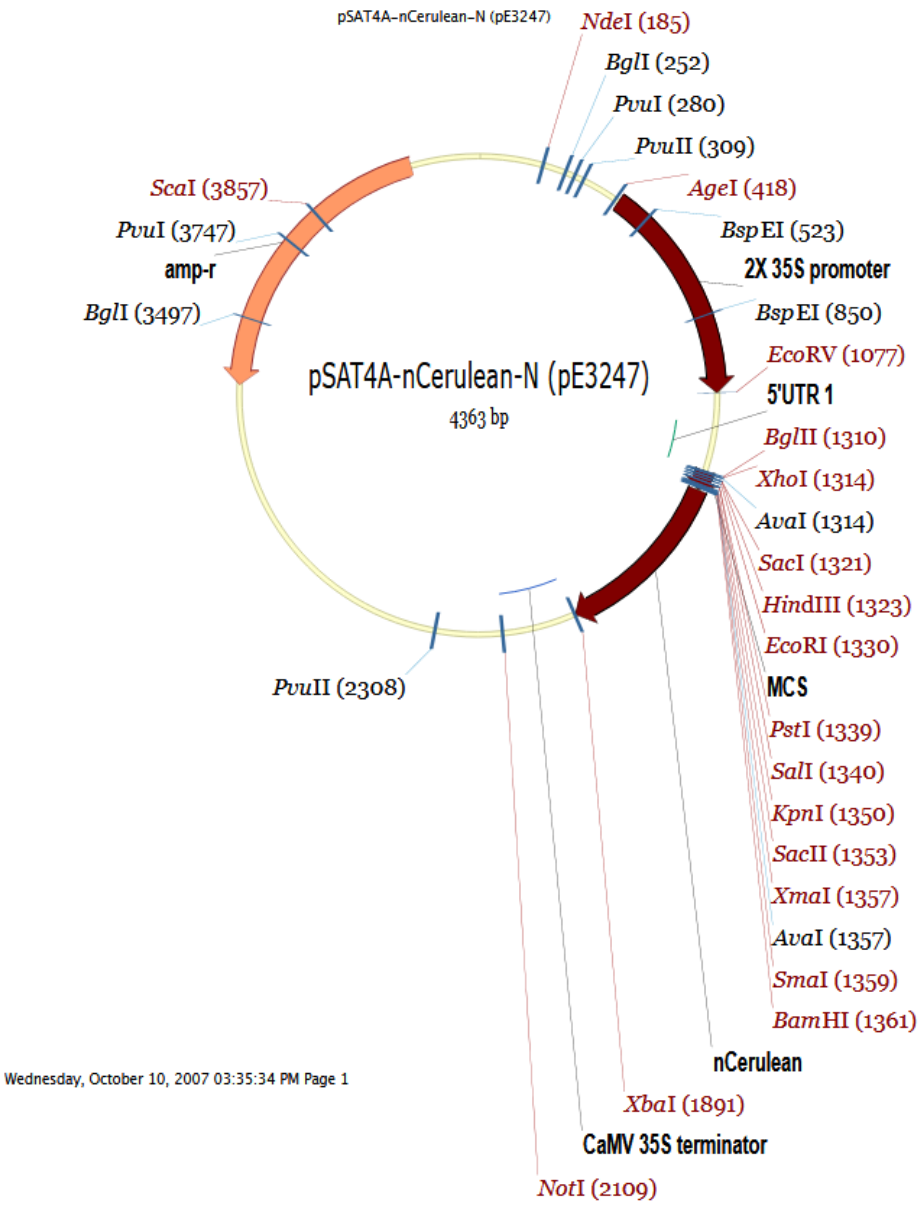

Supplementary Fig. 4 C. Map and multiple cloning sites (MCS) of Pe3247

With nCerulean for mcBiFC (Lee and Gelvin 2014)

Chapter 3. The Regulation of Coordinate Cell-Cycle-Inhibitors by Fb3 Mediated-Degradation in Rice Zygotes

Abstract

From to the previous research, we found that KRP5 and KRP4 coordinately inhibit CDKB1 which may make zygotic cell cycle arrested. According to the studies in yeast and Arabidopsis, the KRP inhibitors are regulated via F-box protein mediated proteasome pathway. In this chapter, we identified Fb3 as a novel rice F-box protein preferentially expressed in rice egg cells and zygotes. It mediates the degradation of both KRP5 and KRP4 via 26S proteasome pathway. This is evidenced in the protein degradation assay and supported by its reversal effect on KRP inhibition to the Kinase activity of CDKB and its interaction with KRP5 and KRP4 as indicated in Y2H, BiFC and cellular localization in rice zygotes at different stages. Our results identify Fb3 as a regulator of the two KRP inhibitors of rice zygotic cell cycle.

Introduction

The Cyclin dependent kinases (CDKs) are major controlling factors in regulating the cell cycle. CDKs are regulated by both positive factors, such as cyclins, and negative ones, CDK inhibitors (CKI), as analyzed in rice zygotes, including KRP5 and KRP4. To control the cell cycle process, these inhibitors must be strictly regulated by the machinery of protein degradation (proteolysis). Without removing these inhibitors from the cell cycle core complexes, CDKA can't be activated for entry into S-phase and CDKB, the controller of mitosis, cannot be activated either (see Introduction Fig. 1). The same will happen for other CDKs to pass other cell cycle checkpoints. According to the studies of the past two decades, the canonical regulation of cell cycle checkpoints is reached by the pathway of ubiquitin-mediated proteolysis (Pagano et al, 1995, Bai

et al 1996, Kipreos and Pagano 2000, Ho et al 2006, Marrocco et al 2010 and Boycheva et al 2015).

The ubiquitin-proteasome pathway is a crucial post-translational mechanism for the well-controlled balance between protein synthesis and degradation in eukaryotic cells. It is essential to maintain and coordinate homeostasis and viability in living organisms. In this pathway, the substrate protein to be targeted is covalently attached with a chain of ubiquitin, which is sequentially catalyzed by three different enzymes: ubiquitin-activating enzyme (E1), ubiquitin-conjugating enzyme (E2), and ubiquitin-ligase enzyme (E3). To activate ubiquitin, E1 consumes ATP to form a thiol-ester-bond between ubiquitin and itself; then E2 receives the thiol-ester-bonded ubiquitin from E1; and finally, E3 (through its component, F-box protein, FBP) binds the specifically targeted protein to the activated ubiquitin-E2 complex and transfers the ubiquitin to the target protein. Multiple rounds of this procedure will provide the poly-ubiquitinated substrate for the degradation by 26S proteasome (Schulman et al 2000 and Cardozo and Pagano 2004).

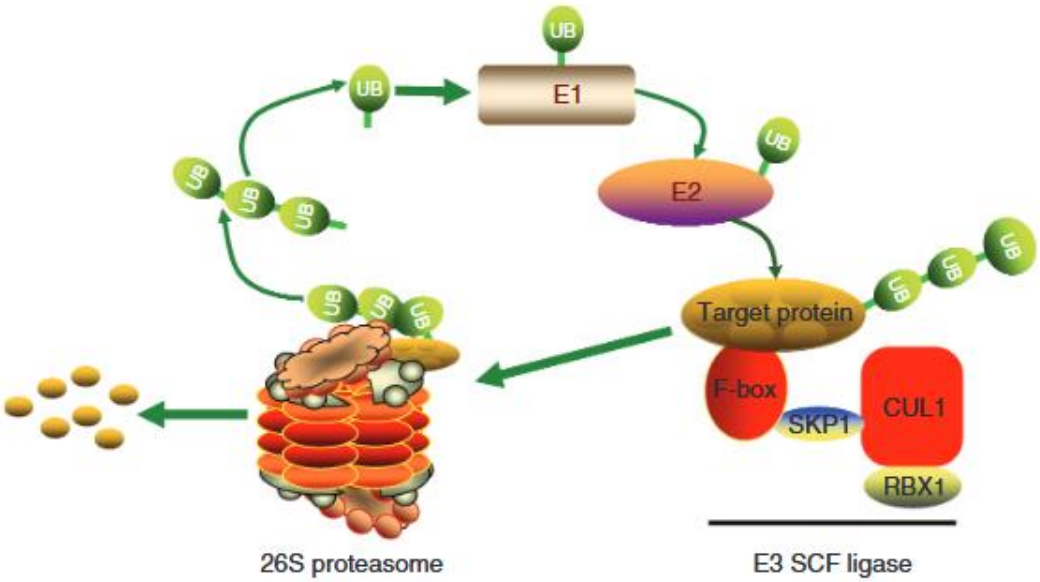

(Zhang et al 2019)

Fig. 1 Diagram of the ubiquitin-proteasome pathway. The target protein is poly-conjugated

with several mono-ubiquitin molecules transferred from E1 and E2 for degradation in 26S proteasome. In the SCF complex, the F-box protein (FBP) provides specificity of the substrate protein, Cul1 serves as a scaffold, Skp1 works as the bridge of Cul1 to FBP and Rbx1 as an adaptor protein to E2.

Based on the sequenced genomes in animal and plant, hundreds of ubiquitin-ligase enzymes (E3s) have been predicted in different classes according to commonly shared sequence motifs, but the most dominant and well characterized one is E3 Skp1-Cul-FBP (SCF) ligase. As shown in Fig. 1 (Zhang et al 2019), the SCF complex is composed of four different components: S-phase kinase-associated protein 1 (Skp1, 163 amino acid residues), Cullin1 (Cul1, 776 amino acid residues), RING-box protein (RBX1, 108 amino acid residues with core catalytic domain) and F-box protein (FBP, 430-1000 amino acid residues). In the SCF complex, the Cul1 serves as an organizing scaffold, Rbx1 acts as an adaptor protein to E2, Skp1 works as the bridge of Cul1 to FBP, and FBP functions as a specific recruiter of protein through 26S proteasome (Hershko and Ciechanover 1998, Gagne et al 2002, Zheng et al 2002, Zhang et al 2019 and Malik et al 2020).

The first F-box protein was identified in 1995. The unique domain was named as F-box since it is discovered at N-terminus of a human protein Cyclin F (Kumar and Paietta 1995, Bai et al 1996 and Kipreos and Pagano 2000). The F-box domain has ~ 50 amino acid residues usually located at the N terminus (see the F-box in OsFb3 in Supplementary Fig.6). It binds to Skp1 in SCF complex and is usually located at the N'-terminus of FBP. In contrast, different FBPs contain various protein-protein interaction domains at their C-termini, which determines the specificity of substrate proteins in the ubiquitin-mediated proteolysis. In plants, some examples of such C-terminal domains are leucine-rich repeats (LRRs, see LRR of OSFb3 in Supplementary Fig. 6), WD-40, TUB, FBO, actin and DEAD-like helicase (Gagne et al 2002 and Xu et al 2009). In

addition, post-translational modifications, such as protein phosphorylation and glycosylation, also play a role in regulating the interaction of a substrate with F-box proteins (Cardozo and Pagano 2004 and Teixeira et al 2013)

During the past over two decades, numerous F-box proteins have been identified. Surprisingly, the number of F-box genes significantly varies with species (Kipreos and Pagano 2000, Xu et al 2009, Cui et al 2015, Gupta et al 2015, Zhang S et al 2019, Zhang X et al 2019 and Malik et al 2020). In budding yeast, fruit-fly, human and nematode, there are 14, 23, 38 and 326 F-box genes identified, respectively, whereas in plants such as rice, maize, *Arabidopsis, Medicago*, cotton, apple, soybean and chickpea, about 678, 359, 694, 972, 592, 517, 509 and 287 F-box genes have been predicted. Because of the importance of protein ubiquitination and degradation, plant F-box proteins have been reported involved in many different processes in plant growth and development including cell cycle control, signal transduction, metabolic regulation, floral organogenesis and senescence. One of striking examples is the study of *Arabidopsis* gametogenesis. It demonstrates that plant sperm cell formation is under the control of two cell cycle inhibitors, AtKRP6 and AtKRP5, and these two inhibitors are degraded by the specific FBP, FBL17, associated SCF complex (Kim et al 2008).

However, fewer studies have been conducted concerning FBP function in the cell cycle control of plant embryogenesis. In this chapter, we present the evidence supporting the interaction of a novel rice F-box protein, OsFb3, with the two-rice zygotic cell cycle inhibitors, OsKRP5 and OsKRP4, and the regulation of the two inhibitors through their degradation mediated by OsFb3 protein.

Material and Methods

Plant material

The growth of rice plants and the cell isolation for leaf protoplasts, egg cells and zygotes are conducted as previously described in Chapter 1.

Methods

I. RNA isolation and RT-PCR

The same procedures as Chapter 2 are followed for RNA isolation and RT-PCR. Specific primers (Supplementary Table 2) were used in PCR for 7 F-box genes (Supplementary Table 1) expressed in rice flowers.

II. Yeast two hybridization (Y2H)

For Y2H, the coding sequences (CDS) of rice KRP4 and KRP5 were amplified in PCR and then cloned into the vector pGBKT7 at the specific restriction sites, respectively, as baits for Y2H; the PCR products of Fb1, Fb2, Fb3, Fb6 and CDKA1;1 were cloned into the vector pGADT7 AD at specific cutting sites, separately, as preys for Y2H. The primers with their respective restriction sites are listed in supplementary Table 2. Y2H assays were conducted with Matchmaker Gold Yeast Two-Hybrid System (Clontech) as described in Chapter 2. The protein-protein interactions are indicted by the yeast spots in blue.

III. Bimolecular Fluorescent Complementation (BiFC)

The procedure for BiFC is the same as Chapter 2. But for the pre-trial of BiFC in rice leaf protoplasts, the CDS of OsKRP5 or OsKRP4 was introduced into pE2913 (Supplemental Fig. 3A, Chapter 2) for the construct KRP5-nEYFP or KRP4-nEYFP, and the CDS of OsFb3, 5’-300 bp of OsFb3 (Fb3m1) or 3’ 324 bp of OsFb3 (Fb3m2), into pE2914 (Supplementary Fig. 3B, Chapter 2).

For the formal BiFC in rice egg cells and zygotes, the CDS of OsKRP5 and OsKRP4 were

cloned into pE2913 separately, then the constructs of OsKRP5-nEYFP and OsKRP4-nEYFP were ligated to the native promoters, OsKRP5 promoter (2 kb) and maize ubiquitin promoter (2 kb), respectively; the CDS of OsFb3 was cloned into pE2914 for OsFb3-cEYFP, and OsFb3-cEYFP was linked to OsFb3 promoter (1.3 kb).

The primers with specific restriction sites for OsFb3, OsFb3 mutants and the native promoters are listed in supplementary Table 2.

IV. Constructs for chemical inducible Fb3 expression system

Two plasmids were made to transform rice plants for high expression of Fb3 driven by the chemically inducible promoters. The construct of OsFb3-EYFP was introduced to the vector pER8 (Supplementary Fig. 3; Xu et al 2009 and Chen et al 2017); and the CDS of OsFb3 was linked to 3' end of GFP coding sequence at SpeI in pUH-GFP2 (Supplementary Fig.4; Sreekala et al 2005 and Hirose et al 2012). The vector pER8 and pUH-GFP2 were provided from the Professor Chua Nam Hai Lab, Rockefeller University). The primers are listed in Supplementary Table 2.

V. Expression of OsFb3 protein in rice protoplasts with suspension culture

1. Expression of OsFb3 in rice protoplasts

Rice protoplasts were prepared as Chapter 1; HA tagged OsFb3 CDS was introduced into pE3449 (Supplementary data) at XhoI and HindIII. The rice protoplasts were transfected with the HA-OsFb3 construct and incubated for 18 hours in dark at room temperature and used for protein extraction and Western blot analysis as Chapter 2.

2. Suspension culture of rice protoplasts transfected with chemically inducible Fb3 expression system

Rice protoplasts were transfected with the construct of GFP-OsFb3 and cultured in darkness (26^{o}C with shaking at 80 rpm) in Chu's medium (3.99g/l, Caisson Cat#CHP03; Chu et al 1975) with Hygromycin (35mg/l, for selection), Ampicillin (100 mg/l) and ß-estradiol (inducer, 20 µM) plus supplementals (Kumlehn et al 1998, Chen et al 2006, Kim TG et al 2008, Main et al 2014 and Chen et al 2017): 2,4-D (2 mg/l), Casamino acids (300 mg/l), L-glutamine (500~1000 mg/l), L-proline (1000 mg/l), Pyridoxine (1.0 mg/l), Kinetin (0.2 mg/l), Biotin (0.01 mg/l) and Retinol (0.01 mg/l) and Sucrose (30,000 mg/l.). The medium was freshly made and sterilized by filtering (0.2 µm).

VI. Rice ovary collection and protein extraction (for the proteasome with SCF complexes)

1. Dissect ~200 rice ovaries from mature florets in 0.3 M mannitol.
2. Freeze in liquid nitrogen and homogenize with Teflon Dounce homogenizer on ice in 0.5 ml protein degradation buffer (25mM Tris pH7.4, 150mM NaCl, 1mM EDTA, 1% NP40 and 5% glycerol with freshly added plant protease inhibitor cocktail, Sigma P9599, and 1 mM PMSF).
3. Pellet cellular debris at 3000 x g, 4^{o}C for 5 min
4. Aliquot the supernatant in 0.1 ml and store at -20^{o}C for later use.

VII. CDKB activity measurement

The yeast cells containing c-Myc or HA tagged constructs (c-Myc-OsKRP5, cMyc-OsKRP4, HA-OsCDKB1, HA-OsCDKB2 and HA-OsFb3) were cultured in medium –Leu-Trp for nuclei isolation as described in Chapter 2; the specific nuclear proteins and protein extract from suspension cultured rice protoplasts containing OsFb3-GFP were purified using Pierce™ Co-Immunoprecipitation Kit (Thermo Scientific™, Cat # 26149) according to manufacturer's

instructions (Chapter 2); then mixed with the crude rice ovary extract for measuring the kinase activity with ADPsensor™ Universal Kinase Activity Assay Kit (BioVision, Cat # K212-100), as stated in Chapter 2.

VIII. Protein degradation assay

The purified proteins of OsKRP5 and OsKRP4 (tagged with c-Myc) from yeast nuclei (as made for CDK activity assay) and OsFb3 protein (tagged with HA from yeast or tagged with GFP from transfected rice protoplasts after suspension culture for 6 ~ 9 days) were used to constitute a degradation assay based on Kim et al (2008). Briefly, the above rice ovary extract (100 µl) was pretreated with the proteasome inhibitor, MG132 (10 µM), to slow down OsKRP protein degradation, then mixed with about 0.5 µg OsKRP5 or OsKRP4 and OsFb3 proteins; in parallel, the same mixture was made with MG132 replaced by DMSO (1%) for normal protein degradation. The two mixtures were incubated at 4^{o}C and sampled (16 µl) every 30 minutes.

Each sample was combined with 4 µl of 5 x SDS-PAGE sample buffer and heated for 5 min at 95^{o}C, electrophoretically separated in 12% SDS-PAGE, and subjected to Western blot (as in Chapter 2), in which OsKRP5 and OsKRP4 were detected with anti-Myc monoclonal antibody (GenScript Cat# 631206). In addition, actin was detected as the internal control for equal loading.

IX. Other methods for high yield of OsFb3 protein

1. Cell-Free System of *E. coli*

NEBExpress® Cell-free *E. coli* Protein Synthesis System (NEB, E5360s) was adopted for high yield of OsFb3 protein. The CDS of OsFb3 were amplified and linked to the T7 RNA Polymerase promoter using PCR specified primers according to the manufacturer's suggestion;

the T7 promoter-Fb3 was used as the template for translation in the cell free system; then the reaction product was analyzed in SDS-PAGE gel.

2. *K. lactis* Protein Expression System

OsFb3 was introduced to pKLAC1-based expression vector, and the yeast cell (*Kluyveromyces lactis,* NEB C1001) was transformed with the vector and cultured following manufacturer's instructions. The protein sample isolated from the yeast cells was analyzed in SDS-PAGE gel.

Results and Discussion

I. OsFb3 is a novel F-box gene and preferentially expressed in rice egg cells and zygotes

Although hundreds of F- box genes are predicted from different plant species based on the sequenced genomes, none is found involved in cell cycle control of the early embryogenesis. One of main reasons is the difficulty in accessing the plant gamete and zygote cells embedded in multiple tissues. However, this barrier has been partially overcome by manual isolation of plant gametes and zygotes (Chapter 1). According to the recent RNAseq data, seven F-box genes (named as Fb1 ~ 7 in this chapter) are expressed in rice sperm cells, egg cells and zygotes as well as other tissues. Their locus numbers are listed in Supplementary Table 1 and their transcription profiles are presented in Supplementary Fig. 1.

As shown in Supplementary Fig.1, in contrast to the other 6 F-box genes, Fb3 is most highly preferentially expressed in rice egg cells and zygotes, although the expression level is not relatively high to other F-box genes. This feature is confirmed by our RT-PCR result (Fig. 1). The transcription level of Fb3 is much higher in the mature rice pistil where the egg cell or zygote located than in leaf, stem, root, anther and lemma/palea.

In addition, the RNAseq data (Supplementary Fig.1) also reveals that the transcription levels of Fb1 to Fb3 increase and those of Fb4 to Fb7 decrease with zygotic development (from 2.5 hours to 9

hours after pollination). This information helps us with RT-PCR cloning for the Y2H assay.

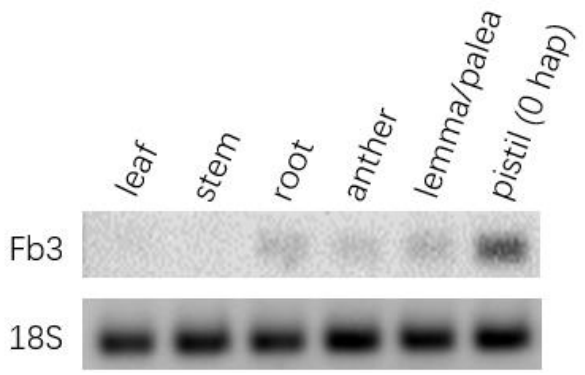

Fig.1 The DNA gel image of RT-PCR product showing the expression profile of Fb3 in six different rice tissues collected from flowering rice plants. 18S rRNA gene was used as the internal control for equal loading.

II. Interactions of OsFb3 protein with the coordinate cell-cycle inhibitors

1. OsFb3 protein interacts with OsKRP5 and OsKRP4 in Y2H

From RT-PCR, we amplified CDSs of Fb1, Fb2, Fb3 and Fb6. It is difficult to obtain those of Fb4, Fb5 and Fb7, partially due to the very high GC content in their CDSs or partially due to their rare transcripts caused by the aforementioned rapid declination during the zygotic development in rice flowers.

The four CDSs were cloned into yeast vector pGADT7 as preys for Y2H assay to test their interactions with the two cell cycle inhibitor proteins, KRP5 and KRP4, respectively. From Fig. 2, we found that KRP5 protein more or less positively interacts with all four F-box proteins, particularly with Fb3, but KRP4 protein interacts with the Fb3 as well. In a word, Fb3 protein interacts with both the KRP5 protein (stronger) and the KRP4 protein (weaker) in yeast.

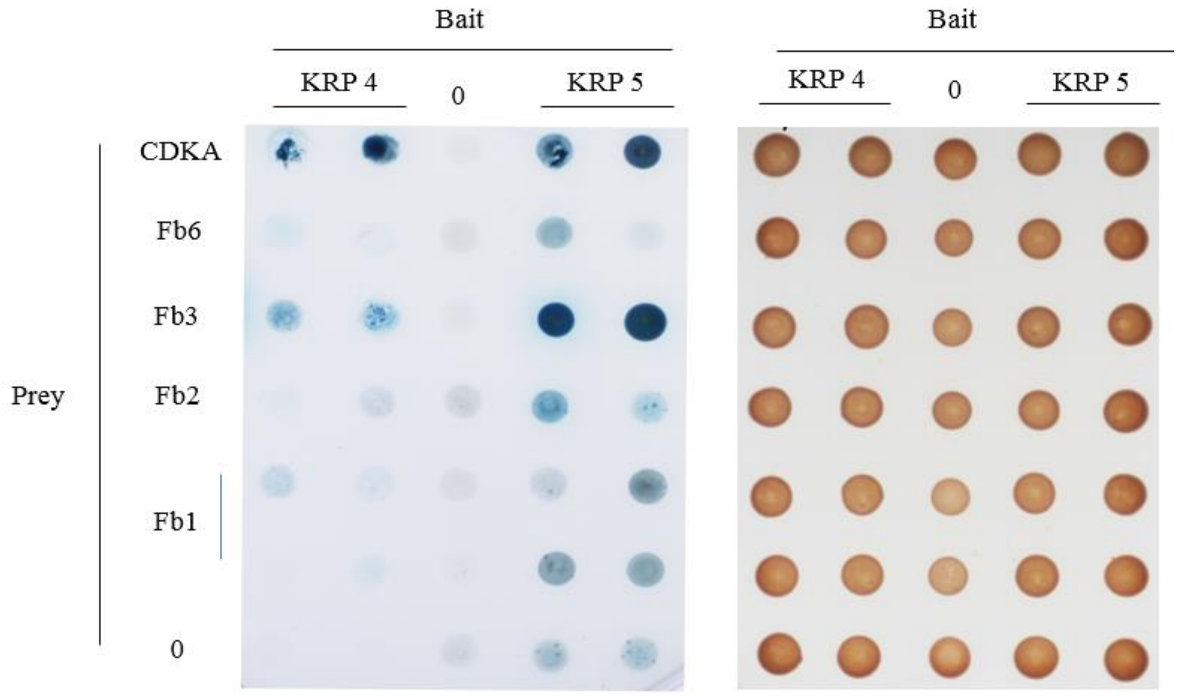

Fig.2 Interactions of four rice F-box proteins with rice CDK inhibitor KRP5 and KRP4 detected in Y2H assy. The preys include CDKA (+control), four F-box proteins (Fb1, Fb2, Fb3 and Fb6) and blank vector, pGADT7 (-control); the baits are KRP4, KRP5 and blank vector, pGBKT7 (-control). Yeast cells were grown on the medium of normal (right, YPDA: Yeast extract, Peptone, Dextrose and Adenine hemi-sulfate) and selective (left: SD/-Leu/-Trp/-His/ -Ade with X-α-gal and antibiotic Aureobasidin A, AbA). The blue spots on selective medium indicate the interactions of F-box proteins with KRP5 and KRP4 proteins, respectively.

2. OsFb3 protein interacts with OsKRP5 and OsKRP4 proteins in rice protoplasts

To test if the interactions of OsFb3 with OsKRP5 and OsKRP4 take place in rice cells, we conducted BiFC first in rice protoplasts as a pre-trial, and then in manually isolated rice egg cells and zygotes. We detected clear signals of yellow fluorescent protein (YFP) and red fluorescent protein (mCherry) from the protoplasts transfeted with Fb3-cYFP and KRP5-nYFP plus $mCherry_{NLS}$ driven by the ubiquitous promoter of Cauliflower mosaic virus (CaMV), P35S (Fig.

3 A), indicating the positive interaction between Fb3 and KRP5 and its location in the nuclear. The mutant Fb3, 3'-300 bp fragment containing the F-box domain or 5'-332 bp fragment containing the leucine rich region domain (LRR), also interacts with KRP5 but relatively weak, as shown in the signals observed from the protoplasts co-transfected with 3' F-box - cYFP plus KRP5-nYFP, or 5' LRR - cYFP plus KRP5-nYFP (Fig. 3 A, the cellular images and the relative

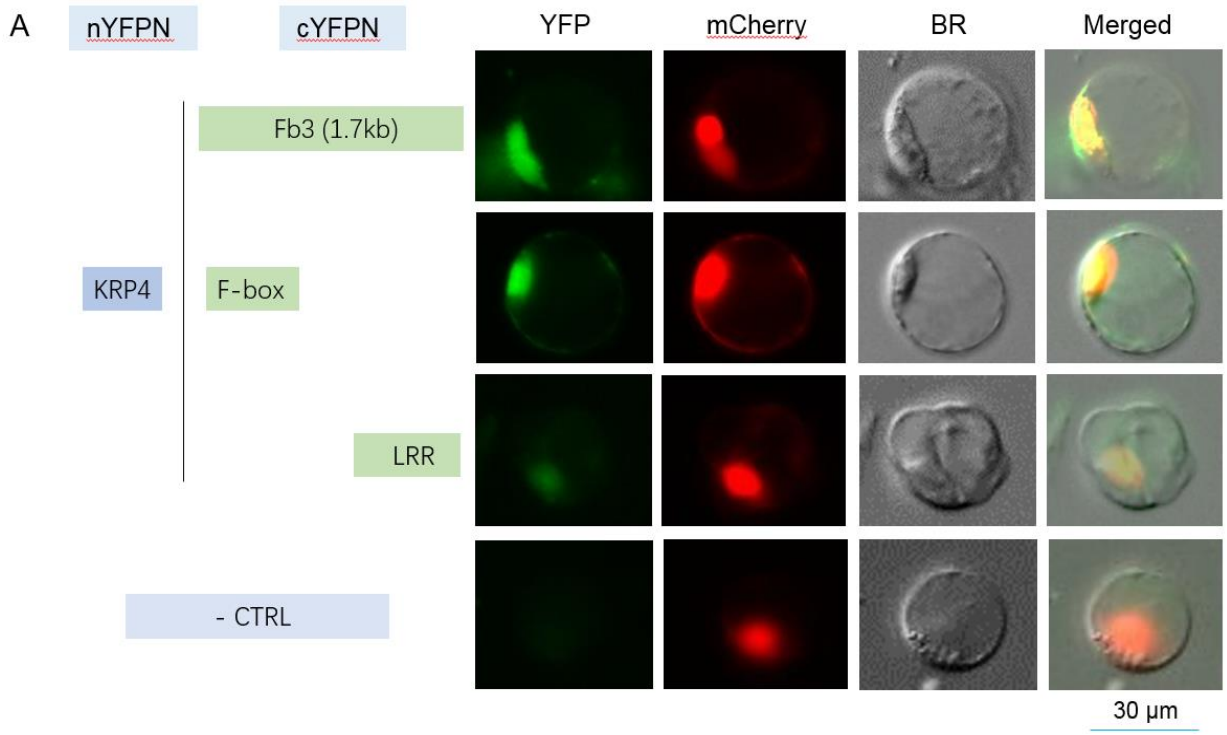

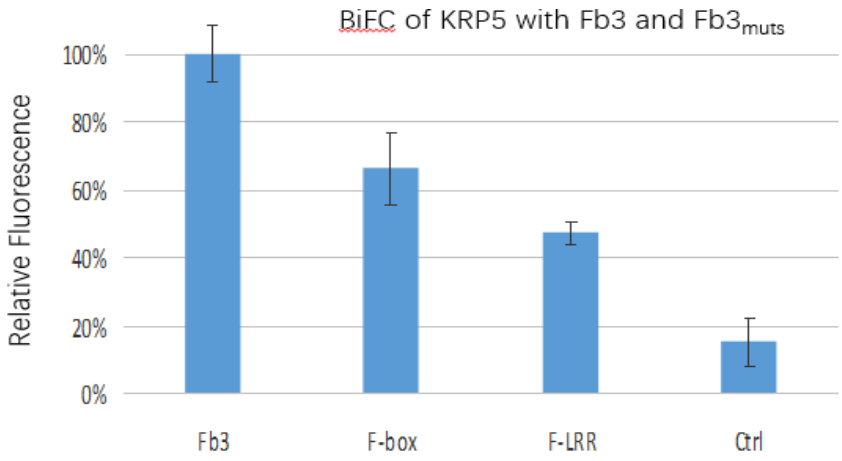

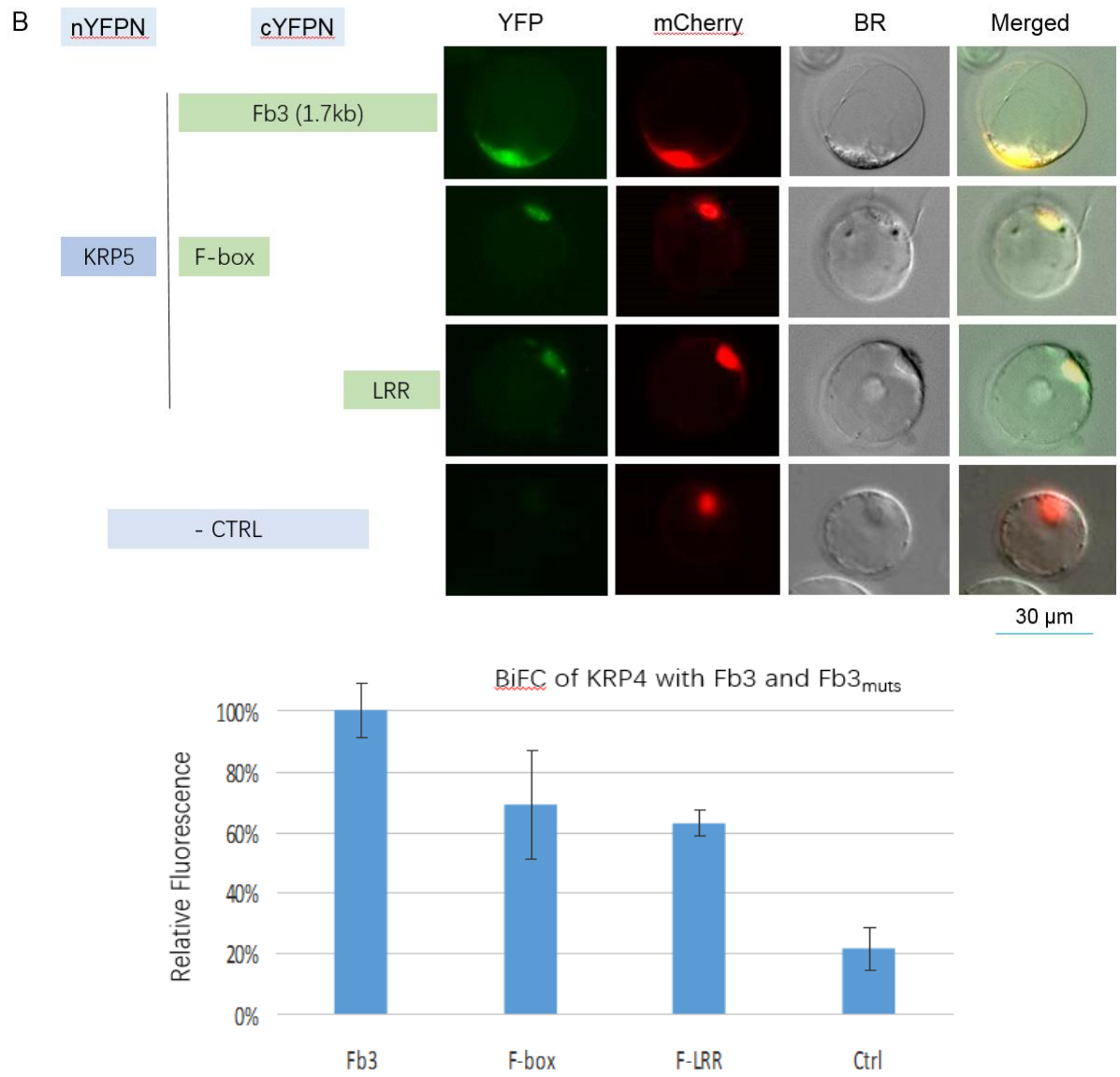

Fig.3 BiFC assay to detect interactions of OsFb3 with OsKRP5 (A) and OsKRP4 (B) in rice protoplasts. The protoplasts were co-transfected with Fb3-cYFP (3' F-box-cYFP or 5' LRR-cYFP) and KRP5-nYFP (A) or KRP4-nYFP (B) plus mCherry$_{NLS}$; The transfection with nYFP + cYFP was used as the negative control. The mCherry$_{NLS}$ represents mCherry linked with Nuclear Localization Sequence (NLS, 12 amino acid residues) and was used as the nuclear marker. BR represents the images of bright field. The Merged refers the overlaid image from the other three in each transfection. The upper panel of A or B shows the representative cellular images; the

lower panel of A or B shows the relative fluorescence of different BiFC images measured in ImageJ (n=3 biological replicates).

fluorescence). The features of interaction of KRP4 with Fb3 and its mutants are similar, as shown in Fig. 3 B.

3. OsFb3 protein interacts with OsKRP5 and OsKRP4 in rice egg cells and zygotes

As shown in Fig. 4 A, the fluorescent signals under the mark BiFC represent the positive interactions between OsFb3 and OsKRP5 in rice egg cell (0 h) and zygotes (2 hours and 9 hours after pollination) transfected with the construct $Fb3_{promoter}$ - Fb3 - cEYFP::$KRP5_{promoter}$ - KRP5 - nEYFP, and these interactions take place in nuclei as indicated by their overlapping with the red signals of $mCherry_{NLS}$. The similar signals are detected for the interaction of Fb3 with KRP4 from rice egg cells and zygotes transfected with $Fb3_{promoter}$ - Fb3 - cEYFP::$Ubiq_{promoter}$ - KRP4 - nEYFP (Fig. 4 B).

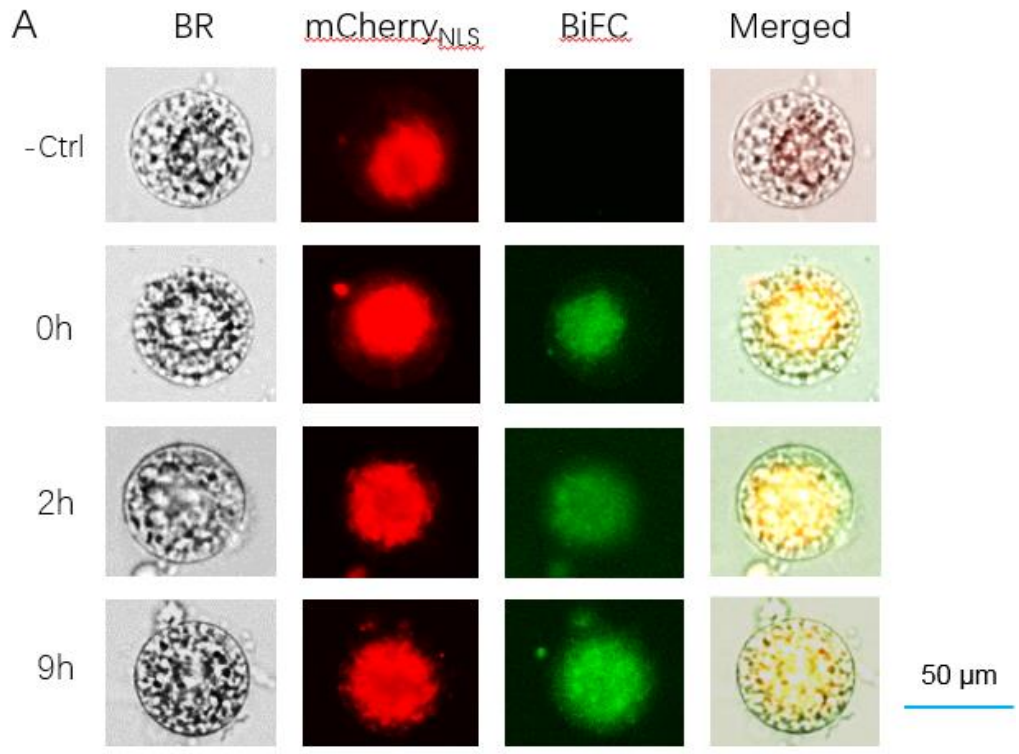

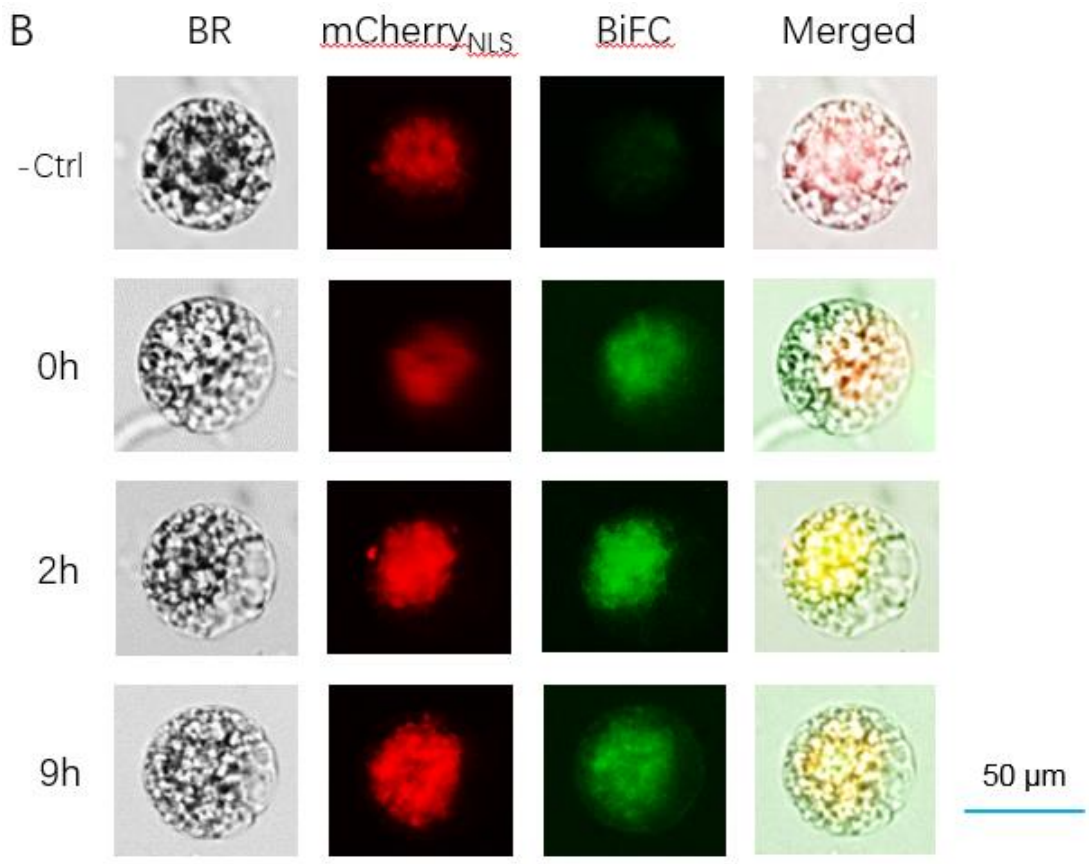

Fig. 4 BiFC assay showing interaction of OsFb3 with OsKRP5 and OsKRP4 in rice egg cells (0 h) and zygotes (2 h and 9 h after pollination). The cells were transfected with the construct Fb3$_{promoter}$-Fb3- cEYFP::KRP5$_{promoter}$-KRP5 -nEYFP (A) and Fb3$_{promoter}$-Fb3-cEYFP::Ubiq$_{promoter}$-KRP4 -nEYFP (B), respectively. The construct nEYFC and cEYFC were used as negative control, mCherry$_{NLS}$ for nuclear localization and BR for cell images in gray under the bright field; the Merged was from overlapping all other images to show that the different fluorescent signals are detected from the same cell.

III. Expression of OsFb3 protein in rice protoplasts and suspension culture

For further examining the function of OsFb3 related to OSKRP5 and OsKRP4, we needed a sufficient amount of these specific proteins expressed and partially purified. OsKRP5 and OsKRP4 were expressed and purified from the nuclei of budding yeast as previously described

(Chapter 2); but due to the lower expression level of OsFb3 or rapid degradation itsself (Kim et al 2008), it is hard to obtain sufficient material from budding yeast following the same procedure. Therefore, we tried other expression systems for better protein yield. Initially, we constructed two promoter-inducible systems (Supplementary Fig. 3 and Supplementary Fig. 4) to get the Fb3 protein from permanantly transformed rice seedling (Kim et al 2008). However, due to the unexpected difficulty in rice transformation and limited funds, this plan became impractical. Therefore, we adopted a cell-free system of *E.coli* (NEB) and a different yeast system (*Kluyveromyces lactis*, NEB), unfortunately, none of them worked for the purpose. That was why we turned to the suspension culture of transfected rice protoplasts as Dr. Libault suggested.

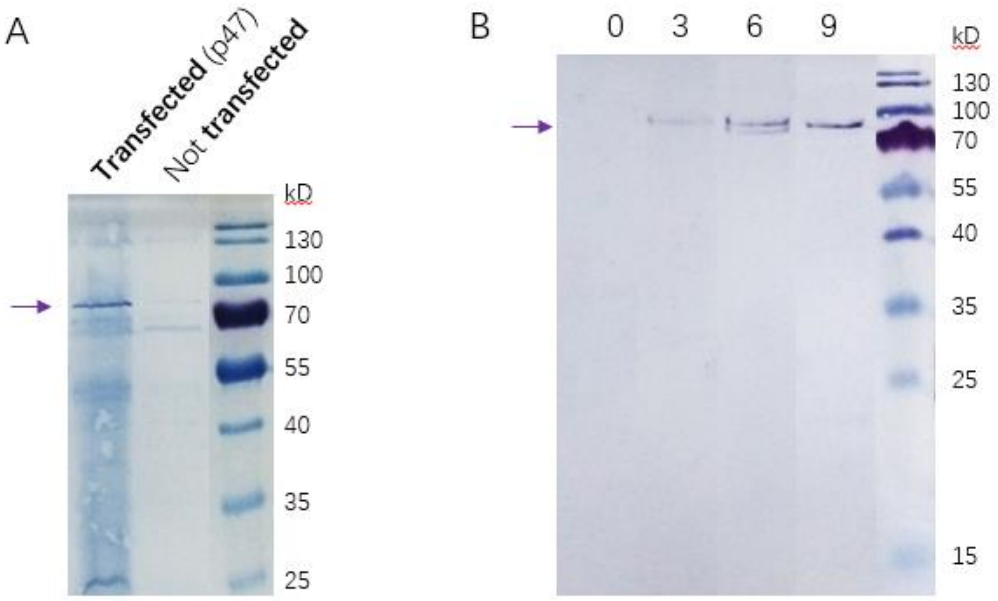

Fig. 5 Western blot assays of OsFb3 protein expressed in rice protoplasts without (A) and with (B) the suspension culture. A. HA tagged OsFb3-cCFP (~ 75 kD, arrow pointed) was detected with anti-HA mAb (Sino Biological, Cat# 100028-MM10) from the protein extract of rice protoplasts transfected with Fb3-HA-cCFP (pOH47). B. GFP tagged OsFb3 (~ 89 kD, arrow point) was detected with anti-GFP mAb (Sino Biological, Cat# 100028-MM10) from the protein extract of

rice protoplasts transfected with GFP-Fb3 (pOH79) and cultured in suspension with Chu's medium plus supplementals. 0, 3, 6 and 9: days after suspension culture. The inducer for suspension culture is ß-estrogen (20 μM).

Prior to the formal trial with suspension culture of transfected rice protoplasts, we tested the expression of HA-tagged OsFb3-cCFP in rice protoplasts. As shown in Fig. 6 A, the expected band (~75 kD) was detected in the Western blot. To obtain sufficient suspension culture product, we optimized an efficient medium recipe (see Methods V. 2) for the rice protoplasts tranfected with the inducible promoter system containing GFP-Fb3 (Supplementary Fig. 3) and grew the cells with the inducer ß-estrogen. As a result, GFP tagged OsFb3 was expressed as expected (Fig. 6 B), which was used for measuring the CDKB activity and the protein degradation assay.

IV. OsFb3 protein reverses the inhibitory effect of OsKRP5 and OsKRP4 on the kinase activity of OsCDKB

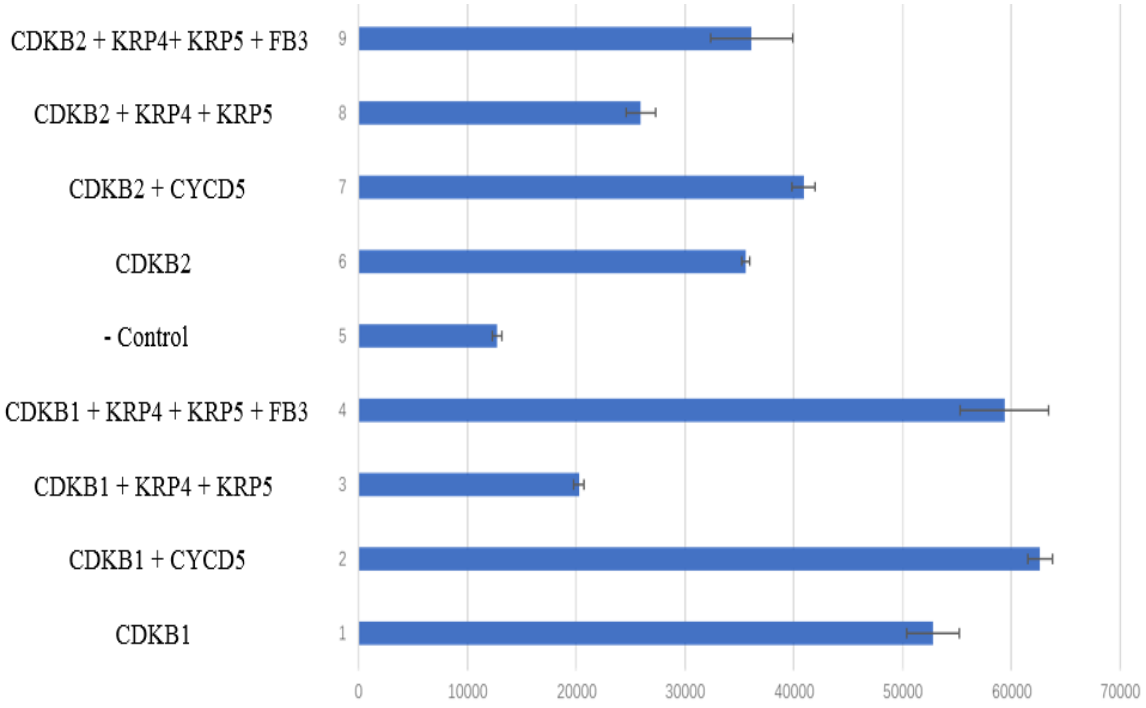

Fig. 6 Rice Fb3 protein counteracts the inhibitory effect of OsKRP5 and OsKRP4 on the kinase activities of OsCDKB1 and OsCDKB2. The activity was measured in relative fluorescent units (RFU) at EX/Em of 535/587 nm. CYCD5, rice Cyclin D5;1. The vector pGBKT7 and pGADT7 were used as the negative control. Error bar, Standard Deviation; n=3 (3 biological replicates).

As described in chapter 2, we are the first in verifying the inhibitory effect of OsKRP5 and OsKRP4 on the activity of OsCDKB1. Interestingly, the coordinate inhibition to OsCDKB1 and OsCDKB2 can be reversed by OsFb3 as demonstrated in Fig. 6. The average activity of OsCDKB1 is ca. 52,000 (RFU); it is raised to ca. 62,000 by OsCYCD5 (CDKB1+CYCD5), but reduced to about 20,000 by the interaction with both OsKRP4 and OsKRP5 (CDKB1+KRP4+ KRP5); however, the kinase activity is bounced back to nearly 60,000 by incubation with the purified OsFb3 protein (CDKB1+KRP4+KRP5+Fb3). These activity changes are similar over the inhibition of OsCDKB2 (Fig. 5). Both scenarios indicate to us that OsKRP5 and OsKRP4 indeed interact with OsFb3 and are likely further degraded via OsFb3 mediated proteasome pathway.

V. Degradation of OsKRP5 and Os KRP4 through OsFb3 associated proteasome pathway

To verify that OsKRP5 and OsKRP4 are regulated by OsFb3 mediated proteolysis, we conducted a protein degradation assay. After 30 to 60 min incubation with GFP-OsFb3 in crude rice ovary extracts, the resulting protein samples were examined using Western blots with anti-Myc monoclonal antibody. As presented in Fig. 7, the abundance of Myc-tagged OsKRP5 or similarly tagged-OsKRP4 decreased faster in DMSO (the control) than in MG132 (the specific 26S proteasome inhibitor), demonstrating that degradation of OsKRP5 and OsKRP4 is 26S proteasome dependent (Kim et al 2008).

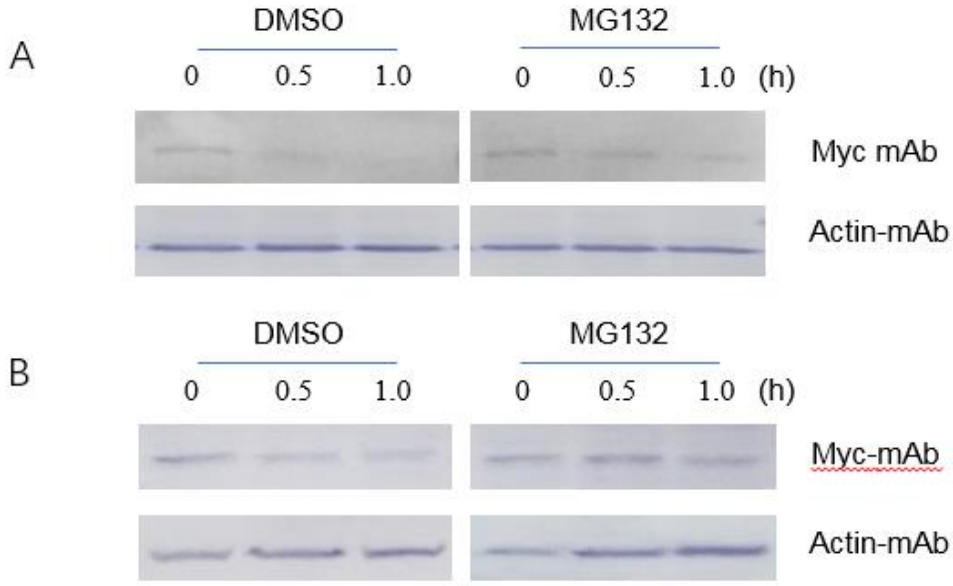

Fig.7 The 26S proteasome-based degradation of KRP5 (A) and KRP4 (B). Purified proteins of Fb3 and KRP5 or KRP4 were mixed with rice ovary extract containing the protease inhibitor cocktail treated with the specific proteasome inhibitor (MG132) and DMSO (control) incubated at 4^{o}C for 0 to 1 hour, and detected with anti-c-Myc mAb.

VI. The protein expression profile in transfected zygotes supports the regulation of OsKRP5 and OsKRP4 by OsFb3 mediated degradation

To reflect the protein expression profile of OsKRP5, OsKRP4 and OsFb3 with zygotic development, we measured the fluorescence intensity of rice egg cells and zygotes transfected with their respective EYFP fusion constructs driven by P35S (see the cellular images in chapter 1 for cellular localization). As indicated in Fig. 8, the expression level of OsKRP5, OsKRP4 and OsFb3 are relatively lower in egg cells, then higher in zygotes 2 hours after pollination (HAP). In contrast, levels of OsKRP4 and OsKRP5 declined to lower levels in the zygotes of 9 HAP, whereas OsFb3 levels rise further. This protein expression profile is consistent with the

transcription profile of OsKRP5, OsKRP4 and OsFb3 genes (Supplementary Fig. 5). In addition, as we previously observed, OsKRPs and OsFb3 are functionally opposite: both OsKRP5 and OsKRP4 coordinate inhibition of OsCDKB (the marker of mitosis for zygotic division), and maintain the arrested cell cycle state, whereas when OsFb3 encounters inhibition (Fig. 6) via mediated degradation (Fig. 7), the two inhibitors release the arrested cell cycle state. Since the rice zygotes at 9 HAP are temporarily close to the stage G2/M, which is the crucial checkpoint of the zygotic cell cycle, the above profile of the three proteins reflects the expected zygotic status as the zygote approaches its first division.

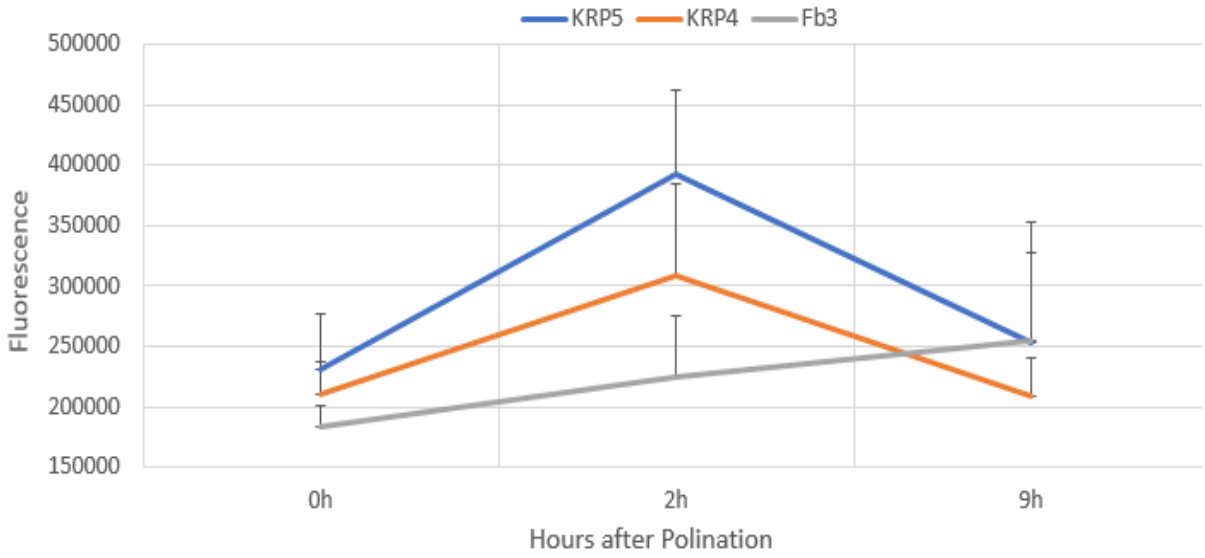

Fig. 8 Protein expression profiles of KRP5, KRP4 and Fb3 in rice egg cells (0h) and zygotic development (at 2 h and 9 h after pollination). Fluorescent intensity was approximated using the ImageJ program with images of rice cells tansfected with KRP5-EYFP, KRP4-EYFP and Fb3-EYFP (driven by P35, as in Chapter 1), respectively; n = 3 (biological replicates).

References

Bai C, Sen P, Hofmann K, Ma M, Goebl M, Harper JW and Elle SJ (1996) SKP1 connects cell cycle regulators to the ubiquitin proteolysis machinery through a novel motif, the F-box. Cell 86, 263–274

Boycheva I, Vassileva V, Revalska M, Zehirov G and Lantcheva A (2015) Cyclin-like F-box protein plays a role in growth and development of the three model species *Medicago truncatula, Lotus japonicus, and Arabidopsis thaliana*. Research and Reports in Biology. 6, 117–130

Chen S, Tao L, Zeng L, Vega-Sanchez ME, Umemura K, Wang GL (2006) A highly efficient transient protoplast system for analyzing defense gene expression and protein-protein interactions in rice. Mol Plant Pathol. 7(5): 417-427

Chen Z, Cheng Q, Hu C, Guo X, Chen Z, Lin Y, Hu T, Bellizzi M, Lu G, Wang GL, Wang Z, Chen S, Wang F (2017) A chemical-induced, seed-soaking activation procedure for regulated gene expression in rice. Front Plant Sci. 8: 1447 (1-13)

Chu CC, Wang CC, Sun CS, Hsu C, Yin KC, Chu YC, Bi FY (1975) Establishment of an efficient medium for anther culture pf rice through comparative experiments on the nitrogen sources. Scientia Sinica, 18 (5), 659-668

Cui H, Zhang Z, Lv W, Xu J and Wang XY (2015) Genome-wide characterization and analysis of F-box protein-encoding genes in the *Malus domestica* genome. Molecular Genetics and Genomics. 290(4), 1435–1446

Gagne JM, Downes BP, Shiu SH, Durski AM and Vierstra RD (2002) The F-box subunit of the SCF E3 complex is encoded by a diverse superfamily of genes in Arabidopsis. PNAS. 99, 11519–11524.

Cardozo T, and Pagano M (2004) The SCF ubiquitin ligase: Insights into a molecular machine. *Nat.* Rev Mol Cell Biol. 5, 739–751

Gupta S, Garg V, Kant C and Bhatia S (2015) Genome-wide survey and expres-sion analysis of F-box genes in chickpea. BMC Genomics16: 67.

Hirose T, Mizutani R, Mitsui T and Terao T (2012) A Chemically inducible gene expression system and its application to inducible gene suppression in rice. Plant Prod Sci. 15(2), 73-78

Hershko A and Ciechanover A (1998) The Ubiquitin system. Annu. Rev Biochem. 67, 425-479

Ho MS, Tsai P I, and Chien C T (2006) F-box proteins: the key to protein degradation. J Biomed Sci. 13, 181-191

Jones D (2014) Reproductive development in two plant models: in situ visualization of the female gametophyte and transcriptomic analysis of cell cycle regulation in Oryza sativa post-fertilization. Master's degree Thesis, University of Oklahoma

Kim HJ, Oh SA, Brownfield L, Hong SH, Ryu H, Hwang I, Twell D and Nam HG (2008) Control of plant germline proliferation by SCFFBL 17 degradation of cell cycle inhibitors. Nature 455, 1134-1137

Kim TG, Baek MY, Lee EK, Kwon TH, Yang MS (2008) Expression of human growth hormone in transgenic rice cell suspension culture. Plant Cell Rep. 27(5), 885-891

Kipreos, E. T. and Pagano, M. (2000). The F-box protein family. Genome Biol. 1, 1-7

Ko SS, Li MJ, Sun-Ben Ku M, Ho YC, Lin YJ, Chuang M H, Hsing HX, Lien YC, Kudla J and Bock R (2016) Lighting the way to protein-protein interactions: recommendations on best practices for Bimolecular Fluorescence Complementation analyses. Plant Cell 28, 1002-1008

Kumar, A. and Paietta, J. (1995). The sulfur controller-2 negative regulatory gene of *Neurospora crassa* encodes a protein with beta-transducin repeats. PNAS. 92 (8), 3343–3347

Kumlehn J, Lörz H and Kranz E (1998) Differentiation of isolated wheat zygotes into embryos and normal plants. Planta. 205, 327–333

Main M, Frame B and Wang K (2014) Chapter 13 Rice, Japonica (*Oryza sativa* L.). In Kan Wang (ed.), *Agrobacterium Protocols: Volume 1*, Methods in Molecular Biology, Springer Science+Business Media New York, vol. 1223, pp160-179

Marrocco, K., Bergdoll, M., Achard, P., Criqui, M. C., and Genschik, P. (2010). Selective proteolysis sets the tempo of the cell cycle. Cur. Opin. Plant Biol. *13*, 631–639

Malik Z, Gul A, Amir R, Munir F, Babar MM, Bakhtiar SM, Hayat MQ, Paracha RZ, Khalid Z and Alipour H (2020) Classification and Computational Analysis of *Arabidopsis thaliana* Sperm Cell-Specific F-Box Protein Gene *3p.AtFBP113.* Front. Genet. 11, 1-17

Schulman BA, Carrano AC, Jeffrey PD, Bowen Z, Kinnucan ER, Finnin MS, Elledge S, Harper JW, Pagano M, and Pavletich NP (2000) Insights into SCF ubiquitin ligases from the structure of the Skp1–Skp2 complex. Nature 408, 381-386

Pagano M, Tam SW, Theodoras AM, Beer-Romero P, Sal GD, Chau V, Yew PR, Draetta GF, Rolfe M (1995) Role of the ubiquitin-proteasome pathway in regulating abundance of the cyclin-dependent kinase inhibitor p27. Science. 269, 682-685

Sadanandom A, Bailey M, Ewan R, Lee J and Nelis S (2012) The ubiquitin-proteasome system: central modifier of plant signaling. New Phytol. 196, 13–28

Sharma B, Joshi D, Yadav PK, Gupta AK, and Bhatt TK (2016). Role of ubiquitin-mediated degradation system in plant biology. Front. Plant Sci. 7:806

Sreekala C, Wu L, Gu K, Wang D, Tian D, Yin Z (2005) Excision of a selectable marker in transgenic rice (*Oryza sativa L.*) using a chemically regulated Cre/loxP system. Plant Cell Reports. 24, 86–94

Teixeira FR, Manfiolli AO, Soares CS, Baqui MMA, Koide T, and Gomes MD (2013) The F-box Protein FBXO25 Promotes the Proteasome-dependent Degradation of ELK-1 Protein.

J Biol Chem. 288(39), 28152–28162

Xu G, Ma H, Nei M and Kong H (2009) Evolution of F-box genes in plants: Different modes of sequence divergence and their relationships with functional diversification. PNAS. 106, 835–840

Xu H, Zhang J, Zeng J, Jiang L, Liu E, Peng C, He Z, Peng X (2009) Inducible antisense suppression of glycolate oxidase reveals its strong regulation over photosynthesis in rice. J Exp Bot. 60(6), 1799-1809

Zhang S, Tian Z, Li H, Guo Y, Zhang Y, Roberts JA, Zhang Xand Miao Y (2019) Genome-wide analysis and characterization of F-box gene family in *Gossypium hirsutum* L. BMC Genomic. 20, 993

Zhang X, Gonzalez-Carranza ZH, Zhang S, Miao Y, Liu CJ and Robert JA (2019) F-box proteins in plants. Annual Plant Reviews. 2, 1–21

Zheng N, Schulman BA, Song L, Miller JJ, Jeffrey PD, Wang P, Chu5 C, Koepps DM, Elledge SJ, Pagano M, Conaway RC, Conaway JW, Harper5 JW and Pavletich NP (2002) Structure of the Cul1-Rbx1-Skp1-F boxSkp2 SCF ubiquitin ligase complex. Nature 416, 703–709

Supplementary Data

Supplementary Table 1 Locus number of F-box genes expressed in rice zygotes

Name	Locus number[1]	CDS length (bp)	RNAseq (TPM)[2]	RT-PCR[3]	Cloned
Fb1	LOC_Os03g43990.1	1875	186 ~ 302	(++)[4]	(Y)[4]
Fb2	LOC_Os12g40860.1	1722	93 ~ 340	(++)[4]	(Y)[4]
Fb3	LOC_Os08g09750.1	1656	45 ~ 300	+	Y
Fb4	LOC_Os06g40360.1	1995	529 ~ 65		
Fb5	LOC_Os05g37690.1	1794	818 ~ 339		
Fb6	LOC_Os05g35110.1	1131	650 ~ 129	++	Y
Fb7	LOC_Os04g32460.1	1728	1501 ~ 488		

1. *Rice genomic database, MSU: http://rice.plantbiology.msu.edu*

2. *RNAseq in rice zygotes (0 ~ 9 HAP) in TPM (transcripts per million) (HRP, hours after pollination): http://sundarlab.ucdavis.edu/cgi-bin/rice_zygote/DEgenescollate.alpha.pl*

3. *RT-PCR by Hengping Xu, 2016*

4. *Partially amplified and cloned without 3' fragment due to the high GC content*

+, signal intensity of RT-PCR product in DNA gel; Y, Yes.

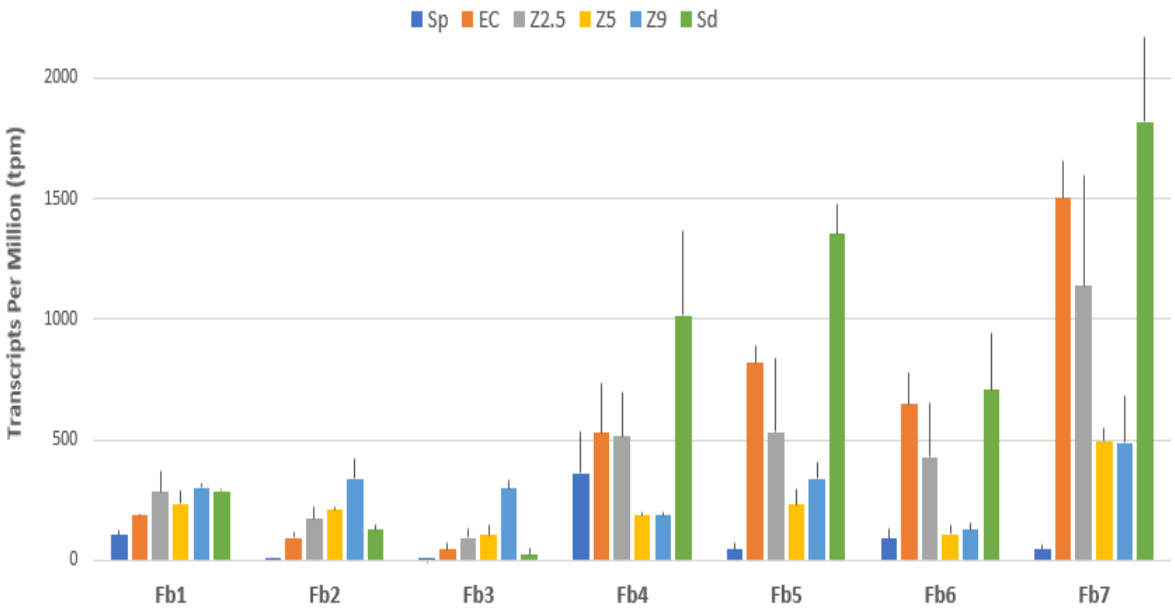

Supplementary Fig.1 RNAseq of 7 F-box genes (see Supplementary Table1) showing the preferencial expression of OsFb3 (and OsFb2) in rice egg cells and zygotes. The transcript

data is based on http://sundarlab.ucdavis.edu/cgi-bin/rice_zygote/DEgenescollate.alpha.pl. Sp, sperm cell; EC, egg cell; Z2.5, zygote at 2.5 hours after pollination (HAP); Z5, zygote of 5 HAP; Z9, zygote of 9 HAP; Sd, seedling.

Supplementary **Table 2** Primer sequences (chapter 3)

Primer names	Sequences 5' -3'
RT-PCR	
Fb1-RT-F (H17)	CGTGCATGGCGTCGCTGCCCAAGC
Fb1-RT-R (H18)	CGTGCTCAATCAAGATGAACGGTGC
Fb2-RT-F (H19)	CGTG*CATGGCCTCCTCCTCCGACG*
Fb2-RT-R (H20)	CGTGCTTAGCTCAGGTGAACGGTGC
Fb3-RT-F (H21)	CGTGCCATGCTCGGGAGGAACGCCA
Fb3-RT-R (H22)	CGTGCTCAGAACTCCATATCTGAATC
Fb4-RT-F (H23)	CTGCATGCCTCCGTTCCACGATT
Fb4-RT-R (H24)	GTCTCTAAGCAAGGATGTCGCA
Fb5-RT-F (H25)	CTGCATGGGAGGGGAGGCACCG
Fb5-RT-R (H26)	GTCTTCACGCAGGATACAAAGGA
Fb6-RT-F- (H27)	CTGCATGGTTAGTGGGAGGTC
Fb6-RT-R- (H28)	GTCTTCAGTATGCGTGGCTAGG
Fb7-RT-F (H29)	CTGCATGACGTACTTCCCGGAG
Fb7-RT-R (H30)	GTCTCTATAGGATTTTAACAAAATTT
18S- RT-F (H177)	TTAGGCCACGGAAGTTTGAG
18S-RT-R (H178)	GCATTCCTCGTTGAAGACCA
Vector construction	
Y2H	
Fb1-F- NdeI (H17)	CGTGCCATATGATGGCGTCGCTGCCCAAGC
Fb1-R- XhoI (H18)	CGTGCCTCGAGTCAATCAAGATGAACGGTGC
Fb2-F- NdeI (H19)	CGTGCCATATGATGGCCTCCTCCTCCGACG
Fb2-R- XhoI (H20)	CGTGCCTCGAGTTAGCTCAGGTGAACGGTGC
Fb3-F- NdeI (H21)	CGTGCCATATGATGCTCGGGAGGAACGCCA
Fb3-R- XhoI (H22)	CGTGCCTCGAGTCAGAACTCCATATCTGAATC

Fb6-F-EcoRI (H27)	CTGCGAATTCATGGTTAGTGGGAGGTC
Fb6-R-BamHI (H28)	GTCTGGATCCTCAGTATGCGTGGCTAGG
KRP4-F-EcoRI (H13)	GAGGCCGAATTCATGGGCAAGTACATGCGCAA
KRP4-R-BamHI (H14)	GTCGACGGATCCTCAGTCTAGCTTGACCCATTC
KRP5-F-EcoRI (H15)	GAGGCCGAATTCATGGGGAAGTACATGCGGAAG
KRP5-R-BamHI (H16)	GTCGACGGATCCCTAGCAGTCTAGCCTTGTCCA
CDKA1;1-Y2Hprey-F-EcoRI (H31)	CTGCGAATTCATGGAGCAGGTGAGCGCCT
CDKA1;1-Y2Hprey-R-BamHI (H32)	GTCTGGATCCTCATTGTACCATCTCAAGGT

BiFC

Fb3-F- XhoI (H59)	TGTCTCGAGCTATGCTCGGGAGGAACGCCAT
Fb3-R- HindIII (H60)	TGCAAGCTTCGGAACTCCATATCTGAATCCTC
Fb3 (5'-300bp)-F- XhoI (H59)	TGTCTCGAGCTATGCTCGGGAGGAACGCCAT
Fb3-(5'-300bp)-R- HindIII (H61)	TGCAAGCTTCGCTCCTCCGGCGGCTCGCT
Fb3-(3'-324bp)-F- XhoI (H59)	TGTCTCGAGCTCTGCGCGATTTCGTGAACC
Fb3-(3'-324bp)-R-HindIII (H60)	TGCAAGCTTCGGAACTCCATATCTGAATCCTC
KRP4-F- KpnI (H124)	TGTGGTACCATGGGCAAGTACATGCGCAA
KRP4-R-SmaI (H125)	TGTCCCGGGCCGTCTAGCTTGACCCATTCAAA
KRP5-F- EcoRI (H65)	GTCGAATTCTATGGGGAAGTACATGCGGAAG
KRP5-R- SalI (H202)	TGCGTCGACCTAGCAGTCTAGCCTTGTCCA
Fb3prom-F-AgeI-NotI (H199)	CGTGTACCGGTGCGGCCGCAGCTCCGATTCATCTA TAGTC
Fb3prom-R-EcoRV (H200)	CGTGTGATATCTCCGCCGAACAGGCTGCG
UBIQprom-F-AgeI (H118)	TGTACCGGTCTGCAGTGCAGCGTGACCC
UBIQprom-R-HindIII (H119)	TGCAAGCTTCTGCAGAAGTAACACCAAACAA
KRP5prom-F-AgeI (H205)	CGTGTACCGGTGGTGACACATCGGTGGAGC
KRP5prom-R-SmaI (H206)	CGTGTCCCGGGGGCCAAGGCGCGCGCGG

Expression of Fb3 in rice protoplasts

Fb3-HA-F-XhoI (H59)	TGTCTCGAGCTATGCTCGGGAGGAACGCCAT
Fb3-HA-R-HindIII (H86)	TGAAGCTTCGAGCGTAATCTGGTACGTCGTAT GGGTACTCCATGAACTCCATATCTGAATCCTC

Fb3-F-SpeI (H189)	CGTGCACTAGTATGCTCGGGAGGAACGCC
Fb3-R-SpeI (H190)	CGTGCACTAGTTCAGAACTCCATATCTGAATC
Fb3-EYFP-F-ApaI (H195)	CGTGTGGGCCCCTATGGTGAGCAAGGGCGAG
Fb3-EYFP-R-SpeI (H190)	CGTGCACTAGTTCAGAACTCCAT TCTGA TC

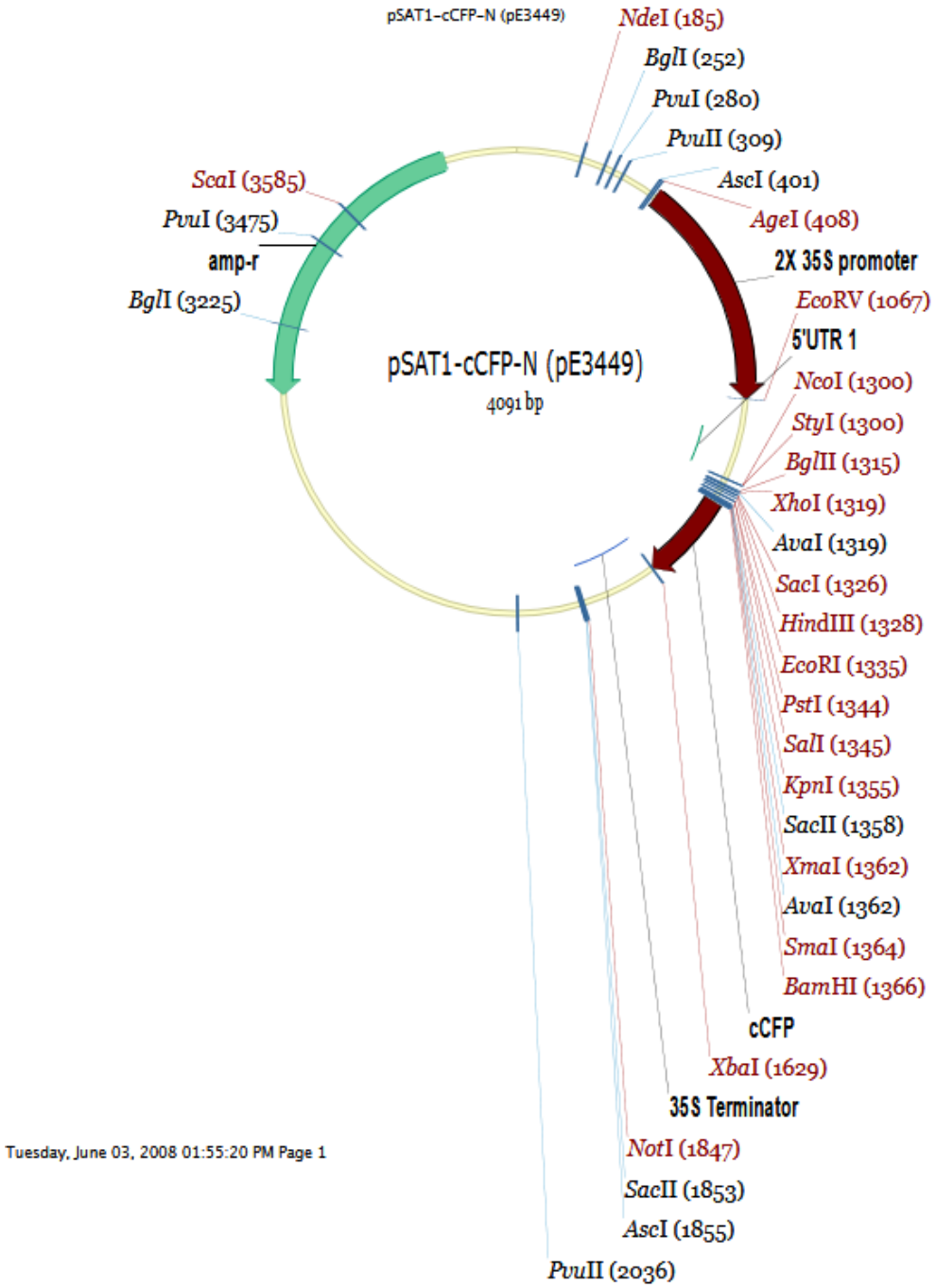

Supplementary Fig. 2 pE3449 for the expression of HA-tagged OsFb3 protein in rice protoplasts (Lee and Gelvin 2014)

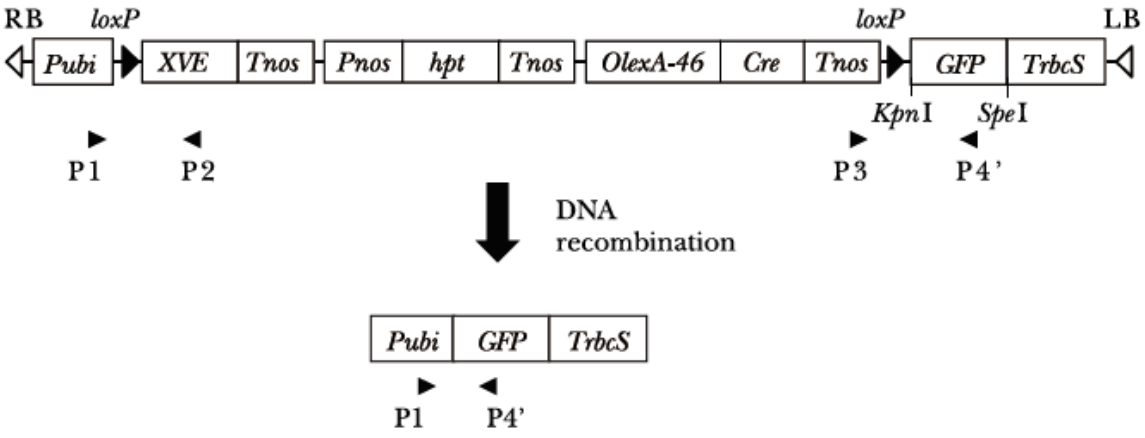

(Hirose et al 2012)

Supplementary Fig. 3 Schematic diagram showingthe structure of the T-DNA region of the promoter inducible vector, pUH-GFP2 (provided by Professor Chua Nam Hai Lab, the Rockefeller University) for the promoter inducible system. Before induction, a constitutive ubiquitin promoter Pubi drives the expression of the chimeric transcriptional activator XVE. When XVE is activated by the estrogen inducer, it stimulates the target promoter Olex-46 to express the Cre DNA recombinase. Cre recombinase excises the region between the two loxP sites, and as a result, Pubi becomes juxtaposed to GFP to drive its constitutive expression. This DNA recombination can be monitored by genomic PCR using the primers P1, P2, P3 and P4'. KpnI and SpeI are restriction sites for replacement of GFP; OsFb3 was introduced at SpeI and its orientation was identified by PCR. hpt, the gene for hygromycin phosphotransferase; Tnos, NOS terminator; TrbcS, Arabidopsis rbcS terminator.

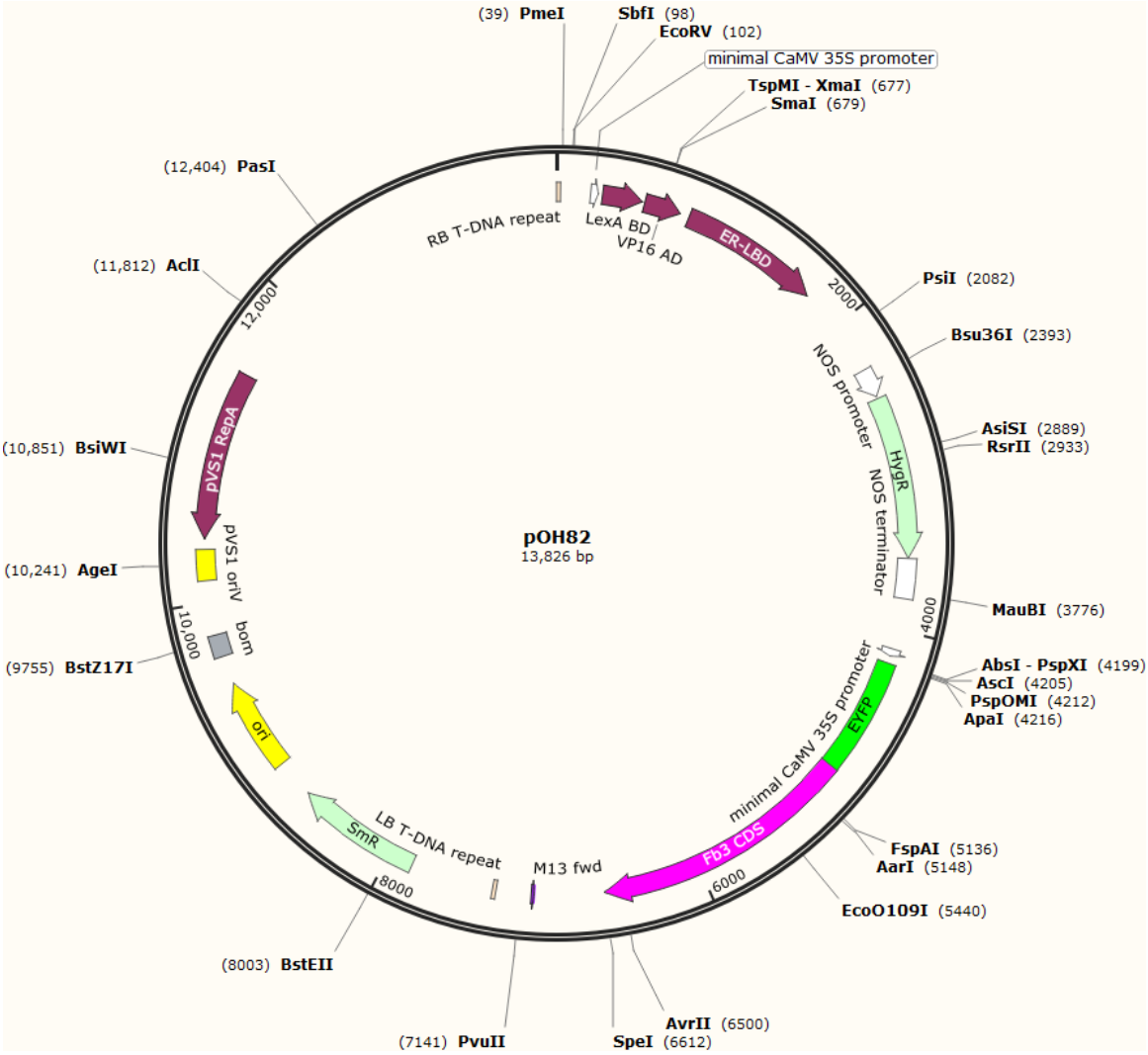

Supplementary Fig.4 Map of pOH82 showing EYFP-Fb3 introduced into the vector, pER8 (provided by Professor Chua Nam Hai Lab, the Rockefeller University), for the promoter inducible system

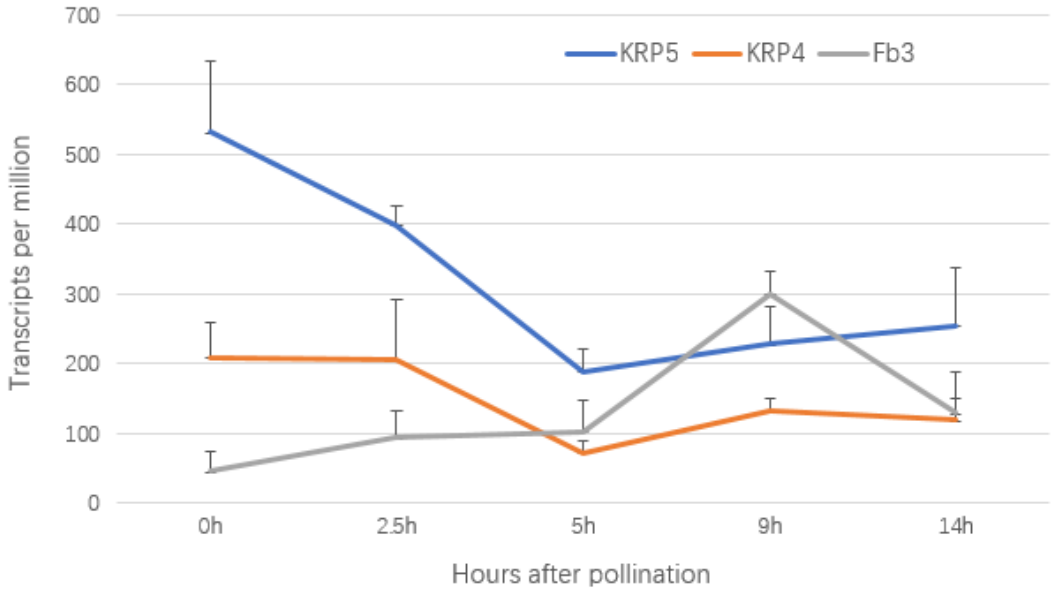

Supplementary Fig. 5 Transcription profile of KRP5, KRP4 and Fb3 in rice egg cells and zygotes with development (0 ~ 14 hours after pollination). The transcript data is based on http://sundarlab.ucdavis.edu/cgi-bin/rice_zygote/DEgenescollate.alpha.pl.

MLGRNAMLGPPRRGEGETSRRGEGSEGDGNGEGDAVDRLSALSDGV
LHHIMSFLKAWEVVRTCVLSRRWRHTWASAPCIDLRVRYNDVDSEPPE
ELRDFVNRLFRRREASAPVDTLRLQSSDPDELFDNDDANAWIRTAINRN
ARFIHLTGHRTEIGVLKHRALVSTHLKILKLSYVLIDDKILKQLSSGCKSLE
ELDLKDCAMTGHEISSASLKILKMDKCKINVDLSITAPNLVLLNLITPYIQVP
SFKNLESLVSCSVILDDFFLGDAYEHSSDEDDIDETTDEDDIDDQKKTYK
TGYGFGFPQKGYGLAGNKDDYGYGSDIESDDNTYEYSEIAKEYGDQQY
AQNSSTIVQGVGTSQQTKTISGGHNFLHGLSNARSLELLAGAGEVVLSR
ELKSCPIFSNLKTLSLGEWCMAAEFDTLIFLLQRSPNLQRLFLKLKLNFNT
RKPLESGAKPMGRSFTCKDLQMVKIRCSKDDVRVHTLACLFRANGIPIE
KIYVRRTGSSYLRGEKFMRDLGKHELEFWGSDSEFCGPNSEFCGSDSE
FEDSDMEF

Supplementary Fig. 6 Predicted amino acid sequence of rice Fb3 protein (551 amino acid residues, 61.9 kD) encoded by LOC_Os08g09750 (1656 bp CDS used as Prey 3 in Y2H); (N') F-box (42~81) and (C') LRR are underlined (based on the rice genome sequences from http://rice.plantbiology.msu.edu)

Chapter 4 Effects of the Three Mutant Cell-Cycle-Genes on Rice Seed Formation

Abstract

In the above two chapters, KRP 5 and KRP4 are identified as the coordinate inhibitors of CDKB and Fb3 as their regulator through proteolysis pathway for rice zygotic cell cycle. We assume that all these three proteins play an essential role in initiation of rice seed formation. Therefore, we conducted the phenotypic observation and genetic analysis in rice mutants. As a result, all five mutant lines show significantly reduced seed setting rate. The mutation (gene knockout or activation) also result in morphologically abnormal female germ units and functionally compromised sperm cells. For the future study, it is interesting to check if the rice sperm cell contributed KRP5 and KRP4 bearing epigenetic codes which might be different from those in rice egg cells.

Introduction

As one of staple cereal crops, rice provides the principal food for nearly 50% of population in the world. Moreover, rice has the smallest genome size (400 Mb) and richer genetic information (such as molecular markers and physical maps) compared to other major cereal crops (Gale and Devos 1998). Therefore, it was the first monocot crop plant chosen for sequencing its whole genome (Feng et al 2002, Goff et al 2002, Sasaki et al 2002 and Yu et al 2002).

However, the most challenging issue in the post-genome era is how to reveal the functions of so many assumed rice genes. One of popular strategies is using insertional mutagenesis in which a gene is tagged with the inserted element and its normal function is interrupted or altered, i.e. so-called knockout or loss-of-function. For this purpose, the transfer DNA (T-DNA) and the transposable element have been used as the mutagenesis (Zupan and Zambryski 1995, Krysan et

al 1999 and Ramachandran and Sundaresan 2001).

T-DNA is a part of tumor - inducing (Ti) plasmid found from the soil bacterium *Agrobacterium tumefaciens*. The Ti plasmid contains the virulence (vir) genes which encode proteins for transporting the T-DNA into the host cell nucleus and integrating it into the plant genome by recombination. The host includes not only plant species and yeast (*Saccharomyces cerevisiae* and *Kluyveromyces lactis*) (Hiei et al 1997 and Bundock 1999). Since the T-DNA insertion takes place randomly in plant genome and transfer to next generations stably, it has been widely adopted as the gene tags to obtain loss-of-function mutants in many plant species, particularly in the model plant *Arabidopsis* (Azpiroz-Leehan and Feldmann 1997; Krysan et al 1999) and rice (Jeong et al 2002, 2006 and Lo et al 2016).

The transposons refer to mobile DNA elements. They are able to change their positions (transposition) in the host genome by the transposon-encoded transposase enzyme. Since this transposition essentially serves as a random mutagenesis agent, it likely changes the expression of a gene depending on its special distance to the coding region. If the insertion takes place within the coding sequence, it may result in the loss - of - function mutant. One striking example is what Barbara McClintock discovered (Mc 1950) unstable pigmentation in maize, the transposition caused mutagenesis. Due to the advantages of transposon-based mutagenesis for easy mutant identification and high throughput assays, transposons have been developed into a powerful tool for functional genomics in various model species (Ramachandran and Sundaresan 2001, Greco et al 2008 and Kawakami et al 2017). In rice, a large number of mutants have been tagged with transposon elements including two maize transposon elements, Activator (Ac)/ Dissociation (Ds) and Spm/dSpm (Greco et al 2008, Ram et al 2019) and the rice retrotransposon, Tos17 (Jun et al 2019).

On the other hand, there are some limitation in the above strategy of gene knockout tagging. For instance, it is difficult to uncover functions of genes when they are redundant or essential for early embryonic development. Moreover, most loss-of-function mutants produce no useful phenotypes for plant breeding thus not valuable in crop improvement. Therefore, the activation tagging is adopted as the alternative strategy. In gene activation tagging, T-DNA or a transposable element still serves as the insertion vector but contains multiple tandemly arranged copies of cauliflower mosaic virus (CaMV) 35S RNA enhancers (Odell et al 1985). When these enhancers are randomly inserted with the T-DNA or transposon into the genome of host cells, the genes proximal to the insertion site will be activated at a distance of several kilo-base pairs away in either upstream or downstream orientation. Any phenotype produced by the activated gene will not interfere with its redundant members in the same family. Thus the activation tagging system has been extensively used for gain-of-function mutants in different plant species including *Arabidopsis* (Weigel et al 2000) and rice (Jeong et al 2002, 2006 and Hsing et al 2007). In addition, there are other methods designed for gain-of-function research (Zhu and Qian 2020) such as CRISPR/Cas9, the full-length cDNA overexpression (FOX) gene hunting system (Ichikawa et al 2006 and Liu et al 2013) and beneficial allele genotype mining (Zhang H et al 2018 and Zhang R et al 2019). Since the FOX and genotype mining are beyond the range of this chapter, only CRISPR/Cas9 will be briefly described due to its potential application to our project in the near future.

CRISPR/Cas9 is abbreviated from Clustered regularly interspaced short palindromic repeat (CRISPR) - associated protein 9 (Cas9). It is an adaptive phage immunity system in archaea and bacteria (Zhu et al 2020). It cuts DNA at a sequence-specific site based on DNA-RNA recognition by base paring. Therefore, it has been quickly programmed into a genome

engineering tool for any desired target site at economical cost. Since its first application in plants in 2013 (Li et al 2013, Nekrasov et al 2013 and Shan et al 2013), this system has been applied foe genome editing in various crop plant species.

To investigate further biological functions of OsKRP5, OsKRP4 and OsFb3 genes, we collected and studied multiple rice mutants and examined their seed-setting related phenotypic changes. As shown in the results, the disruption of these three genes by either knockout or activation significantly lowered the rice seed-set rate, which is likely resulted from the abnormal gametes and retarded zygotic development.

Material and Methods

Plant material

Rice plant growth in green house is same as the previous description in chapter 3.

Rice mutant lines were searched from RiceGE: Rice Functional Genomic Express Database (*http://signal.salk.edu/cgi-bin/RiceGE*) by input of the chromosome number and location and purchased (with the USDA permit) from South Korea (Crop Biotech Institute, Kyung Hee University), Taiwan (Department of Intellectual Property and Technology Transfer, Academia Sinica) and UC-Davis (Department of Plant Biology).

Methods

I. Genomic DNA isolation and genotyping

For isolation of genomic DNA, each ~ 200 mg (~ 1 cm long) rice leaf was collected from young plants (2 – 4 weeks after planting in pots) into a 2 ml plastic tube containing 3 small metal beads (two in 2 mm and one in 4 mm in diameter) and frozen in liquid nitrogen followed by grinding in

Geno Grinder (SPEX SamplePrep 2010) at 1450 rpm for 60 seconds. The sample was added on ice with 200 μl of Extraction Buffer (100 mM Tris-Cl, pH 8.0, 1 M KCl and 10 mM EDTA), vortexed briefly and incubated at 60^{o}C for 30 minutes; then added with 600 μl of dH_2O, mixed by inverting several times and centrifuged at the maximum speed and room temperature for 10 minutes in the bench centrifuge. One μl of the supernatant was used for PCR and the rest was saved at -20^{o}C.

The genotyping was carried out by routing PCR but with 3 specific primers (Supplementary Table 2).

II. RT-PCR and qRT-PCR

RNA was isolated from freshly dissected rice ovaries for RT-PCR and qRT-PCR with specific primers (Supplementary Table 2) following the same procedure as previously described in other chapters.

III. Seed-setting assay

Rice seeds were harvested from three or more plants of each wild type or mutant line. The seed setting rate is calculated using the formula: number of filled seeds / number of (filled seeds + half-filled + not filled seeds). Every seed setting assay has three or more biological replicates.

IV. Pollen staining with DAPI and FDA

To stain with DAPI, the rice pollen from 3-5 opening florets was incubated in an Eppendorf tube in dark for 10-30 minutes with 20 μl DAPI solution (0.4 μg DAPI in 1 ml of 0.1 M sodium phosphate pH7.0, 1 mM EDTA and 0.1% Triton X-100), then viewed under the fluorescent microscope (ZEISS, Germany).

For staining with FDA, the rice pollen was treated in dark for 5-10 minutes with FDA solution,

0.2 µl FDA stock (1 mg/ml acetone at 4ºC in dark) to 1 ml of 0.6 Mannitol followed by the fluorescent microscopy.

V. Light microscopy of rice ovary

The procedure was modified from the previous description (Newman GR et al, 1982, Skepper and Powell 2008).

For fixation, 3-5 rice ovaries were dissected from mature florets at 0 HAP and fixed immediately with the fixative: 2% paraformaldehyde (PFA) and 2% glutaraldehyde (GA) in 50 mM PIPES (pH 6.8), with 1 mM MgSO4, 5 mM EGTA (fixative: tissue in volume, 20:1). To reduce the inhibition of the resin polymerization by air, the sample was fixed under vacuum for 1 hour at room temperature and overnight with rotation at 4°C.

Then, the sample was washed three times in PBS buffer (10 min each) for dehydration and embedded with the following four steps:

1. Dehydrate by incubation with rotation at 4 °C in an ascending ethanol series: 10, 20, 30, 50, 70, 90 % (v/v), two times 100 %, and each for 30 min.

2. Infiltrate samples with resin by incubation in an ascending resin series of 30, 50, and 90 % (v/v) resin in ethanol with 1 h incubation at 4 °C for each solution. Finally transfer samples to 100 % (v/v) resin and incubate for overnight, 8 h, and then overnight.

3. Transfer samples to gelatin capsules (with lid) containing fresh resin and ensure appropriate orientation of plant material; fill to the top with resin and seal rapidly to exclude air.

4. Allow polymerization of resin either at 60 °C for 24–48 h using heat block in hood.

To Section with Ultramicrotome and stain with Toluidine Blue O, four steps were conducted:

1. Cut the resin block with a new razor blade to make the sample visible at the cut face; then trim the block to a trapezium with the sample in the middle and the widest edge at the bottom.

The upper and lower edges of the block should be parallel with the knife edge.

2. Prepare a glass knife and make 2 μm sections onto water. A ribbon with good quality should have a glassy surface (to view egg/zygote cells, cut from style side to the bottom).
3. Transfer a section to a drop of water on Gelatin coated slides and dry it on a hot plate.
4. Stain sections with Toluidine Blue O (0.5% in 2% Sodium Borate for 3 min, wash slowly in dH_2O, air dry, mount it with non-aqueous media (100% glycerol) and observe in bright field.

VI. Cross pollination

Cross hybridization of the rice in greenhouse was conducted in the procedure modified from what Dr. Susan McCouch described (Department of Plant Breeding and Genetics, Cornell University, *https://ricelab.plbr.cornell.edu/panicle_rice_mite_manual*). Briefly, the top half of each mature floret (spikelet) in a panicle was cut off at a slight angle using small scissors and each anther was gently removed (emasculation) by grabbing and pulling away the filament with thin forceps; then the panicle with emasculated florets was placed to the proximity of the panicle of pollen parent plant in which anthers are beginning to be extruded for pollen to be shed; finally, the two panicles were tied together and covered with a glassine bag. To ensure the pollination, the bags were tapped every half hour from ~ 11 am to 2 pm for 2-3 days. The seeds can be counted in 1 or 2 weeks and harvested in about 4 weeks after the pollination.

VII. Vector construction for stable transformation of rice mutants to express KRP5 and Fb3 driven by native promoters

The specific primers (Supplementary Table 2, Chapter 3) were used for making $Promoter_{KRP5}$-mCherry-KRP5 and $Promoter_{Fb3}$-EYFP-Fb3. These two constructs were cloned into the binary vector pE3055 (Lee and Gelvin 2014) as the plasmid p119cds and p118cds separately

(Supplementary Fig. 2 and 3). The 2 final plasmids were used for the stable transformation of rice KRP5KO mutant line (#05609) and Fb3KO mutant line (#2792), respectively, to entirely or partially restore the reduced seed-setting rate (Complementation) in the Plant Transformation Facility, Cornell University.

Results and Disscussion

I. Collection of rice mutant lines and observation of the seed-setting related traits

To further investigate the functions of OsKRP5, OsKRP4 and Fb3 genes in rice embryogenesis and rice seed formation, we did the search in Rice Functional Genomic Express Database and

Table 1 Observation of seed-setting related traits in ten rice mutant lines

Line #	Mutation	Height (cm)	Til # / Pl	Gr # / Pan	Seed setting (%)	1000 Gr Wt (g)
5609	KRP5 KO-1	75 ~ 90	~ 5	57	33.1 **	21.4
WT (DJ)		80 ~ 90	~ 6	54	89	24
18132	KRP5 KO-2	80 ~ 100	~ 9	81	28**	19.2
WT (HY)		80 ~ 90	~ 6	60	91.7	24.56
43987	KRP5 AC-1	50 ~ 60	2 ~ 3	54	62.4**	22.2
WT (Tn)		65 ~ 85	3 ~ 6	112	96.4	22.5
40246	KRP5 AC-2	50 ~ 60	~ 6	54	34.3**	18.1
WT (HY)		80 ~ 90	~ 6	60	91.7	24.56
6157	KRP4 AC	70 ~ 90	~ 10	60	34 **	20.6
WT (DJ)		80 ~ 90	~ 6	60	89	24
6385A	KRP4 KO-1	50 ~ 60	7 ~ 8	54	56.1**	22
WT (Nip)		60 ~ 80	3 ~ 6	70	86.6	22
36527	KRP4 KO-2	50 ~ 60	1 ~ 2	112	87.2**	21.5
WT (Tn)		65 ~ 85	3 ~ 6	134	96.4	22.8
2792	Fb3 KO-1	60 ~ 70	3 ~ 6	65	46.1 **	22.1
WT (Nip)		60 ~ 80	3 ~ 6	70	86.6	22
40994	Fb3 KO-2	60 ~ 80	~ 3	76	87.7*	22.9
WT (Tn)		65 ~ 85	3 ~ 6	70	96.4	25.7
9125	Fb3 KO-3	65 ~ 85	~ 3	83	68.4**	19.3
WT (Tn)		65 ~ 85	3 ~ 6	70	96.4	22

*The data is based on the analysis of 3 - 6 plants in each mutant line; Til, tiller; Pl, plant; Gr, grain; Pan, panicle; Wt, weight; DJ, Dongjin; HY, Huayoung; Tn, Tainung 67; Nip, Nipponbare; Gr#, including grains filled, half-filled and filled; KO, Knockout; AC, Activation; Seed setting = # of filled / # of (filled + half-filled + unfilled) x 100 %; *, the difference to WT could be significant at the 0.05 level in t-test; **, the difference to WT could be significant at 0.01 level in t-test.*

collected 10 rice mutant lines from South Korea, Taiwan and UC-Davis (Supplementary Table 1), including two KRP5 knockout (KO) lines and two KRP5 activation (AC) lines; one KRP4 AC line and two KRP4 KO lines; and 3 Fb3 KO lines. Then, we had a preliminary observation of seed-setting related traits in 3 - 6 individual plants from each line. As listed in Table 1, all of the ten mutant lines shows significantly reduced seed-setting rate, particularlly in KRP5 KO mutants (#05606 and #18132), KRP5 AC mutant (#40246), KRP4 KO mutant (#06157) and Fb3 KO mutant (#2792). In addition, most mutants produced lower-weight seed grains (in 1000 Grain Weight, gram) than their WT parents except KRP4 KO line (#6385A) and Fb3 KO line (#2792).

II. Identification and selection of the rice mutant lines

We identified all the above mutant lines based on the analysis of genotyping, DNA sequencing, RT-PCR or qRT-PCR, and seed-setting rate. Five lines are selected for the further study.

1. KRP5 KO-1 mutant (line# 05609)

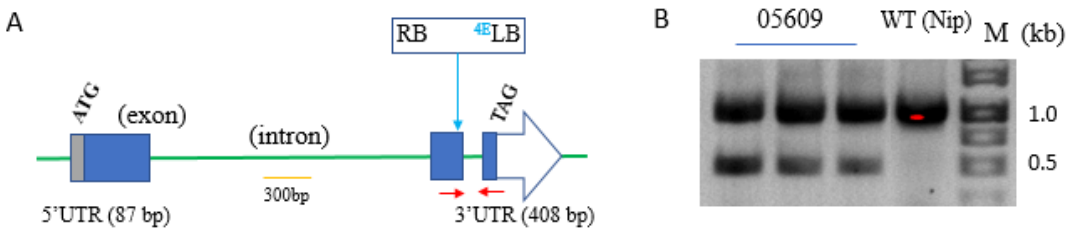

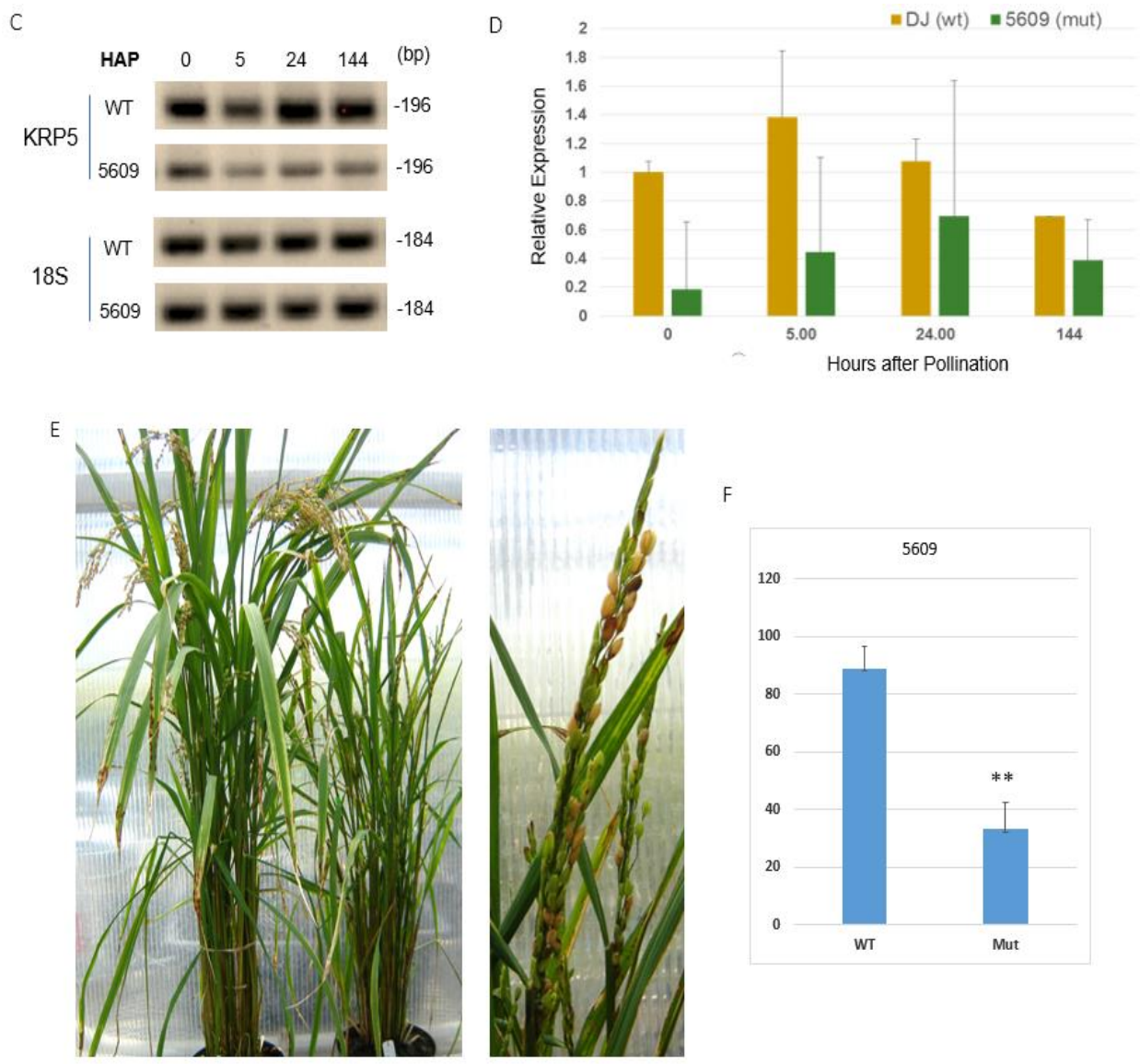

Fig. 1 Effects of KRP5 gene Knockout-1 (KO-1) in heterozygous mutant line 05609 on KRP5 transcription level and seed setting rate. ***A****. The diagram showing the gene structure of KRP5 (http://rice.plantbiology.msu.edu/ analyses_search.shtml) and T-DNA insertion site exactly determined by DNA sequencing (Supplementary Fig. 1); the red arrows show the location of primer pair for RT-PCR (C) and qRT-PCR (D).* ***B****. The gel image of genotyping with specific primers (Supplementary Table 2) in multiplex PCR: the 1 kb band shows the PCR product from*

genomic DNA, and the 0.5 kb band shows the chimeric product from the T-DNA insertion region; the heterozygous individual plants are identified by the presence of both products. ***C****. The gel image of RT-PCR showing reduced KRP5 transcription level in the ovaries of mutant line at different developmental stages (HAP, hours after pollination).* ***D****. The result of qPCR showing reduced KRP5 transcription level in the ovaries of mutant line at different developmental stages. 18S rRNA gene was used as the internal control for equal loading in both C and D.* ***E****. Representative plants of WT, Dongjin (the bigger plant in the left photo) and the mutant (the smaller one in the left photo and the close-up of mutant panicles in the right).* ***F****. The reduced seed-setting rate in the mutant (3 biological replicates; each has about 1000 seeds counted).* *******, the s*ignificant difference to WT is at the level of p<0.01*.

As shown in Fig. 1 B, KRP5 KO mutant (#05609) is identified as heterozygous because of the presence of both 1 kb PCR product amplified from the genomic DNA and the 0.5 kb chimeric product from the T-DNA insertion region (using the gene specific forward primer and T-DNA border reverse primer). The exact insertion site of T-DNA was determined by DNA sequencing (Supplementary Fig. 1): it is between the nucleotide #530 (G) and #531 (T) in the codon AGT encoding amino acid #175, S (Serine). Both RT-PCR and qRT-PCR (Fig. 1 C and D) consistently indicate the reduced transcription level of KRP5 in this line at different ovary developmental stages. Obviously, the lower expression is caused by the knockout of KRP5 gene with the T-DNA insertion within the coding reagion. More importantly, this KO mutant results in much lower seed-setting rate (Fig.1 E and F).

2. KRP5 KO-2 mutant (line# 18132)

The second KRP5 KO line (# 18132) has the insertion at the 3' terminus of KRP5 coding sequence, and it is identified as heterozygous in the same way for KRP5 KO-1 line (Fig. 2 A and

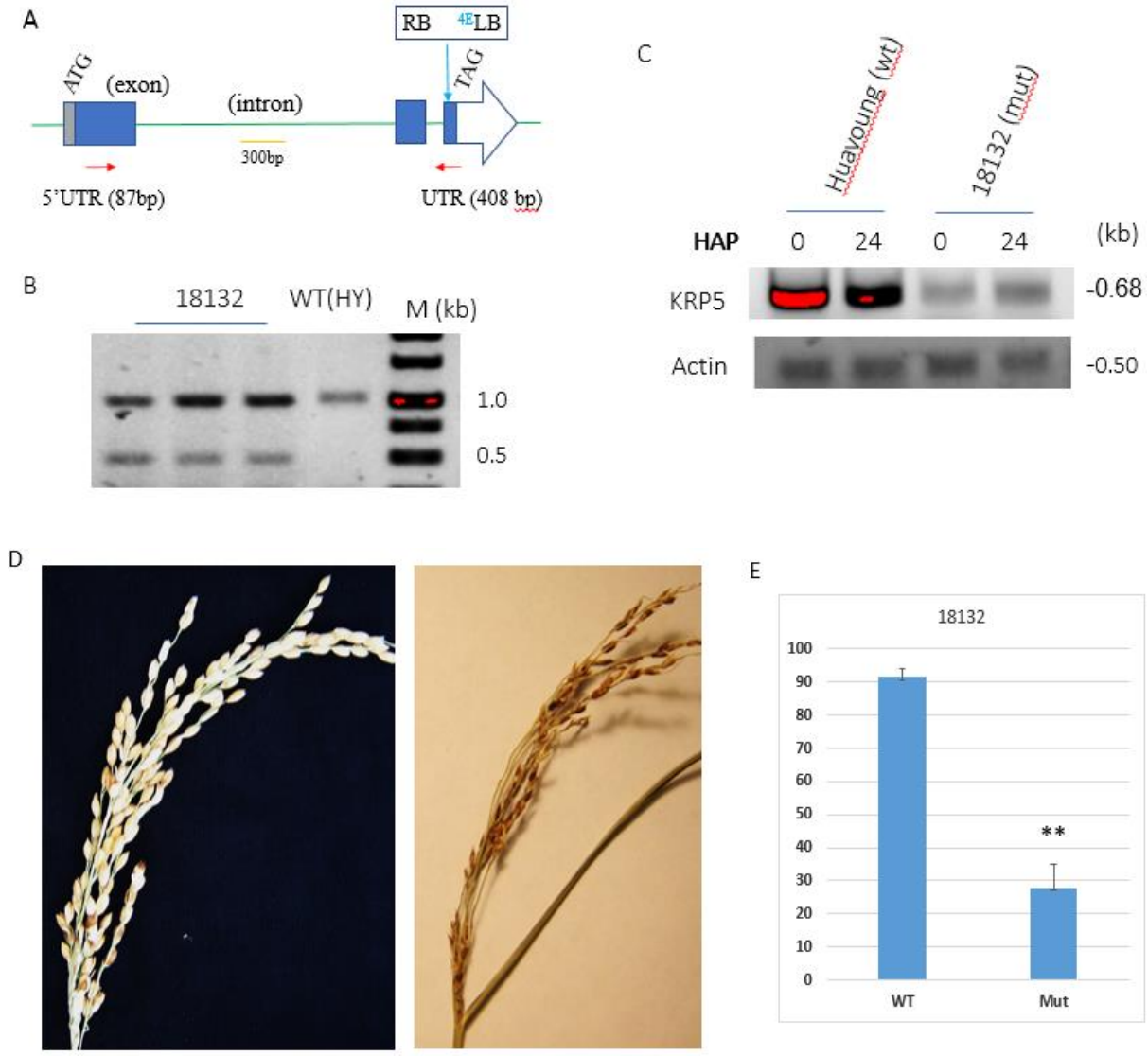

Fig. 2 Effects of KRP5 gene Knockout-2 (KO-2) in heterozygous mutant line 18132 on KRP5 transcription level and seed setting rate. ***A****. The diagram showing the gene structure of KRP5 (http://rice.plantbiology.msu.edu/ analyses_search.shtml) and T-DNA insertion site confirmed by DNA sequencing; the red arrows show the location of primer pair for RT-PCR (C).* ***B****. The gel image of genotyping with specific primers (Supplementary Table 2) in multiplex PCR: the 1 kb*

band shows the PCR product from genomic DNA, and the 0.5 kb band shows the chimeric product from the T-DNA insertion region; the heterozygous individual plants are identified by the presence of both products. ***C****. The gel image of RT-PCR showing reduced KRP5 transcription level in the ovaries of mutant line at 0 and 24 HAP; Actin gene was used as the internal control.* ***D****. Representative panicle of WT, Huayoung (the left) and the mutant (the right).* ***E****. The reduced seed-setting rate in the mutant (3 biological replicates; each has about 1000 seeds counted).* ***,*** the s*ignificant difference to WT is at the level of p<0.01*.

B). RT-PCR also shows the reduced KRP5 transcription in ovaries of this mutant at 0 and 24 HAP (Fig. 2 C). Moreover, the mutant has very lower seed-setting rate (Fig. 2 D and E).

Since the T-DNA insertion sites of the two KRP5 KO mutant lines are very close (Fig. 1 A and Fig. 2 A), it is reasonable for the both to have the similar reduced KRP5 expression and lower seed-setting rate, demonstrating the role of KRP5 gene in rice seed formation.

3. KRP4 AC mutant (line# 06157)

The KRP4 mutant line (# 06157) is identified as heterozygous by genotying (Fig. 3. B) but it is an Activation line due to the insertion of four copies of cauliflower mosaic virus (CaMV) 35S RNA enhancers carried by T-DNA (Fig. 3 A). By DNA sequencing of the chimeric PCR product, the exact insertion site was determined at the nucleotide #540 downstream the KRP4 STOP codon. As expected, the transcription of KRP4 is increased in the mutant ovaries at 0 and 24 HAP compared to the WT as indicated by RT-PCR (Fig. 3 C). However, increased KRP4 expression level did not result in any better seed-setting rate (Fig. 3 D and E); in contrast, the rate is around 34%, only about one third of WT (~ 89%).

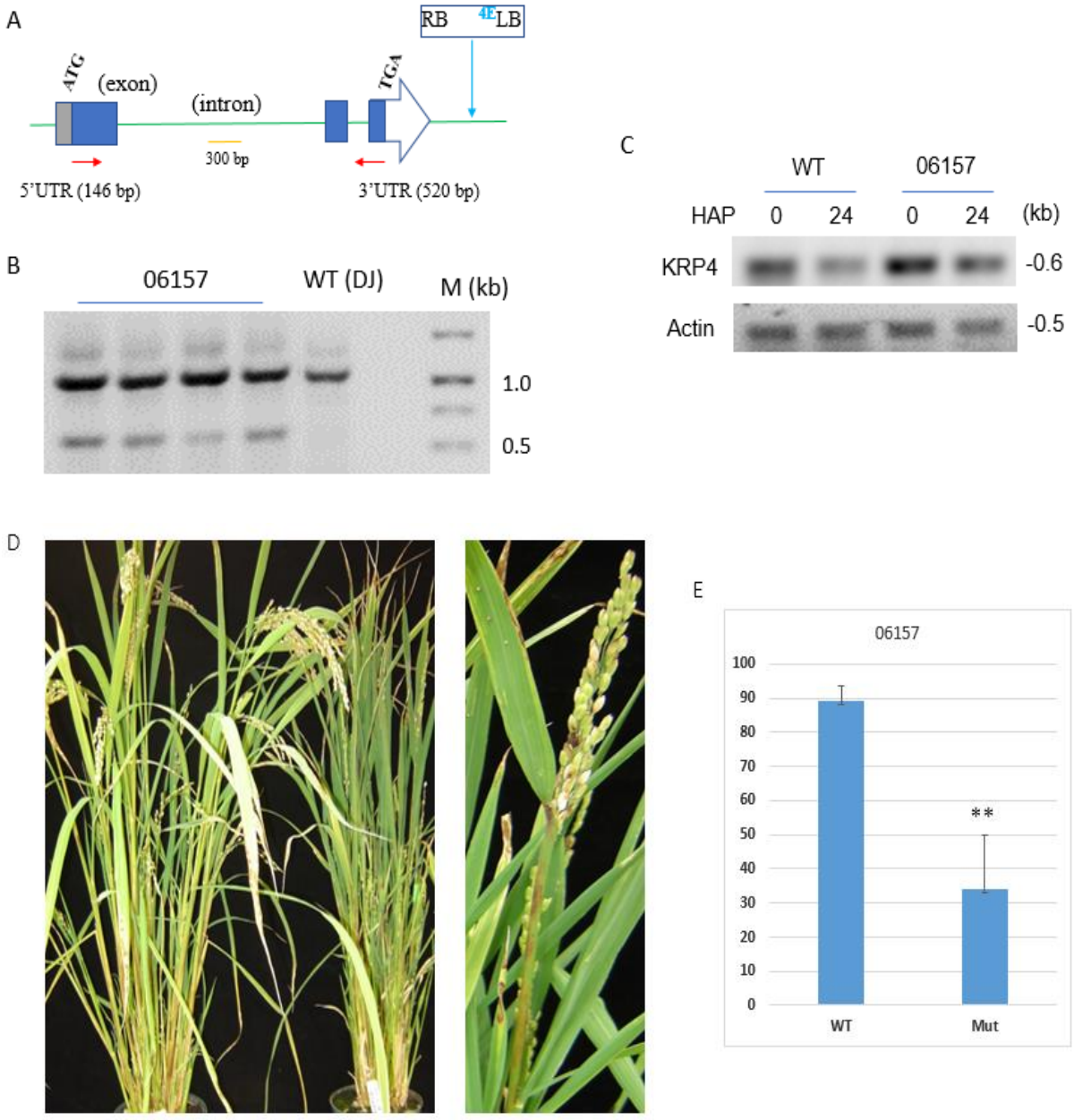

Fig. 3 Effects of KRP4 gene Activation (AC-1) in heterozygous mutant line 06157 on KRP4 transcription level and seed setting rate. ***A****. The diagram showing the gene structure of KRP4 (http://rice.plantbiology.msu.edu/ analyses_search.shtml), T-DNA insertion site, exactly determined by DNA sequencing and primer location (red arrows) for RT-PCR (C).* ***B****. The gel image of genotyping with specific primers (Supplementary Table 2) in multiplex PCR: the 1 kb*

band shows the PCR product from genomic DNA, and the 0.5 kb band shows the chimeric product from the T-DNA insertion region; the heterozygous individual plants are identified by the presence of both products. ***C****. The gel image of RT-PCR showing enhanced expression of KRP4 gene in the ovaries of mutant line at 0 and 24 HAP; Actin gene was used as the internal control.* ***D****. Representative plants of WT, Dongjin (the bigger plant in the left photo) and the mutant (the smaller one in the left photo and the close-up of mutant panicles in the right).* ***E****. The reduced seed-setting rate in the mutant (3 biological replicates; each has about 1000 seeds counted). **,* the s*ignificant difference to WT is at the level of p<0.01.*

4. KRP4 KO mutant (line# 6385A)

The KRP4 KO mutant line (# 6385A) has the transposon, dSpm, inserted within the intron (Fig. 4 A) at the nucleotide #1895 as verified by DNA sequencing. It is identified as homozygous by genotying (Fig. 4 B) due to the absence of 1.1 kb PCR product amplified from genomic DNA (of WT, Nipponbare) with the gene specific primers. As expected, the transposon insertion

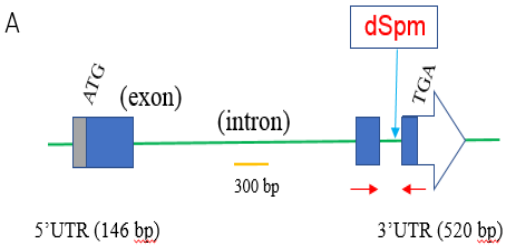

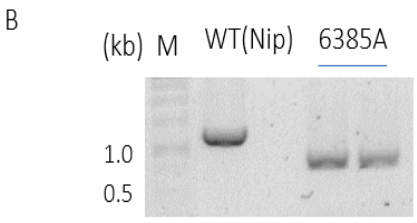

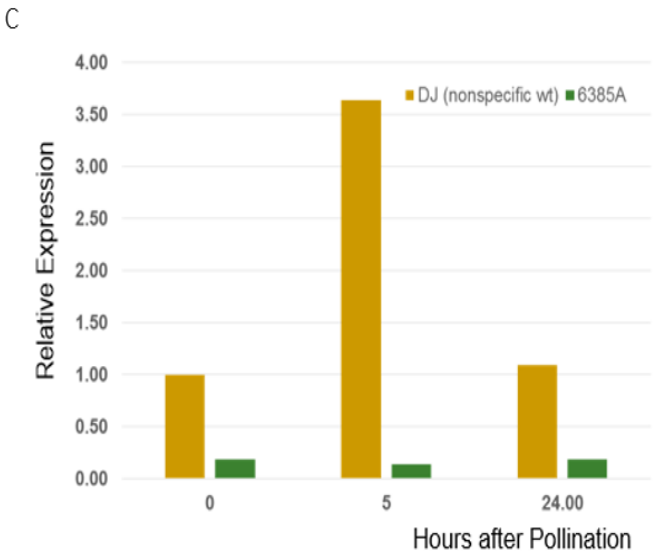

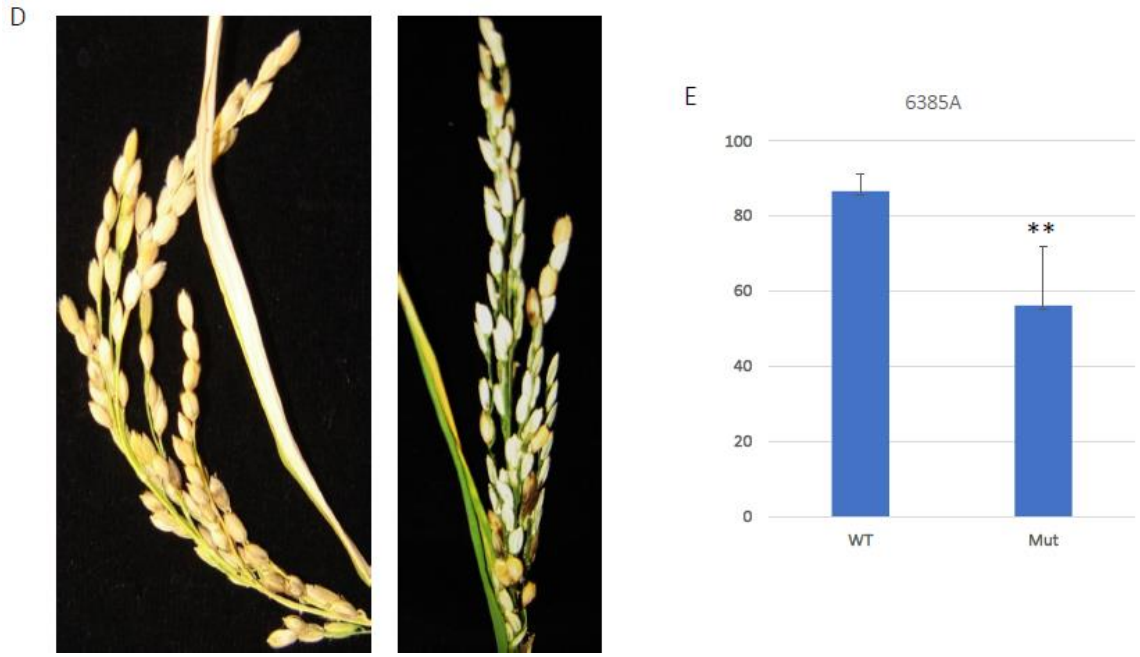

Fig. 4 Effects of KRP4 gene Knockout (KO-1) in homozygous mutant line 6385A on KRP4 transcription level and seed setting rate. ***A****. The diagram showing the gene structure of KRP4 (http://rice.plantbiology.msu.edu/ analyses_search.shtml) with primer location (red arrows) for qRT-PCR (C) and the insertion site of transposon dSpm within intron upstream of the STOP, confirmed by DNA sequencing.* ***B****. The gel image of genotyping with specific primers (Supplementary Table 2) in multiplex PCR: the 1.1 kb band shows the PCR product from genomic DNA of WT, and the 0.7 kb band shows the chimeric product from the T-DNA insertion region; the homozygous individuals are identified by the absence of 1.1 kb product.* ***C****. The gel image of qRT-PCR showing reduced expression of KRP4 gene in the ovaries of mutant line at 0, 5 and 24 HAP; 18S rRNA gene was used as the internal control.* ***D****. Representative panicle of WT, Nipponbare (left) and the mutant (right).* ***E****. The reduced seed-setting rate in the mutant (three biological replicates; each has ~ 1000 seeds counted).* **, the *significant difference to WT is at the level of* $p<0.01$.

results in the disruption of KRP4 transcription in the mutant ovaries at 0, 5 and 24 HAP as reflected in qRT-PCR (Fig. 4 C) and also significant lower seed setting rate (Fig.4 D and E).

The two KRP4 mutant lines, AC and KO, present different changes in KRP4 transcription (Fig. 3 C and Fig. 4 C), one increased against the other decresed, but both give reduced seed setting rate, indicating the importance of stable KRP4 transcription to rice embryogenesis and grain yield.

5. Fb3 KO mutant (line# 2792)

The Fb3 KO mutant line (# 2792) also has the insertion of transposon dSpm within the Exon 1 (Fig. 5 A). As determined by DNA sequencing, it takes place between nucleotide #561 and 562, i.e. between the codon CTT and TCT encoding amino acid Leucine and Serine, repsectively. The mutant plants in analysis were identified as heterozygous in genotyping (Fig. 5 B).

As expected, the transcription of Fb3 is reduced at 0, 24 and 144 HAP, but unexpectedly raised at 2.5, 5 and 9 HAP (Fig. 5 C), indicating the mechanism of compensation for Fb3 expression exists in this mutant line. Meanwhile, the same qRT-PCR shows us the greatest differnce of Fb3

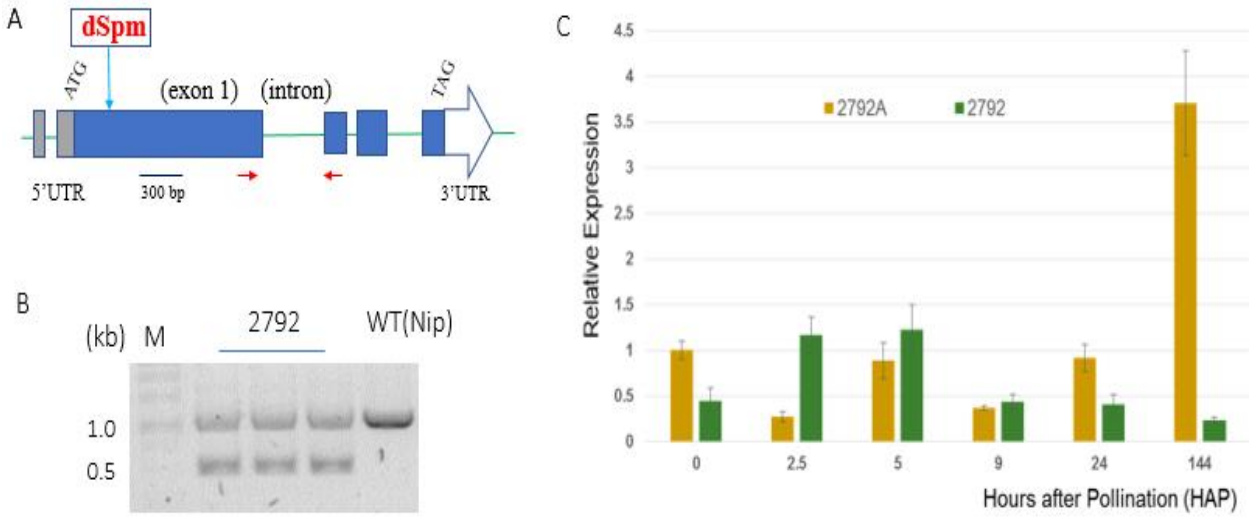

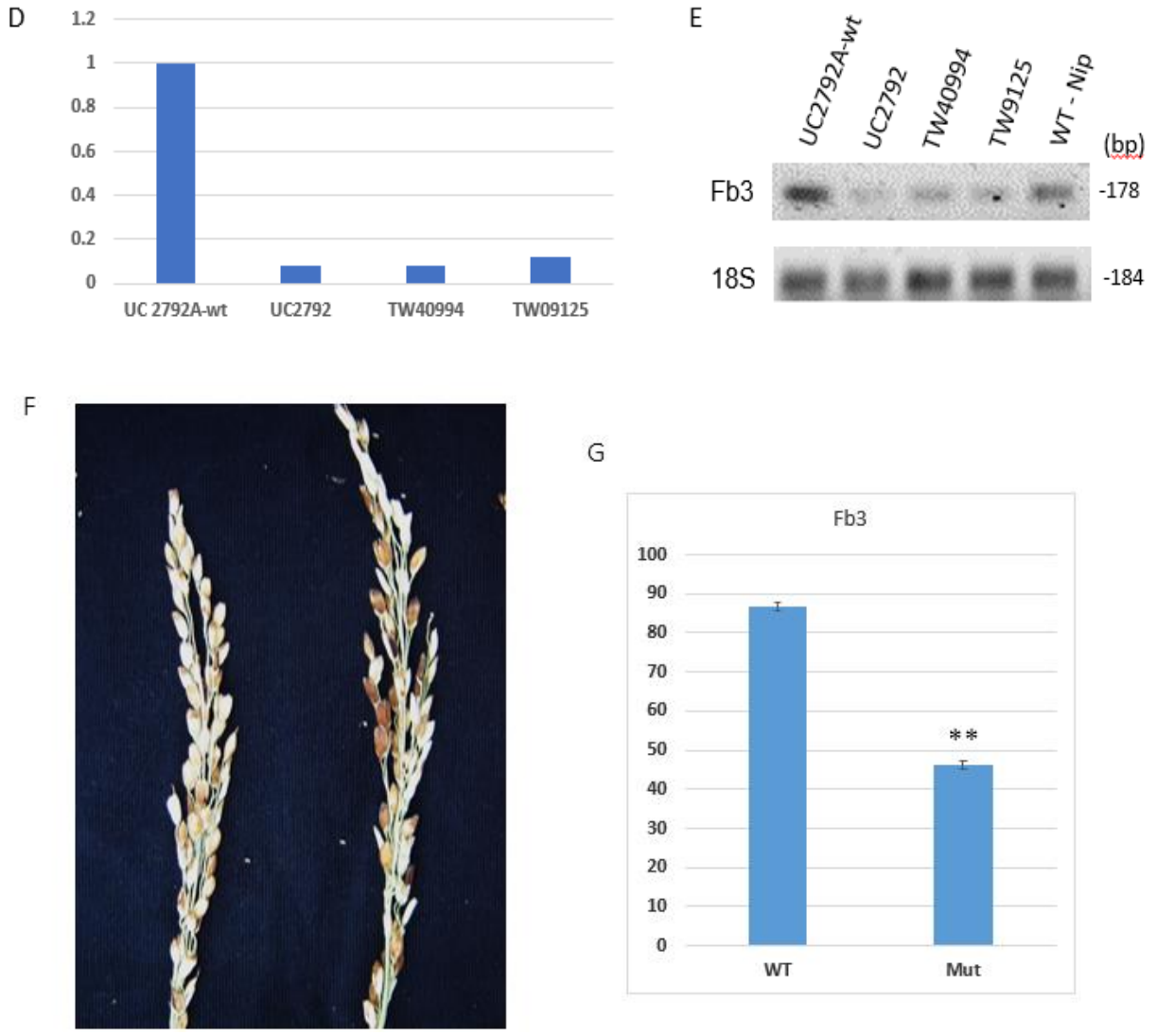

Fig. 5 Effects of Fb3 gene Knockout (KO) in heterozygous mutant line 2792 on Fb3 transcription level and seed setting rate. ***A****. The diagram showing the gene structure of Fb3 (http://rice. plantbiology.msu.edu/ analyses_search.shtml) with primer location (red arrows) for qRT-PCR (C-E) and the insertion site of transposon dSpm within the Exon 1, exactly determined by DNA sequencing.* ***B****. The gel image of genotyping with specific primers (Supplementary Table 2) in multiplex PCR: the 1.0 kb band shows the PCR product from genomic DNA of WT, and the 0.5 kb*

band shows the chimeric product from the T-DNA insertion region; the heterozygous individuals are identified by the presence of both products. ***C****. The gel image of qRT-PCR showing reduced expression of Fb3 gene in the ovaries of mutant line at 0, 5 and 144 HAP with 3 biological replicates and 18S rRNA gene was used as the internal control.* ***D****. qRT-PCR showing Fb3 expression in different Fb3 mutant lines at 144 HAP.* ***E****. RT-PCR to show Fb3 expression in different Fb3 mutant lines at 144 HAP, consistent with the result of qRT-PCR. 18S rRNA gene was used as the internal control in C-E.* ***F****. Representative panicle of WT, Nipponbare (left) and the mutant (right).* ***G****. The reduced seed-setting rate in the mutant (3 biological replicates; each has ~ 1000 seeds counted).* **, the s*ignificant difference to WT is at the level of p<0.01*.

expression between the mutant (#2792) and WT at 144 HAP. To confirm it, we repeated it in the different qRT-PCR and RT-PCR together with other two Fb3 mutant lines (TW40994 and TW 9125). The results (Fig. 5 D and E) are consistent with the previous at 144 HAP (Fig. 5 C), suggesting that the mutant ovaries have reduced Fb3 expression at HAP of 0, 24 and the later stage, but compensated during 2-9 HAP.

Similar to other mutant lines, the line 2792 presents significantly lower seed setting rate (Fig. 5 F and G), indicating the function of Fb3 in rice seed formation.

In addition, from the ovaries of this Fb3 mutant line, we detected the higher transcription levels of KRP4 at 0, 5 and 24 HAP and KRP5 at 0 and 5 HAP (Fig. 6); but the expression of KRP5 at 24 HAP is rather lowor, which is likely related to the aforementioned stage specific Fb3 compensation mechnism in the heterozygous mutant plants.

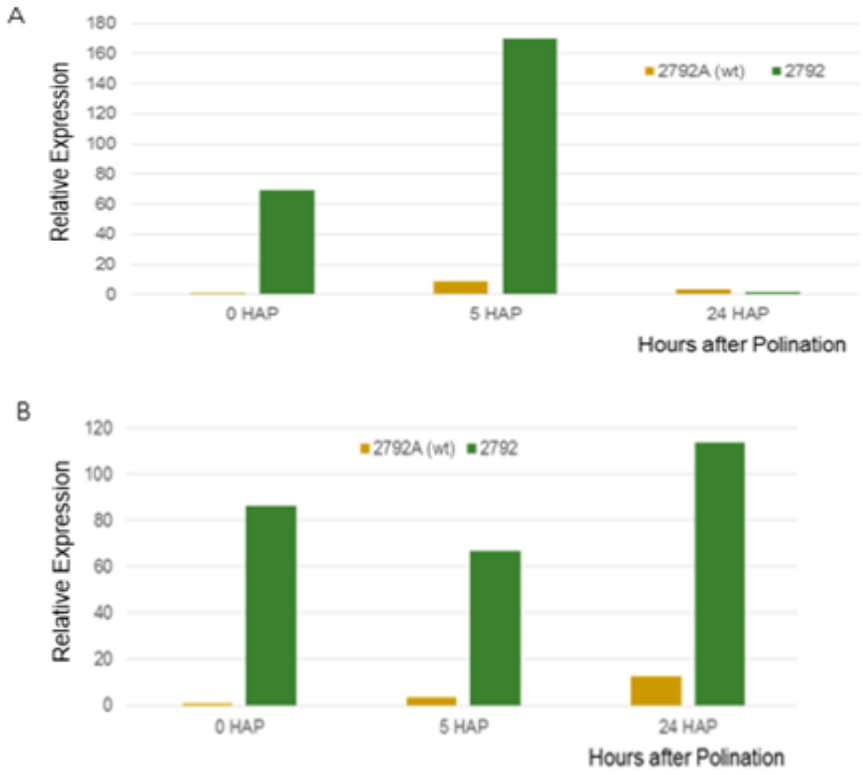

Fig. 6 The qRT-PCR showing enhanced expression level of KRP5 gene at 0 and 5 HAP (A) and KRP4 gene at 0, 5 and 24 HAP (B) in the ovaries of rice Fb3 KO mutant (2792). The relative expression is normalized with WT at 0 HAP.

III. Examination of cellular structure in pollen grains and ovaries of the rice mutants

In the regular plant reproduction, the seed formation is initiated from zygotes, the fertilized egg cell and central cell. Therefore, the reduced seed - setting rate in the above rice mutants are possibley resulted from the mutation caused abnormal male gametes, female gamets and/or zygotes. To address this issue, we examined the rice mutants in pollen grains and ovaries, separately. We stained the pollent using fluorescein diacetate (FDA), the substrate of intracellular esterase, as a viability probe, and 4', 6-diamidino-2-phenylindole (DAPI), a fluorescent molecule strongly binding to A-T rich regions in DNA, as the nuclear probe of rice sperm cells.

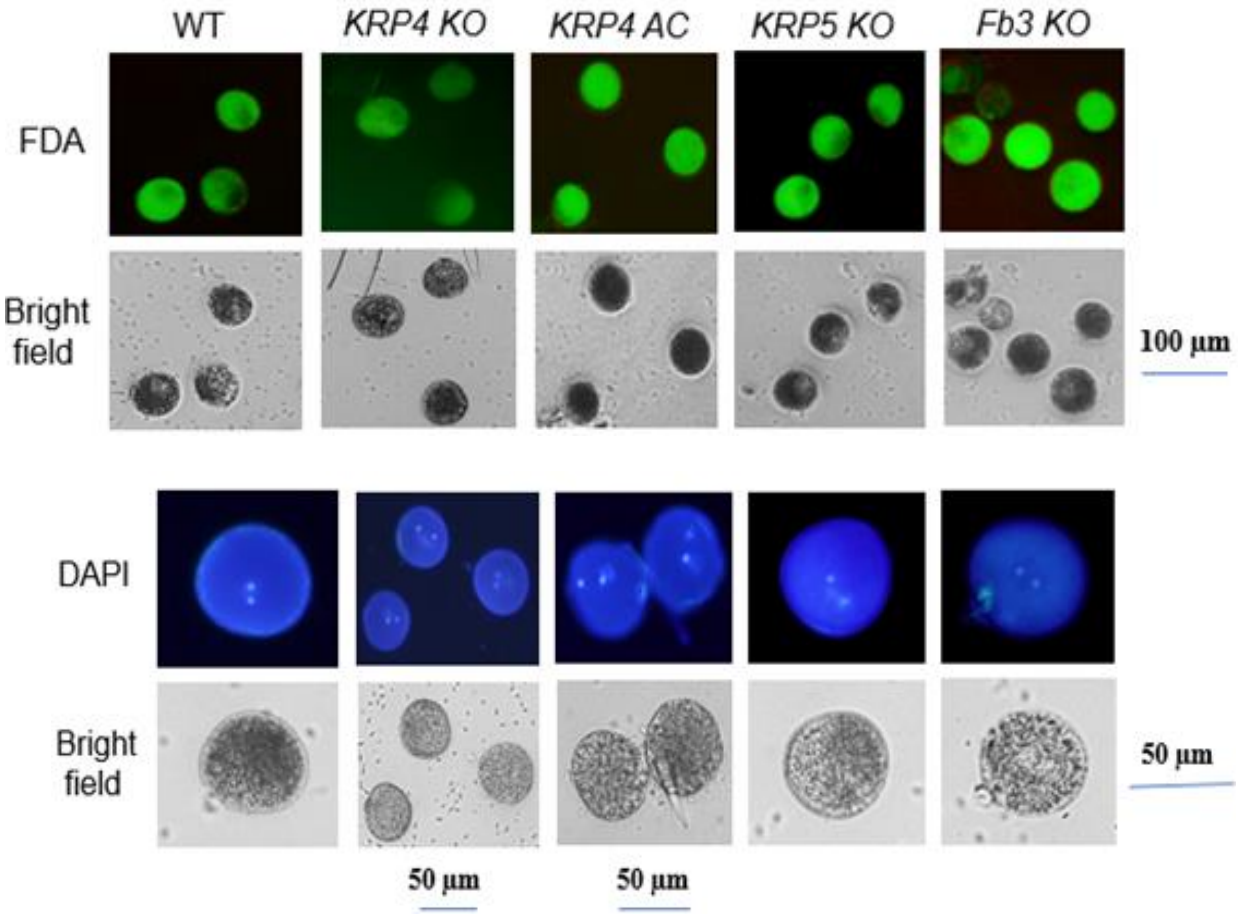

Fig. 7 Rice pollen grains stained with FDA and DAPI. KRP4KO mutant, line# 6385A; KRP4AC mutant, line# 06157; KRP5KO mutant, line# 05609; Fb3KO mutant, line# 2792. FDA staining is to show the normal pollen viability in different mutant lines; staining with DAPI indicates the normal morphology of sperm cells within pollen grains.

As shown Fig. 7, FDA stained pollen grains from the four mutant lines have the same viability as the WT; and each DAPI stained pollen grain from the mutants contains two sperm cells (the two bright spots), same as the WT. According to Kim et al (2008), only single germ cell nucleus presented in the fbl17 mutant pollen, indicating the disrupted sperm cell formation by the F-box

gene knockout in Arabidopsis. However, it is not the case in our mutant lines of either Fb3 or KRP5 and KRP4.

On the other hand, we did the ovary microscopy of three mutant lines and WT with the staining of Toluidine Blue O. Compared to the WT (green arrows in Fig. 8), the cellular structure within the mutant ovaries is obviously abnormal. Unlike in WT, the egg cells and two synergid cells look collapsed, completely undistinguishable in mutant ovaries (red arrows in Fig. 8).

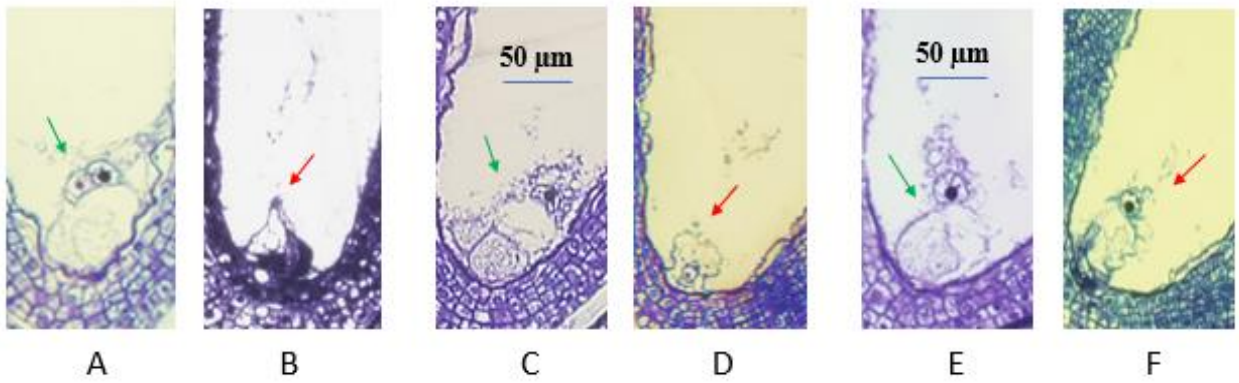

Fig. 8 Cellular structure within ovaries of rice mutants and WT at 0 HAP stained with Toluidine Blue O. A and B, WT and Fb3 KO mutant (# 2792); C and D, WT and KRP4 AC mutant (# 06157); E and F, WT and KRP5 KO mutant (# 05609). The green arrows indicate the egg cell and synergids in WT ovaries and red arrows point to the abnormal cellular structure in mutant ovaries. The dark purple spots represent cellular nuclei.

IV. Cross pollination for the double mutants and complementation

We conducted the cross pollination between two rice mutant lines for two purposes. One is to get the double mutants in KRP5 and KRP4 using two different KRP mutants in KO or AC to further explore the functions of the two rice zygotic inhibitors of cell cycle; the other is for complementing the knockout KRP mutant with the activated KRP mutant, considering that the

successful gene identification usually requires complementation of the mutant phenotype by transformation with a wild-type allele.

The results are summerized as Table 2. Although a few seeds obtained (mostly half filled), no new plant was survived, further demonstrating the crucial role of coordinate KRP5 and KRP4 (Chapeter 2) in rice zygote development and seed grain formation.

Regarding the cross pollination for complementation, it is successful between KRP4 KO mutant (line 6385A) and KRP4 AC mutant (line 06157). Only 3 fully filled seeds harvested, but in the new plants, the seed-setting rate was restored to 74.3% (Table 2), which is higher than that of their parents: 34% of KRP4 AC mutant (line 06157) and 56.1% of KRP4 KO mutant (line 6385A) (Table 1). Unfortunately, it was unsuccessful in other two pairs of cross pollination using KRP5 mutants (Table 2). That is why we turned to stable rice transformation for the complementation of KRP5 mutant using mCherry labeled KRP5 CDS driven by its native promoter (see the next part, VI).

Table 2 Cross pollination between two rice mutant lines

Cross pollination	# of pollination	# of seeds harvested	Seedset of new plant
For double mutant line			
KRP4-KO(6385A) x KRP5-KO(5609)	200	1 filled + 5 falf filled	No survival
KRP4-AC(6157) x KRP5-AC(40246)	200	4 half filled	No survival
For Complementation			
KRP4-KO(6385A) x KRP4-AC(6157)	100	3 filled + 5 falf filled	74.30%
KRP5-AC(40246) x KRP5-KO(5609)	85	3 filled + 11 falf filled	No survival
KRP5-AC(43987) x KRP5-KO(5609)	94	8 filled + 4 falf filled	23.40%

Cross pollination didn't work for the double mutants.

Complementation works in cross pollination for the 2 KRP4 mutants but not for KRP5 mutants.

V. Reciprocal pollination of the mutant and WT

The reciprocal pollination of mutant and WT was conducted not only for the complementation and also for checking further which parent is responsible for the reduced seed-setting rate in the mutants. Because of normal viability and morphology of the pollen and its contained two sperm cells in the examined mutants (Fig. 7), we didn't expect the male side would be involved in any change of seed-setting rate from the reciprocal hybridization. As summerized in Fig. 9, it is true for Fb3 KO mutant vs its WT (Nipponbare x #2792 and #2792 x Nipponbare). But surprisingly, other cross pollinations show that WT pollen always significantly improve the seed-setting rate for mutants of KRP5 and KRP4, suggesting that disturbed expression of KRP5 and/or KRP4 results in more damage to the function of rice sperm cells in fertilization or their contribution to zygote, and particullarly indicating the possibility that KRP5 and KRP4 carried by oppsite gametes may bear different epigenetic codes. Therefore, it is interesting and important to investigate the epigentic modifications of KRP5 and KRP4 in rice gametes and zygotes.

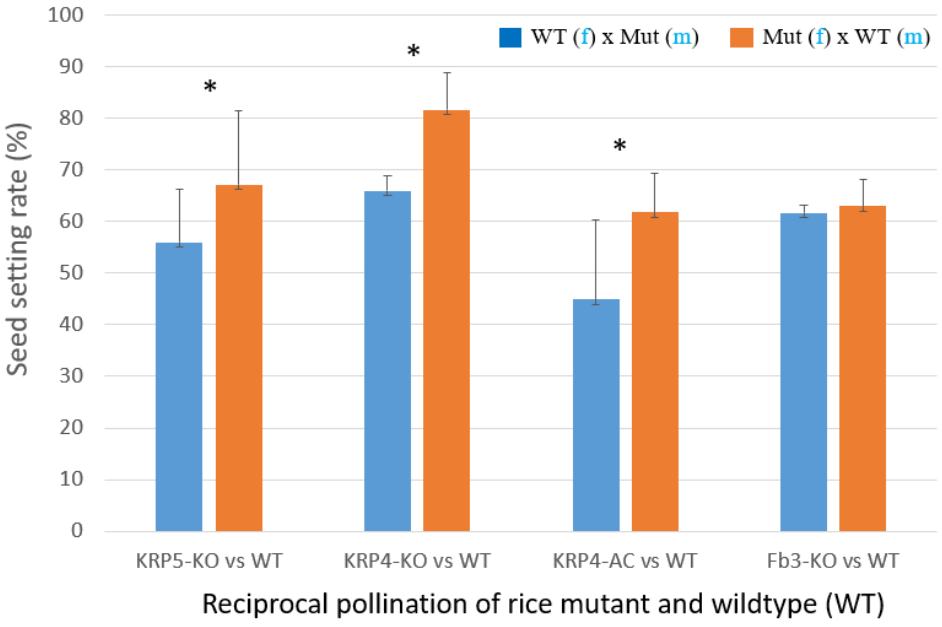

*Fig. 9 Seed setting rate from reciprocal pollination of rice mutant lines and WT. Each cross pollination is expressed in the way that parent 1 is **female (f)** and parent 2 is **male (m)** as following: KRP5-KO vs WT: DJ x 05609, 05609 x DJ; KRP4-KO vs WT: Nip x 6385A; 6385A x Nip; KRP4-AC vs WT: DJ x 06157, 06157 x DJ; Fb3-KO vs WT: Nip x 2792, 2792 x Nip; DJ and Nip are WT (Dongjin and Nipponbare). Mutant line 05609, 06157 and 2792 are heterozygous; Mutant 6385A is homozygous. * The significant difference in t-test is at the level of $P < 0.05$.*

VI. Stable transformation of rice mutants to express KRP5 and Fb3 driven by native promoters

To make the complementation in rice KRP5 KO mutant as well as Fb3 KO mutants, we constructed the cassette of red fluorescent (mCherry) labeled KRP5 under its native promoter and that of EYFP marked Fb3 with the native promoter, and then cloned them into the binary vector pE3055 (Lee and Gelvin 2014) for stable transformation of the corresponding mutants. The transformation have been initiated in the Plant Transformation Facility, Cornell University since January 2018. Due to well-known difficulty in transforming rice plant, especially its mutant, we hadn't got any transformed products until the mid of March, 2021.

The growing plantlets will be identified in PCR with specific primers, then observed for complementation in seed-setting rate assay and detected for gene expression in egg cells and zygotes with development under epi-fluorescent microscope.

References

Azpiroz-Leehan R and Feldmann KA (1997) T-DNA insertion mutagenesis in Arabidopsis: going back and forth. Trends Genet 13, 152 – 156

Bundock P, MroÂczek K, Winkler AA, Steensma HY, Hooykaas PJJ (1999) T-DNA from

Agrobacterium tumefaciens as an efficient tool for gene targeting in *Kluyveromyces lacti*. Mol Gen Genet. 261, 115 – 121

Feng Q, Zhang Y, Hao P, et al (2002) Sequence and analysis of rice chromosome 4. Nature. 420, 316 – 320

Gale MD, Devos KM (1998) Comparative genetics in the grasses. Proc Natl Acad Sci USA 95, 1971 – 1974

Goff SA, Ricke D, Lan TH, et al (2002) A draft sequence of the rice genome *(Oryza sativa L. ssp. japonica)*. Science. 296, 92 – 100

Greco R, Ouwerkerk PBF, Sallaud C, Kohli A, Favalli C, Beguiristain T, Colombo L, Pè E, Puigdomènech P, Guiderdoni E, Christou E, Hoge JHC and Pereira A (2008) Transposons and functional genomics in rice. Rice Genetics IV, 263-277

Hiei Y, Komari T and Kubo T (1997) Transformation of rice mediated by *Agrobacterium tumefaciens*. Plant Molecular Biology. 35 (1–2), 205 – 18

Hsing YI, Chern CG, Fan MJ, Lu PC, Chen KT, Lo SF, et al (2007) A rice gene activation/knockout mutant resource for high throughput functional genomics. Plant Mol Biol. 63, 351 – 364

Ichikawa T, Nakazawa M, Kawashima M, Iizumi H, Kuroda H, Kondou Y, Kondou Y, Tsuhara Y, Suzuki K, Ishikawa A, Seki M, Fujita M, Motohashi R, Nagata N, Takagi T, Shinozaki K, Matsui M et al. (2006) The FOX hunting system: an alternative gain-of-function gene hunting technique. Plant J. 48, 974 – 985

Jeong DH, An S, Kang HG, Moon S, Han JJ, Park S, Lee HS, An K, An G (2002) T-DNA insertional mutagenesis for activation tagging in rice. Plant Physiol. 130, 1636 – 1644

Jeong DH, An S, Park S, Kang HG, Park GG, Kim SR, Sim J, Kim YO, Kim MK, Kim SR, Kim

J, Shin M, Jung M and An G (2006) Generation of a flanking sequence-tag database for activation tagging lines in japonica rice. Plant J. 45, 123 – 132

Jun KM, Kim JS, Chae S, Pahk YM, Lee GS, Chung JH, Kim YK and Nahm BH (2019) Development of Tos17 insertion mutants from Korean cultivars ‘Ilmibyeo’ and ‘Baegjinju1ho’ (*Oryza sativa L.*). Appl Biol Chem. 62 (31), 1-9

Kawakami K, Largaespada DA and Ivics Z (2017) Transposons as tools for functional genomics in vertebrate models. Trends in Genetics. 33 (11), 784 – 801

Kim TG, Baek MY, Lee EK, Kwon TH, Yang MS (2008) Expression of human growth hormone in transgenic rice cell suspension culture. Plant Cell Rep. 27(5), 885-891

Krysan PJ, Young JC and Sussman MR (1999) T-DNA as an insertional mutagen in Arabidopsis. Plant Cell. 11, 2283 – 2290

Kuromori T, Takahashi S, Kondou Y, Shinozaki K and Matsui M (2009) Phenome Analysis in Plant Species Using Loss-of-Function and Gain-of-Function Mutants. Plant Cell Physiol. 50 (70), 1215-1231

Lee L and Gelvin SB **(**2014**)** Bimolecular Fluorescence Complementation for imaging protein interactions in plant hosts of microbial pathogens. In Annette C. Vergunst and David O’Callaghan (eds.), Host-Bacteria Interactions: Methods and Protocols, Methods in Mol. Biol., Springer Science+ Business Media New York *1197*, pp185-208

Li JF, et al (2013) Multiplex and homologous recombination 1 mediated genome editing in Arabidopsis and *Nicotiana benthamiana* using guide RNA and Cas9. Nat. Biotechnol. 31, 688–691

Liu YY, Wu JX and Lu TG (2013) Advance and application of FOX gene hunting system in plant. Current Biotechnology. 3, 324–327

Lo SF, Fan MJ, Hsing YI, Chen LJ, Chen S, Wen IC, Liu YL, Chen KT, Jiang MJ, Lin MK, Rao MY, Yu LC, Ho THD and Yu SM (2016) Genetic resources offer efficient tools for rice functional genomics research. Plant, Cell and Environment. 39, 998-1013

Mc, C.B. (1950) The origin and behavior of mutable loci in maize. Proc. Natl. Acad. Sci. U. S. A. 36, 344–355

Odell JT, Nagy F and Chua NH (1985) Identification of DNA sequences required for activity of the cauliflower mosaic virus 35S promoter. Nature. 313, 810–812

Nekrasov V, Staskawicz B, Weigel D, Jones J D and Kamoun S (2013) Targeted mutagenesis in the model plant *Nicotiana benthamiana* using Cas9 RNA-guided endonuclease. Nat. Biotechnol. 31, 691–693

Newman GR, Jasani B and Williams ED (1982) The preservation of ultrastructure and antigenicity. J. Microscopy, 127(3), RP5-RP6

Ram H, Soni P, Salvi1 P, Gandass N, Sharma A, Kaur A and Sharma TR (2019) Insertional mutagenesis approaches and their Use in rice for functional genomics. Plants. 8(310), 1-14

Ramachandran S and Sundaresan V (2001) Transposons as tools for functional genomics. Plant Physiol Biochem. 39, 243 – 252

Sasaki T, Matsumoto T, Yamamoto K, et al (2002) The genome sequence and structure of rice chromosome 1. Nature. 420, 312 – 316

Skepper JN and Powell JM (2008) Ultrastructural Immunochemistry: Immunostaining of London Resin (LR) White section for TEM. Cold Spring Harbor Protocols.3 (6), 1-5

Weigel D, Ahn JH, Blazquez MA, Borevitz JO, Christensen SK, Fankhauser C, Ferrandiz C, Kardailsky I, Malancharuvil EJ, Neff MM, Nguyen JT, Sato S, Wang ZY, Xia Y, Dixon RA, Harrison MJ, Lamb CJ, Yanofsky MF, Chory J (2000) Activation tagging in Arabidopsis. Plant

Physiol 122:1003– 1013

Shan Q, et al (2013) Targeted genome modification of crop plants using a CRISPR-Cas system. Nat. Biotechnol. 31, 686–688

Yu J, Hu S, Wang J, et al (2002) A draft sequence of the rice genome *(Oryza sativa L. ssp. indica)*. Science. 296, 79 – 92

Zhang H, Si X, Ji X, Fan R, Liu J, Chen K, Wang D and Gao C (2018) Genome editing of upstream open reading frames enables translational control in plants. Nature Biotechnology. 36, 894–898.

Zhang R, Liu J, Chai Z, Chen S, Bai Y, Zong Y, Chen K, Li J, Jiang L and Gao C (2019) Generation of herbicide tolerance traits and a new selectable marker in wheat using base editing. Nature Plants. 5, 480–485

Zhu H, Li C and Gao C (2020) Applications of CRISPR - Cas in agriculture and plant biotechnology. Nature Reviews Molecular Cell Biology. 21, 661–677

Zhu L and Qian Q (2020) Gain-of-function mutations: key tools for modifying or designing novel proteins in plant molecular engineering. Journal of Experimental Botany. 71 (4), 1203 – 1205

Zupan JR, Zambryski P (1995). Transfer of tDNA from Agrobacterium to the plant cell. Plant Physiology. 107 (4), 1041 – 7

Supplementary Data

Supplementary **Table 1** Basic information of ten mutant lines of *Oryza sativa*

Line #	Full name	Mutation	Locus #	Wildtype	Provider	Reference
5609	PFG_3A-05609.R	KRP5 KO	LOC_Os03g04490.1	Dongjin	Korea	*Jeong et al 2006, Jeon et al 2000*
18132	PFG_1A-18132.L	KRP5 KO	LOC_Os03g04490.1	Huayoung	Korea	*Jeong et al 2006, Jeon et al 2000*
43987	M0043987	KRP5 AC	LOC_Os03g04490.1	Tainung67	Taiwan	*Hsing et al 2007, Ho et al 2000*
40246	PFG_2A-40246.L	KRP5 AC	LOC_Os03g04490.1	Huayoung	Korea	*Jeong et al 2006, Jeon et al 2000*
6157	PFG_3A-06157.L	KRP4 AC	*LOC_Os10g33310.1*	Dongjin	Korea	*Jeong et al 2006, Jeon et al 2000*
6385A	RdSpm6385A_3.1	KRP4 KO	*LOC_Os10g33310.1*	Nipponbare	UC-Davis	*Sundaresan V 2005 (unpublished)*
36527	M0036527	KRP4 KO	*LOC_Os10g33310.1*	Tainung67	Taiwan	*Hsing et al 2007, Ho et al 2000*
2792	RdSpm2792_3.1	Fb3 KO	LOC_Os08g09750	Nipponbare	UC-Davis	*Sundaresan V 2005 (unpublished)*
40994	M0040994	Fb3 KO	LOC_Os08g09750	Tainung67	Taiwan	*Hsing et al 2007, Ho et al 2000*
9125	M0009125	Fb3 KO	LOC_Os08g09750	Tainung67	Taiwan	*Hsing et al 2007, Ho et al 2000*

**The mutants were searched from RiceGE: Rice Functional Genomic Express Database at http://signal.salk.edu/cgi-bin/RiceGE*

CDS of KRP5 gene (LOC_Os03g04490.1, 666 bp)

```
ATGGGGAAGTACATGCGGAAGGGGAAGGTGTCGGGGGAGGTGGCGGTGATGGAGGTGGGC   (60)
GGGGCGCTGCTCGGCGTCCGCACCCGCTCCCGCACGCTCGCGCTGCAGCGGACGACCTCG
TCGCAGAAGCCGCCGGAGAAGGGGGAGGGGGACCCCGGTGCGGGCGCGGGCGCGGGGGCG  (180)
GAGTACCTCGAGCTCAGGAGCCGGAGGCTCGAGAAGCCGCCTCCGCACACGCCGCCGGCC
AAGGAGAAGGAGACCGCCAGGAGGGCTTCCGCCGCCGCCGCCGCCGCCGTGAGGATGCCG  (300)
GCGGCGCCGCAAGCGGCCGAGGAGTTCGAGGCGGAGGTCGAGGTGTCCTTCGGCGACAAC
GTTCTTGACCTCGACGGCGACGCCATGGAGAGGAGTACCAGGGAGACAACGCCTTGCAGT  (420)
TTAATTAGGAGCTCAGAAATGATAAGCACCCCTGGCTCCACAACTAAAACCAACACCTCG
ATCAGTTCCCGGCGCAGAATGGAGACCTCTGTTTGTCGTTACGTTCCGAGTTCTTGAG   (540)
ATGGAAGAGTTCTTTGCAGCTGCTGAACAACAGCAACATCAGGCTTTCAGAGAGAGGTAT
AACTTCTGTCCTGTGAACGACTGCCCACTTCCTGGACGGTACGAATGGACAAGGCTAGAC  (660)
TGCTAG
```

Encoding KRP5 protein (221 aa)

```
MGKYMRKGKVSGEVAVMEVGGALLGVRTRSRTLALQRTTSSQKPPEKGEGDPGAGAGAGA   (60)
EYLELRSRRLEKPPPHTPPAKEKETARRASAAAAAAVRMPAAPQAAEEFEAEVEVSFGDN
VLDLDGDAMERSTRETTPCSLIRSSEMISTPGSTTKTNTSISSRRRMETSVCRYVPSSLE  (180)
MEEFFAAAEQQQHQAFRERYNFCPVNDCPLPGRYEWTRLDC*
```

The code AGT for aa #175, S (Serine), is interrupted at G/T

Supplementary Fig. 1 T-DNA Insertion Site at KRP5 Gene of the Line 05609

Supplementary **Table 2** Primer sequences (chapter 4)

Primer names	Sequences 5' -3'
Genotyping	
KRP5mut05609-F (H77)	AGATGCAACCTCGTGAAAGG
KRP5mut05609-R1 (H78)	AGCAGGTTTATGTGGCCAAG
KRP5mut05609-R2 (H76)	AGTTTTCGCGATCCAGACTG
KRP5mut18132-F (H80)	TCGTCCAAAGCTGAATGTTG
KRP5mut18132-R1 (H81)	GGTAAACAGAAGGCAGCTGC
KRP5mut18132-R2 (H163)	ACCTCCGGAATCACTGCAA
KRP4mut06157-F1 (H82)	TTCTTGCAGGAATACCAGGG
KRP4mut06157-F2 (H160)	CCTGTGCCATTATTGCTACC
KRP4mut06157-R (H83)	CCCACTAAGCCTGAGCAGAG
KRP4mut6385A-F (H72)	AAACAAGAAAAATGCACCGG
KRP4mut6385A-R1 (H73)	ATCTCACCACCCACCTCAAG
KRP4mut6385A-R2 (H71)	GAGCGTCCATTTTAGAGTGAC
Fb3mut2792A-F (H69)	AATGAGGCCTCGTTTGAATG
Fb3mut2792A-R1 (H70)	GCGCAGTCCTTAAGATCCAG
Fb3mut2792A-R2 (H71)	GAGCGTCCATTTTAGAGTGAC
RT-PCR	
KRP4-RT-F (H13)	GAGGCCGAATTCATGGGCAAGTACATGCGCAA
KRP4-RT-R (H14)	GTCGACGGATCCTCAGTCTAGCTTGACCCATTC
KRP5-RT-F (H15)	GAGGCCGAATTCATGGGGAAGTACATGCGGAAG
KRP5-RT-R (H16)	GTCGACGGATCCCTAGCAGTCTAGCCTTGTCCA
qRT-PCR	
KRP5-qRT-F (H185)	ACCAACACCTCGATCAGTTCC
KRP5-qRT-R (H186)	CTAGCAGTCTAGCCTTGTCC
Fb3-qRT-F (H181)	TGGAGATCAGCAGTATGCCC
Fb3-qRT-R (H182)	GCAGCTTTTCAACTCCCTAGAA
18S-qRT-F (H177)	TTAGGCCACGGAAGTTTGAG
18S-qRT-R (H178)	GCATTCCTCGTTGAAGACCA

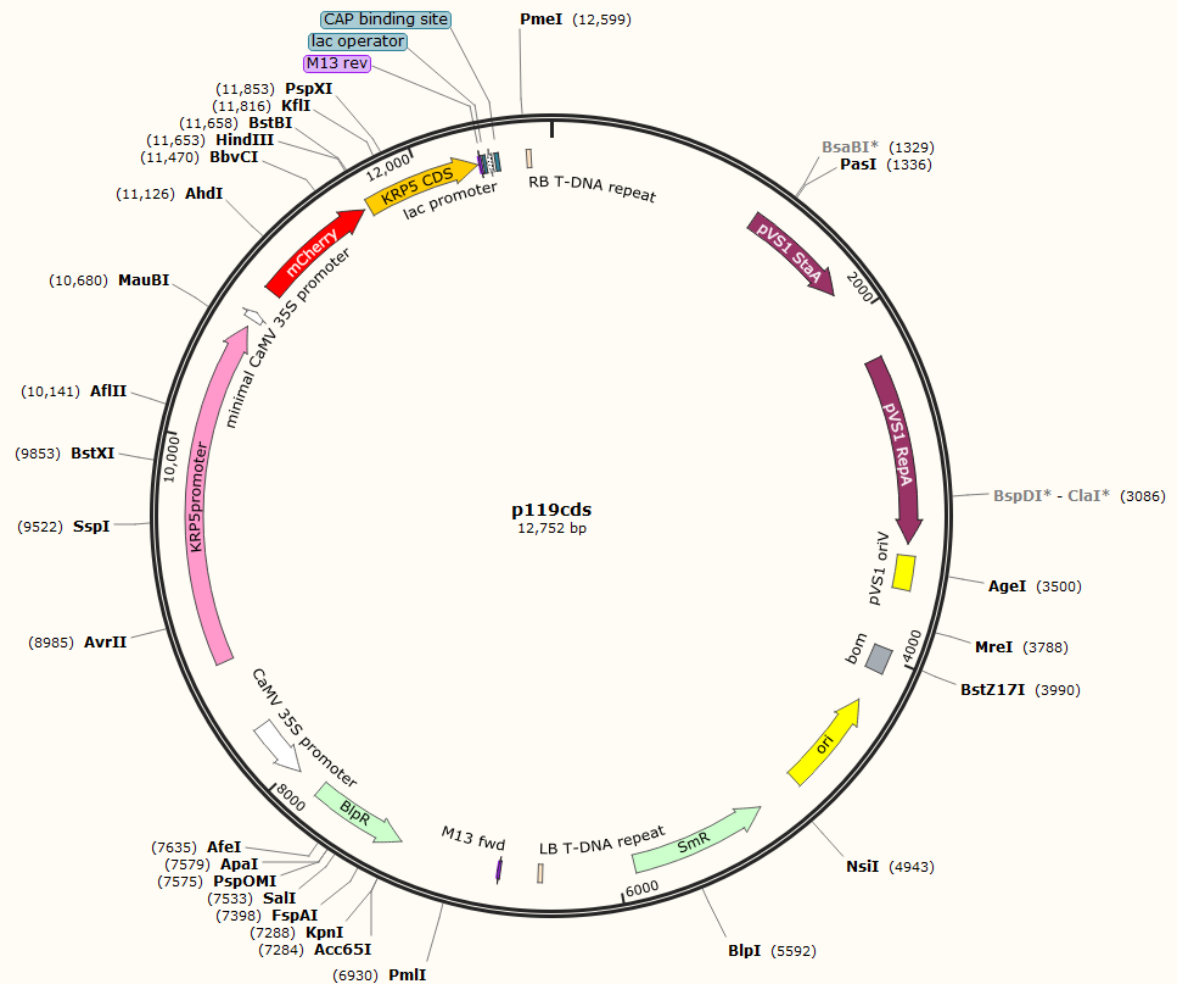

Supplementary Fig 2. Map of p119cds showing the construct Promoter$_{KRP5}$-mCherry-KRP5 cloned into the binary vector pE3055 (Lee and Gelvin 2014) for the stable transformation of rice KRP5KO mutant line (#05609)

Supplementary Fig 3. The map of p118cds showing the construct Promoter$_{Fb3}$-EYFP-Fb3 cloned into the binary vector pE3055 (Lee and Gelvin 2014) for the stable transformation of rice Fb3KO mutant line (#2792)

Conclusions

Based our study, we can make four conclusions as the following.

1. The isolated rice gametes and zygotes provide us a unique system for research in cellular and molecular biology and biochemistry due to their purity, viability, transparency and intactness. On the other hand, they are very vulnerable, therefore, the manipulation demands patience and caution.
2. We established a specific model (Fig. 1) called arrested core complex for rice zygotic cell cycle control, in which KRP5 and KRP4 coordinately inhibit kinase activity of the basic core complex, CDKB1-CYCD5 to arrest the zygotic cell cycle at the checkpoint 2 (G2-M). This model is supported by the results from Y2H, yeast growth in serial dilutions, Kinase activity assay of CDKB and BiFC in living rice egg cells and zygotes.
3. Fb3 is identified as a regulator of the two KRP inhibitors of rice zygotic cell cycle through proteasome pathway (Fig.1). This is evidenced by the protein degradation assay and supported by the interactions of Fb3 with KRP5 and KRP4 detected in Y2H, cellular localization and BiFC, and the reversal effect of Fb3 on KRP inhibition to the kinase activity of CDKB.
4. Five rice lines with mutation in KRP5, KRP4 andFb3 show significantly reduced seed setting rate, demonstrating the essential roles of the three proteins in initiation of rice seed formation. We also found that these mutations result in abnormal morphology in rice female germ units and compromised function in rice sperm cells.

The above finding helps better understand the cell cycle control in the early embryogenesis and provides a reference for genetic engineering to get higher rice grain yield.

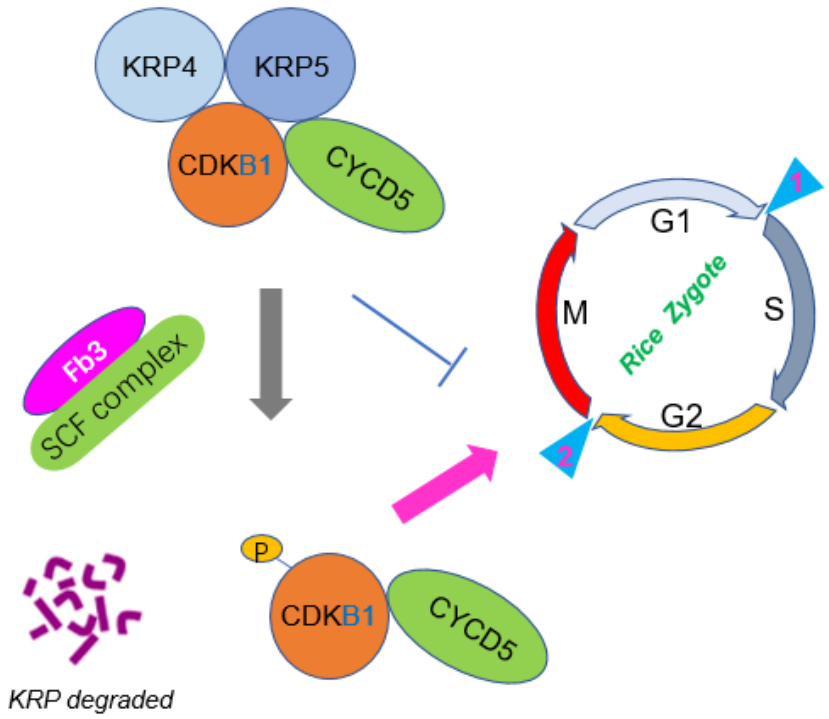

Fig.1 The arrested core complex model for rice zygotic cell cycle control at Checkpoint 2 (G2-M) and the regulation of KRP inhibitors via Fb3 mediated proteasome pathway

However, this is just the beginning for the study of plant zygotic cell cycle control. More issues remain to be solved or verified. For example, the CDKA based core complex may be involved in the S phase entry yet its components need to be verified by Co-IP; besides Fb3, we need to clarify if there is any other F-box proteins which may also participate in the regulation of KRP inhibitors via the proteolysis pathway.

Moreover, our finding and practice may have other potential applications for the future research. Here are some of examples.

1. Our efficient and skillful manipulation in isolation of rice gametes make it possible to collect enough isolated cells for purification and characterization of gamete plasma membrane

glycoproteins to identify the surface determinants in the cell-cell recognition required for plant double fertilization.

2. It is well known that it is difficult to get the stably transformed rice plants from the callus in the traditional way; but our technique and experience in transfecting rice egg cells and zygotes with plasmid DNA, as for we did for the cellular localization and BiFC, can be promisingly applied for an relatively easier way to generate stably transformed rice plantlets.
3. According to the RNAseq of rice gametes and zygote (Supplementary Fig.1, Chapter 2), KRP1 and KRP3 are preferentially expressed in rice sperm cells. It is interesting to investigate if they are involved in the cell cycle control of rice spermatogenesis.
4. From the reciprocal pollination between the mutant line and WT, we found that the wild type father (pollen) always significantly rescue more mutation damage (reduced seed setting rate) than the wild type mother (Fig. 9, Chapter 4). One of possibilities is that the rice sperm cell contributed KRP5 and KRP4 bear some more important epigenetic codes which are different from those in rice egg cells. It is interesting to check further on this issue.

Prior and Planned Publications

1. Li C., Xu H*, Russell SD and Sundaresan V (2019) Step-by-step protocols for rice gamete isolation. Plant Reprod. 32, 5–13

   **The first co-author*

2. Li C, Xu H*, Fu FF, Russell SD, Sundaresan V and Gent JI (2020) Genome-wide redistribution of 24-nt siRNAs in rice gametes. Genome Res. 30, 173-184

   **The first co-author*

3. Li C, Gent JI, Xu H*, Fu H, Russell SD and Sundaresan V (2021) Resetting of 24-nt siRNA landscape is initiated in the unicellular zygote in rice. (submitted to Genome Biology)

   **The first co-author*

4. Xu H, Fu H and Russell SD (2021) Isolation and transfection of rice gametes and zygotes (in preparation)
5. Xu H, Russell SD, Bartley L, Fu H, Libault M and Bourne C (2021) The coordinate function of OsKRP5 and OsKRP4 in rice zygotic cell cycle control. (in preparation)
6. Xu H, Russell SD, Bartley L, Fu H, Dunn A and Sundaresan V (2021) Regulation of the coordinate cell-cycle inhibitors by Fb3 mediated degradation in rice zygotes. (in preparation)

Acknowledgements

What has been presented in this dissertation is a summary of the recent progress made in Dr. Russell Lab, OU, on a very fundamental but little explored spot in plant reproduction. Over six years have elapsed since 2015. It consumed me almost every day and night regardless of holidays and weekends. It is due to the importance and difficulty of the project, and also needs to be attributed to the support from numerous sources.

Therefore, I thank Professor Dr. Scott Russell, my supervisor, and Dr. Anne Dunn, the Department Chair, for their efforts in guiding, funding and caring every stage of the project. I also thank the other members of my Advisory Committee including (the current members) Dr. Laura Bartley, Dr. Marc Libault, and Dr. Christina Bourne and (the previous members) Dr. Ann West and Dr. Sharon Kesslller (Purdue University) for their valuable advice and practical help, lab facilities and aid with developing experimental material and methods.

I also thank Joshua Chesnut and Daniel Jones for demonstrating the procedure of manual isolation of rice gametes and zygotes; Kangmei Zhao and Chengcheng Zhang for their assistance with analyzing rice mutants; Professor Chua Nam Hai (Rockefeller University) for his generous providing vector pER8 and pUH-GFP2; Dr. Christina Bourne and Dr. Paul Sims for help using the fluorescent plate reader to measure Kinase activity; Dr. Ben Smith and David Thomas for instructing epi-fluorescence microscopy; Dr. Venkatesan Sundaresan and Chenxin Li (UC-Davis) for their coordination in our epigenetic study of rice gametes and zygotes; Mr. Michael Keeter, Mr. Lynn Nichols and Mr. Mike Todd for their important assistance with chemical ordering, rice plant management and instrument maintenance.

In addition, I must mention Hong Fu, my wife, for her diligent hands especially her voluntary daily work since summer 2020 in rice plant growth and maintenance, and manual isolation of one thousand and two hundred of rice egg cells and zygotes.

In a word, without the support as above numerated, no results could have been obtained.